THE PHOSPHORYLATION AND NUCLEAR LOCALIZATION OF THE CO-CHAPERONE MURINE STRESS-INDUCIBLE PROTEIN 1

THESIS

Submitted in fulfillment of the Requirements of the Degree of

DOCTOR OF PHILOSOPHY
(BIOCHEMISTRY)

in the

DEPARTMENT OF BIOCHEMISTRY, MICROBIOLOGY AND BIOTECHNOLOGY
FACULTY OF SCIENCE
RHODES UNIVERSITY

by

VICTORIA MARY LONGSHAW

November 2002

ABSTRACT

The co-chaperone murine stress-inducible protein 1 (mSTI1), a heat shock protein 70 (Hsp70)/ heat shock protein 90 (Hsp90) organizing protein (Hop) homologue, mediates the assembly of the Hsp70/Hsp90 chaperone heterocomplex. mSTI1 is phosphorylated *in vitro* by cell cycle kinases, proximal to a putative nuclear localization signal (NLS), substantiating a predicted CKII-cdc2-NLS (CcN) motif at position 189-239. Stable transfectants of NIH 3T3 fibroblasts that expressed mSTI1-EGFP, NLS^{mSTI1}-EGFP and EGFP, were prepared. Fluorescence microscopy revealed mSTI1 was cytoplasmically localized, and that this localization was not affected by the fusion of mSTI1 with the EGFP moiety. NLS^{mSTI1}-EGFP was targeted to the nucleus compared to EGFP, suggesting that the NLS^{mSTI1} was a functional NLS. The localization of mSTI1 was determined under normal and heat shock conditions, inhibition of nuclear export (leptomycin B), inhibition of CKII (5,6-dichlorobenzimidazole riboside, DRB), inhibition of cdc2 kinase (olomoucine), and G1/S phase arrest (hydroxyurea). mSTI1-EGFP and mSTI1 were excluded from the nucleus in the majority of resting cells, but accumulated in the nucleus following leptomycin B treatment, implying that mSTI1 possibly undergoes a functional import process, and export via the chromosomal region maintenance 1 (CRM-1)-mediated export pathway. Hydroxyurea and olomoucine (but not DRB or heat shock) treatment increased the proportion of cells in which mSTI1-EGFP exhibited cytoplasmic and nuclear localization. 2D gel electrophoresis detected three endogenous mSTI1 isoforms, which changed following hydroxyurea treatment. Furthermore, point inactivation and mimicking of phosphorylatable residues in mSTI1 altered the translocation of the protein and the isoform composition. Modification of mSTI1 at S189 and T198 decreased the number of isoforms of mSTI1-EGFP, suggesting that the protein is modified at these sites *in vivo*. The removal of the *in vitro* cdc2 kinase site at T198 promoted a nuclear localization during G1/S phase arrest. Therefore active cdc2 kinase, but not CKII, may be required for cytoplasmic localization of mSTI1. The CKII site appears to have no regulatory role under heat shock conditions or during the cell cycle. *In vitro* phosphorylation studies on untagged mSTI1 further supported the

prediction that S189 is the only site recognised by CKII. The cdc2 kinase site at T198, however, although the major site, was not the only site phosphorylated *in vitro*. However, mSTI1 and cdc2 kinase did not interact in a detectable stable complex. Bioinformatic analysis of mSTI1 revealed NLS residues were conserved in STI1 proteins, and the NLS and TPR2A motifs were in close proximity. This may have mechanistic implications for the formation of the Hsp90-mSTI1 heterocomplex. The cytoplasmic or nuclear localization of mSTI1 is predicted to be the result of a dynamic equilibrium between nuclear import and nuclear export, the fulcrum of which may be shifted under different cell cycle conditions. These data provide the first evidence of regulated nuclear import/export of a major Hsp70/Hsp90 co-chaperone, and the regulation of this nuclear import by cell cycle status and cell cycle kinases.

TABLE OF CONTENTS

CHAPTER 1
LITERATURE REVIEW

CHAPTER 2

BIOINFORMATIC ANALYSIS OF mSTI1

CHAPTER 3

THE SUBCELLULAR LOCALIZATION OF mSTI1

CHAPTER 4
MECHANISTIC AND INHIBITION STUDIES ON THE SUBCELLULAR LOCALIZATION OF mSTI1

CHAPTER 5
IN VIVO ANALYSIS OF THE POTENTIAL CKII AND CDC2 KINASE PHOSPHORYLATION SITES OF mSTI1

CHAPTER 6

IN VITRO ANALYSIS OF THE POTENTIAL CKII AND CDC2 KINASE PHOSPHORYLATION SITES OF mSTI1

APPENDIX B

GENERAL PROCEDURES

APPENDIX C

PRIMERS

APPENDIX D

SUPPLEMENTARY RESULTS

APPENDIX E

PLASMID VECTORS

REFERENCES

LIST OF FIGURES

LIST OF TABLES

LIST OF SYMBOLS

UNIT ABBREVIATIONS

%	Percent or g/100ml
α	alpha subunit
β	beta subunit
γ	gamma atom radioactively labeled
λ	Lamda DNA
μg	microgram
μl	microlitre
μm	micrometer
μmol	micromole
Å	angstrom
A^{260}	absorbance at 260 nanometers
A^{280}	absorbance at 280 nanometers
bp	base pair
Ci	curie
Da	Dalton
g	gram
kDa	kiloDalton
l	litre
M	molar
mg	milligram
ml	milliliter
mm	millimitre
mol	mole
nm	nanometer
^{o}C	degrees Celcius

pmol	picomole
U	units
V	volt
v/v	volume per volume
w/v	weight per volume
x g	relative centrifugal force to gravity

PREFIXES

10^{3}	kilo	k
10^{-3}	milli	m
10^{-6}	micro	μ
10^{-9}	nano	n
10^{-12}	pico	p

NOMENCLATURE

NOMENCLATURE

Anti-	antibody
BSA	Bovine serum albumen
cdc	cell division cycle
cdc2 kinase	cell division cycle kinase 2
cdk	cyclin dependent kinase
cDNA	complementary DNA
CKII	casein kinase II
DMEM	Dulbecco's Modified Eagle's Medium
DNA	Deoxyribonucleic acid
DTT	Dithiothreitol
EDTA	Ethylenediaminetetraacetic acid
FKBP	FK506-binding protein
GAP	GTPase activating protein
GST	Glutathione *S*-transferase
Hip	Hsp70/Hsc70-interacting protein
Hop	Hsp70/Hsp90-organising protein
Hsc70	Heat shock cognate protein 70
HSF	Heat shock factor
Hsp	Heat shock protein
Hsp40	Heat shock protein 40
Hsp70	Heat shock protein 70
Hsp90	Heat shock protein 90
IPTG	Isopropyl-β-D-thiogalactoside
MAPK	Mitogen activated protein kinase
MOPS	3-(N-morpholino)propanesulfonic acid
mRNA	messenger ribonucleic acid

mSTI1	murine stress-inducible protein 1
OD	optical density
PAGE	polyacrylamide gel electrophoresis
PBE	polybuffer exchanger
PBS	phosphate buffered saline
PCR	polymerase chain reaction
pI	isoelectric point
PMSF	Phenylmethylsulfonyl fluoride
PP5	protein phosphatase 5
RNA	Ribonucleic acid
Rnase	Ribonuclease
SDS	sodium dodecyl sulphate or sodium lauryl sulphate
STI1	stress-inducible protein 1
SV40	simian virus 40
TBE	Tris-borate-EDTA
TBS	Tris-buffered-saline
TBST	Tris-buffered-saline-Tween 20
TEMED	N,N,N’,N’-tetramethylethylenediamine
TPR	tetratricopeptide repeat
UV	ultraviolet
NPC	Nuclear pore complex
Ras	
Ran	Ras-related nuclear protein
NLS	Nuclear localization sequence
NTF2	nuclear transport factor-2
CRM1	chromosomal region maintenance 1
CcN	CKII ("C") and cdc2 kinase ("c") sites and the NLS ("N")
Cdk	cyclin-dependent protein kinases
Cdc	cell division cycle
MPF	Mitosis promoting factor
S phase	DNA synthesis phase

G1 phase	First growth phase
G2 phase	Second growth phase
M phase	Mitosis
CKII	casein kinase II
Bag 1	Bcl2-associated anthogene 1
Hip1	Hsp70 interacting protein
PPIase	polyproline isomerase
FKBP	FK506 binding protein
GR	Glucocorticoid receptor
CNS	central nervous system
AR	androgen receptor
STI1	Stress inducible protein 1
TPR	Tetratricopeptide repeat
N-	amino-terminal
C-	Carboxy-terminal
ATP	adenosine triphosphate
ATPase	adenosine triphosphate hydrolysis activity
MAPKAP kinase 2	MAP kinase-activated protein kinase 2
$pp90^{rsk}$	heat-activated S6 kinase

ACKNOWLEDGEMENTS

I would like to acknowledge my supervisor and mentor, Professor Greg Blatch, for his unflagging enthusiasm, empathy and patience. His conduct, both in and out of the lab, gives all his students a standard in scientific excellence, as well as a personal dignity. He is a true academic and teacher.

I would also like to thank:

- The Foundation for Research and Development for project funding, as well as Rhodes University for personal financial assistance during this project. The financial assistance from the Henderson Postgraduate Scholarship towards this research is hereby acknowledged. Opinions expressed and conclusions arrived at, are those of the author and are not necessarily to be attributed to Rhodes University or the donor.
- Drs M. Cheetham and P. Chapple, Department of Pathology, Institute of Ophthalmology, University College London, U.K., who kindly allowed me the opportunity to use the facilities at the Institute of Ophthalmology, and Drs Karl Matter, Tracy Bailey, Jacqueline van der Spuy, Celene Grayson and Simon Wilkins, for their valuable advice.
- Prof H. Karasuyama, Head of Department of Immunology, Tokyo Metropolitan Institute of Medical Science, Tokyo, Japan, who kindly provided me with BCMGSNeo vector.

A big thank you to my colleagues in Lab 301 for their company and support. And to all my friends, especially Jess Arjun, Judith Hornby and Ansuya Nassen for their on-the-spot friendship. Thank-you to Janice Limson, Aileen Boschoff and Ansuya Nassen for their generous and stoical help in proofreading this manuscript.

A special thank you to Clark Ehlers, for his continuous empathy and good fun, which kept me sane for 3 years. And for always starting my car when I drain the battery by leaving the lights on…

DEDICATION

This work is dedicated to my excellent parents, Geoff and Jenny Longshaw,
and to the best of brothers, James Longshaw.
They have stood tall beside me through all my hurricanes, and without them the privilege of this achievement would not have been possible.
They are my North and my Sunshine.

And in loving memory of a most beloved grandmother, Peggy Longshaw,
my refuge in many things.
I hope she knows that all the gels finally gelled.

Most people don't know how brave they really are.
In fact, many heroes
live out their lives in self-doubt.
R. E. Chambers

A little bit of what you fancy
does you good…
My Grandmother
Peggy Longshaw

CHAPTER 1

LITERATURE REVIEW

SUMMARY: The co-chaperone mSTI1 (murine stress-inducible protein 1), a Hop (heat shock protein 70 (Hsp70)/ heat shock protein 90 (Hsp90) organizing protein) homolog, mediates the assembly of the Hsp70/Hsp90 chaperone heterocomplex. This study investigates the nucleocytoplasmic distribution of mSTI1. A nuclear localization signal (NLS) in mSTI1 is here proposed to cause the nucleocytoplasmic distribution, which has implications for the subcellular localization of the Hsp70/Hsp90 chaperone heterocomplex. Furthermore, the evidence presented in this work suggests that the regulation of the localization of mSTI1 is cell cycle related in the form of a phosphorylation-regulated NLS, the CcN motif, in mSTI1. Therefore, in this chapter, the relevant research areas are reviewed, namely nucleocytoplasmic transport of proteins, aspects of cell cycle control, and chaperone protein functions.

1.1 NUCLEOCYTOPLASMIC TRANSPORT

1.1.1 The nuclear pore complex (NPC)

The mammalian nucleus is a highly dynamic organelle of about 10 μm, surrounded by a double membrane (separate inner and outer bi layers) to form the nucleus. Passage through the nuclear envelope occurs through NPCs (nuclear pore complexes), which penetrate the double lipid bilayer (Feldherr *et al.,* 1984, Panté and Aebi, 1995). The NPC is a large proteinaceous structure, about 90-100 nm in diameter, having a molecular mass of approximately 125 MDa and is currently thought to consist of 50-100 distinct polypeptides in vertebrates (Davis, 1995, Goldberg and Allen, 1995). The NPC is made up of octagonal spoke-ring structures, of which a short fibre-like structure extends into the cytoplasm from the cytoplasmic ring, while an unusual basket-like structure (possibly to exclude loops of DNA) extends from the nucleoplasmic ring (Panté *and* Aebi, 1995, Davis, 1995, Goldberg and Allen, 1995). Many nuclear pore proteins (nucleoporins) are characterised by O-linked N-acetylglucosamine modifications and the presence of multiple FxFG or GLFG peptide repeats (Davis, 1995). The pore complex contains an aqueous diffusion channel, approximately 10 nm in diameter. In principle, molecules of up to 9 nm in diameter (~60 kDa) should pass freely through this channel by diffusion. However, only relatively small molecules (< 20 kDa) such as ions and metabolites, actually pass by simple diffusion (Yoneda, 1997).

1.1.2 Nuclear import is coupled to a motive force

The processes of nuclear transport are energy dependent, driven by the Ras-like small GTPase protein Gsp1p (Ran, Ras-related nuclear protein) (Nachury and Weiss, 1999; Izaurralde *et al*., 1997). Ran-GTP acts as a marker of the nuclear compartment for both nuclear import and export (Görlich and Kutay, 1999; Nakielny and Dreyfuss, 1999; Weiss, 1998). This model remarkably predicts that only a single molecule of GTP is hydrolysed per import/export cycle; it strictly requires that Ran-GTP is highly enriched in the nucleus. A steep Gsp1p-GTP-Gsp1p–GDP gradient is generated by the cellular

compartmentalization of regulators of the Gsp1p cycle. Specifically, the guanine-nucleotide exchange factor of Gsp1p(RanGEF or RCC1), which regenerates Ran-GTP, is nuclear and bound to chromatin (Bischoff and Ponstingl, 1991). In contrast, the main GTPase activating protein (RanGAP), and the Ran-binding proteins, RanBP1 and RanBP2, which stimulate GTP hydrolysis by Ran, are found in the cytoplasm (Bischoff *et al.,* 1994). This asymmetric distribution predicts that Gsp1p is present mainly in the GTP-bound form in the nucleus, whereas Gsp1p is immediately converted to a GDP-bound state in the cytoplasm (Ström and Weiss, 2001).

1.1.3 Nucleocytoplasmic transport of proteins

Macromolecules of up to 25 nm in diameter (~25 MDa) are shuttled bi-directionally through the FxFG repeat-rich NPC by association with karyopherins (Chook and Blobel, 2001). Individual members of the karyopherin-β-like protein family can function both as import and export receptors (Yoshida and Blobel, 2001). The multitude of filamentous FxFG repeat NPC proteins form a gel-like mesh due to weak hydrophobic interactions (Ribbeck and Görlich, 2001), such that molecules pass through with increasing difficulty as size increases, and beyond an upper size limit, they are totally excluded. Most karyopherins have binding sites for FxFG repeats and thus interact with components of the NPC, through their FxFG-binding sites (Ribbeck and Görlich, 2001). The direction of transport is determined by sequence signals in the transport substrate: nuclear localization signals (NLS) direct a substrate to the nuclear import pathway, while nuclear export signals (NES) direct a substrate to exit the nucleus.

Nuclear import involves recognition of a substrate NLS by a karyopherin (Figure 1.1). There are more than 22 putative karyopherin β members in mammals (Ström and Weis, 2001). The heterodimer karyopherin complex contains the subunits karyopherin-α (also called importin-α, or Kap60p) and karyopherin-β (also called importin-β or Kapβ1), and is required for active transport through the NPC (Talcott and Moore, 1999). Karyopherin-α contains the NLS binding site and karyopherin-β is responsible for the docking of the karyopherin-substrate complex to the cytoplasmic filaments of the NPC and its translocation through the pore (Conti and Izaurralde, 2001).

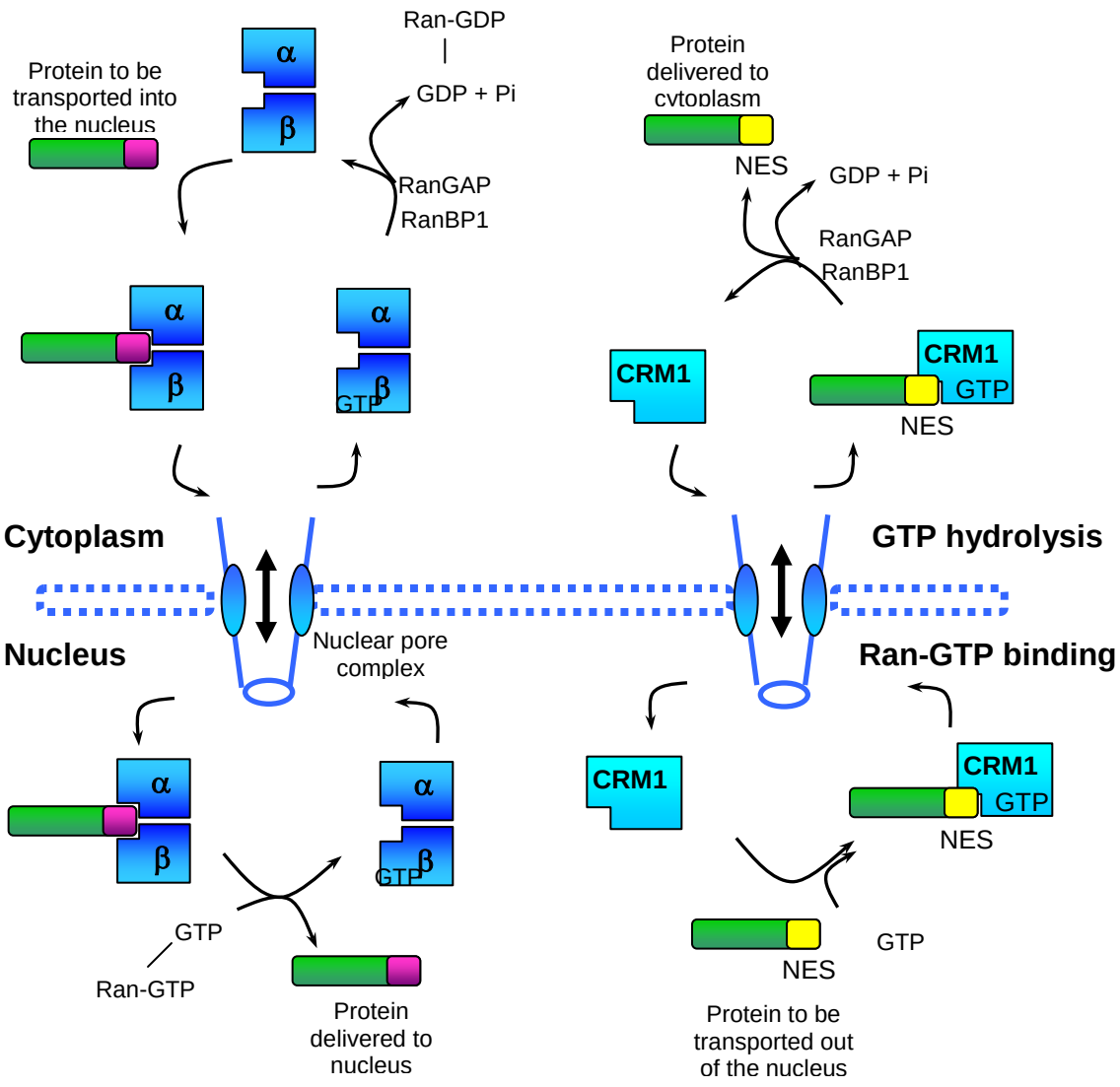

Figure 1.1: NLS- and NES-containing proteins are transported through the NPC

Karyopherin-α binds a substrate protein bearing the NLS sequence, then binds to karyopherin-β to form a trimeric karyopherin-substrate complex (Morianu *et al.*, 1995). Karyopherin-β docks the karyopherin-substrate complex to the cytoplasmic filaments of the NPC (ATP-independent binding), and facilitates ATP-dependent translocation through the pore. This transfer is facilitated by Gsp1p and NTF2 (Gorlich and Mattaj, 1996, Melchior and Gerace, 1995, Yoneda, 1996a). Translocation is terminated by the binding of Ran-GTP to karyopherin-β, which causes a conformational change, and the dissociation of the import complex. Karyopherin-α becomes autoinhibited and is returned to the cytoplasm by the exportin CAS (also called Kap109p). The substrate protein is released into the nucleoplasm. Ran-GTP-karyopherin-β is transferred back through the nuclear pore by binding to FxFG repeats. On the cytoplasmic side, Ran-GTP binds to RanGAP, stimulating GTP hydrolysis. The resulting conformational switch in Gsp1p releases karyopherin-β for interaction with a new substrate (Ström and Weiss, 2001). CRM1 binds to substrates containing a leucine-rich NES in the nucleus, forming a trimeric complex with Ran-GTP. The complex is transferred to the cytoplasm by a mechanism involving binding of CRM1 to the NPC. Once in the cytoplasm, GTP hydrolysis results in dissociation of Gsp1p from the complex, allowing CRM1 to release the substrate protein. Free CRM1 re-enters the nucleus to bind and export additional substrate proteins (Ström and Weiss, 2001).

There are other examples of karyopherins including Transportin 1, Transportin-SR, Importin 5, Importin 7 and Importin 11 (Ström and Weis, 2001). Different karyopherins possess distinct NLS-binding specificities, allowing modulation of the system through differencial expression of karopherins and through competition between different karyopherins for the same protein (Jans *et al.,* 2000). The proteins Ran, and nuclear transport factor-2 (NTF2) facilitate the actual transfer through the pore (for recent reviews see: Adam, 1999; Hood and Silver, 1999; Talcott and Moore, 1999). Nuclear export involves recognition of a substrate NES by one of many export proteins (Figure 1.1). Examples of exportins include CRM1, CAS, exportin-t and exportin 4. CRM1 (chromosomal region maintenance 1) (also called exportin 1, Crm1p, and Xpo1p) is of the karyopherin-β protein family, and is often required for export from the nucleus. CRM1 is a receptor for leucine-rich NES-containing proteins (Fornerod *et al.,* 1997; Stade *et al.,* 1997). CRM1 is a specific target of leptomycin B, an anti-fungal and anti-tumor antibiotic with cell cycle arresting activity (Kudo *et al.,* 1997).

1.1.4 The Nuclear Localization Sequence (NLS)

The molecular mechanism of nuclear protein import into the nucleus has been modelled on the NLS-containing simian virus (SV40) large T-antigen (T-ag) (Garcia-Bustos *et al.*, 1991). Other NLSs have been identified in a variety of karyophilic proteins by deletion or point mutagenesis of their corresponding genes (Garcia-Bustos *et al.*, 1991). Nuclear localization signals are short peptide sequences that are necessary and sufficient for the nuclear localization of their respective proteins (Hall *et al.*, 1984, Kalderon *et al.*, 1984, Lanford and Butel, 1984). The identification of these sequences requires firstly, mutation or deletion of the NLS to lead to cytoplasmic localization of the protein, and that secondly, the NLS is active in nuclear targeting of a normally cytoplasmic localized carrier protein, either as a peptide covalently coupled to the carrier or when encoded in the same reading frame as a fusion protein (Jans and Hübner, 1996).

Nuclear localization sequences function via recognition/ligand-receptor-like interactions (e.g. with NLS-binding proteins) and not through DNA or histone binding. The NLS is an entry rather than a retention signal since NLS-deficient carrier proteins microinjected into

the nucleus remain nuclear (Lyons *et al*., 1987, Schmidt-Zachmann *et al*., 1993). However nuclear retention by nuclear-targeting sequences has been observed (Briggs *et al.,* 2000). Nuclear accumulated NLS-containing proteins are highly laterally mobile (Rihs and Peters, 1989), and binding to chromatin or nucleoskeleton is unlikely to be the mechanism by which NLSs function (Dingwall *et al*., 1982). The NLS sequence is not deleted during or after translocation, and remains a part of the mature molecule, unlike the signal sequences for the targeting of proteins into rough endoplasmic reticulum (rough ER) or mitochondria (Yoneda, 1997). This is because, in contrast to ER and other targeting signals, NLSs are required to function many times, through a number of cell divisions, which in the case of most eukaryotes involves dissolution of the nuclear envelope (Agutter and Prochnow, 1994). NLS-dependent transport is temperature and ATP-dependent, as shown by the addition of NLS sequences to small proteins (Breeuwer and Goldfarb, 1990).

1.1.5 The consensus sequence for the NLS

There is no general consensus sequence for NLSs, the best characterised being that of SV40 T-antigen (PKKKRKV^{132}). A single amino acid substitution of N or T for the critical K^{128} residue of the SV40 T-antigen NLS abolishes its function and results in complete cytoplasmic localization (Jans and Hübner, 1996). This short 7 amino acid stretch of lysine-and arginine-rich sequence is sufficient to confer nuclear localization, even when it has been conjugated as a synthetic peptide to serum albumin (Kalderon *et al.,* 1984; Goldfarb *et al.,* 1986; Lanford *et al.,* 1986; Moore and Blobel, 1992). Although not all NLSs resemble that of T-ag, a number of them have been identified on the basis of similarity to the T-antigen NLS (Jans and Hübner, 1996). Several secondary structure prediction analyses predict NLSs to be hydrophilic, and preceded by a β-turn random coil region with highly antigenic surface structures (Lanford and Butel, 1984, Roberts, 1989). Secondary structure, however, is known to play a role in the nuclear localization of many NLS-bearing proteins, presumably through influencing the accessibility of the NLS (Jans and Hübner, 1996).

1.1.6 The Bipartite NLS

A variant of multiple NLSs are bipartite NLSs (Dingwall and Laskey, 1991), which consist of two series of basic residues separated by a 10 - to 12 - amino acid spacer. Although in a significant proportion of these sequences, one of the necessary elements shows a striking similarity to the SV40 NLS, it is not sufficient by itself to target a protein to the nucleus (Dingwall and Laskey, 1991). Although varying the length of the spacer, which can be increased to 22 amino acids in nucleoplasmin, has no effect on nuclear targeting efficiency, introduction of hydrophobic and bulky residues into the spacer markedly reduces targeting efficiency (Robbins *et al*., 1991). This implies that conformation and/or hydrophobicity may be important, perhaps for co-recognition of the two arms of the NLS. The finding that there is no strict requirement for spacers of a given length could be explained, if a flexible region of polypeptide need only connect the two basic domains. This flexible region of polypeptide may be needed in order to contact separate binding sites on a nuclear targeting sequence receptor, or perhaps different binding sites on two separate receptor molecules (Dingwall and Laskey, 1991). The structure of karyopherin-α was recently resolved, in complex with NLS peptides (Fontes *et al.,* 2000). The two basic clusters in the bipartite NLS occupy the two binding sites in karyopherin α used by the monopartite NLS, while the sequence linking the two basic clusters is poorly ordered, consistent with its tolerance to mutations (Kambach and Mattaj, 1992). It is thought that the increased length of NLS-functioning sequences existing in various proteins (Kambach and Mattaj, 1992), as in the case of the 70 kDa stress-induced chaperone cognate (Hsc70) (Mandell and Feldherr, 1992), are as a result of secondary structure influences on NLS accessibility which have affected nuclear localization (Mandell and Feldherr, 1992). More complex NLSs involve the presence of zinc fingers (Matheny *et al*., 1994) and specific glycosylation signals (Duverger *et al*., 1993). Larger carrier proteins presumably have more stringent targeting requirements than smaller proteins (Yoneda *et al*., 1992, Jans and Hübner, 1996). Structural analyses of the bipartite NLS in the glutocorticoid receptor indicate that the first pair of basic amino acids, and the first few amino acids in the spacer region, lie in an α-helix, such that the basic amino acids are on the face of the helix and exposed to the solvent (Dingwall and

Laskey, 1991). The remainder of the spacer region and the downstream basic cluster are disordered in solution. Computer modelling indicates that the spacer region can be looped out to juxtapose the two basic clusters, which suggests a mechanism whereby two domains can mimic a shorter basic sequence (Dingwall and Laskey, 1991).

The frequency of occurrence of this bipartite NLS sequence motif in nuclear and non-nuclear proteins has been determined by computer search of the SwissProt data base to be 50% of the nuclear proteins, but less than 5% of non-nuclear proteins (Dingwall and Laskey, 1991). The bipartite motif is thus a considerably more reliable indicator of nuclear localization *in vivo* than the SV40 sequence (relaxed to any five consecutive basic residues) (Dingwall and Laskey, 1991). The presence of the bipartite motif in many nonnuclear proteins will not necessarily cause them to be directed to the nucleus, as many are directed to other specific locations within the cell by alternative signals that probably function in a dominant manner (Dingwall and Laskey, 1991).

1.1.7 NLS number, dominance and absence

A number of proteins possess two or more NLSs that are required in concert to achieve "complete" nuclear localization, for example, the polyoma large T antigen, c-*myc*, N1/N2, influenza virus NS1, Matα2, and the yeast ribosomal protein L29 (Jans and Hübner, 1996). Multiple copies of an NLS are more efficient than one copy, especially in the case of a "weak" NLS. The maize R protein requires two or three NLSs to be nuclear (Sheih *et al*., 1993). The presence of additional copies of a NLS increases the initial rate and final steady-state level of nuclear accumulation (Dingwall and Laskey, 1991).

The possession of an NLS may not be sufficient to effect the nuclear localization (Roberts, 1989, Garcia-Bustos *et al*., 1991). Protein context may play a role in the efficiency of an NLS, i.e. the position of the NLS within a protein (Roberts *et al*., 1987). The NLS has to be solvent exposed to be accessible for recognition (Roberts *et al*., 1987). Signals for localization to subcellular compartments other than the nucleus can overide NLSs (Garcia-Bustos *et al*., 1991). If signals for targeting to different subcellular compartments are in competition, in particular competition between NLSs and mitochondrial localization and secretory signals (Garcia-Bustos *et al*., 1991, Kiefer *et al*., 1994) the most NH_2-terminal signal dominates.

Many proteins greater than 45 kDa are predominantly nuclear, but lack a functional NLS. The mechanism of nuclear transport of these proteins is often via an association with NLS-bearing proteins effecting co-transport into the nucleus ("piggy backing"). The glutocorticoid receptor (GR) contains a proto-nuclear localization signal (DeFranco *et al.,* 1995). Cytoplasmically localized mutant steroid hormone receptors can be transported to the nucleus by the specifically interacting 90 kDa heat shock protein (Hsp90), if the latter is fused to the NLS of nucleoplasmin. The expression of wild type progesterone receptor can lead to nuclear localization of Hsp90, which is normally cytoplasmic (Kang *et al.,* 1994). An alternate nuclear import pathway has been reported, which uses the M9 sequence, originally identified as a stretch of approximately 40 amino acids in the C terminus of the RNA-binding protein hnRNPA1. A nuclear transporter termed transportin (also called karyopherin β2), with significant similarity (~22%) to karopherin β, can mediate the nuclear import of M9-containing proteins *in vitro* (Fridell *et al.,* 1997). This nuclear import is different from the import of basic NLS proteins, because no karyopherin α is required. The M9 sequence also contains a signal for import and export, which cannot be separated (Michael *et al.,* 1995), whereas the classic NLS exclusively promotes import.

1.1.8 Phosphorylation regulation of nuclear import

We are well aware there are many karyopherin proteins in the karyopherin superfamily. Interestingly, many karyophilic proteins are regulated by cell cycle signals. Proliferating cells have a higher import capacity than serum-starved quiescent cells (Görlich and Mattaj, 1996), and nuclear pores appear to be most permeable just after the envelope has reassembled after mitosis (Feldherr and Akin, 1990, Feldherr and Akin, 1993). The kinetics of NLS-dependent nuclear localization are regulated by phosphorylation in the vicinity of the NLS (Jans and Hübner, 1996), as nuclear import is regulated by phosphorylation-dephosphorylation reactions (Mishra and Parnaik, 1995). Moreover, synthetic NLS-containing peptides have been found to stimulate the phosphorylation of several cellular proteins both *in vitro* and *in vivo* (Kurihara *et al.*, 1996). There appears to be a consensus of phosphorylation sites close to the NLSs of several proteins, which

modify NLS activity. The phosphorylation sites, together with the NLS, constitute phosphorylation mediated regulatory modules for nuclear protein localization (Jans *et al.*, 1995). Phosphorylation can enhance or inhibit NLS-dependent nuclear transport. For example, Protein Kinase C phosphorylation of lamin B_2 (Hennekes *et al.*, 1993) and CaMPK phosphorylation of the actin binding protein cofilin (Abe *et al.*, 1993) inhibit nuclear localization; while Protein kinase A phosphorylation of the c-*rel* proto-oncogene enhances nuclear localization (Mosialos *et al.,* 1991). CKII increases the rate of import of SV40 T-antigen (Jans and Jans, 1994) and nucleoplasmin (Vancurova *et al.*, 1995). Phosphorylation regulated NLSs therefore constitute a highly specific mechanism of cuing nuclear protein import precisely according to the stage of the cell cycle or to the signal transduction, metabolic, proliferative, or differentiation state of the cell (Jans and Hübner, 1996).

.

1.1.9 The CcN motif: a specialized phosphorylation regulated NLS

SV40 T-antigen comprises both enhancing and inhibitory phosphorylation sites proximal to the NLS (Figure 1.2 A). The CKII site increases the rate of NLS-dependent nuclear import, whereas cdc2 kinase site inhibits transport, markedly reducing the level of maximal nuclear accumulation. The cdc2 kinase and CKII sites appear to function independently of one another in terms of both regulating T-antigen nuclear transport and influencing phosphorylation at the other site. This regulatory module for T-antigen nuclear transport, comprising CKII ("C") and cdc2 kinase ("c") sites and the NLS ("N") has been termed the "CcN motif" (Jans *et al.*, 1991). The mechanism of cdc2 kinase-mediated inhibition appears to be through cytoplasmic retention (Jans and Jans, 1994) (Figure 1.2 B), while that of CKII phosphorylation-mediated enhancement is through increasing the affinity of association with the karyopherin complex (Jans and Jans, 1994), enhancing the docking rate at the NPC. Flanking sequences and phosphorylation at the CKII site are mechanistically important in NLS recognition by karyopherin α in both T-antigen (Hübner *et al.*, 1997) and Dorsal transcription factor from Drosophila (Briggs *et al.,* 1998). Similar CcN motifs have been found in a variety of nuclear proteins, including

p53 (Shaulsky *et al.*, 1990, Bischoff *et al.*, 1990), lamin (Loewinger and McKeon, 1988), nucleoplasmin (Dingwall *et al.*, 1988, Robbins *et al.*, 1991), SW15 (Jans *et al.*, 1995) and the interferon-induced nuclear factor IFI 16 (Briggs *et al.*, 2001), implying a general role for the CcN motif in regulating nuclear protein transport.

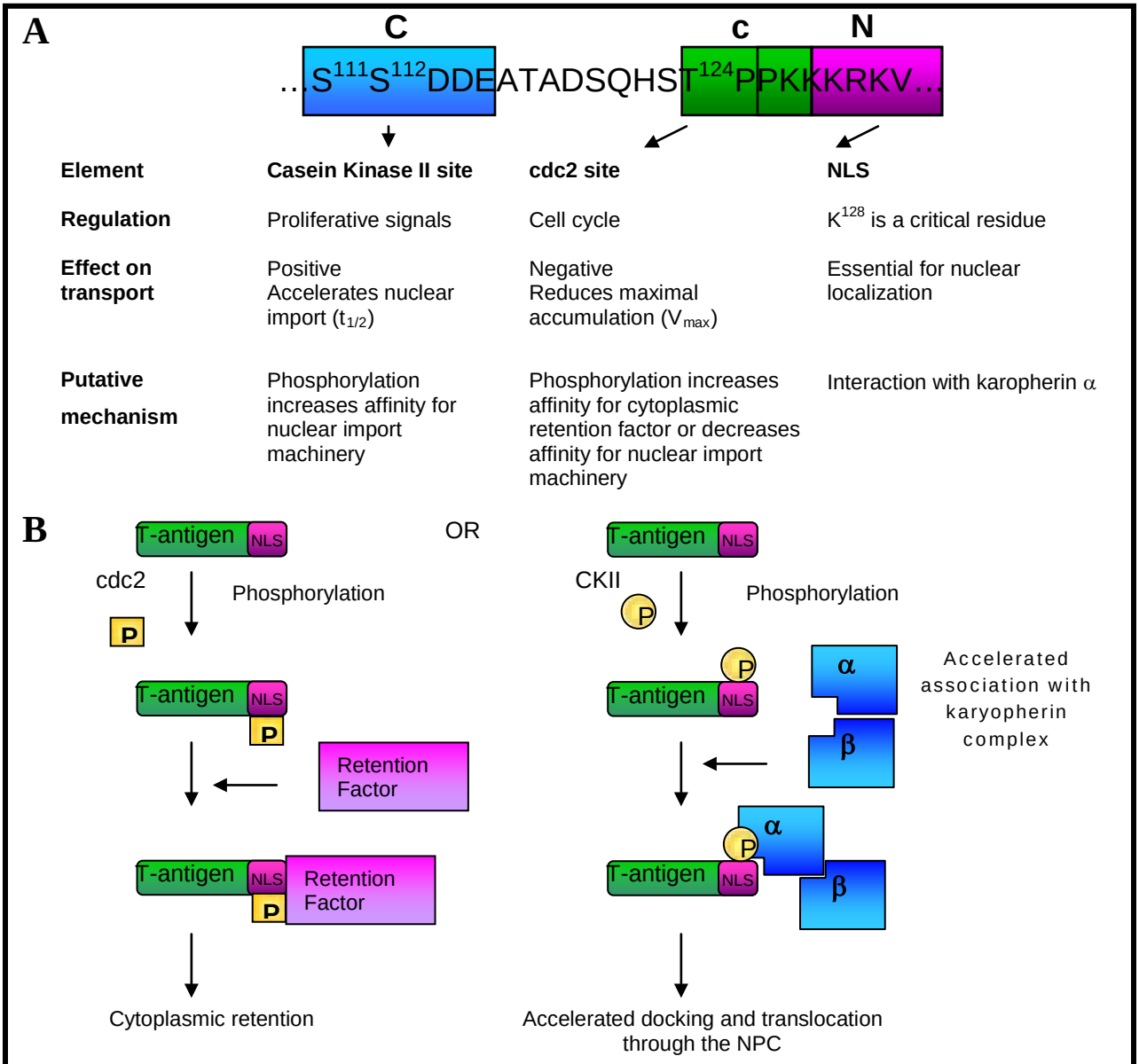

Figure 1.2: SV40 T-antigen nuclear transport is regulated by phosphorylation

(A) Diagrammatic representation of the SV40 T-antigen CcN motif. Single letter amino acid code is used, with phosphorylated residues numbered and CKII (blue box) and cdc2 kinase sites (green box), and NLS (pink box) (Jans and Hübner, 1996). (B) The regulatory mechanism of nuclear transport of SV40 T-antigen. Phosphorylation by cdc2 kinase results in the cytoplasmic retention of T-antigen, probably through increasing affinity for a cytoplasmic anchor protein. Phosphorylation at the CKII site increases nuclear import rate, probably by increasing the kinetics of docking at the nuclear envelope/NPC and regulating interactions with the karyopherin complex (Jans and Hübner, 1996).

1.1.10 Nuclear localization of cell cycle components

In order to understand the link between nuclear localization of karyophilic proteins and the cell cycle machinery, it may be useful to compare the nuclear localization mechanisms used by the cell cycle machinery, to those used to effect conventional nuclear transport. Most cdc2 kinase/cyclin complexes are required to be localized in the nucleus when active in order to effect reversible phosphorylation of nuclear proteins, a requirement for both DNA replication and entry into mitosis. Consequently, most cyclin-dependent kinase/cyclin complexes are localized to the nucleus when active. These complexes however lack obvious nuclear localization sequences. Nuclear import machinery recognizes these cdk/cyclin complexes through direct interactions with the cyclin component. Cyclin E behaves like a classical basic nuclear localization sequence-containing protein, binding to karyopherin-α. In contrast, cyclin B1 is imported via a direct interaction with a site in the NH_2 terminus of karyopherin-β that is distinct from that used to bind karyopherin-α (Moore *et al.,* 1999). Cyclin B1, which accumulates in the cytoplasm during S and G2 phases, translocates to the nucleus before nuclear envelope breakdown during prophase (Ookata *et al.,* 1992). This cytoplasmic localization of cyclin B1 in interphase is directed by its NES-dependent transport mechanism. Expression of a NES-disrupted derivative of cyclin B1 in mammalian cells is able to override the DNA damage-induced G2 checkpoint, suggesting a role for the NES-dependent cytoplasmic localization of cyclin B1 in the DNA damage-induced checkpoint (Toyoshima *et al.,* 1998). The phosphorylation in the region of the NES of cyclin B1 plays a regulatory role in the mediation of the nuclear localization and hence biological activity of cyclin B1. Nuclear localization of Cyclin B1 controls mitotic entry after DNA damage (Jin *et al.,* 1998). Nuclear targeting of cyclin B1 occurs in G2 arrest caused by DNA damage, where it greatly reduces the damage-induced G2 arrest. Thus, nuclear targeting of cyclin B1 contributes to the control of mitotic entry and exit in human cells. The control of the subcellular localization of cyclins plays a key role in regulating the biological activity of cdk-cyclin complexes (Li *et al.,* 1997).

1.2 THE CELL CYCLE

1.2.1 Cyclin-dependent protein kinases and cyclins

The cell cycle is ordered into dependent pathways such that the initiation of late events is dependent on the completion of early events. The cell cycle is composed of four phases: the gap before DNA replication (G1), the DNA synthetic phase (S), the gap after DNA replication (G2), and the mitotic phase which culminates in cell division (M) (Alberts *et al.*, 1994). The cell cycle is controlled by cyclin-dependent protein kinases (cdk's, also known as cdc's) and cyclins. Cdks induce downstream processes by phosphorylating serine and threonine residues on selected proteins (Alberts *et al.*, 1994). Cyclins bind to cdks or cdc2 proteins and control their ability to phosphorylate appropriate target proteins (Alberts *et al.*, 1994). The cyclic assembly, activation, and disassembly of cyclin-cdk/cdc complexes are the pivotal events driving the cell cycle (Figure 1.3). There are two main classes of cyclins: mitotic cyclins, which bind to cdk/cdc proteins during G2, and are required for entry into mitosis, and G1 cyclins, which bind to cdk/cdc proteins during G1 and are required for entry into S phase (Alberts *et al.*, 1994). These cdk/cyclin complexes are regulated by metabolites. Important metabolites in the regulation of cell proliferation are sphingolipids, which inhibit protein kinase C, activate cellular kinases, and stimulate DNA synthesis and cell division in quiescent cultures (Rani *et al.,* 1995). Steroids have been found to regulate transcription of early genes, cell cycle-controlling genes and cyclin-dependent kinase activity (Planas-Silva and Weinberg, 1997). Non-transcription action of oestradiol and progestin play a major role in cell cycle progression (Castoria *et al.,* 1999).

1.2.2 cdc2 kinase and cell cycle checkpoints

In yeast, the best characterized transitions are those from G1 to S phase, and from G1 to mitosis, which are monitored by checkpoints (cell cycle control mechanisms) such as DNA replication in the case of mitosis (Hartwell and Weinert, 1989).

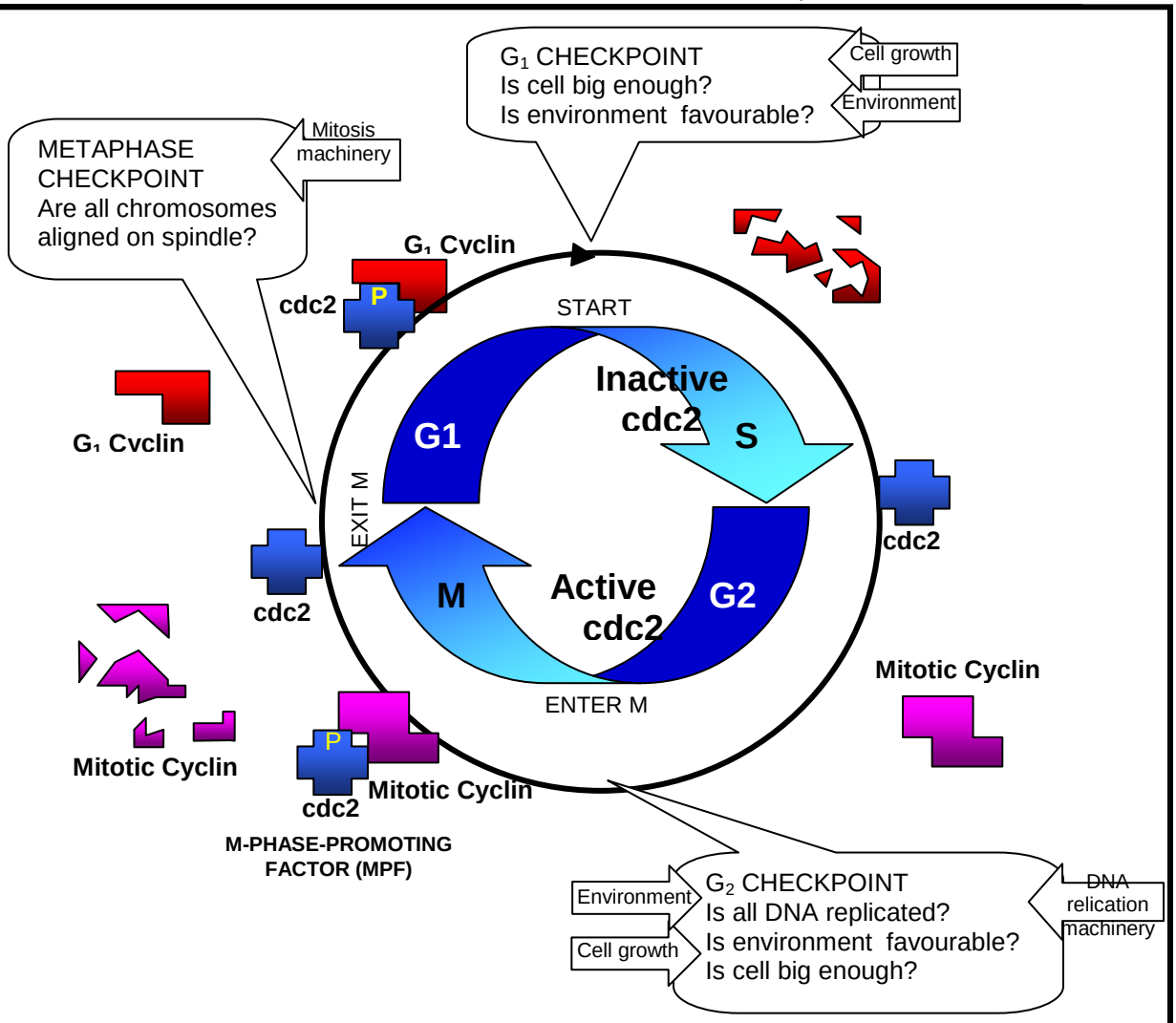

Figure 1.3: cdc2 kinase associates with different cyclins in yeast.

Cdc2 kinase is permanently present, but its state of association with cyclins changes, defining the division - cycle phase of the cell. The subunits of the cdc2 kinase in yeast are similar to those in vertebrates, however, vertebrates have many more different cyclin genes and many different *cdc2* genes. Their products also act in different combinations at different stages of the cell cycle. Cyclins A and B in vertebrates are thought to be the functional equivalent of the mitotic cyclin in yeast and cyclin E is thought to be the functional equivalent of the G_1 cyclin in yeast (Alberts *et al.*, 1994).

Mitotic cyclin accumulates gradually during G2, and binds to the cdc2 subunit to form the M-phase-promoting factor (MPF) (Figure 1.3). MPF is a heterodimer (Labbé *et al.*, 1989) containing regulatory and catalytic subunits. The catalytic subunit (cdc2 subunit) is homologous to the mammalian cdc2 kinase (Hartwell and Weinert, 1989). This complex is activated by phosphorylation, and propels the cell into mitosis. MPF is inactivated by the degradation of mitotic cyclin at the metaphase-anaphase boundary, enabling the cell

to exit from mitosis (Alberts *et al*., 1994). In yeast, passage through both G1 and G2 checkpoints is regulated by the same protein kinase, the product of the *cdc28* or *cdc2+* gene for *Saccharomyces cerevisiae* or *Schizosaccharomyces pombe* respectively. Previously it was thought that inhibition of DNA synthesis triggers down-regulation of cdc2 kinase activity. However, the mechanism for cell-cycle arrest in response to incomplete DNA synthesis is not dependent on the attenuation of cdc2 kinase activity (Knudsen *et al.,* 1996).

In mammalian cells there are at least two different cdk proteins, one for each checkpoint. Multi-cellular eukaryotes have developed a higher degree of regulation. They express multiple cyclins, like yeast, but also contain multiple catalytic subunits that interact with these cyclins. Whereas cdc2 kinase is active and essential at the G2/M transition, a closely related kinase, $p33^{cdk2}$, has been implicated in the initiation of DNA replication (van den Heuvel and Harlow, 1993). Twelve human protein kinases have been described that share extensive amino acid sequence identity with cdc2 kinase (van den Heuvel and Harlow, 1993). They are often named temporarily according to their amino acid sequence in the PSTAIRE-region, a domain that is conserved between yeast and human cdc2 kinase. Alternatively they are designated as cyclin-dependent kinases either when a cyclin partner is identified, or when they complement yeast *cdc2-cdc28* mutations. In mammalian cells, cdc2 kinase associates mainly with A- and B-type cyclins; cdk2 associates with cyclins A, E, and D; and cdk4 (formerly PSK-J3), cdk5 (previously PSSALRE), and cdk6 (previously PLSTIRE) associate with D-type cyclins (van den Heuvel and Harlow, 1993). In mammalian cells, progression through the G1 phase initially depends on holoenzymes composed of one or more of the D type cyclins (D_1, D_2, and/or D_3), in association with either cdk4 or cdk6 (Sherr and Roberts, 1995). This step is followed by the activation of the cyclin E- and A- cdk2 as cells approach the G1/S transition (Sherr and Roberts, 1995). Kip proteins control both assembly and disassembly of different cyclin-cdk complexes. The Kip proteins $p21^{Cip1}$, $p27^{Kip1}$, and $p57^{Kip2}$, positively regulate cyclin D-cdk complex assembly, and remain bound to catalytically active cyclin D-cdk complexes. However, if cyclin D_1 transcription is inhibited, the turnover of this protein is accelerated, leading to the rapid disassembly of cyclin D-cdk

complexes and to the release of Kip proteins from this latent pool. When released from cyclin D-cdk complexes, $p21^{Cip1}$, $p27^{Kip1}$ and $p57^{Kip2}$ act as potent inhibitors of cyclin E-cdk2 and cyclin A-cdk2, thus preventing S phase entry and resulting in G1 phase arrest, usually within a single cell cycle (Brewer *et al.,* 1999).

1.2.3 cdc2 kinase phosphorylates CKII

CKII is a widely distributed cyclic-AMP-independent kinase that phosphorylates serine and threonine residues, which are followed by several consecutive acidic amino acid residues (Dingwall and Laskey, 1991). This ubiquitous kinase phosphorylates a broad spectrum of endogenous substrates and has been implicated in cell division and differentiation. The cdc2 kinase phosphorylates CKII, increasing CKII activity up to five-fold, suggesting that CKII could be regulated during cell division by cdc2 kinase and could mediate some of the pleiotropic effects of the MPF. CKII activity parallels the changes of mitotic cdc2 kinase activity through the cell cycle. CKII activity increases 10-fold during G2/M transition, and decreases at interphase. cdc2 kinase drives cells to mitosis by triggering activation of a protein kinase cascade which is accelerated by CKII (Mulner-Lorillon *et al.*, 1988).

1.2.4 Chaperones and cell cycle regulation

Many studies have indicated that chaperones and stress proteins are involved in the regulation of cell growth and transformation. In general, the level of chaperones or stress proteins is increased in proliferating cells compared to those in the stationary state or differentiated cells (Sainis *et al.,* 1994; Helmbrecht and Rensing, 1999). Cell cycle components, regulatory proteins and members of the mitogenic signal cascade associate with chaperones and stress proteins for different periods of time. Chaperones are localized in different cell compartments and assist newly synthesized proteins to fold or translocate through membranes, stabilize certain protein conformations and help to eliminate denatured proteins by way of degradation (Becker and Craig, 1994; Hartl, 1996). Chaperones also play a role within the regulatory network of the cell cycle and

within signal cascades. The cell cycle and its control processes can be upset by stress as induced by external factors such as heat shock, irradiation, toxic substances, by reactive oxygen species, viral infections and other perturbations. Stress also affects the mitogen-activated signal cascade and alters its signalling drastically (Helmbrecht *et al.,* 2000). The accumulation of improperly folded proteins triggers a stress response that represses overall protein synthesis and causes cell cycle arrest. This cell cycle arrest is due to a decrease in cyclin D_1 translation, decreasing in cyclin D- and E-dependent kinase activities and resulting in G1 phase arrest (Brewer *et al.*, 1999).

1.2.4.1 Heat shock protein 90 (Hsp90) and the cell cycle

The cytosolic chaperone Hsp90 acts as a dimer and forms complexes with protein kinases and transcription factors with the function of chaperoning the partner protein to its ultimate location, assisting in its conformational maturation and/or stabilising its conformation (reviews: Scheibel and Buchner, 1997b; Beissinger and Buchner, 1998). The expression of Hsp90 is cell cycle regulated with Hsp90a mRNA accumulating during the G1/S transition (Jérôme *et al.,* 1993), and inhibition of Hsp90 function causes G1/S arrest (Srethapakdi *et al.,* 2000, Basso *et al.,* 2002). Paradoxically, exogenous expression of Hsp90 also causes a decrease in cell growth and an arrest at the G1/S transition (Zhao *et al.,* 2002), implying the function of Hsp90 during G1/S to be highly regulated. In addition to the chaperone activity of Hsp90, there is evidence of an interaction between Hsp90 homologs and the cell cycle machinery. Hsp90 associates with and affects the assembly of telomerase, the polymerase enzyme responsible for maintaining telomeric DNA during the cell cycle (Forsythe *et al.,* 2001). Hsp75, an Hsp90 homolog, has been identified as a pRB binding protein (Chen *et al.,* 1996a) and cell cycle regulators Wee-1 and CDKs are chaperoned by Hsp90 (Aligue *et al.,* 1994). The homolog of Hsp90, SWO1, also co-immunoprecipitates with Wee1 (Alique *et al.,* 1994). Wee-1 is a protein kinase that regulates the length of the G2 phase by carrying out the inhibitory tyrosyl phosphorylation of cdc2 kinase-cyclin B kinase.

The association of Hsp90 with cdks requires other chaperones such as p23 and cdc37, which together stabilize cdks and inhibit kinase activity (Stepanova, 1996). The cdc37 protein is a chaperone involved in chaperoning protein kinases together with Hsp90 , and binds to Hsp90 (Abbas-Terki *et al .,* 2000) regulating the ATPase activity of Hsp90 (Siligard *et al.,* 2002). Cdc37 in *Saccharomyces cerevisiae* is required for the start event of the cell division cycle (Reed, 1980) , for cyclin dependent kinase activation and functions in signal transduction (Kimura *et al*., 1997), and for chromosome segregation and cytokinesis in high eukaryotes (Lange *et al.,* 2002). In addition, cdc37 interacts with CKII (McCann and Glover, 1995) and acts as a molecular chaperone specifically on cell cycle protein kinases, directing them to Hsp90 (Kimura *et al.,* 1997). The yeast cell cycle kinase cdc28 (Mort-Bontemps-Soret *et al .,* 2002) is the functional equivalent of mammalian cdc2. Furthermore, genetic interactions between Hsp90 and cdc2 mitotic machinery have been found (Muňoz and Jimenez, 1999). Down-regulation of Hsp90 could change cell cycle distribution and increase drug sensitivity of tumor cells (Lui *et al.,* 1999).

1.2.4.2 Hsp70 and the cell cycle

Tumorigenic cells depend on the constitutive high expression of the anti-apoptotic chaperone Hsp70 to suppress death (Nylandsted *et al .,* 2000). Hsc73, a constitutive member of the Hsp70 family is directly associated with pRB, a major regulatory molecule of the cell cycle (Inoue *et al .,* 1995). Specifically, Hsc73 binds to nonphosphorylated pRB. The Hsc73/Hsp40 complex may therefore act as a molecular chaperone for the active form of pRB, which in turn could act as a suppressor molecule of the cell cycle. The stress-induced translocation of Hsc73 into the nucleus may also increase the probability of rescuing active nuclear pRB from stress-induced denaturation and degradation. In fact, heat shock induces cell-cycle specific regulation of Hsp70 (Hang and Fox, 1995). An increase of Hsp70, or Hsc70 mRNA and protein, occurs in S-phase (Milarski and Morimoto, 1986; Zeise *et al.,* 1998; Hunt *et al.,* 1999; Helmbrecht and Rensing, 1999). During this increase, a translocation of Hsp70, or Hsc70, into the nucleus during S-phase has also been observed (Zeise *et al.,* 1998). In some cell lines the

expression of Hsp70 is suppressed by treatment with the inhibitor of DNA synthesis AraC (Milarski and Morimoto; 1986; Hang and Fox, 1995), indicating a potential involvement of Hsp70 in DNA replication, which occurs in the S-phase. Hsp73 also interacts with $p27^{Kip1}$, an inhibitor of cdks, during the G1/S transition (Nakamura *et al*. 1999). Hsp70 is also required for cdc2 kinase activity (Zhu *et al.*, 1997).

1.2.4.3 Co-chaperones and the cell cycle

There is increasing evidence of interaction between cell cycle components and co-chaperones. FKBP12 has a regulatory role in the cell cycle by downregulating TGFβ receptor signaling (Aghdasi *et al*., 2001). FKBP12 deficient mice manifested cell cycle arrest in the G1 phase (Aghdasi *et al*., 2001). Phosphorylation of murine Hsp25 and human Hsp27 by MAPKAP kinase 2 (Stokoe *et al.*, 1992), heat shock transcription factor 1 (HSF1) by cdc2 kinase (Reindl *et al.*, 1997), and Hsp90 (Shi *et al.*, 1994), calnexin (Ou *et a.l*, 1992) and the immunosuppressant FK506-binding protein 52 (FKBP52) (Miyata *et al.*, 1997) by CKII, has been reported. Phosphorylation of Hsp28 may be coupled to the inhibition of DNA synthesis in mouse osteoblastic MC3T3-E1 cells (Shibanuma *et al*., 1992). Co-chaperones Bag1, Hop and Hsp40 regulate Hsc70 and Hsp90 interactions with wild-type or mutant p53 (King *et al.,* 2001). The cdc37 co-chaperone, which regulates the ATPase activity of Hsp90 (Siligard *et al.,* 2002), has been found to interact with cdc28 in *Saccharomyces cerevisiae* (Mort-Bontemps-Soret *et al*., 2002).

The exact details of the role of chaperones in the cell cycle are not yet fully understood. Stress such as heat shock or oxidative stress, upsets many cellular processes including the cell cycle, which is arrested mainly at the G1/S and the G2/M transitions (Kühl and Rensing, 2000). After cells have responded to stress through an increased synthesis of Hsps, they reach a state of acquired thermotolerance, where they are less sensitive to further stress exposures. This is also true for heat shock effects on the cell cycle (Kühl *et al.,* 2000), a result that supports the idea of a stabilizing role of Hsps/chaperones for cell cycle processes. Increased amounts of Hsps apparently counteract the effects of stress on regulatory cell cycle proteins as well as on basic cell cycle-sustaining processes

(Helmbrecht *et al*., 2000). The roles of Hsp70 and Hsp90 in cell cycle control known so far appear to be that of either a molecular stabilizer of cell cycle suppressors or an inhibitor of cell cycle accelerators. This evidence may explain the molecular mechanism of growth suppression induced by stress conditions (Sato and Torigoe, 1998). Chaperones may have an essential function in the initiation of DNA replication by stabilizing parts of the DNA replication pre-initiation complex. Chaperones may also have an auxiliary role in stabilizing the conformation of active/inactive forms of essential cell cycle or signal cascade proteins such as Cdk4, pRB (retinoblastoma protein), p27, Wee-1, Src and Raf. An alternative auxiliary function may be the chaperoning of DNA initiation factors and the transcription factors such as E2F to the nucleus or in the transport of cell cycle inhibitors to the degradation machinery (Helmbrecht *et al.,* 2000).

1.3 HEAT SHOCK PROTEINS

1.3.1 *In vitro* protein folding

The folding of a newly synthesized polypeptide is an intrinsic feature of its primary amino acid structure. However, most polypeptides quickly collapse into a compact "molten globule" *in vitro* (Jaenicke, 1991), despite favourable *in vitro* folding conditions, of low protein concentration (limiting inter-polypeptide aggregation) and low temperatures (attenuating hydrophobic interactions) (Jaenicke, 1991). The molten globule possesses extensive native-like secondary structure, unstable disulphide bonds, and exposed hydrophobic groups, which may lead to aggregation. *In vivo* intracellular conditions consist of higher temperatures and protein concentrations, which in principle lead to less favourable folding conditions (Georgopoulos and Welch, 1993).

1.3.2 *In vivo* protein folding

Polypeptide chains emerging from the ribosomes, may be subjected to premature interactions with other intra- or inter-polypeptide domains, leading to misfolding and aggregation (Georgopoulos and Welch, 1993, Jaenicke, 1991). Proteins collectively referred to as chaperones bind to the reactive surfaces of polypeptides. Such reactive surfaces often constitute the hydrophobic surfaces exposed by the molten globule intermediates of various proteins (Creighton, 1988). Chaperones function by sequestering these reactive surfaces from others present in their vicinity, thereby favouring proper folding pathways by preventing aggregation. This occurs with neither covalent modification of the substrate polypeptide by the chaperone, nor inclusion of the chaperone in the final product (Creighton, 1988). As high temperatures favour protein unfolding and hydrophobic interactions, the need to prevent protein aggregation *in vivo* increases on heat shock, as both nascent and mature polypeptides begin to partially unfold and/or aggregate (Georgopoulos and Welch, 1993). Many members of the heat shock protein (Hsp) family have been reported to exhibit chaperone-like properties, while many chaperones are expressed at increased levels after heat shock (Welch, 1991). Most

Hsps are constitutively expressed in normal cell physiology (cognates), their molecular chaperone function being essential for normal cell growth. Hsps regulate the heat shock response, assembling/disassembling structures, to provide a molecular shuttle service for polypeptides by chaperoning in tandem (Hightower, 1991). Cellular proteins are thus maintained in a refolding competent state for "resurrection" during recovery after heat shock (Skowyra *et al.*, 1990).

The heat shock response can be induced by a broad variety of stressors besides heat. Such stressors include amino acid analogs, puromycin, ethanol, heavy metal ions, arsenicals, tissue explantation and infection by certain viruses (Hightower, 1991). Glucose deprivation, exposure to glycosylation inhibitors and Ca^{2+} ionophores (agents that perturb calcium homeostasis), result in the glucose-regulated proteins which are also considered as stress proteins (Hightower, 1991). The accumulation of abnormally folded proteins induces the heat shock response (Hightower, 1980), as supported by the adverse effect heat has on protein conformation, the effect of the antibiotic puromycin (which results in the premature release of nascent polypeptide from the translation machinery), and the short half-lives of proteins containing amino acid analogues (Hightower, 1980). Injection of a collection of denatured proteins into living cells also increased the expression of Hsps (Ananthan *et al.*, 1986).

1.3.3 Subcellular localization of chaperone-mediated protein folding

In the presence of heat shock protein 70 (Hsp70), heat-unfolded nuclear luciferase accumulated in foci in the nucleoli. This translocation required Hsp70 chaperone activity, indicating that Hsp70 is involved in holding heat-unfolded nuclear proteins and translocating them to the nucleolus during stress. This prevents indirect damage to other nuclear components (Nollen *et al.* 2001). Under normal conditions, Hsp70 is localized in the cytoplasm, however during heat stress, Hsp70 translocates to the nucleus and the nucleolus, from which it retracts during recovery (Welch and Suhan, 1986). This movement of Hsp70 could be associated with repair of heat-induced nucleolar damage

(Pelham, 1984), as the nucleolus is especially sensitive to heat. Upon heat shock, nucleoli become swollen and small granules present in normal nucleoli become large electrodense structures. Nucleolar processes, such as ribosomal RNA synthesis and assembly of ribosomal precursor particles, are inhibited (Welch and Suhan, 1986). The nucleolar morphological changes observed during heat shock are due to translocation of unfolded nonnuclear proteins to the nuclei. This reduces random aggregation and damage of other cellular components, interfering with the assembly of ribosomes essential for protein synthesis (Nollen *et al.,* 2001). In the cytosol, misfolded or heat-unfolded proteins are transported to the proximity of the centrisome for degradation by the proteosome (Garcia-Mata *et al.,* 1999; Johnston *et al.,* 1998; Vidair *et al.,* 1996; Wigley *et al.,* 1999).

1.3.4 Stress and nuclear localization

Stress, such as starvation, ethanol, heat or oxidants have been shown to inhibit specific NLS-dependent nuclear import (Stochaj *et al.,* 2000). This may be due to a collapse in the nucleocytoplasmic concentration gradient of Gsp1p (Ran) (Stochaj *et al.,* 2000). During the stress of viral infection, interferon regulatory factors (INFs) are mobilized from the cytoplasm to the nucleus to induce expression of interferon. INFs contain a conserved bipartite NLS and NES (Lau *et al.,* 2000). During DNA damage, the DNA-dependent protein kinase (DNA-PK) complex is involved in the repair of DNA double-strand breaks by physically protecting the broken ends of DNA from degradation. This DNA repair kinase transports to the nucleus by a bipartite NLS, which is recognized by karyopherin (Koike *et al.,* 1999). The nuclear chaperone nucleoplasmin enters the nucleus via its functional NLS in order to mediate the assembly of nucleosomes (Shackleford *et al.,* 2001) and centrisome duplication (Okuda *et al.,* 2000). Hsc70 co-localizes with karyophilic proteins into the nucleus during their transport *in vitro* (Okuno *et al.,* 1993). In mammalian cells cytosolic Hsc70 is involved in the transport of proteins to lysosomes (Chiang *et al.,* 1989), to mitochondria (Sheffield *et al.* 1990) and to the nucleus (Shi and Thomas, 1992).

1.3.5 Chaperone folding machinery

1.3.5.1 Heat shock protein 90 (Hsp90)

The major chaperone Hsp90 constitutes up to 1-2% of cellular protein under physiological conditions, and is upregulated under stress (Yonehara *et al*., 1996). Members of the Hsp90 family have been found in the cytosol, the endoplasmic reticulum and chloroplasts (Scheibel and Buchner, 1997b). Although isoforms of Hsp90 have interchangeable functions (Borkovich *et al*., 1989), the respective genes are differentially regulated. In most eukaryotic cells, one of the two cytosolic members is expressed constitutively at a high level at physiological temperatures and is induced only two to three times more by heat shock. The second Hsp90 gene is expressed at a low basal level at normal temperatures, but expression is enhanced strongly under restrictive growth conditions like heat treatment (Borkovich *et al*, 1989, Krone *et al*, 1994). The structure of the N-terminal domain of Hsp90 consists of nine helices and an anti-parallel β-sheet of eight strands that fold into an α-β sandwich (Prodomou *et al*., 1997). The tertiary fold of the N-terminal domain of Hsp90 is similar to the N-terminal ATP-binding fragment of the bacterial type II topoisomerase, DNA gyrase B protein (Wigley *et al*., 1991). Hsp90 contains two independent chaperone sites, which differ in substrate specificity and nucleotide dependence (Scheibel *et al*., 1998). The native protein is a flexible elongated dimer, the association sites of which lie in the extreme C-terminal region of the protein (Buchner, 1999). Recently, Hsp90 has been proposed to be a capacitor for phenotypic variation by buffering the release of genetic variation (Queitsch, *et al*., 2002). Also, the chaperone function of Hsp90 may be regulated by phosphorylation (Zhao *et al*., 2001)

1.3.5.2 Heat shock cognate/protein 70 (Hsc/Hsp70)

Hsp70 has been characterized in bacteria (DnaK), in yeast (Ssa and Ssb) and in higher eukaryotes (Table 1.1). Hsp70 interacts with the nascent polypeptide chain as it emerges from the ribosome (Georgopoulos and Welch, 1993) and for some proteins, the activity of the Hsp70 chaperone is sufficient for folding (Georgopoulos and Welch, 1993). Hsp70s are composed of a highly conserved 44 kD a N-terminal nucleotide-binding domain, a less well conserved 18 kDa peptide-binding domain, and a C-terminal 10 kDa

variable domain of unknown function (James *et al.*, 1997). The nucleotide-binding domain contains an ATPase site (Flahery *et al.*, 1990). The ATPase activity is weak, 0.1 to 1.0 ATP molecules hydrolyzed per minute per monomer (Georgopoulos and Welch, 1993). The Hsp70's bind short, extended peptide segments of seven or eight residues, which are enriched in hydrophobic amino acids (Flynn *et al.*, 1991, Blond-Elguindi *et al.*, 1993). Through a cycle of ATP binding, hydrolysis and nucleotide exchange, denatured proteins are alternately bound to Hsp70 and released to effect protein folding (Hartl, 1996). Substrates bind transiently to the ATP-bound form of Hsp70, but when ATP is hydrolysed, the binding is stabilized (Greene *et al.*, 1995).

Table 1.1: The Hsp70 family of proteins contains many members

Hsp70 Family	Name	Locale	Size (kDa)	Comments
Bacteria	DnaK	Cytosol	70	Mutants grow poorly, constitutive / inducible
Yeast	Ssa1-4	Cytosol	70	Multiple members, essential family
	Ssb1-2	Cytosol	70	Multiple members, mutants - cold sensitive
	Pdr13p		70	Binds ribosomes
	Ssc	Mitochondria	70	Essential for viability
	Kar2	ER	70	Essential for viability
Mammalian	Hsc70	Cytosol / nucleus	70	Constitutive
	Hsp70	Cytosol / nucleus	70	Stress - inducible
	Grp75	Mitochondria	75	Most homology to DnaK
	Hsp70	Chloroplasts	70	Constitutive
	Grp78 (BiP)	ER	78	ADP - ribosylated

(Georgopoulos and Welch, 1993, Frydman, 2001)

1.3.6 The assembly of the glucocorticoid receptor (GR) by the Hsp90-based chaperone system

Many co-chaperones have been reported to interact with Hsp90 and Hsp70 (Table 1.2), modifying their functions within heterocomplex structures (Chen *et al.*, 1996b). The importance of Hsp90 is demonstrated by its abundance in all species with a remarkable 40% amino acid identity from *E. coli* to humans (Lindquist and Craig, 1988, Johnson *et al.*, 2000). Although a number of cell-signalling proteins such as kinases and steroid

receptors require Hsp90 function to reach their active state within the cell, Hsp90 does not act alone and requires the aid of several co-chaperone proteins (Buchner, 1999).

The interaction of Hsp90 with its co-chaperones had been studied most extensively in the assembly of steroid receptor complexes (DeFranco, 2002). The assembly of steroid complexes is relevant to the study of progressive central nervous system (CNS) neurodegenerative diseases such as Huntington's disease, caused by abnormal polyglutamine tract expansion in the androgen receptor (AR) gene. Activation of the wild-type GR suppressed the aggregation of expanded polyglutamine proteins derived from these diseased systems and controlled their cellular effects of nuclear localization and cellular toxicity (Welch and Diamond, 2001).

The GR forms a complex with chaperones Hsp90 and Hsp70, and co-chaperones Hop, Hsp40 and p23, resulting in the hormone-binding domain of the receptor being converted to its high affinity steroid binding state (Murphy *et al*., 2001). Some groups report the association of these co-chaperones in this complex to optimise assembly of the GR (Dittmar and Pratt, 1997; Murphy *et al*.,2001, Johnson *et al*., 2000), while others report only Hsp70 and Hsp90 to be necessary to activate hormone binding by GR (Rajapandi *et al.,* 2000). Morishima *et al*. (2000a) found that although Hop is not required for the formation of the GR-Hsp90 heterocomplex assembly, it enhances the rate of the process. Hop binds independently to both Hsp70 and Hsp90, to produce the Hsp70/Hop/Hsp90 chaperone complex, which is sufficient (Dittmar and Pratt, 1997) and necessary to bind specifically to the GR (Kaul *et* al., 2002), and open the GR steroid-binding site (Murphy *et al.,* 2001) for access by steroid. The stoichiometry of association of Hsp90:Hop:Hsp70 is 2:1:1 (Murphy *et al.,* 2001). Under hypothermic stress conditions, both constitutive and inducible forms of the Hsp70 protein associate in this GR-Hsp90 heterocomplex (Cvoro and Matic, 2002). However, stressor-induced Hsp70 accumulation, above normal Hsc70 levels, may impair glucocorticoid-dependent metabolic adjustments (Boone *et al.,* 2002).

The first step to assembly of the GR activating complex is the ATP-dependent and Hsp40-dependent binding of Hsp70 to the GR, priming the receptor for subsequent ATP-

dependent activation by Hsp90, Hop, and p23 (Figure 1.4). The ATP-bound form of Hsp70 is predicted to interact initially with the GR and is then converted to the ADP-dependent form with high affinity for hydrophobic substrate (Morishima *et al.,* 2000b). The GR-Hsp70 complex (initial complex) rapidly binds Hsp90 in a nucleotide-independent manner, which is Hop-dependent (intermediate complex). The N-terminal ATP-binding site of Hsp90 is required for the subsequent rate limiting ATP-dependent opening of the steroid binding cleft (Kanelakis *et al.,* 2002), such that the hydrophobic binding form of Hsp90 must be converted to its ATP-dependent conformation for the pocket of the GR to be accessible by steroid (Morishima *et al.,* 2000b). As the steroid receptor progresses to the mature receptor, more Hsp90 enters the complex while Hsp70 and Hop levels decrease. The mature receptor is characterized by the appearance of p23 (mature complex), which stabilizes the ATP-dependent conformation of Hsp90 (Dittmar *et al.,* 1997), and one of the three large immunophilins FK506 binding proteins: FKBP51, FKBP52 or Cyp40. These complexes have also been found in the absence of substrate protein, suggesting the existence of pre-assembled multiprotein complexes (Johnson *et al.,* 2000).

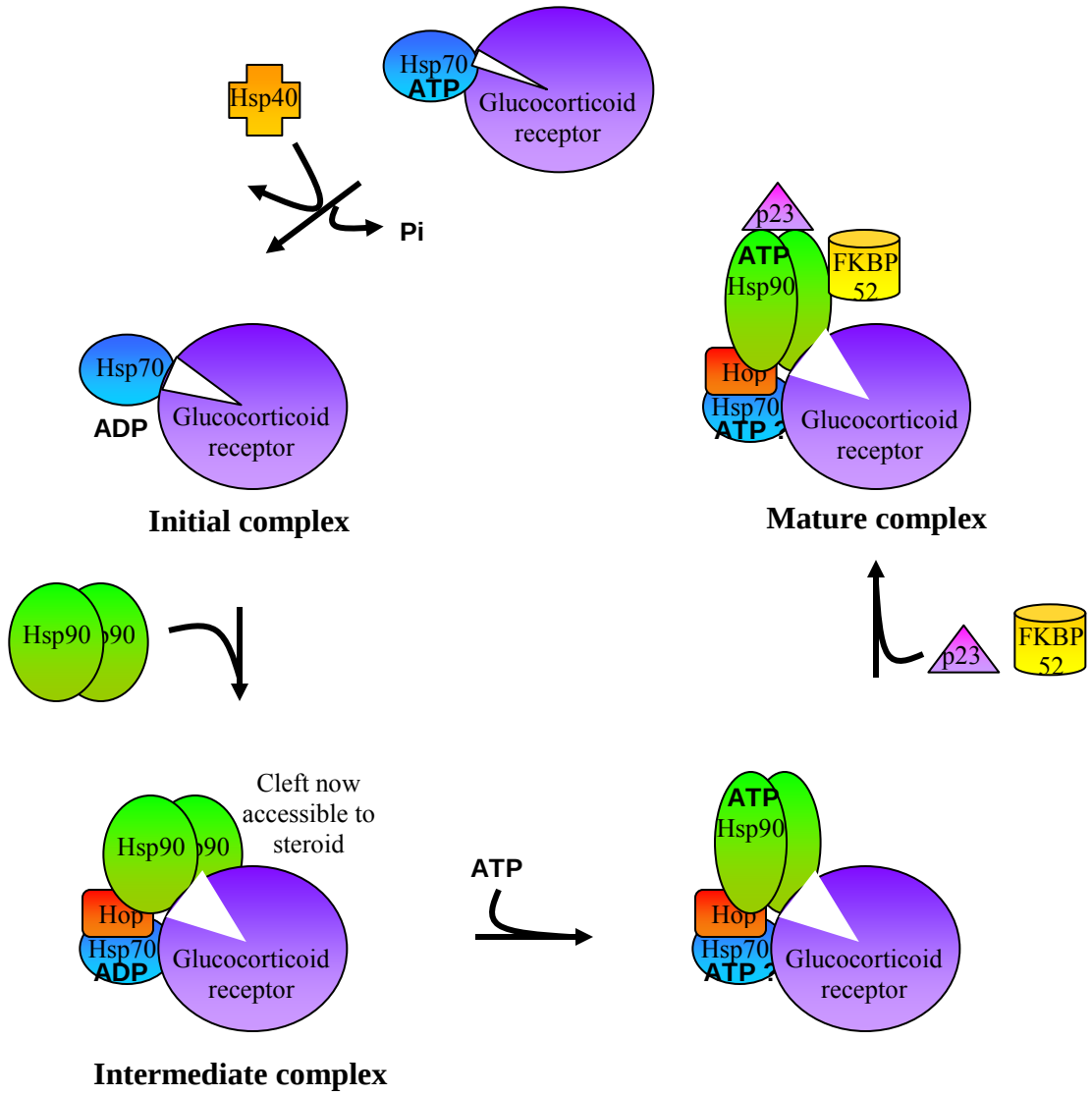

Figure 1.4: The stepwise assembly of the GR-Hsp90 heterocomplex.

A graphical representation of the assembly of the GR. The initiation of the pathway involved Hsp40-dependent and ATP-dependent binding of Hsp70 to the receptor. Hop binds independently to Hsp90 and Hsp70. Hsp90 and Hsp70 are necessary for the opening of the steroid-binding cleft. Hop increases the rate of this process, brings Hsp70 and Hsp90 together, and inhibits the ATPase activity of Hsp90. Hsp40 modulates the ATPase activity of Hsp70, increasing the heterocomplex assembly by ensuring that Hsp70 is in the ADP bound state. p23 binds to and stabilizes the ATP-dependent conformation of Hsp90 (Murphy *et al.,* 2001, Morishima *et al.,* 2000a, Hernández *et al.,* 2002).

1.3.7 The movement of the mature GR to the nucleus

Steroid receptors move in and out of the nucleus in a dynamic manner, depending on their hormone bound or unbound state, exerting their effects on cellular physiology through regulating the rate of transcription from unique target genes (DeFranco, 2002). The hormone-free GR-Hsp90 heterocomplex is localized in the cytoplasm of most cells, and after steroid binding it translocates to the nucleus (Picard and Yamamoto, 1987), thought to be through an association with the multiprotein Hsp90-based chaperone system (DeFranco, 2000) and the Hsp90-binding immunophilin FKBP52 (Pratt *et al.,* 1999). This movement to the nucleus requires the ATPase activity of Hsp90, since geldanamycin, an benzoquinone ansamycin that binds to the nucleotide binding site on Hsp90 impedes steroid induced movement of the GR from the cytoplasm to the nucleus (Galigniana *et al.,* 1998). Non-steroidal compounds which bind to the receptor associated proteins have been shown to alter the GR-Hsp90 heterocomplex subcellular localization (Prima *et al.,* 2000), implicating the Hsp90-based chaperone system in receptor transfer to the nucleus. FKBP52 is proposed to target retrograde movement of the GFP-GR along microtubules by linking the receptor to the dynein motor (Galigniana *et al.,* 2001). Dyenin is a cytoplasmic motor protein involved in retrograde transport of vesicles toward the nucleus (Bloom and Goldstein, 1998). The earliest known event in steroid receptor signalling has been identified as immunophilin interchange, of either FKBP51 or FKBP52 (Davies *et al.,* 2002). GR-Hsp90 heterocomplexes in the cytoplasm have been shown to contain dyenin in a manner that is competed by the PPIase (polyproline isomerase) domain of FKBP52 (Galigniana *et al.,* 2001), implicating FKBP52 in targeting the NLS-directed movement of the GR (containing a proto-NLS) along microtubular pathways to the nucleus. FKBP52 binds to Hsp90 via a conserved protein interaction involving tetratricopeptide repeat (TPR) domains. FKBP52 also binds directly to the Hsp90-free GR, and a 35 amino acid segment spanning the proto-NLS of the GR (Pratt *et al.,* 2001)

1.3.8 The tetratricopeptide repeat motif (TPR)

The tetratricopeptide repeat motif (TPR) is a degenerate 34 amino acid sequence repeated in a wide variety of proteins, where it is often present in tandem arrays of 3-16 motifs (Das *et al.,* 1998). These repeats have been found to be packed together in a parallel arrangement to form a regular series of anti-parallel α-helices, defining a right-handed super-helical structure and creating an amphipathic groove suitable for the recognition of target proteins (Das *et al.,* 1998). Such TPR structures form scaffolds, which mediate protein-protein interactions in the assembling of heterocomplexes, many TPR-containing proteins being reported to be associated with multiprotein complexes (Das *et al.,* 1998, reviewed by Blatch *et al.*, 1999). Many of the co-chaperones interacting with Hsp70 and Hsp90 contain TPR motifs, including most of the immunophilins (Owens-Grillo *et al.,* 1996), Hop (Scheufler *et al.,* 2000) and mSTI1 (Blatch *et al.*, 1997, van der Spuy *et al.*, 2000). However, in the case of Hsp90-FKBP52 and Hsp90-Cyp40 binding, the TPR motifs are necessary but not sufficient for protein-protein interaction, since TPR flanking regions in addition to the TPR have been found to be required (Ratajczak and Carrello, 1996). This may be explained if the regions flanking the TPR domain also contain a number of charged residues predominantly localized to a n amphipathic α-helical microdomain in each region (Blatch *et al.*, 1999). Depending on the number of tandem TPR motifs, and hence, the size of the TPR groove generated, a number of multiple simultaneous interactions with target proteins could be accommodated by a single TPR-containing protein (Blatch *et al.*, 1999).

1.3.9 The modulation of Hsp70 and Hsp90 activities by co-chaperones

1.3.9.1 Heat shock 40 (Hsp40) and Bcl2-associated anthogene 1 (Bag1)

Hsp70 function is modulated by members of the heat shock protein 40 (Hsp40) family in higher eukaryotes, Ydj1 in yeast, and DnaJ in bacteria. These proteins are known to

stimulate the ATPase activity and therefore the action of their respective Hsp70s (Cyr *et al.*, 1992, Liberek *et al.,* 1991, Chevalier *et al.,* 2000) since conformation of Hsp70 is affected by its nucleotide binding state. Hsp70 has been shown to bind to the GR as the Hsp70-ATP form (Kanelakis *et al.,* 2002). Hsp40 plays an integral role in this assembly of the GR-chaperone complex, enhancing the binding of Hsp70 to Hop by stimulating the conversion of Hsp70-ATP to Hsp70-ADP, the Hsp70 conformation favoured for Hop binding (Hernández *et al.,* 2002).

Bcl2-associated anthogene 1 (Bag1), initially identified as a anti-apoptotic molecule and binding partner of the cell death inhibitor Bcl2, modulates Hsc70's chaperone activity (Höhfeld, 1998). Bag1 acts as a nucleotide exchange factor in the Hsc70 ATPase cycle, competing with the co-factor Hsp70 interacting protein (Hip) which stabilizes the ADP-bound state of Hsc70. Bag1 is a family of co-chaperones consisting of at least four polypeptides Bag1l, Bag1m/Rap46, Bag1, and p29 (Cato and Mink, 2001). Bag1 negatively regulates the action of the GR possibly by inhibiting the hormone binding activity of the GR or by regulating the trans-activation function of the receptor. Bag1 repress DNA binding by the GR in a process that requires prior binding of Hsp70 to the receptor (Cato and Mink, 2001).

The co-operative assembly of large multi-component chaperone complexes like the Hsp90-based chaperone system (Table 1.2), has recently been suggested to promote a disassembly of transcriptional regulatory complexes, thus enabling regulatory machineries to detect and respond to signalling changes (Freeman and Yamamoto, 2002). Such a disassembly activity of the chaperones would contribute to the rapid inactivation of the receptors upon hormone withdrawal (Young and Hartl, 2002).

Table 1.2: Many molecular co – chaperones interact with Hsp90 and Hsp70

Class	Members	Alternative names	Associated proteins	Comments
Immunophilins	FKBP51 FKBP52 FKBP54 CyP40	 Hsp56	Hsp90	Binding between immunophilins to Hsp90 is competitive (Ratajczak *et al.,* 1993, Owens - Grillo *et al.*, 1996)
p60	Hop mSTI1 STI1	STI1	Hsp90 and Hsp70	Functions as physical links between Hsp90 and Hsp70 (Johnson *et al*, 1998)
p48	p48	Hip	Hsp70	Interacts with the ATPase domain of Hsp70 in a manner dependent on Hsp40 (Owens - Grillo *et al.*, 1996)
p23	p23	-	Hsp90	Binds efficiently to non - native protein (Owens - Grillo *et al.*, 1996)
Hsp40	DnaJ, Ydj1, Hdj1	DnaJ	Hsp70	Modulates ATPase activity of Hsp70 (Owens - Grillo *et al.*, 1996)
Cdc37	Cdc37	p50 Cdc37p	Hsp90	Kinase - specific co - factor (reviewed by Buchner, 1999)
PP5	PP5	-	Hsp90	Protein - serine phosphatase (reviewed by Buchner, 1999)
Bag1	Bag1-5	-	Hsp70	Functions as a nucleotide exchange factor in the Hsc70 ATPase cycle, thereby competing with the co-factor p48 / Hip (Höhfeld, 1998)

1.3.9.2 Hsp70/Hsp90 organising protein (Hop) and its homologs murine stress inducible protein 1 (mSTI1) and stress inducible protein 1 (STI1)

Hop is an abundant, stress-induced 60 kDa protein characterized by its ability to bind the two chaperones, Hsp70 and Hsp90 (Smith *et al*., 1993, Boguski *et al*., 1990). It was originally observed in reconstituted progesterone complexes when ATP was limiting (Smith *et al*., 1992), and is a homolog of the yeast STI1 (Boguski *et al*., 1990) and the murine stress-inducible protein 1 (mSTI1) (Blatch *et al.*, 1997). STI1 is a stress inducible

phosphoprotein implicated in mediating the heat shock response in *Saccharomyces cerevisiae* (Nicolet and Craig, 1989).

The subcellular localization of mSTI1 is mostly cytoplasmic, although a nuclear fraction does exist (Lässle *et al.*, 1997). Recently, STI1 has been shown to also be localized at the cell membrane in prion-infected cells (Zanata *et al.*, 2002). A putative bipartite NLS sequence has been reported in the central region of mSTI1 (Blatch *et al.*, 1997). Furthermore, CKII and cdc2 kinases phosphorylate mSTI1, proximal to the NLS, supporting a predicted CcN motif (Longshaw *et al.,* 2000) (Figure 1.5).

The main function of mSTI1 appears to be its association with Hsp70 and Hsp90. The simultaneous interaction of mSTI1 with Hsp70 and Hsp90 at its N- (TPR1) and C-termini (TPR2A) respectively is mediated by the TPR motifs in these regions (Figure 1.5). The N-terminal TPR motifs of mSTI1, without flanking regions, are sufficient for Hsp70 interaction (van der Spuy *et al.,* 2000). Hsp70 and Hsp90 are not associated with one another in the absence of Hop (Chen *et al.*, 1996b). The interaction of the Hop TPR2A with a C-terminal pentapeptide of Hsp90 (MEEVD) has been identified as the core contact for Hop binding to Hsp90. In contrast, formation of the Hsp70-Hop complex depends not only on recognition of the C-terminal Hsp70 heptapeptide (PTIEEVD) by TPR1, but also on additional contacts between Hsp70 and Hop. Asp0 and Val-1 of the EEVD motif have been identified as general anchor residues, but the highly conserved glutamates of the EEVD sequence, which are critical in Hsp90 binding by TPR2A, do not contribute appreciably to the interaction of Hsp70 with TPR1 of Hop. Hydrophobic residues in these positions are preferred for binding by TPR1. Furthermore, both TPR domains tend to interact preferentially with hydrophobic aliphatic and aromatic side chains in positions –4 and –6 of their respective peptide ligands (Brinker *et al.,* 2002). These two TPR domains have been suggested to form two globular domains, separated by an extended polyproline II helix which could possibly serve as a linker region within the protein (Blatch *et al.,* 1997).

Hop does not of itself have any chaperone activity (Bose *et al*., 1996, Freeman *et al*., 1996). Hsp70 binds with low affinity to Hop (K_d = 1.3 μM) on its own, but this affinity is increased (K_d = 250 nM) in the presence of Hsp90. Hsp90 binds with high affinity to Hop (K_d = 90 nM), and Hsp70 does not affect this binding. The binding of Hsp90 to Hop reduces the number of Hsp70 binding sites on the Hop dimer from two sites in the absence of Hsp90 to one site in its presence. Hop can inhibit the ATP binding and p23 binding activity of Hsp90, which can be reversed if Hsp70 is present in the complex (Hernández *et al*., 2002). Although Hop is not required for the formation of the GR-Hsp90 chaperone system assembly, it has been shown to enhance the rate of the process (Morishima *et al.,* 2000a).

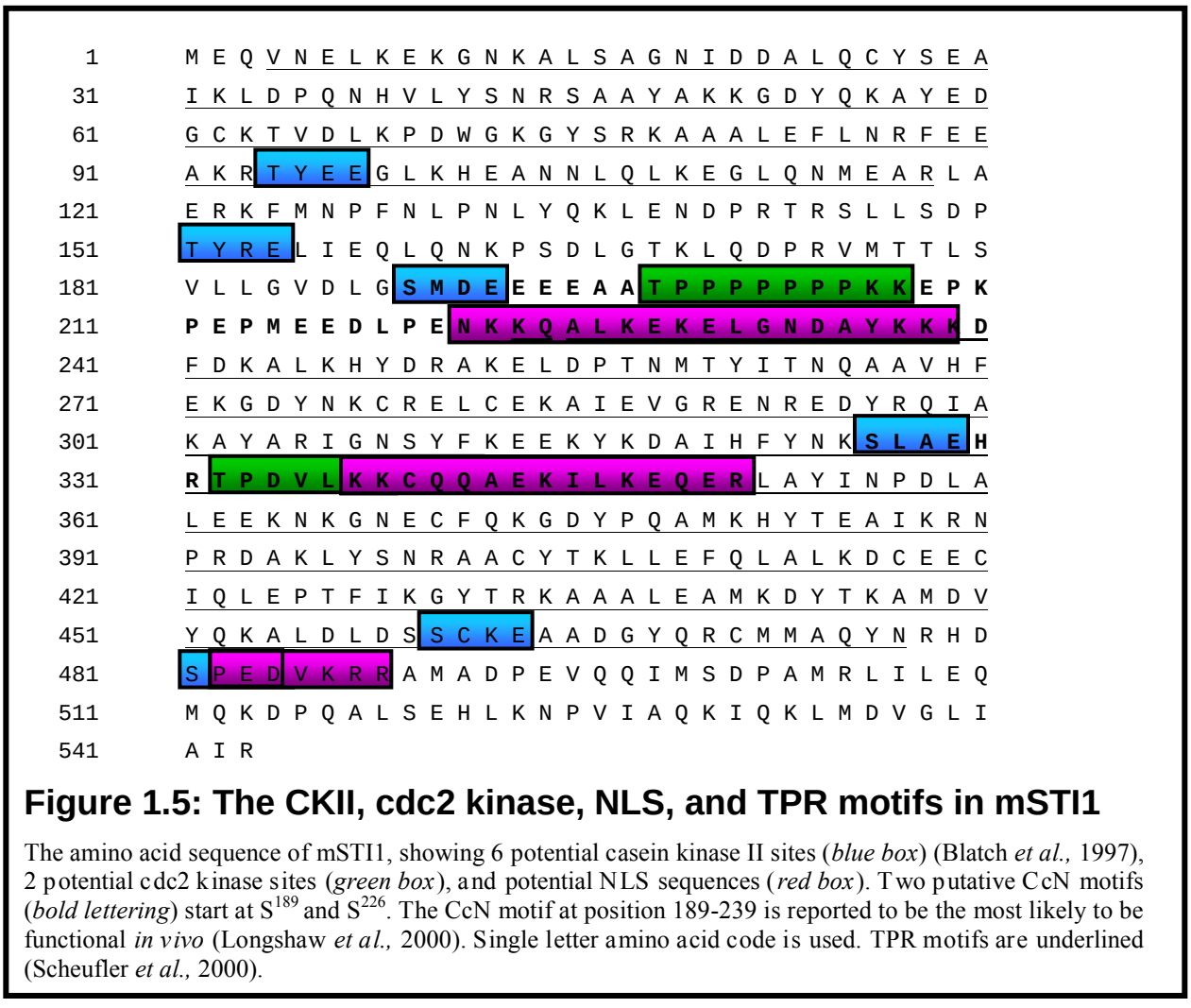

Figure 1.5: The CKII, cdc2 kinase, NLS, and TPR motifs in mSTI1

The amino acid sequence of mSTI1, showing 6 potential casein kinase II sites (*blue box*) (Blatch *et al.,* 1997), 2 potential cdc2 kinase sites (*green box*), and potential NLS sequences (*red box*). Two putative CcN motifs (*bold lettering*) start at S^{189} and S^{226}. The CcN motif at position 189-239 is reported to be the most likely to be functional *in vivo* (Longshaw *et al.,* 2000). Single letter amino acid code is used. TPR motifs are underlined (Scheufler *et al.,* 2000).

In addition, the weak ATPase activity of human Hsp90, which is stimulated by binding to GR, is inhibited by both p23 and Hop (McLaughlin *et al.,* 2002). The rate-limiting ATP-dependent opening of the steroid binding cleft after Hsp90 binding (Kanelakis *et al.,* 2002) may thus be highly regulated by the co-chaperones p23 and Hop. All Hop in reticulocyte lysate is present in an Hsp70-Hop-Hsp90 complex (Murphy *et al.,* 2001).

Prior to this work, there was little information available on the possible phosphorylation of mSTI1, Hop or STI1. No phosphorylation of mSTI1 by MAP kinase-activated protein kinase 2 (MAPKAP kinase 2), a heat activated kinase, has been detected (Lässle *et al.*, 1997). However, a heat-activated S6 kinase, $pp90^{rsk}$ has been shown to phosphorylate an N-terminal peptide of mSTI1, albeit with low activity (Lässle *et al.*, 1997). A shift in the *in vivo* isoform composition of Hop, to more acidic (and therefore possibly more phosphorylated) forms, occurs after viral transformation as well as after heat shock, suggesting the stress-induced phosphorylation of a Hop subpopulation (Honoré *et al.*, 1992). Investigations into a direct interaction of Hop homologs and cell cycle machinery have reported a direct physical interaction of the *Candida albicans* STI1 and cdc2 kinase (Ni *et al.,* 2001) and of the *Saccharomyces cerevisiae* STI1 and cdc37 (Abbas-Terki *et al.,* 2002). STI1 is specifically retained from yeast extracts by immobilized cdc37 and is proposed to interact directly with cdc37 in a complex *in vivo*. Previously, Hsp90 has been thought to mediate interactions between co-chaperones and cdc37, however STI1 has now been shown to interact directly with cdc37, indicating a further level of complexity in Hsp90-based chaperone interactions (Abbas-Terki *et al.,* 2002). *Cdc37* and *sti1* mutations of *Saccharomyces cerevisiae* have been shown to be synthetically lethal, further supporting a direct contact between cdc37 and STI1 *in vivo* (Abbas-Terki *et al.,* 2000).

1.4 HYPOTHESIS, AIMS AND OBJECTIVES

The GR forms a complex with chaperones Hsp90 and Hsp70, and co-chaperones Hop, Hsp40 and p23, resulting in the hormone-binding domain of the receptor being converted to its high affinity steroid binding state (Murphy *et al*., 2001). This hormone-free GR-Hsp90 heterocomplex is localized in the cytoplasm of most cells, and after steroid binding it translocates to the nucleus (Picard and Yamamoto, 1987), propsed to be through an association with the multiprotein Hsp90-based chaperone system (DeFranco, 2000) and NLS-directed movement via the proto-NLS in the GR (Pratt *et al*., 2001). mSTI1 is a homolog of Hop, localized in the cytoplasm (Lässle *et al*., 1997) and CKII and cdc2 kinases phosphorylate mSTI1, proximal to a predicted NLS, supporting a predicted CcN motif (Longshaw *et al.,* 2000).

In broad terms, it is therefore hypothesized that a nucleocytoplasmic distribution of mSTI1 occurs as a result of nuclear import and export of mSTI1, and that nuclear import is regulated by cell cycle status and cell cycle kinases.

In specific terms, nuclear localization is proposed to be directed by a functional NLS in mSTI1 at amino-acid position 222-239, and nuclear export of mSTI1 through the classical CRM-1 export pathway. Furthermore, the NLS in mSTI1 is hypothesized to be regulated via interactions with cell-cycle machinery, substantiating a predicted CcN motif. This CcN motif may consist of amino-acid positions 189-239 in mSTI1, with a functional CKII site at S189 and a functional cdc2 kinase site at T198. Modifications at the S189 and T198 positions, and inhibition of CKII and cdc2 kinases, may therefore affect the nucleocytoplasmic distribution of mSTI1.

CHAPTER 2

BIOINFORMATIC ANALYSIS OF mSTI1

SUMMARY: The primary amino acid sequence of mSTI1 was assessed and compared to the primary sequence of other STI1 proteins. The NLS, but not the proximal phosphorylation sites were conserved in STI1 proteins. The CKII site residues, D^{191} and E^{194}, contacted the conserved NLS first basic arm residue, K^{222} and the cdc2 kinase site residue T^{198} contacted the conserved NLS spacer region residue K^{229}. The bioinformatic assessment of mSTI1 presented in this work suggests a role for these proximal CKII and cdc2 kinase phosphorylation sites in mSTI1 in the electrostatic stabilization of the NLS for binding to karyopherin-α. Phosphorylation at the S^{189} and T^{198} sites is predicted to affect the binding of the mSTI1 NLS to karyopherin-α. The NLS coincides with the Hsp90-binding TPR2A domain of mSTI1. It is predicted that mSTI1 may not be able to simultaneously bind Hsp90 and karyopherin α, due to the sterically close proximity of their respective binding sites. This alternate binding of Hsp90 or karyopherin α may have mechanistic implications for the formation of the Hsp70/mSTI1/Hsp90 chaperone complex and its localization.

2.1 INTRODUCTION

2.1.1 The Fasta and Blast methods for database searches

The program ENTREZ (http://www.ncbi.nlm.nih.gov/Entrez), a derivative from the original menu-driven program called GEN-INFO, allows rapid and flexible searching through a simple windows-interface for similar sequences on the basis of previous similarity comparisons.

The program FASTA, developed by Pearson and Lipman (1988) is now extensively used as it rapidly performs a database scan for similarity. An even more rapid program for searching sequence databases is the BLAST program (http://www.ncbi.nlm.nih.gov/BLAST) developed by Altschul *et al*. (1990). The BLAST server is probably the most widely used search facility, providing similarity searching to all currently available sequences. Both FASTA and BLAST prepare a table of short sequence words, however BLAST also determines which of these words are most significant, confining the search to these words. More recent versions of BLAST include GAPPED-BLAST, which is three-fold faster than the original BLAST and PSI-BLAST (position-specific-iterated BLAST). These programs can find more distant matches to a test protein sequence by repeatedly searching for additional sequences that match an alignment of the query. BLAST assigns an expectation value (E value), which is the number of matches expected by chance between the query sequence and random or unrelated database sequences.

2.1.2 The functional significance of sequence alignment

With the advent of genome analysis and large-scale sequence comparisons, it is important to recognize that sequence similarity may be an indicator of several possible types of ancestor relationships. Recent theories have suggested evolution of genes, and therefore proteins, to be through gene duplication creating tandem copies of the same gene, and subsequent mutation of the two copies, allowing them to evolve along different pathways. Furthermore, genetic rearrangement allows reassortment of domains within proteins resulting in a complex evolutionary history. Homologous genes that share a common ancestry and function in the absence of evidence of gene duplication are termed orthologs. The conserved functional and structural domains of a protein family may be resolved using multiple sequence alignments of orthologs.

2.1.3 Sequence analysis programs

Initial methods for comparing sequences involved the dot matrix method (Gibbs and McIntyre, 1970), which required the first sequence to form the x-axis and the second the y-axis of a graph. Whenever the same letter appeared in both sequences, a dot was placed at the intersection, and the resulting graph scanned for a diagonal line fit. More recently, methods have been developed that allow the aligning of three or more sequences at the same time. The programs most commonly used are the GCG program PILEUP (http://www.gcg.com) and CLUSTALW (Thomson *et al*.) (Baylor College of Medicine, http://dot.imgen.bcm.tmc.edu:9331/multi-align/multi-align.html). Two matrix representations of the multiple sequence alignment called a PROFILE and a POSITION-SPECIFIC SCORING MATRIX (PSSM) are useful computational tools.

CLUSTALW is a more recent version of CLUSTAL, with the "W" standing for "weighting" to represent the ability of the program to provide weights to the sequence and program parameters, while CLUSTALX provides a graphic interface. CLUSTALW aligns the most closely related sequences first, and then additional sequences and groups of sequences are added and guided by the initial alignments (Higgins and Sharp, 1988;

Thompson *et al*. 1994; Higgins, *et al*. 1996). As more sequences are added to the profile of the existing alignment, gaps may accumulate and influence the alignment of further sequences. This may be regarded as a criticism of this approach to multiple sequence alignments. However, CLUSTALW has been designed to calculate these gaps in a novel way and place them in regions between conserved domains, in an attempt to compensate for the scoring matrix, the expected number of gaps (alignment with more identities should have fewer gaps) and differences in sequence length. Thus CLUSTALW is designed to provide an adequate alignment of a large number of sequences and provide a very good indication of the domain structure of those sequences (Pascarella and Argos, 1992). CLUSTALW uses a more global alignment of sequence similarity compared to the local alignment used by BLAST. This can provide a better overview of sequence similarity and therefore ancestral relationship, whereas a local alignment is useful for the investigation of functional motifs, which are conserved in ancestrally unrelated but functionally related proteins.

2.1.4 Predicting protein secondary structure

Although the number of known protein sequences is large, the number of protein sequences for which the structure has been resolved is relatively small. This is due to the expensive and time-consuming nature of X-ray crystallography and nuclear magnetic resonance spectroscopy (NMR). The amino acid sequence of the protein directs the folding pathway, often assisted by chaperones. Computational methods have been used to find protein structures with similar structural folds. Proteins have therefore been reported to have a limited number of structural folds (Chothia, 1992), suggested to be due to chemical restraints on protein folding or the existence of a single evolutionary pathway for protein structure (Gibrat *et al.* 1996).

Several algorithms are now available to predict the secondary structure content of proteins. The Chou-Fasman approach (Chou and Fasman, 1974) is based on statistically observed propensities of all 20 amino acids to occur in various protein secondary structures. For instance, valine and isoleucine have high beta-sheet probabilities, alanine and glutamic acid have high helical probabilities, and glycine and proline tend to appear

in random coil structures. The simplified rules of Williams *et al*. (1987) have improved the accuracy and utility of the original approach to within a 57.5% level of accuracy. A random three-state prediction (helix, beta and coil) is expected to be only 33.6% correct, based on the disposition of the secondary structures in structural databases. The GOR method (Garnier *et al*. 1978) is a statistical technique that predicts secondary structure on the basis of parameters obtained from information theory. The GOR method takes into account the positional preferences of amino acids within helices, beta sheets and coils. This method has since been modified (Gibrat *et al*., 1987) and is rated as among the most accurate of known methods, attaining a 63.4% level of accuracy (using the structural assignments available in structural databases). Homology based secondary structure prediction (Nishikawa and Ooi, 1986; Sweet, 1986; Levin *et al*., 1986) makes use of short stretches of homologous sequences within the protein of interest and compares them to known protein structures. For proteins sharing greater than 25% sequence similarity with any protein in the structure databases, this method approaches a level of accuracy of 87%. For proteins possessing no significant homology, the prediction is 66% correct.

Bowie *et al*. (1991) also developed a method for predicting whether a given protein sequence can occupy the same three dimensional conformation as another based on the properties of the amino acids. Furthermore, it is now possible to search for protein sequences that may form proteins with a common biochemical activity, deduced by the pattern of amino acids responsible for that activity. The patterns were collected into the PROSITE database (http://www.expasy.ch/prosite). Alignments of protein sequences making up motifs were used to generate the BLOCK database (http://www.blocks.fhcrc.org/) to determine the possible biochemical activity of an unknown protein. Similarly, ungapped patterns in alignments may be extracted to produce blocks using BLOCKS (http://www.blocks.fhcrc.org/blocks/process_blocks.html) from alignments in FASTA or CLUSTAL formats. The MOTIFS server (http://dna.stanford.edu/emotif/) similarly extracts motifs from multiple sequence alignments. The changes in the patterns of these matrices made it possible to generate a new set of amino acid matrices, called Blocks Amino Acid Substitution Matrices (BLOSUM) (Henikoff and Henikoff, 1992), of which

BLOSUM62 is the more frequently used in searching and aligning sequences from databases.

2.1.5 Modeling of protein structures

In performing structural modeling, the three-dimensional structure of the molecular backbone of a matched sequence is superimposed upon the one-dimensional structure of a second protein sequence, such that the average deviation of distance between the respective atoms is minimal. While statistically significant sequence similarity is an indicator of an evolutionary relationship between sequences, structural similarity is common, even among proteins not sharing any sequence similarity or evolutionary relationship. Molecular distances, angles and energies of the superimposed sequence may then be analyzed and manipulated by the SPDBViewer. Useful programs for modeling are Modeler (http://guitar.rockefeller.edu/modeller.modeller.html), Swiss-model (http://www.expansy.ch/swissmod/SWISS-MODEL.html) and WhatIF (http://www.cmbi.kun.nl/whatif/) (Mount, 2001).

2.1.6 Bioinformatic analysis of mSTI1

Bioinformatic studies of mSTI1 have mainly been to further the investigation of the structure and function of the TPR domains in mSTI1. Ten potential TPR motifs have been identified in mSTI1 (Blatch *et al.,* 1997). The mSTI1 homolog Hop was predicted to contain nine TPR motifs, forming two TPR domains (Scheufler *et al.,* 2000). These TPR domains enable Hop and mSTI1 to carry out their apparent main function of association with the EEVD motifs in both Hsp70 and Hsp90. The simultaneous interaction of mSTI1 with Hsp70 and Hsp90 at its N- (TPR1) and C- termini (TPR2) respectively is mediated by the TPR motifs in these regions (Lässle *et al.,* 1997; Van der Spuy *et al.,* 2000; Odunuga *et al.,* 2002). Hsp70 and Hsp90 bind with high affinity to Hop (K_d = 250 nM and K_d = 90 nM respectively) (Hernández *et al.,* 2002). A pentapeptide of Hsp90 (MEEVD) is reported to be the core binding residues required for specific binding to the TPR2A of Hop. Hsp70 binding to Hop, however, requires the Hsp70 heptapeptide

(PTIEEVD) binding by TPR1, as well as additional contacts between Hsp70 and Hop. Asp0 and Val-1 of the EEVD motif have been identified as general anchor residues for the binding of the EEVD sequence to the TPR residues in Hop. The highly conserved glutamates of the EEVD sequence are critical in Hsp90 binding by TPR2A. However, these glutamates do not contribute appreciably to the interaction of Hsp70 with TPR1 of Hop (Brinker *et al.,* 2002). These two TPR domains have been suggested to form two globular domains, separated by an extended polyproline II helix which could possibly serve as a linker region within the protein (Blatch *et al.,*1997). Previously, bioinformatic analysis of mSTI1 has been restricted to the modeling of the TPR1 (three TPR motifs) and TPR2 (six TPR motifs) regions for binding studies to Hsp70 and Hsp90 respectively (Van der Spuy, 2000; Odunuga *et al*., 2002). These models have used the structural coordinates of the resolved PP5, and the Hop TPR1 and TPR2 structures. Structural information, real or predicted, of the CcN motif has previously not been available.

2.1.7 Specific hypothesis, aims and objectives

Hop, the human homolog of mSTI1 (Lässle *et al.,* 1997), is involved in mediating the Hsp90 based chaperone complex that binds to the GR, converting the hormone-binding domain of the receptor to its high affinity steroid binding state (Murphy *et al*., 2001). After steroid binding, this hormone-free GR-Hsp90 heterocomplex is translocated from the cytoplasm to the nucleus (Picard and Yamamoto, 1987), via NLS-directed movement via the proto-NLS in the GR (Pratt *et al.,* 2001) and through association with the multiprotein Hsp90-based chaperone system (DeFranco, 2000). The translocation of the GR-Hsp90 chaperone complex may also be brought about by the predicted NLS in mSTI1, implying a translocation regulatory role of mSTI1 in this complex.

It is hypothesized that mSTI1 contains a CcN motif that conforms structurally to the CcN motif initially described for SV40 T-antigen, and that this CcN motif is structurally integrated with other motifs in mSTI1, namely TPR motifs.

In this work, the potential NLS in mSTI1 at positions 222-239 will later be tested for its functionality in targeting a non-nuclear protein to the nucleus. In this chapter, the conservation of this NLS was determined for all STI1 proteins, as well as the conservation of the proximal phosphorylation sites to this NLS, which make up the predicted CcN motif (Longshaw *et al.,* 2000). The usefulness of this analysis would be towards an understanding of which residues contained within the mSTI1 NLS are potentially critical, for further analysis of their potential mechanistic interactions. The potential CcN motif region was modelled on a potentially structurally similar protein to produce a 3D model of this region of mSTI1. The residues in the NLS found to be conserved in STI1 proteins were analyzed for significant contacts with other residues using this 3D model of the potential CcN motif in mSTI1. Although the structures of fragments of the mSTI1 homolog Hop in complex with Hsp70 and Hsp90 peptides have been resolved, these structures do not include the full potential CcN motif. The template for the modelling of this region was therefore carried out on the TPR-rich PP5 protein structure. Furthermore, the CcN motif region in mSTI1 was analyzed for its proximity to other motif structures in mSTI1, namely the TPR motifs, which mediate protein-protein interaction. The TPR2 in mSTI1 binds Hsp90, while the predicted NLS in mSTI1 would probably bind the NLS receptor protein, karyopherin-α. The functional significance of the proximity of these motifs was discussed.

2.2 EXPERIMENTAL PROCEDURES

2.2.1 The analysis of the mSTI1 amino acid sequence

The primary amino acid sequences of mSTI1 and of proteins demonstrating homology to mSTI1 were downloaded from the NCBI database (http://www.ncbi.nlm.nih.gov/Entrez), the Saccharomyces Genome Database (SGD) (http://genome-www.stanford.edu/Saccharomyces), European Molecular Biology Laboratory (EMBL) (http://www.embl-heidelberg.de), SWISS-PROT, TrEMBL (http://www.expasy.org/sprot/) and the Protein Information Resource database (PIR) (http://pir.georgetown.edu/).

2.2.2 The alignment of protein sequences

Protein sequences were pairwise aligned using CLUSTALW at the BCM Launcher (BCM) server (http://searchlauncher.bcm.tmc.edu/seq-search/alignment.html). Protein sequences were multiple-aligned using the GCG program ClustalW 1.8 (Corpet, 1988) at the European Bioinformatics Institute (EBI) server (http://www2.ebi.ac.uk/clustalw/) (Thompson *et al*. 1994). The multiple-alignment in FASTA format was then assessed for conserved blocks using the BLOCK server (http://www.blocks.fhcrc.org/blocks/process_blocks.html) to determine significantly conserved residues in conserved blocks in the regions of the identified CcN motifs.

2.2.3 The prediction of secondary structure of mSTI1

Secondary structure predictions were used to assess the secondary structure content of mSTI1, especially of the CcN motif, such that an appropriate 3D coordinate file could be used for subsequent homology modeling. The program PepTools with the Chou-Fasman, the GOR, and the homology algorithms, was used.

2.2.4 The modeling of the mSTI1 CcN motif

A preliminary homology model was carried out with protein phosphatase 5 (PP5) as a template using the SWISS-MODEL program at http://www.expasy.org/swissmod/SWISS-MODEL.html (Guex and Peitsch, 1997). The PP5 template was used instead of the Hop template because the Hop structure(1ELR.pdb) does not include the full CcN motf. The model was visualized using Deep View SwissPDB viewer at http://www.expasy.ch/spdbv/mainpage.html. The mSTI1 identified CcN motif sequence V^{181}-F^{241} was then modeled against the PP5 coordinate file 1A17.pdb as downloaded from the Protein Data Bank, using the modeling program WhatIF (Vriend, 1990). Potentially significant distances between side-chains were visualized using the SwissPDB viewer and Molscript (Kraulis, 1991).

2.2.5 The structure of the bipartite NLS in Hop, and as recognized by karyopherin α

The coordinate files for the TPR2 of Hop in complex with a C-terminal peptide of Hsp90 (1ELR.pdb), and for mouse karyopherin α in complex with the nucleoplasmin bipartite NLS (1EJY.pdb), were downloaded from the Protein Data Bank. These structures were visualized in Molscript (Kraulis, 1991).

2.3 RESULTS AND DISCUSSION

2.3.1 The NLS in the CcN motif is conserved

The primary amino acid sequence of the predicted CcN motif at positions 189-239 in mSTI1 was found to resemble similar CcN motifs reported for other proteins (Figure 2.1). A second CcN motif was identified in mSTI1 at positions 326-251, however this CcN motif is unlikely to be phosphorylated, since removal of the S189 CKII site and the T198 cdc2 kinase site abolished phosphorylation of GST-mSTI1 by CKII and cdc2 kinase respectively (Longshaw *et al.,* 2000)

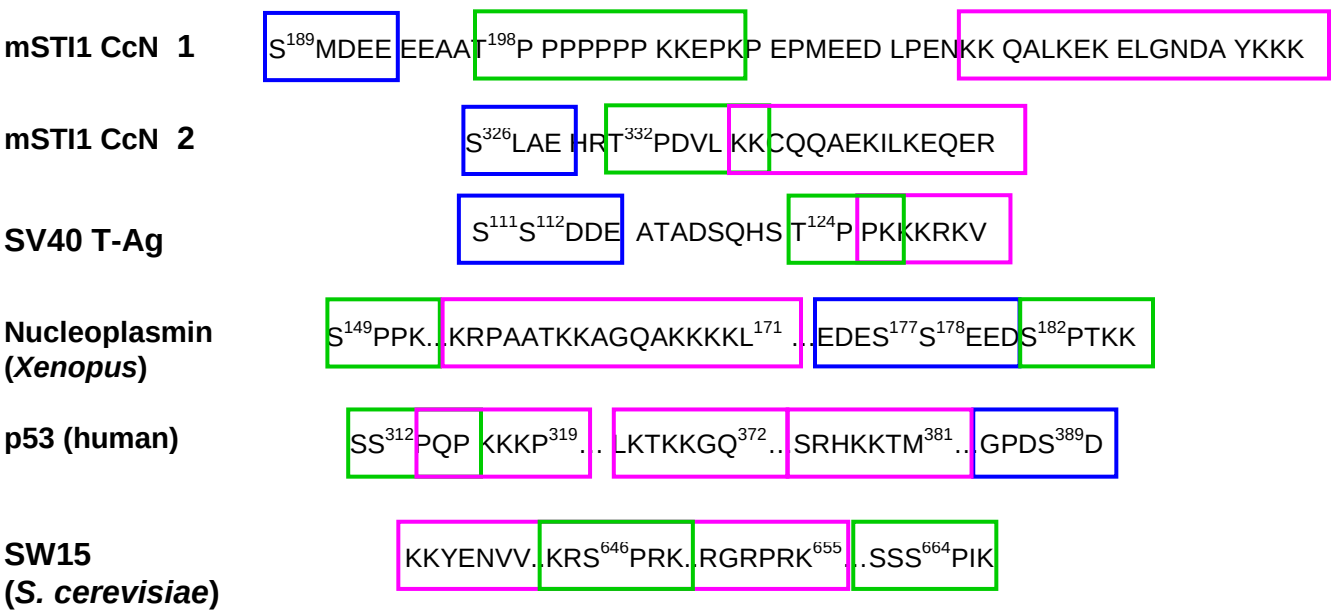

Figure 2.1: Comparison of CcN motifs

Identified mSTI1 CcN motifs were compared to those reviewed by Jans and Hübner (1996). Single letter amino acid code is used. The CKII consensus site comprises an acidic amino acid 3 residues C-terminal to phosphorylatable S/T, with an elevated number of acidic residues in the vicinity increasing its affinity for CKII. Amino acid sequences corresponding to this CKII consensus site are indicated by a blue box. Cdk/p34^{cdc2} kinase phosphorylates S/T residues C-terminal to proline residues, if a basic amino acid is present 1 or 2 residues C-terminal to the proline. Amino acid sequences corresponding to this p34^{cdc2} consensus site are indicated by a green box. Amino acid sequences showing similarity to the SV40 NLS are indicated by a red box. Confirmed *in vitro* or *in vivo* phosphorylation sites for CKII, Cdk/p34^{cdc2} kinase, and NLS are indicated by +. Phosphorylated residues are numbered.

The mSTI1 primary acid sequence (accession number NP_058017) was used to search the entire database through the BLAST search program, using the Entrez Browser. The search yielded 11 significant hits, mostly against the TPR regions. The proteins identified by BLAST were compared to mSTI1 using a pairwise BCM Launcher alignment. Mammalian or higher vertebrate STI1 proteins had a high identity to mSTI1 (Table 2.1, Figure 2.2) and were highly conserved in the CcN motif region. *rn*STI1 was found to have the highest pairwise identity to mSTI1, and lowest gap frequency, followed by *cg*STI1, *hs*STI1 and *xl*STI1 (Table 2.1). STI1 proteins from yeast, simple vertebrate or of plant origin, were less similar to mSTI1, and showed a higher gap frequency (Table 2.1, Figure 2.3). Sequence analysis limits predictions of residue interactions as it cannot include three-dimensional data, but can be positively used to assess possible conservation of residues and therefore their possible mechanistic importance.

The CcN motif in the less similar STI1 proteins showed little similarity in phosphorylation sites proximal to the NLS, however residues in the NLS sequence were highly conserved and constituted a conserved block (Figure 2.4). The CcN motif (conserved block 222-256) was found to contain significantly conserved residues K^{223}, A^{225}, E^{228}, K^{229}, G^{232}, N^{233}, Y^{236}, K^{237}, K^{238} and K^{239} (Figure 2.4). This therefore included the first (K^{223}) and second (K^{237}, K^{238} and K^{239}) basic clusters of the bipartite NLS. Although in a significant proportion of bipartite NLS sequences, one of the necessary bipartite clusters shows a striking similarity to the SV40 NLS, it is not sufficient by itself to target a protein to the nucleus (Dingwall and Laskey, 1991). Therefore, the conservation of both clusters of the NLS implies a conservation of the STI1 NLS function. The phosphorylation sites proximal to the NLS, on the other hand, are not highly conserved among STI1 homologs. If the NLS is functional in STI1 proteins that lack kinase sites proximal to the NLS, the conserved STI1 NLS may not require proximal phosphorylation to function.

Residues in the NLS spacer region were also conserved and included negatively charged (E^{228}); positively charged (K^{229}); polar (G^{232}, N^{233}) and non-polar residues (A^{225}, Y^{236}). Although varying the length of the bipartite NLS spacer has been found to have no effect

on nuclear targeting efficiency, the introduction of hydrophobic or bulky residues into the spacer markedly reduces targeting efficiency (Robbins, *et al.*, 1991). The conservation of charged residues implies the formation of salt bridges for electrostatic stabilization of the protein. The conservation of the hydrophobic Y^{236}, on the other hand, could indicate its participation in a hydrophobic binding pocket between helices, also for stabilization purposes. The conservation of the small G^{232} and A^{225} residues (Figure 2.2) implies that this region is closely packed. The introduction of hydrophobic or bulky residues, therefore, into this spacer may certainly affect the closely packed electrostatic interactions of this site.

Table 2.1: Pairwise alignments of mSTI1 homologs

Organism	**Protein**	**Accession number**	**BLAST *E* value**	**%Identity to mSTI1**	**%Gap frequency**
Rattus norvegicus	*rn*STI1	NP_620266	0.0	99.3	0.0
Cricetulus griseus	*cg*STI1	AAB94760	0.0	97.8	0.0
Homo sapiens	*hs*STI1	NP_006810	0.0	97.4	0.0
Xenopus laevis	*xl*STI1	AAM77586	0.0	85.5	0.0
Caenorhabditis elegans	*ce*STI1	NP_503322	5e-91	56.1	0.9
Arabidopsis thaliana	*at*STI1	AAF19538	e-110	43.1	9.0
Glycine max	*gm*STI1	CAA56165	3e-91	41.8	5.9
Acanthamoeba castellanii	*ac*STI1	AAB49720	e-113	45.7	3.6
Schizosaccharomyces pombe	*sp*STI1	NP_588123	7e-96	39.8	8.8
Saccharomyces cerevisiae	*sc*STI1	NP_014670	8e-86	38.7	7.9
Leishmania major	*lm*STI1	AAB37318	5e-91	39.6	1.7

Protein sequences were pairwise aligned using BLOSUM62 at the BCM Launcher (BCM) server (http://searchlauncher.bcm.tmc.edu/seq-search/alignment.html).

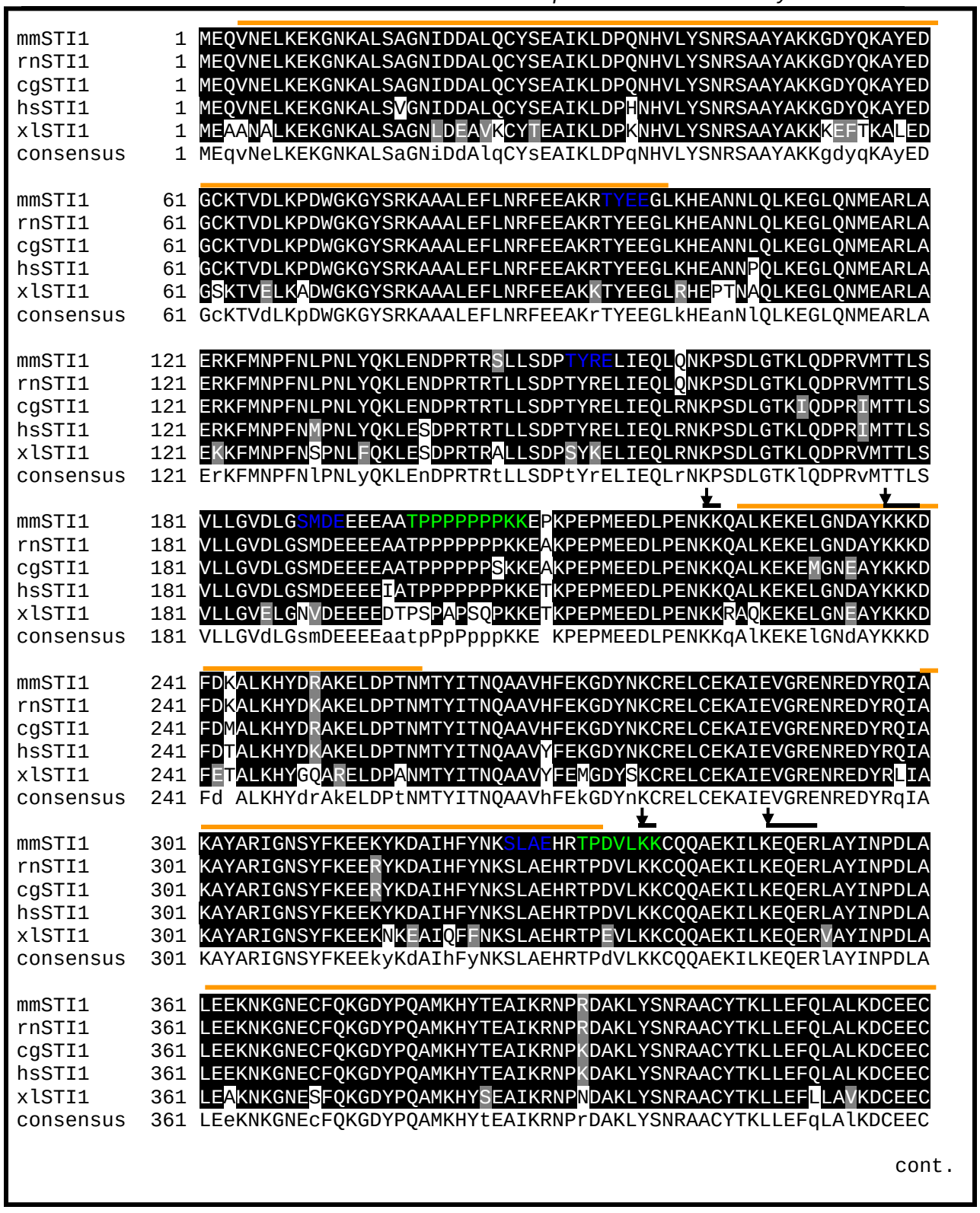
mmSTI1 1 MEQVNELKEKGNKALSAGNIDDALQCYSEAIKLDPQNHVLYSNRSAAYAKKGDYQKAYED
rnSTI1 1 MEQVNELKEKGNKALSAGNIDDALQCYSEAIKLDPQNHVLYSNRSAAYAKKGDYQKAYED
cgSTI1 1 MEQVNELKEKGNKALSAGNIDDALQCYSEAIKLDPQNHVLYSNRSAAYAKKGDYQKAYED
hsSTI1 1 MEQVNELKEKGNKALSVGNIDDALQCYSEAIKLDPHNHVLYSNRSAAYAKKGDYQKAYED
xlSTI1 1 MEAANALKEKGNKALSAGNLDEAVKCYTEAIKLDPKNHVLYSNRSAAYAKKKEFTKALED
consensus 1 MEqvNeLKEKGNKALSaGNiDdAlqCYsEAIKLDPqNHVLYSNRSAAYAKKgdyqKAyED
mmSTI1 61 GCKTVDLKPDWGKGYSRKAAALEFLNRFEEAKRTYEEGLKHEANNLQLKEGLQNMEARLA
rnSTI1 61 GCKTVDLKPDWGKGYSRKAAALEFLNRFEEAKRTYEEGLKHEANNLQLKEGLQNMEARLA
cgSTI1 61 GCKTVDLKPDWGKGYSRKAAALEFLNRFEEAKRTYEEGLKHEANNLQLKEGLQNMEARLA
hsSTI1 61 GCKTVDLKPDWGKGYSRKAAALEFLNRFEEAKRTYEEGLKHEANNPQLKEGLQNMEARLA
xlSTI1 61 GSKTVELKADWGKGYSRKAAALEFLNRFEEAKKTYEEGLRHEPTNAQLKEGLQNMEARLA
consensus 61 GcKTVdLKpDWGKGYSRKAAALEFLNRFEEAKrTYEEGLkHEanNlQLKEGLQNMEARLA
mmSTI1 121 ERKFMNPFNLPNLYQKLENDPRTRSLLSDPTYRELIEQLQNKPSDLGTKLQDPRVMTTLS
rnSTI1 121 ERKFMNPFNLPNLYQKLENDPRTRTLLSDPTYRELIEQLQNKPSDLGTKLQDPRVMTTLS
cgSTI1 121 ERKFMNPFNLPNLYQKLENDPRTRTLLSDPTYRELIEQLRNKPSDLGTKIQDPRIMTTLS
hsSTI1 121 ERKFMNPFNMPNLYQKLESDPRTRTLLSDPTYRELIEQLRNKPSDLGTKLQDPRIMTTLS
xlSTI1 121 EKKFMNPFNSPNLFQKLESDPRTRALLSDPSYKELIEQLRNKPSDLGTKLQDPRVMTTLS
consensus 121 ErKFMNPFNlPNLyQKLEnDPRTRtLLSDPtYrELIEQLrNKPSDLGTKlQDPRvMTTLS
mmSTI1 181 VLLGVDLGSMDEEEEAATPPPPPPPKKEPKPEPMEEDLPENKKQALKEKELGNDAYKKKD
rnSTI1 181 VLLGVDLGSMDEEEEAATPPPPPPPKKEAKPEPMEEDLPENKKQALKEKELGNDAYKKKD
cgSTI1 181 VLLGVDLGSMDEEEEAATPPPPPPSKKEAKPEPMEEDLPENKKQALKEKEMGNEAYKKKD
hsSTI1 181 VLLGVDLGSMDEEEEIATPPPPPPPKKETKPEPMEEDLPENKKQALKEKELGNDAYKKKD
xlSTI1 181 VLLGVELGNVDEEEEDTPSPAPSQPKKETKPEPMEEDLPENKKRAQKEKELGNEAYKKKD
consensus 181 VLLGVdLGsmDEEEEaatpPpPpppKKE KPEPMEEDLPENKKqAlKEKElGNdAYKKKD
mmSTI1 241 FDKALKHYDRAKELDPTNMTYITNQAAVHFEKGDYNKCRELCEKAIEVGRENREDYRQIA
rnSTI1 241 FDKALKHYDKAKELDPTNMTYITNQAAVHFEKGDYNKCRELCEKAIEVGRENREDYRQIA
cgSTI1 241 FDMALKHYDRAKELDPTNMTYITNQAAVHFEKGDYNKCRELCEKAIEVGRENREDYRQIA
hsSTI1 241 FDTALKHYDKAKELDPTNMTYITNQAAVYFEKGDYNKCRELCEKAIEVGRENREDYRQIA
xlSTI1 241 FETALKHYGQARELDPANMTYITNQAAVYFEMGDYSKCRELCEKAIEVGRENREDYRLIA
consensus 241 Fd ALKHYdrAkELDPtNMTYITNQAAVhFEkGDYnKCRELCEKAIEVGRENREDYRqIA
mmSTI1 301 KAYARIGNSYFKEEKYKDAIHFYNKSLAEHRTPDVLKKCQQAEKILKEQERLAYINPDLA
rnSTI1 301 KAYARIGNSYFKEERYKDAIHFYNKSLAEHRTPDVLKKCQQAEKILKEQERLAYINPDLA
cgSTI1 301 KAYARIGNSYFKEERYKDAIHFYNKSLAEHRTPDVLKKCQQAEKILKEQERLAYINPDLA
hsSTI1 301 KAYARIGNSYFKEEKYKDAIHFYNKSLAEHRTPDVLKKCQQAEKILKEQERLAYINPDLA
xlSTI1 301 KAYARIGNSYFKEEKNKEAIQFFNKSLAEHRTPEVLKKCQQAEKILKEQERVAYINPDLA
consensus 301 KAYARIGNSYFKEEkyKdAIhFyNKSLAEHRTPdVLKKCQQAEKILKEQERlAYINPDLA
mmSTI1 361 LEEKNKGNECFQKGDYPQAMKHYTEAIKRNPRDAKLYSNRAACYTKLLEFQLALKDCEEC
rnSTI1 361 LEEKNKGNECFQKGDYPQAMKHYTEAIKRNPRDAKLYSNRAACYTKLLEFQLALKDCEEC
cgSTI1 361 LEEKNKGNECFQKGDYPQAMKHYTEAIKRNPKDAKLYSNRAACYTKLLEFQLALKDCEEC
hsSTI1 361 LEEKNKGNECFQKGDYPQAMKHYTEAIKRNPKDAKLYSNRAACYTKLLEFQLALKDCEEC
xlSTI1 361 LEAKNKGNESFQKGDYPQAMKHYSEAIKRNPNDAKLYSNRAACYTKLLEFLLAVKDCEEC
consensus 361 LEeKNKGNEcFQKGDYPQAMKHYtEAIKRNPrDAKLYSNRAACYTKLLEFqLAlKDCEEC
cont.

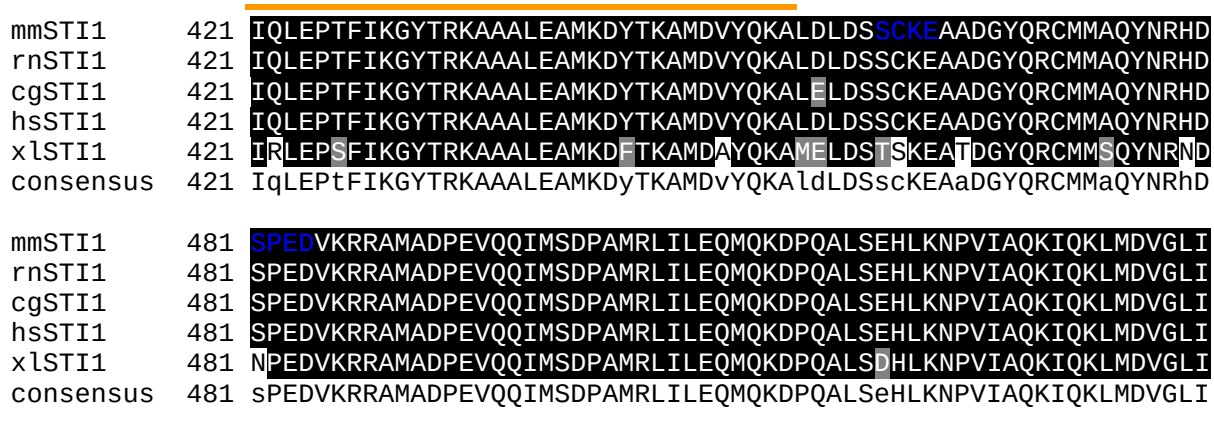

Figure 2.2: The multiple sequence alignment of mSTI1 and similar homologs

The amino acid sequences of the STI1 orthologs were aligned. The dark boxes represent the identical and thus conserved residues, and the gray boxes, the structurally similar residues. mmSTI1: *Mus musculus* (NP_058017), rnSTI1: *Rattus norvegicus* (NP_620266), cgSTI1: *Cricetulus griseus* (AAB94760), hsSTI1: *Homo sapiens* (NP_006810), and xlSTI1: *Xenopus laevis* (AAM77586). The identified CcN motif in mSTI1 is highlighted in red. The basic NLS clusters are indicated with arrowheads. The mSTI1 phosphorylation sites are shown: the CKII site in blue and the cdc2 kinase site in green. The TPRs are indicated with orange lines.

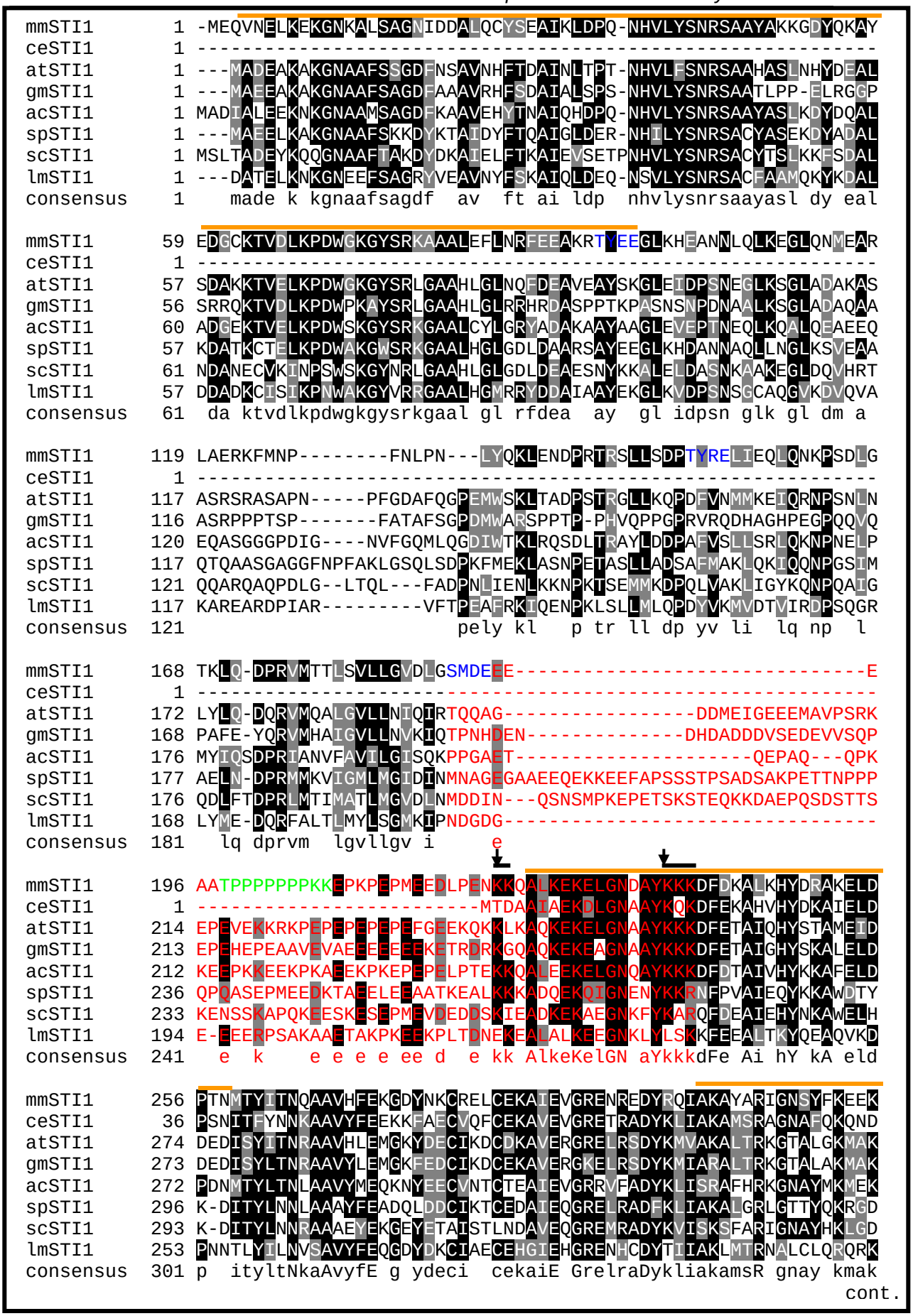
mmSTI1 1 -MEQVNELKEKGNKALSAGNIDDALQCYSEAIKLDPQ-NHVLYSNRSAAYAKKGDYQKAY
ceSTI1 1 ----------
atSTI1 1 ---MADEAKAKGNAAFSSGDFNSAVNHFTDAINLTPT-NHVLFSNRSAAHASLNHYDEAL
gmSTI1 1 ---MAEEAKAKGNAAFSAGDFAAAVRHFSDAIALSPS-NHVLYSNRSAATLPP-ELRGGP
acSTI1 1 MADIALEEKNKGNAAMSAGDFKAAVEHYTNAIQHDPQ-NHVLYSNRSAAYASLKDYDQAL
spSTI1 1 ---MAEELKAKGNAAFSKKDYKTAIDYFTQAIGLDER-NHILYSNRSACYASEKDYADAL
scSTI1 1 MSLTADEYKQQGNAAFTAKDYDKAIELFTKAIEVSETPNHVLYSNRSACYTSLKKFSDAL
lmSTI1 1 ---DATELKNKGNEEFSAGRYVEAVNYFSKAIQLDEQ-NSVLYSNRSACFAAMQKYKDAL
consensus 1 made k kgnaafsagdf av ft ai ldp nhvlysnrsaayasl dy eal
mmSTI1 59 EDGCKTVDLKPDWGKGYSRKAAALEFLNRFEEAKRTYEEGLKHEANNLQLKEGLQNMEAR
ceSTI1 1 ----------
atSTI1 57 SDAKKTVELKPDWGKGYSRLGAAHLGLNQFDEAVEAYSKGLEIDPSNEGLKSGLADAKAS
gmSTI1 56 SRRQKTVDLKPDWPKAYSRLGAAHLGLRRHRDASPPTKPASNSNPDNAALKSGLADAQAA
acSTI1 60 ADGEKTVELKPDWSKGYSRKGAALCYLGRYADAKAAYAAGLEVEPTNEQLKQALQEAEEQ
spSTI1 57 KDATKCTELKPDWAKGWSRKGAALHGLGDLDAARSAYEEGLKHDANNAQLLNGLKSVEAA
scSTI1 61 NDANECVKINPSWSKGYNRLGAAHLGLGDLDEAESNYKKALELDASNKAAKEGLDQVHRT
lmSTI1 57 DDADKCISIKPNWAKGYVRRGAALHGMRRYDDAIAAYEKGLKVDPSNSGCAQGVKDVQVA
consensus 61 da ktvdlkpdwgkgysrkgaal gl rfdea ay gl idpsn glk gl dm a
mmSTI1 119 LAERKFMNP--------FNLPN---LYQKLENDPRTRSLLSDPTYRELIEQLQNKPSDLG
ceSTI1 1 ----------
atSTI1 117 ASRSRASAPN-----PFGDAFQGPEMWSKLTADPSTRGLLKQPDFVNMMKEIQRNPSNLN
gmSTI1 116 ASRPPPTSP-------FATAFSGPDMWARSPPTP-PHVQPPGPRVRQDHAGHPEGPQQVQ
acSTI1 120 EQASGGGPDIG----NVFGQMLQGDIWTKLRQSDLTRAYLDDPAFVSLLSRLQKNPNELP
spSTI1 117 QTQAASGAGGFNPFAKLGSQLSDPKFMEKLASNPETASLLADSAFMAKLQKIQQNPGSIM
scSTI1 121 QQARQAQPDLG--LTQL---FADPNLIENLKKNPKTSEMMKDPQLVAKLIGYKQNPQAIG
lmSTI1 117 KAREARDPIAR---------VFTPEAFRKIQENPKLSLLMLQPDYVKMVDTVIRDPSQGR
consensus 121 pely kl p tr ll dp yv li lq np l
mmSTI1 168 TKLQ-DPRVMTTLSVLLGVDLGSMDEEE----------E
ceSTI1 1 ----------
atSTI1 172 LYLQ-DQRVMQALGVLLNIQIRTQQAG----------DDMEIGEEEMAVPSRK
gmSTI1 168 PAFE-YQRVMHAIGVLLNVKIQTPNHDEN----------DHDADDDVSEDEVVSQP
acSTI1 176 MYIQSDPRIANVFAVILGISQKPPGAET----------QEPAQ---QPK
spSTI1 177 AELN-DPRMMKVIGMLMGIDINMNAGEGAAEEQEKKEEFAPSSSTPSADSAKPETTNPPP
scSTI1 176 QDLFTDPRLMTIMATLMGVDLNMDDIN---QSNSMPKEPETSKSTEQKKDAEPQSDSTTS
lmSTI1 168 LYME-DQRFALTLMYLSGMKIPNDGDG----------
consensus 181 lq dprvm lgvllgv i e
mmSTI1 196 AATPPPPPPPKKEPKPEPMEEDLPENKKQALKEKELGNDAYKKKDFDKALKHYDRAKELD
ceSTI1 1 ----------MTDAAIAEKDLGNAAYKQKDFEKAHVHYDKAIELD
atSTI1 214 EPEVEKKRKPEPEPEPEPEFGEEKQKKLKAQKEKELGNAAYKKKDFETAIQHYSTAMEID
gmSTI1 213 EPEHEPEAAVEVAEEEEEEEKETRDRKGQAQKEKEAGNAAYKKKDFETAIGHYSKALELD
acSTI1 212 KEEPKKEEKPKAEEKPKEPEPELPTEKKQALEEKELGNQAYKKKDFDTAIVHYKKAFELD
spSTI1 236 QPQASEPMEEDKTAEELEEAATKEALKKKADQEKQIGNENYKKRNFPVAIEQYKKAWDTY
scSTI1 233 KENSSKAPQKEESKESEPMEVDEDDSKIEADKEKAEGNKFYKARQFDEAIEHYNKAWELH
lmSTI1 194 E-EEERPSAKAAETAKPKEEKPLTDNEKEALALKEEGNKLYLSKKFEEALTKYQEAQVKD
consensus 241 e k e e e e ee d e kk AlkeKelGN aYkkkdFe Ai hY kA eld
mmSTI1 256 PTNMTYITNQAAVHFEKGDYNKCRELCEKAIEVGRENREDYRQIAKAYARIGNSYFKEEK
ceSTI1 36 PSNITFYNNKAAVYFEEKKFAECVQFCEKAVEVGRETRADYKLIAKAMSRAGNAFQKQND
atSTI1 274 DEDISYITNRAAVHLEMGKYDECIKDCDKAVERGRELRSDYKMVAKALTRKGTALGKMAK
gmSTI1 273 DEDISYLTNRAAVYLEMGKFEDCIKDCEKAVERGKELRSDYKMIARALTRKGTALAKMAK
acSTI1 272 PDNMTYLTNLAAVYMEQKNYEECVNTCTEAIEVGRRVFADYKLISRAFHRKGNAYMKMEK
spSTI1 296 K-DITYLNNLAAAYFEADQLDDCIKTCEDAIEQGRELRADFKLIAKALGRLGTTYQKRGD
scSTI1 293 K-DITYLNNRAAAEYEKGEYETAISTLNDAVEQGREMRADYKVISKSFARIGNAYHKLGD
lmSTI1 253 PNNTLYILNVSAVYFEQGDYDKCIAECEHGIEHGRENHCDYTIIAKLMTRNALCLQRQRK
consensus 301 p ityltNkaAvyfE g ydeci cekaiE GrelraDykliakamsR gnay kmak
cont.

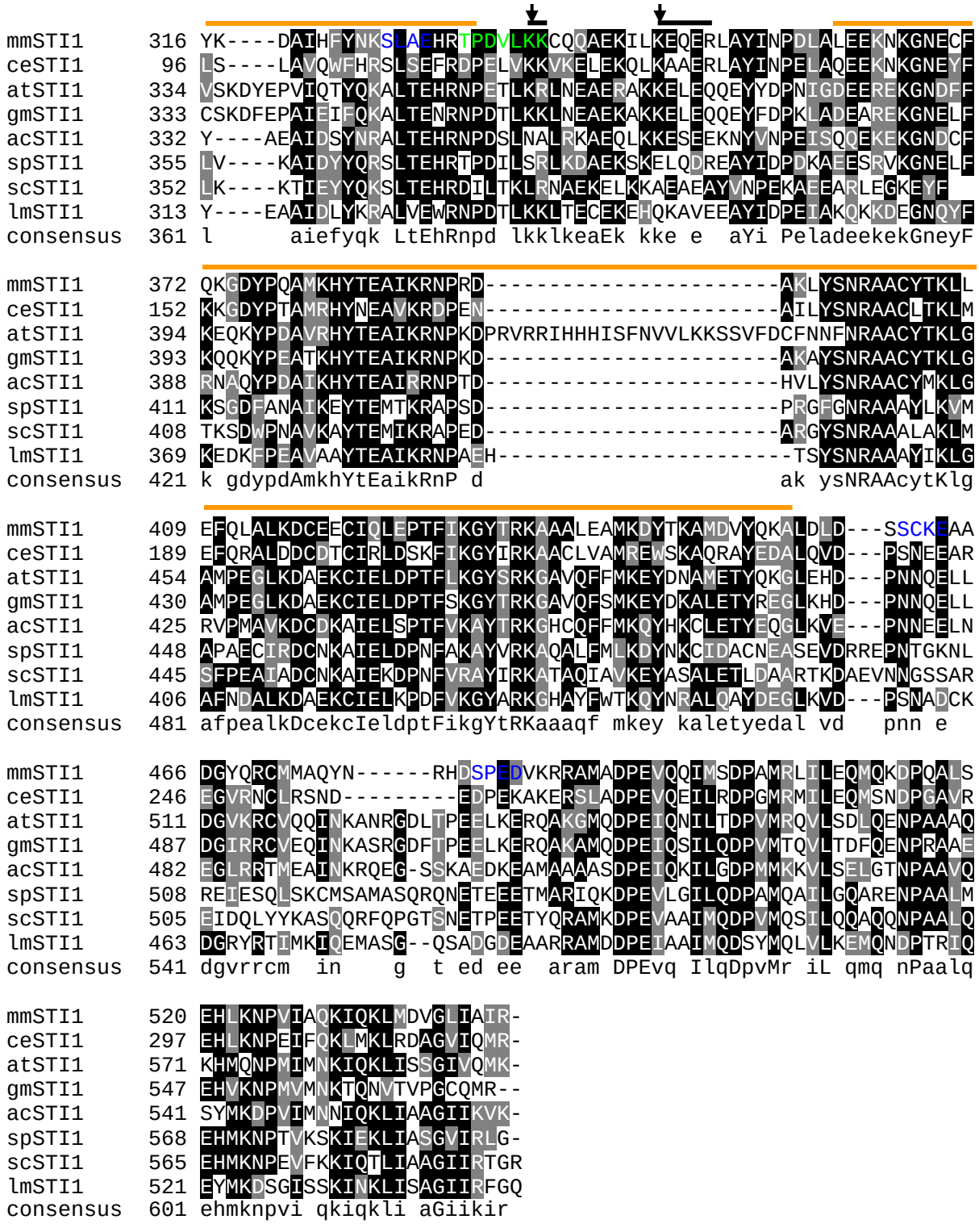

Figure 2.3: The multiple sequence alignment of low e value STI1 proteins

The dark boxes represent the identical and thus conserved residues, and the gray boxes, the structurally similar residues. m mSTI1: *Mus m usculus* (NP_058017), c eSTI1: *Caenorhabditis e legans* (NP_503322), a tSTI1: *Arabidopsis thaliana* (AAF19538), gmSTI1: *Glycine max* (CAA56165), acSTI1: *Acanthamoeba castellanii* (AAB49720), s pSTI1: *Schizosaccharomyces pom be* (NP_588123), s cSTI1: *Saccharomyces cer evisiae* (NP_014670), lmSTI1: *Leishmania major* (AAB37318). The identified CcN motif in mSTI1 is highlighted in red. The basic NLS clusters are indicated with arrowheads. The mSTI1 phosphorylation sites are shown: the CKII site in blue and the cdc2 kinase site in green. The TPRs are indicated with orange lines.

```
mmSTI1 222  NKKQALKEKELGNDAYKKKDFDKALKHYDRAKELDP 256
ceSTI1      MTDAAIAEKDLGNAAYKQKDFEKAHVHYDKAIELDP
atSTI1      KKLKAQKEKELGNAAYKKKDFETAIQHYSTAMEIDD
gmSTI1      RKGQAQKEKEAGNAAYKKKDFETAIGHYSKALELDD
acSTI1      EKKQALEEKELGNQAYKKKDFDTAIVHYKKAFELDP
spSTI1      LKKKADQEKQIGNENYKKRNFPVAIEQYKKAWDTYK
scSTI1      SKIEADKEKAEGNKFYKARQFDEAIEHYNKAWELHK
lmSTI1      NEKEALALKEEGNKLYLSKKFEEALTKYQEAQVKDP
```

Figure 2.4: Conserved blocks in the region of identified CcN motif

The multiple-alignment was assessed for conserved blocks using the BLOCK server. The BLOCK server only identifies significantly conserved blocks of residues. Conserved residues in the region of the identified mSTI1 CcN motif 1 (222-239) (*pink*) together made up a conserved block (222-256). Residues considered to be significantly conserved, K^{223},A^{225}, E^{228}, K^{229}, G^{232}, N^{233}, Y^{236}, K^{237}, K^{238} and K^{239}, are represented as larger letters.

2.3.2 CKII and cdc2 kinase phosphorylation sites are implicated in stabilization of the NLS

The secondary structure prediction showed the mSTI1 protein to be highly helical in nature. The average predicted alpha helix content was 77.3%, the beta sheet content 0.0% and the coil content 22.7%. The CcN motif itself was predicted to be helical with stretches of random coil between 3 helices. The coordinates of the highly helical PP5 protein were therefore considered to be appropriate for modeling of this region using the program WhatIF.

The structures of fragments of Hop in complex with peptides of Hsp70 and Hsp90 have been resolved. However, only the C-terminal fragment of Hop in complex with a peptide of Hsp90 includes any of the predicted mSTI1 CcN motif and only the NLS portion is present. Therefore, the full CcN motif of mSTI1 was modeled on a suitable template such

that the proximal CKII and cdc2 kinase sites at positions S189 and T198 respectively were included. PP5 demonstrated a 34.8% pairwise identity with mSTI1 when the amino acid sequences were compared by pairwise alignment, and therefore was acceptable for homology modeling. However, the program only limited sections of the mSTI1 protein were accepted as being sufficiently similar. The mSTI1 region V^{181}-F^{241} was successfully modeled on PP5 (average score of all contacts –0.191), and produced a helix-turn-helix TPR-like structure comprising 3 helices (Figure 2.5 A). This section of mSTI1 fortunately contained the CcN motif. A long helix containing the CKII (189) and cdc2 kinase (198) sites was terminated by the poly-proline region (199-205) and joined by a coil to a short helix. The NLS region was joined to this short helix by a coil.

Residues involved in the phosphorylation sites from the first helix were significantly close to conserved residues within the NLS in the third helix. A significant side chain contact of 2.87Å was noted between the cdc2 kinase site residue T^{198} and the conserved NLS spacer region residue K^{229} (Figure 2.5 B). This electrostatic contact may stabilize the CcN motif, such that the two lysine-rich ends of the NLS helix are appropriately presented to karyopherin α for recognition and binding. If the cdc2 kinase site residue T^{198} were to be phosphorylated, this T^{198}-K^{229} interaction would be greatly affected. The introduction of a highly negatively charged phosphate group onto T^{198} may increase the attraction of K^{229} for T^{198}. However, the electrostatic environment in the area would be significantly changed, and most likely result in the formation of new and different electrostatic contacts. The new contacts would occur to stabilize the high negative charge, and may especially involve the neighboring positively charged stretch of lysines (K^{237}, K^{238}, K^{239}) at the end of the NLS helix. The NLS helix displayed the conserved lysine residues (K^{222}, K^{223} and K^{237}, K^{238}, K^{239}) to extend from the NLS, on either end of the helix.

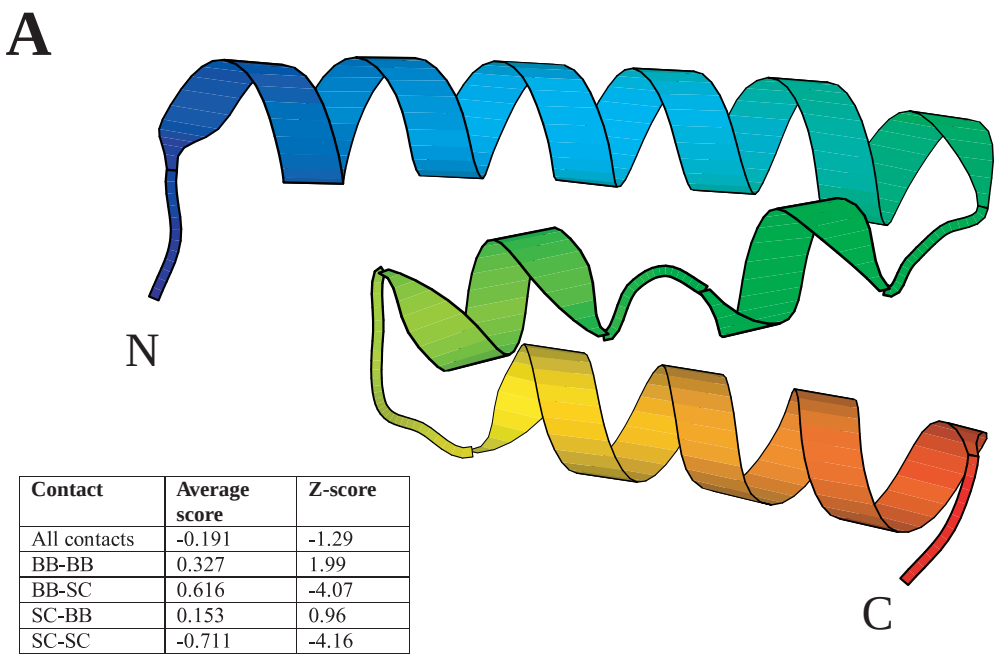

Contact	Average score	Z-score
All contacts	-0.191	-1.29
BB-BB	0.327	1.99
BB-SC	0.616	-4.07
SC-BB	0.153	0.96
SC-SC	-0.711	-4.16

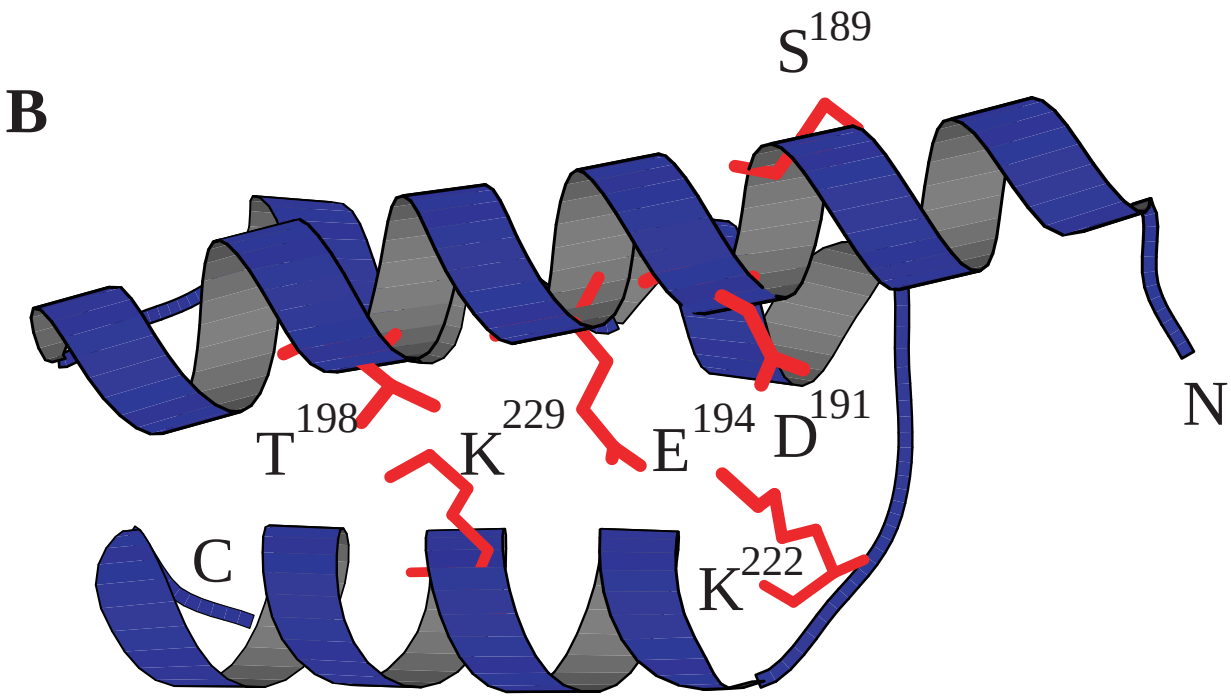

Figure 2.5: Ribbon representation of the predicted structure for the mSTI1 region (V^{181}-F^{241}) that incorporates the CcN motif (S^{189}-K^{239}) using Pp5 as a template

(A) A ribbon representation of the proposed tertiary structure of the mSTI1 CcN motif of mSTI1 (189-239), as modeled on the structural coordinates of the (B) PP5 N-terminal TPR domain. The average contact scores are inserted. The model was generated using WhatIF (Vriend, 1990) and the figure was generated using Molscript (Kraulis, 1991).

The modeling of this section of the CcN motif in mSTI1 is useful since it contributes to an understanding of potential interactions occurring within the CcN motif and between CcN motif residues, namely the flanking phosphorylation sites and the NLS. The T-antigen CcN motif was not modeled because firstly, although it bears significant overall structure similarity to the mSTI1 predicted CcN motif, the NLS of T-antigen is monopartite and therefore differs in structure to the bipartite NLS of mSTI1. Two significant side chain contacts were noted between the CKII site and the first basic arm of the bipartite NLS. The CKII site residue D^{191} and the conserved NLS first basic arm residue K^{222} were 2.95 Å apart (Figure 2.5B). Similarly K^{222} was a distance of 2.91Å from the CKII site residue E^{194} (Figure 2.5B). These two electrostatic contacts may similarly stabilize the basic end of the NLS helix as suggested for the T^{198}-K^{229} contact. The CKII site phosphorylatable residue S^{189}, despite its proximity, may not be directly involved in these contacts as it faces away and outwards from the other side of the helix. Thus, in the limitations of this partial protein model, phosphorylation of this serine residue may not have any significant structural effects on the conformation of the NLS residues included in the model, as has been suggested for the phosphorylation of the T^{198} phosphorylatable residue. Phosphorylation at the S^{189} site in the full mSTI1 protein may, however, certainly change the electrostatic environment of this region of the protein, and induce other conformational changes, potentially influencing the recognition of the NLS by karyopherin-α.

2.3.3 The STI1 NLS interacts with Hsp90

The NLS sequence in mSTI1 was noted to overlap the TPR2 domain, the binding site of Hsp90. The resolved structure of the TPR2 domain of Hop in complex with a peptide (containing the EEVD binding motif) of Hsp90 (Scheufler *et al*., 2000) included the upstream NLS sequence (Figure 2.6). The reported residues of TPR2 involved with electrostatic binding of the EEVD motif of the Hsp90 peptide were K^{229}, N^{233}, N^{264}, K^{301}, and R^{305} (Scheufler *et al.*, 2000). These contact the D^0 of the MEEVD motif of the Hsp90 peptide, to form a two-carboxylate clamp, which is the basis of the Hsp90 binding. In relation to the NLS, the conserved residues K^{229} and N^{233} in the NLS spacer sequence were in close proximity (2.68Å and 3.00Å) to D^0 of the MEEVD motif of the Hsp90 peptide (Figure 2.6A), mediating the peptide binding. The methionine M^{-4} of the Hsp90 peptide engaged in tight hydrophobic interactions with a cavity mainly formed by the sidechains of Y^{226} and E^{271}, and V^{-1} of the EEVD region bound in a hydrophobic pocket formed by N^{233}, N^{264} and A^{267} (Scheufler *et al*., 2000) (Figure 2.6B). Furthermore, Y^{236} contacted E^{-3} (Å) (Figure 2.6B). K^{229}, N^{233} and Y^{236} are conserved in STI1 proteins, and are located in the NLS spacer sequence. These NLS spacer residues may therefore be involved in either Hsp90 binding or karyopherin-α binding, such that this NLS in mSTI1 becomes inaccessible to karyopherin-α when Hsp90 is bound to mSTI1. Structural analyses of the bipartite NLS in the glutocorticoid receptor indicate that the first pair of basic amino acids, and the first few amino acids in the spacer region, lie in an α-helix, such that the basic amino acids are on the face of the helix and exposed to the solvent (Dingwall and Laskey, 1991). The remainder of the spacer region and the downstream basic cluster are disordered in solution. Interestingly, an mSTI1 derivative, which included a K^{229} to alanine amino acid substitution, could not be heterologously expressed in *E. coli* (Tanner, 2001). The NLS spacer K^{229} residue may therefore be critical to maintaining overall mSTI1 protein structural integrity.

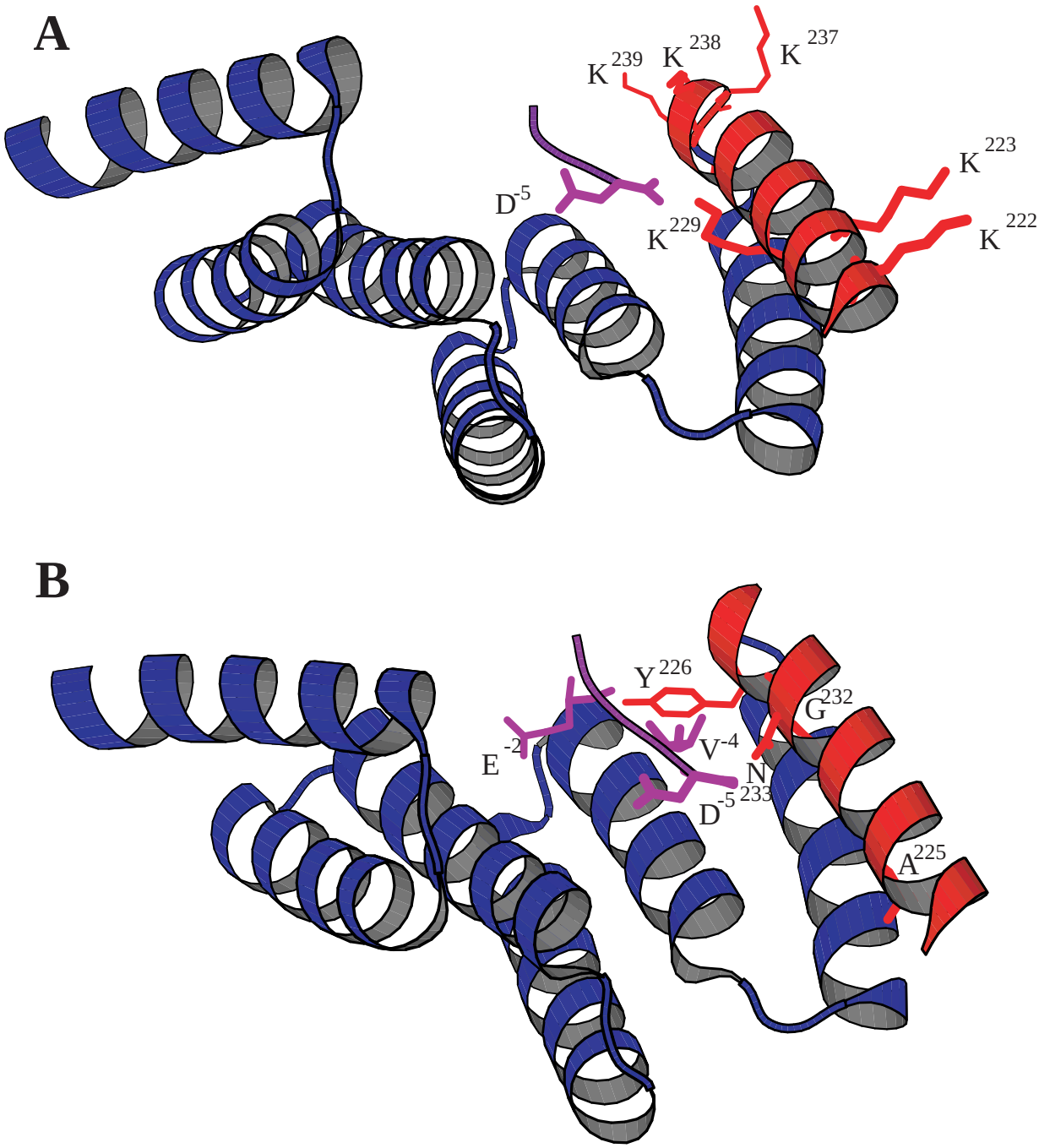

Figure 2.6: The TPR2 domain of Hop in complex with a peptide ofHsp90

A diagrammatic representation of the tertiary structure of the TPR2 domain of Hop in complex with a peptide of Hsp90 (1ELR.pdb). The molecular backbone of the TPR2 domain is depicted in blue with the region identified as the conserved NLS in red. Sidechains are shown in red. The conserved lysines of the bipartite NLS (A), and other significantly conserved residues, which are in close proximity to the Hsp90 peptide (B) are shown. The figure was generated using Molscript (Kraulis, 1991).

The nucleoplasmin bipartite NLS, a similar NLS to the mSTI1 NLS, binds to karyopherin α (Figure 2.7). The nucleoplasmin bipartite NLS consists of two basic clusters which occupy the two bindings sites of karyopherin α used by the monopartite NLS. The sequence linking the two basic clusters is poorly ordered, consistent with its tolerance to mutations (Fontes *et al.,* 2000). This mode of binding explains the structural basis for binding of diverse NLSs to the sole receptor protein (Fontes *et al.,* 2000). This supports previous predictions that the NLS spacer region can be looped out to juxtapose the two basic clusters, suggesting a mechanism whereby two domains can mimic a shorter basic sequence (Dingwall and Laskey, 1991). A direct interaction of mSTI1 and karyopherin α remains to be shown, however the mSTI1 NLS may similarly bind to the binding pocket of karyopherin α, such that the basic clusters of the NLS juxtapose one another, and the spacer region is looped out.

Unfortunately there is no current structural data available for an entire STI1 protein, making predictions of the proximity of the Hsp90 binding domain to the karyopherin α binding site difficult. However, since these proteins are relatively large (Hsp90: 90kDa, karyopherin α: 58 kDa), it is proposed that mSTI1 may not be sterically able to simultaneously bind Hsp90 and karyopherin α, due to the close proximity of their respective binding sites. This alternate binding of Hsp90 or karyopherin α may have mechanistic implications for the formation of the Hsp70/mSTI1/Hsp90 chaperone complex and its localization. Furthermore, conformational changes induced by phosphorylation at various sites proximal to these overlapping binding sites may allow preferential binding of either Hsp90 or karyopherin α. Phosphorylation of sites within the CcN motif may therefore not only be a level of regulation of the import kinetics of the NLS, but also of the assembly of the Hsp70/mSTI1/Hsp90 chaperone complex. Future work could include mSTI1/karyopherin binding assays and competitive binding assays involving ratios of mSTI1, Hsp90 and karyopherin protein.

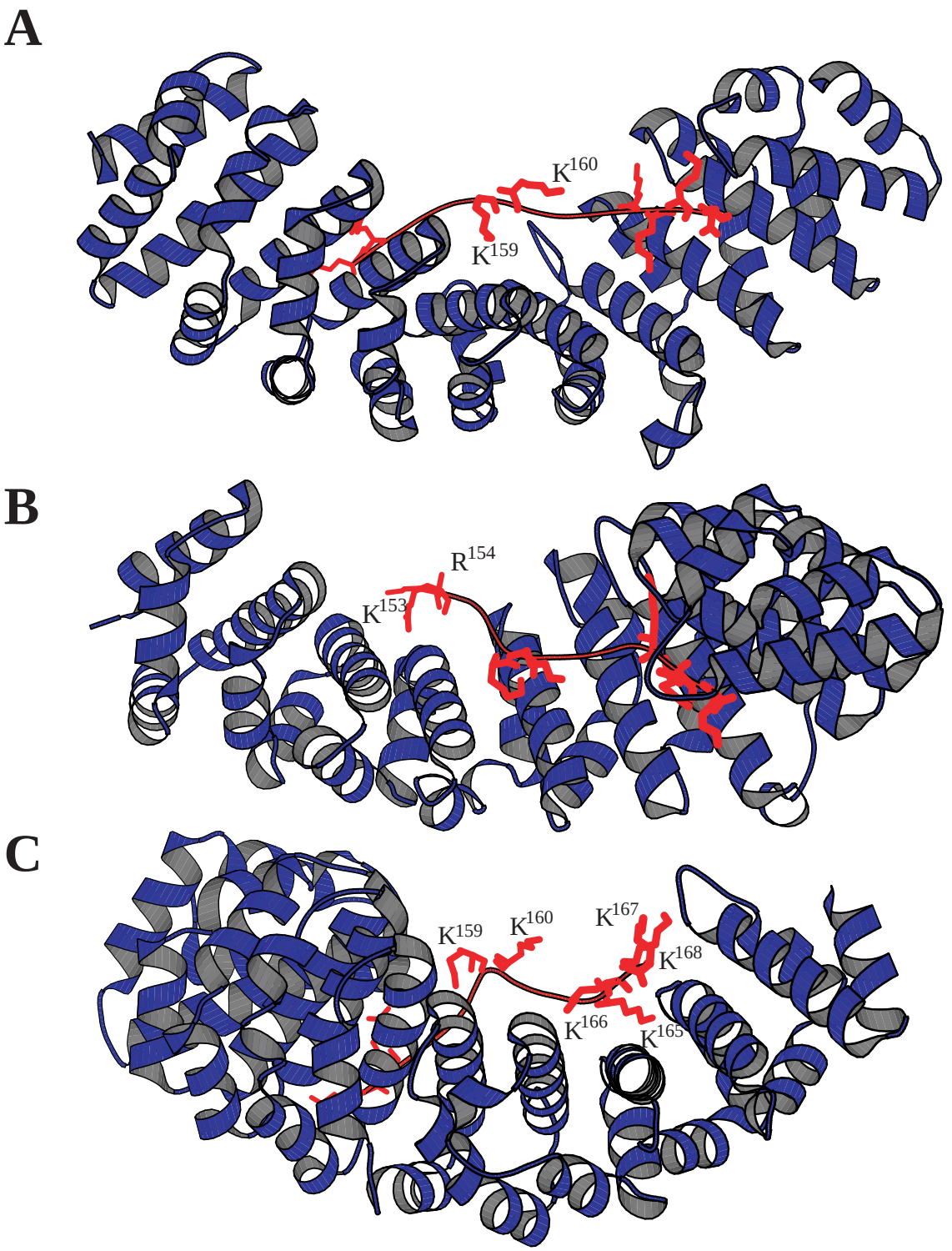

Figure 2.7: The NLS-binding site of mouse karyopherin in complex with the nucleoplasmin bipartite NLS

A diagrammatic representation of the tertiary structure of the NLS-binding site of karyopherin in complex with the nucleoplasmin bipartite NLS (1EJY.pdb). The molecular backbone of the NLS-binding site is depicted in blue and the bipartite NLS in red. Conserved lysine sidechains are shown in red. The conserved lysines of the bipartite NLS are shown from two perspectives (A and B), to bind into two binding pockets of the binding site. The figure was generated using Molscript (Kraulis, 1991).

2.4 CONCLUSIONS

The primary amino acid sequence of mSTI1 was assessed and compared to the primary sequence of other STI1 proteins. The NLS was conserved in STI1 proteins, however the proximal phosphorylation sites to the NLS were not conserved in many STI1 proteins. The NLS, but not the CcN motif, may therefore be conserved in STI1 proteins. In mSTI1 these proximal CKII and cdc2 kinase phosphorylation sites may be involved in stabilization of the NLS, since a model of the CcN motif suggested the CKII site residues, D^{191} and E^{194}, contacted the conserved NLS first basic arm residue, K^{222}. Furthermore, a significant side chain contact was between the cdc2 kinase site residue T^{198} and the conserved NLS spacer region residue K^{229} was noted. These contacts may indicate a electrostatic stabilization of the NLS by the proximal phosphorylation sites such that the NLS is correctly presented for binding to karyopherin-α. This electrostatic stabilization may be affected by phosphorylation at the S^{189} and T^{198} sites, thus affecting the binding of the mSTI1 NLS to karyopherin-α.

In the TPR2 of Hop, the NLS conserved residues K^{229} and N^{233} contacted D^{0} of the MEEVD motif of the Hsp90 peptide. Furthermore, Y^{236} contacted E^{-3} and M^{-4} of the Hsp90 peptide. Hsp90 and karyopherin-α are relatively large (Hsp90: 90kDa, karyopherin-α: 58 kDa), and it is therefore proposed that mSTI1 may not be sterically able to simultaneously bind Hsp90 and karyopherin α, due to the close proximity of their respective binding sites. This alternate binding of Hsp90 or karyopherin α may have mechanistic implications for the formation of the Hsp70/mSTI1/Hsp90 chaperone complex and its localization. Furthermore, conformational changes induced by phosphorylation at various sites proximal to these overlapping binding sites may allow preferential binding of either Hsp90 or karyopherin α. Phosphorylation of sites within the CcN motif may therefore not only be a level of regulation of the import kinetics of the NLS, but also of the assembly of the Hsp70/mSTI1/Hsp90 chaperone complex.

CHAPTER 3

THE SUBCELLULAR LOCALIZATION OF mSTI1

SUMMARY: Endogenous mSTI1 was cytoplasmically localized in all cells, although a small nuclear fraction was observed. An EGFP tag did not affect mSTI1-EGFP localization compared to that of endogenous mSTI1, and the EGFP fusion system was therefore regarded as appropriate for the study of mSTI1 localization. The nuclear fraction of mSTI1 implied the existence of a nuclear import process for mSTI1, suggested to be NLS-dependant nuclear localization. The mSTI1 amino acids 222-239 functioned as an NLS by directing nuclear localization when fused to EGFP. The cytoplasmic localization of mSTI1 could therefore be as a result of cytoplasmic retention or a dynamic nucleocytoplasmic shuttling process.

3.1 INTRODUCTION

3.1.1 The technology of reporter genes

There are a number of *in vitro* reporter genes available for use as markers of gene expression and protein subcellular distribution. Such systems include secreted alkaline phosphatase [SEAP](Berger *et al*., 1988); β-galactosidase [β-gal] (Alam *et al*., 1990); firefly luciferase (De Wet *et al*., 1987); chloramphenicol acetyltransferase [CAT](Gorman *et al*., 1982); and green fluorescent protein [GFP](Chalfie *et al*., 1994). The use of most of the enzymatic reporter gene systems involves the generation of cellular extracts or fractions of transfected cells and subsequent activity assays. This provides only an indirect measurement of gene transfection and expression and of protein distribution. *In vivo* reporter assays are also available for detecting gene transfection in either fixed cells or tissue sections, such as *in situ* β-gal staining (Alam *et al*., 1990); *in situ* β-glucuronidase [GUS](Jefferson *et al.*, 1987); and *in situ* luciferase (Bronstein *et al.*, 1994), assays which allow visualization of transfected cells following staining with enzymatic substrates or antibodies (Kain and Ganguly, 1995). The cultures used for staining experiments, however, must often be produced separately from those utilized to analyze the specific gene of interest.

3.1.2 The green fluorescent protein (GFP) reporter system

The green fluorescent protein (GFP) from the jellyfish *Aequorea victoria* has become an important reporter for monitoring gene expression and protein localization in a variety of cells and organisms. Proteins fused to GFP provide a powerful system to analyze protein expression and targeting to different organelles in living cells (Chalfie *et al.*, 1994; Kain *et al.*, 1995; Rizzuto *et al.*, 1995, Wang and Hazelrigg, 1994).

GFP and GFP-fusion proteins have been successfully expressed in many mammalian cell lines, including COS-1, chicken embryonic retina and EPC carp epithelial tumor cells

(Ogawa *et al*., 1995); CHO-K1 Chinese hamster ovary, BHK-21 baby hamster kidney, and HeLa human cervical carcinoma cells (Zhang *et al*., 1996); PCL human hepatoma B104 rat neuroblastoma, C2C12 mouse muscle and CHO-7 Chinese hamster ovary cells (Ludin *et al*., 1996); GH3 rat pituitary tumor cells (Plautz *et al*., 1996); PA317 and NIH 3T3 murine fibroblast cells (Cheng *et al*., 1996); COS-7, HeLa and NIH 3T3 cells (Pines, 1995); C 127 murine adenocarcinoma cells (Htun *et al*., 1996); and RBL 2H3 cells (Yokoe and Meyer, 1996).

GFP expressed in eukaryotic cells yields green fluorescence when cells are excited by ultraviolet (UV) or blue light. The chromophore in GFP is intrinsic to the primary structure of the protein. The artificial addition of a tag to the protein of interest is offset by the advantages of not requiring additional co-factors, substrates, or additional gene products (Chalfie *et al*., 1994; Stearns, 1995). In addition, GFP fluorescence is species independent and can be monitored non-invasively using techniques of fluorescence microscopy, flow cytometry, and macroscopic imaging (Chalfie *et al*., 1994; Kain *et al*., 1995; Inouye and Tsuji, 1994). GFP has been shown to tolerate both C- and N-terminus fusions to proteins without affecting their normal functionality (Cubitt *et al*., 1995; Ludin *et al*., 1996; Ogawa *et al*., 1995). Recently, variants in GFP that fluoresce at different wavelengths (cyan and yellow fluorescent proteins) have been used simultaneously for co-localization studies. This technology has been termed FRET (Flourescence Resonance Energy Transfer) and allows the study of conformational changes in proteins at a single molecule level as well as in the native *in vivo* context of a living cell (Heyduk, 2002). Direct *in vivo* protein interactions can be investigated using FRET, as well as oligomerization and dimerization of proteins (Overton and Blumer, 2002) and detection of the kinetics of *in vivo* protein folding (Ratner *et al.,* 2002). Another recent application of GFP variants has been termed FRAP (Fluorescence Recovery After Photobleaching) and allows the detection of GFP-protein translocation in the cell to an area lacking fluorescence (Falk, 2002) and the examination of cellular dynamics (Klonis *et al*. 2002). GFP-GR, expressed in mammalian cells, has been shown to be cytoplasmic using FRAP studies, but translocates to foci in the nucleus in a hormone-dependent manner (Htun *et*

al., 1996). Recently, the use of GFP fusion proteins has been extended into investigations of nuclear import and export of cytoplasmic proteins (Hanaka *et al.,* 2002).

3.1.3 The EGFP variant

Enhanced GFP (EGFP) is a unique GFP variant (Zhang *et al*., 1996) which contains chromophore mutations (Phe64 to Leu; Ser65 to Thr) that enhance the fluorescence 35 times above that of wild-type GFP (Cormack *et al*., 1996). The EGFP variant is also codon-optimized for higher expression in mammalian cells, by using the favoured codons of highly expressed human proteins in place of the corresponding *Aequorea victoria* codons (Chiu *et al*., 1996). The greater fluorescence and improved folding characteristics allows earlier detection of expression. The codon optimization allows increased translation efficiency (5-10 fold) (Cormack *et al*., 1996). These features of EGFP overcome many of the disadvantages found to be associated with the use of wild-type GFP, namely low fluorescence signal, a lag in the development of fluorescence after protein synthesis, as well as poor expression in several mammalian cell types (Stearns, 1995; Haas *et al*., 1996; Heim *et al*., 1995). The EGFP variant is often routinely used as a better detection system than many of the original GFP variants (Bunnell *et al.,* 2002).

3.1.4 The distribution of GFP in the cell

The fluorescence of GFP, when expressed in mammalian cells, independent of cell type examined but with some exceptions, has been found to be uniformly distributed throughout the cytoplasm and nucleus (Carey *et al*., 1996; Chiochetti *et al*., 1997; Ludin *et al*., 1996; Ogawa *et al*., 1995; Pines, 1995), but excluded from the nucleoli (Dobson *et al*., 1996; Plautz *et al*., 1996) and vesicular organelles (Cubitt *et al*., 1995). No noticeable binding to any intracellular structures has been observed (Ludin *et al*., 1996). There have been reports of a slight concentration of GFP in the nucleus of wild-type GFP expressing CHO-T cells (Dobson *et al*., 1996) and mutants S65T GFP in GH3 cells (Plautz *et al*., 1996).

3.1.7 The use of NLS-GFP fusions in subcellular localization studies

The correct localization of proteins in eukaryotes involves complex targeting reactions. The NLS is recognized by cytoplasmic NLS receptors that dock at the nuclear pore complex, which subsequently catalyzes the translocation across the nuclear envelope (Görlich and Mattaj, 1996). Transport across the nuclear membrane is mediated by nuclear pore complexes that allow proteins that are 40 kDa or less to enter by passive diffusion (Stochaj and Silver, 1992; Paine, 1975; Paine *et al.*, 1975; Harootunian, 1993). By contrast, proteins that exceed the size of the diffusion channel, 40 kDa, enter the nucleus by a facilitated process that requires energy and an NLS. Polypeptides larger than 70 kDa are excluded from nuclei if they do not carry a functional NLS (Paine *et al.*, 1975; Harootunian, 1993).

Previously developed systems to study nuclear protein traffic in higher eukaryotes have been based on *in vitro* reconstitution or on injection of nuclear substrates into single cells; both time-consuming and laborious approaches (Stochaj and Silver, 1992). These techniques however, do not allow post-translation modification studies such as phosphorylation, which can modulate nuclear traffic (Jans *et al.*, 1995). Hybrid GFP proteins containing N-terminal nuclear localization sequences have also been used to establish functionality of such NLS sequences by their ability to localize the hybrid GFP protein to the nucleus (Chatterjee *et al.*, 1997). GFP diffuses into the nucleus via passive diffusion and not by active recognition of an NLS, since multiple copies of GFP, excluded by its size from diffusion across the nuclear pore, did not enter the nucleus (Chatterjee *et al.*, 1997). Since no NLS has yet been recognized in GFP, the fusion of an NLS to GFP and a subsequent change in localization from the typical diffuse ubiquitous GFP distribution, to one on nuclear localization is significant, since this requires continual active nuclear import to overcome passive diffusion out of the nucleus. This makes NLS-GFP fusions valuable tools for the analysis of nuclear transport.

3.1.8 Specific hypothesis, aims and objectives

The subcellular localization of mSTI1 is mostly cytoplasmic, although a nuclear fraction does exist (Lässle *et al.*, 1997). Recently, STI1 has been shown to also be localized at the cell membrane in prion-infected cells (Zanata *et al.*, 2002). The nuclear fraction of mSTI1 implied the existence of a nuclear import process for mSTI1. Previous localization studies of mSTI1 or its homologs, however, used an immunostaining approach against mSTI1, limiting these studies to that of unmodified endogenous mSTI1. The exogenous EGFP fusion expression system was an appropriate system for localization studies of mSTI1 and modified mSTI1 under controlled conditions. Therefore, a pB-mSTI1-EGFP construct was produced for the expression of mSTI1, fused in-frame to EGFP, in mouse NIH 3T3 fibroblasts. The expression of exogenous mSTI1 therefore allowed the study of modified mSTI1, under controlled conditions.

It is hypothesized that the localization of mSTI1 is controlled by NLS-dependent nuclear localization of mSTI1. A putative bipartite NLS sequence has been reported in the central region of mSTI1 (Blatch *et al.,* 1997). This sequence conforms to the consensus sequence for bipartite NLSs, which consists of two series of basic residues separated by a 10 - to 12 - amino acid spacer (Dingwall and Laskey, 1991). The identification of NLS sequences requires that the NLS is active in nuclear targeting of a normally cytoplasmic localized carrier protein, either as a peptide covalently coupled to the carrier or when encoded in the same reading frame as a fusion protein (Jans and Hübner, 1996). Therefore, to establish functionality, the mSTI1 NLS (amino acids 222-239) was expressed as an N-terminal in-frame fusion with EGFP in mouse NIH 3T3 fibroblasts. In addition, the co-localization of mSTI1-EGFP and endogenous mSTI1 was established and thus any effect of the EGFP fusion on the localization of mSTI1 determined.

3.2 EXPERIMENTAL PROCEDURES

The vendors of the materials used are described in Appendix A (A) and the general procedures used are described in Appendix B (B). The identity and characteristics of the primers used are described in Appendix C (C) and subcloning steps are described in Appendix D (D). The maps of the plasmid vectors used are shown in Appendix E (E).

3.2.1 The PCR amplification of mSTI1 cDNA

The mSTI1 open reading frame (ORF) was amplified from the pGEX3X2000 template plasmid DNA (Lässle *et al*., 1997, vector map E.1), by PCR (B.1), using the mSTI1-specific forward primer: PCRmSTI1pCineoF and the reverse primer: PCRmSTI1pCineoR (C, Table C.1). PCRmSTI1pCineoF was designed such that a Kozak sequence (Kozak, 1983) was introduced immediately preceding the start codon. The resultant PCR product encompassed the mSTI1 open reading frame immediately preceded by a *Nhe*I site, and followed by a *Sac*II site downstream of the deleted mSTI1 stop codon. The PCR product was resolved by agarose gel electrophoresis and gel-purified (B.2).

3.2.2 The ligation of the PCR product into pGEM(T) and screening of transformants

The PCR product was ligated to pGEM(T) vector DNA (B.3, E.2), and transformed into *E. coli* XL1Blue supercompetent cells (B.4). Transformants were screened for putative pGEM(T)mSTI1[*Nhe*I/*Sac*II] plasmid DNA (B.5). Plasmid DNA was extracted from *E. coli* cultures of transformants forming white colonies, by a modified alkaline lysis method (Birnboim and Doly, 1979; Joly, 1996) and using the High Pure Plasmid Isolation Kit (B.5). Putative pGEM(T)mSTI1[*Nhe*I/*Sac*II] plasmid DNA was restricted separately with *Nhe*I, in medium salt buffer, and with *Sac*II in Tris-acetate buffer (B.6). Plasmid DNA *Nhe*I and *Sac*II restriction fragments were resolved by agarose gel electrophoresis (B.2) and those plasmid digestions containing fragments migrating

expected distances corresponding to sizes of 3015-bp and 1600-bp were regarded as pGEM(T)mSTI1[*Nhe*I/*Sac*II] (D.1).

3.2.3 The directional ligation of mSTI1 cDNA into the pCineo-EGFP construct

The PCR-amplified mSTI1 cDNA was inserted in-frame with EGFP cDNA: Bulk pGEM(T)mSTI1[*Nhe*I/*Sac*II] and pCineo-EGFP (kindly provided by Prof Arbuthnot, University of the Witwatersrand, vector map E.3) were separately restricted in double digests, with *Nhe*I and *Sac*II (B.7) and resolved by agarose gel electrophoresis (B.2). The appropriate bands (6207-bp and 1600-bp for pCineo-EGFP and mSTI1 cDNA respectively) were excised and extracted from the agarose gel (B.2). The 1600-bp mSTI1 cDNA insert was ligated to the 6207-bp pCineo-EGFP construct such that mSTI1 cDNA was ligated 5' to, and in-frame with, EGFP cDNA present in the pCineo-EGFP construct. Ligation reactions were transformed into competent *E. coli* XL1Blue cells (B.8), plasmid DNA extracted and screened by *Hind*III restriction in potassium buffer (B.6). Plasmid DNA *Hind*III restriction fragments were resolved by agarose gel electrophoresis (B.2) and those plasmid digestions containing fragments migrating expected distances corresponding to sizes of 3815-bp, 2748-bp and 1239-bp, were regarded as pCineo-mSTI1-EGFP (D.2). The insert region of pCineo-mSTI1-EGFP was not yet sequenced due to the low copy number and poor extraction of pCineo-mSTI1-EGFP (characteristics typical of a mammalian construct). Further cloning was first performed before sequencing of the mSTI1-EGFP insert was attempted.

3.2.4 The directional ligation of EGFP and mSTI1-EGFP cDNA into the pSK vector

Bulk pCineo-mSTI1-EGFP and pCineo-EGFP were restricted in a double digest with *Nhe*I and *Sac*II in medium salt restriction buffer (B.6, B.7). DNA overhangs were filled in using T4 polymerase (B.9). *Not*I was subsequently added to the digestions, as well as

high salt buffer (B.6). Restricted plasmid DNA was ethanol precipitated (B.7) and resolved by agarose gel electrophoresis (B.2). The appropriate bands (2378-bp and 764-bp, for mSTI1-EGFP and EGFP cDNA respectively) were excised and extracted (B.2). Bulk pSK was restricted with *Eco*RV and *Not*I in high salt restriction buffer, ethanol precipitated and resolved by agarose gel electrophoresis (B.7). The appropriate band (3000 -bp for pSK DNA) was excised and extracted (B.2).

The gel-purified 2378-bp mSTI1-EGFP cDNA insert and the 764 -bp EGFP cDNA insert were separately ligated to the restricted, gel-purified 3000 -bp pSK vector (B.7, E.4). Ligation reactions were transformed into *E. coli* XL1Blue (B.8). Putative pSK-mSTI1-EGFP and pSK-EGFP plasmid DNA were screened by *Xho*I and *Not*I restriction, in high salt buffer and resolved by agarose gel electrophoresis (B.5, B.6). Those plasmid digestions containing fragments migrating expected distances corresponding to the size of 5378 -bp (linearized pSK-mSTI1-EGFP), 3000-bp and 2378 -bp (pSK and released mSTI1-EGFP cDNA insert), were regarded as pSK-mSTI1-EGFP (D.3). Those plasmid digestions containing fragments migrating expected distances corresponding to the size of 3764-bp (linearized pSK-EGFP), 3000-bp and 764-bp (pSK and excised EGFP cDNA insert), were regarded as pSK-EGFP (D.3).

The insert regions of pSK-EGFP and pSK-mSTI1-EGFP were sequenced according to the chain termination method (Fangan *et al.,* 1999), using the Big Dye™ ready reaction kit (B.10).

3.2.5 The directional ligation of EGFP and mSTI1-EGFP cDNA into the pB vector

The mammalian expression vector pB (BCMGSNeo, Karasuyama and Melchers, 1988) was used in this study for cloning (via a subcloning step using the pSK vector) and transfection of the required cDNA sequences. BCMGSNeo (hereafter referred to as pB, E.5) is a shuttle vector containing an *Escherichia coli* origin of replication, a β-lactamase-encoding gene for ampicillin resistance (for selection of transformed *E. coli*

cells), as well as neomycin resistance genes for mammalian cell plasmid maintenance, and elements for gene expression in mammalian cells. An existing bovine papilloma virus (-BPV)-based expression vector, pBV-1MTHA, was modified by Karasuyama and Melchers (1988) to produce pB to allow transformed X63Ag8-653 myeloma cells, NIH 3T3 fibroblasts and C127 mammary tumor cells to stably carry multiple copies of the vector, as well as express the inserted cDNA constitutively and in high quantities. pB is maintained Episomally, and cell lines transformed with pB stably carry 30-100 copies of the plasmid per cell (Karasuyama and Melchers, 1988). Plasmids containing certain -BPV DNA sequences have been found in many cases to be propagated as stable extrasomal elements in transformed cells (Sarver *et al.*, 1981). Transformed cells usually carry a high copy number of -BPV plasmids (20-100 copies/cell), which carry transcriptional enhancer elements (Lusky *et al.*, 1983) and therefore often produce high levels of recombinant proteins. The episomal nature of pB made this vector an attractive option for the expression of mSTI1-EGFP in NIH 3T3 murine fibroblasts, and for the generation of transfectants that could be pooled to form episomally stable cell lines.

Bulk pSKmSTI1-EGFP, pSK-EGFP and pB vector were separately restricted with *Xho*I and *Not*I in high salt restriction buffer, ethanol precipitated and resolved by agarose gel electrophoresis (B.7). The appropriate bands (14.5-kbp, 2378-bp and 764-bp for pB, mSTI1-EGFP and EGFP cDNA respectively) were excised and extracted from the agarose gel (B.2). The gel-purified 2378-bp mSTI1-EGFP cDNA insert and the 764-bp EGFP cDNA insert were separately ligated to the restricted and gel-purified 14.5-kbp pB vector (B.7). Ligation reactions were transformed into *E. coli* XL1Blue (B.8). Putative pSK-mSTI1-EGFP and pSK-EGFP plasmid DNA was screened by *Hin*dIII restriction, in medium salt buffer, and resolved by agarose gel electrophoresis (B.5, B.2). Those plasmid digestions containing fragments migrating expected distances corresponding to the sizes of 7700-bp, 5000-bp, 3790-bp and 902-bp were regarded as pB-mSTI1-EGFP. Those plasmid digestions containing fragments migrating expected distances corresponding to the sizes of 7700-bp, 4350-bp and 3310-bp, were regarded as pB-EGFP.

3.2.6 The PCR amplification of EGFP and insertion into pGEM(T)

The EGFP ORF was amplified from the pCineo-EGFP template DNA plasmid (300 ng) by PCR (B.1) using the EGFP-specific forward primer: EGFP-NLSmSTI1-F (a 95-mer including a Kozak sequence followed by the cDNA encoding the mSTI1 NLS at amino acid positions 222-239) and the reverse primer: EGFP-NLS-R (C). The cycling parameters were as described in B.1 except that an annealing temperature of 50 °C was used instead of 55 °C. The resultant PCR product encompassed the EGFP open reading frame immediately preceded by the NLS^{mSTI1} cDNA at the 5' end, and including EGFP's own stop codon at the 3' end. Restriction endonuclease sites were engineered such that the resultant NLS^{mSTI1}EGFP PCR product was flanked by *Xho*I and *Not*I sites at the 5' and 3' terminals, respectively. The PCR product was resolved by agarose gel electrophoresis (B.2), ligated to pGEM(T) plasmid DNA (B.3, E.2), and transformed into *E. coli* XL1Blue cells (B.4). Transformants containing putative pGEM(T)NLS^{mSTI1}EGFP[*Xho*I/*Not*I] were screened (B.5). Plasmid DNA was extracted from cultures of transformants forming white colonies (B.6). Putative pGEM(T)NLS^{mSTI1}EGFP[*Xho*I/*Not*I] plasmid DNA was restricted with *Xho*I and with *Sal*I in high salt restriction buffer (B.6). A double digest, such that putative pGEM(T)NLS^{mSTI1}EGFP[*Xho*I/*Not*I] plasmid DNA was restricted with both *Nhe*I and *Sac*II, was performed in Tris-acetate buffer (B.6). Plasmid DNA exhibiting fragments migrating the expected distances corresponding to sizes of 3015-bp and 1600-bp (pGEM(T) vector and mSTI1 insert respectively) were regarded as pGEM(T)NLS^{mSTI1}EGFP[*Xho*I/*Not*I] (D.5).

3.2.7 The directional insertion of NLS^{mSTI1}EGFP cDNA into the pB vector

Bulk pGEM(T)NLS^{mSTI1}EGFP[*Xho*I/*Not*I] and pB vector were separately restricted in double digests, with *Xho*I and *Not*I, ethanol precipitated and gel-purified (B.7, B.2). The

appropriate bands (815-bp and 14.5-kbp for NLS^{mSTI1}EGFP and pB respectively) were excised and extracted from the agarose gel (B.2). The 815-bp NLS^{mSTI1}EGFP cDNA insert was ligated to the 14.5 k-bp pB vector (B.7, E.5) to produce pB-NLS^{mSTI1}EGFP. Ligation reactions were transformed into *E. coli* XL1Blue (B.8). Putative pB-NLS^{mSTI1}EGFP plasmid DNA was screened by *Hin*dIII restriction, in medium salt buffer, and resolved by agarose gel electrophoresis (B.5, B.2). Those plasmid digestions containing fragments migrating expected distances corresponding to the sizes of 7700-bp, 5000-bp, 3790-bp and 902-bp were regarded as pB-NLS^{mSTI1}EGFP.

3.2.8 Localization of EGFP, mSTI1-EGFP and endogenous mSTI1 in mouse NIH 3T3 fibroblasts

Purified preparations of pB-mSTI1-EGFP and pB-EGFP plasmid DNA were prepared using a modified alkaline lysis procedure (Birnboim and Doly, 1979; Joly, 1996) and the QIAGEN Maxiprep kit (B.11). Mouse NIH 3T3 fibroblasts were cultured (B.12) and transfected either transiently or stably (B.13) and visualized by confocal laser scanning fluorescence microscopy (B.14). Transient pB-mSTI1-EGFP transfectants were prepared (B.13), immunostained using the mSTI1-specific SF1 antibody (Lässle *et al*., 1997)(B.15) and visualized by confocal laser scanning fluorescence microscopy (B14).

3.3 RESULTS AND DISCUSSION

3.3.1 Mammalian constructs expressing chimeric proteins are successfully produced

3.3.1.1 pB-EGFP and pB-mSTI1-EGFP

We have shown previously that mSTI1 is predominantly localized in the cytoplasm, using immunostaining techniques (Lässle *et al.,* 1997). To determine the subcellular localization of mSTI1 *in vivo* in a system that could be subsequently engineered to produce modified mSTI1 proteins, a fusion of mSTI1 with EGFP at its C-terminus (mSTI1-EGFP) was constructed.

The mSTI1 cDNA PCR amplification reaction successfully yielded a 1600-bp DNA product which was ligated into pGEM(T) (D.1) and into pCineo-EGFP (D.2). The EGFP and mSTI1-EGFP cDNA from pCineo-EGFP and pCineo-mSTI1-EGFP were further subcloned into the vector pSK (D.3) to introduce the *Xho*I restriction site, so that further cloning into pB was possible. The EGFP cDNA from pSK-EGFP was finally inserted into the vector pB to produce pB-EGFP (Figure 3.1A) which, upon *Hind*III digestion, yielded the expected 7700-bp, 4350-bp and 3310-bp fragments (Figure 3.1D, lane 4). The mSTI1-EGFP cDNA from pSK-mSTI1-EGFP were finally inserted into the vector pB to produce pB-mSTI1-EGFP (Figure 3.1B) which, upon *Hind*III digestion resulted in 7700-bp, 5000-bp, 3790-bp and 902-bp fragments (Figure 3.1E, lane 4). The digestion of pB with *Hind*III, by comparison, produced 7700-bp and 6880-bp fragments (Figure 3.1D and 4E, lanes 3). Sequencing of the subclone pSK-mSTI1-EGFP plasmid confirmed the in-frame fusion of the mSTI1 with the EGFP cDNA. Transfectants of these plasmids exhibited bright fluorescence, indicating the correct translation in-frame as well as correct folding of the EGFP moiety at least, since the GFP chromophore is fluorescent only when encapsulated inside the correctly folded protein (Cubitt *et al.,* 1995).

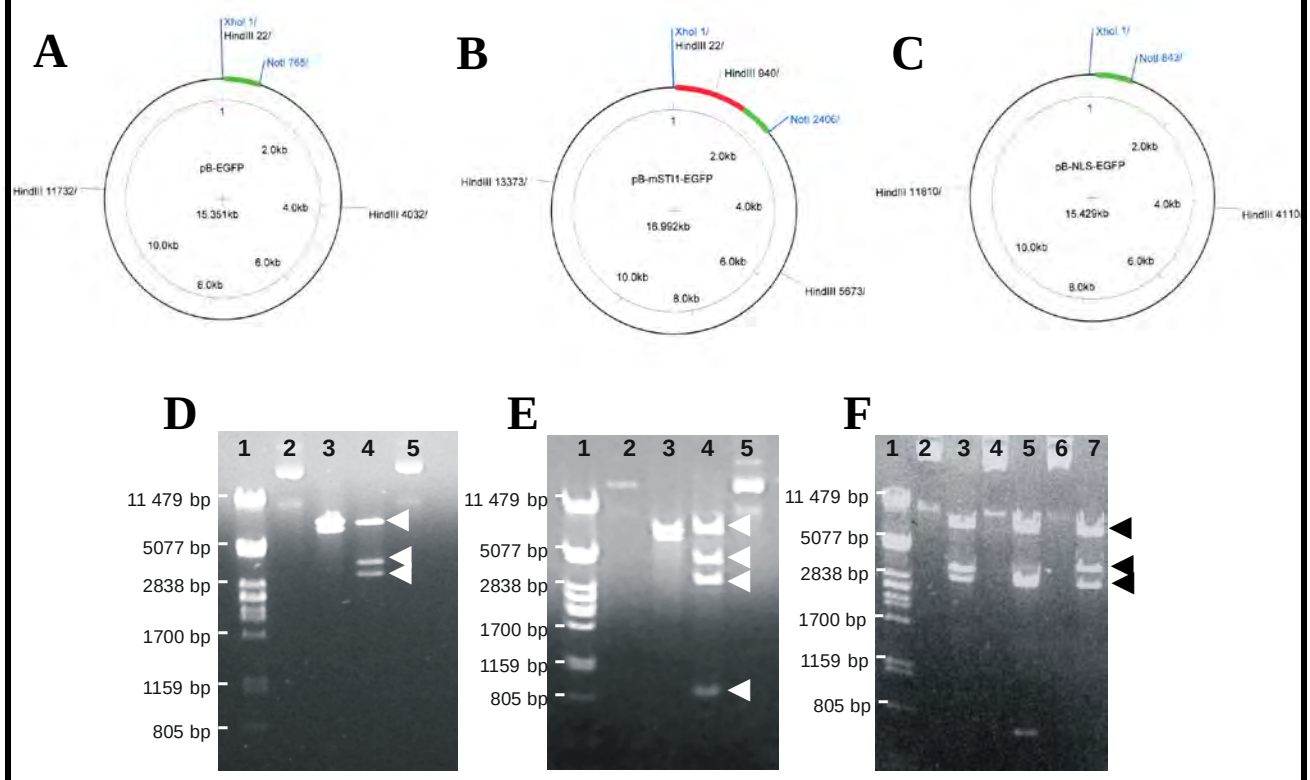

Figure 3.1: Mammalian constructs expressing chimeric proteins are successfully produced

The products of *Hind*III digested pB-EGFP(A), pB-mSTI1-EGFP (B) and pB-NLS^{mSTI1}EGFP (C) were resolved by agarose (0.7% w/v) gel electrophoresis. Lambda DNA digested with *Pst*I was used as a molecular marker (D-F, lanes 1). (D) The *Hind*III digest of pB-EGFP (lane 4) produced the expected 7700-bp, 4350-bp and 3310-bp fragments compared to the 7700-bp and 6880-bp fragments produced by *Hind*III digestion of pB (lane 3). Undigested pB (lane 2) and pB-EGFP (lane 5) were included. (E) The *Hind*III digest of pB-mSTI1-EGFP (lane 4) produced the expected 7700-bp, 5000-bp, 3790-bp and 90 -bp fragments compared to the 7700-bp and 6880-bp fragments produced by *Hind*III digestion of pB (lane 3). Undigested pB (lane 2) and pB-mSTI1-EGFP (lane 5) were included. (F) The *Hind*III/*Not*I double digest of pB-NLS^{mSTI1}EGFP (lane 7) produced the expected 7700-bp, 4100-bp and 3260-bp fragments compared to the 7700-bp, 3300-bp, 3260 and 800-bp fragments produced by *Hind*III/*Not*I digestion of pB-EGFP (lane 5) and 7700-bp, 3600-bp and 3300-bp fragments by *Hind*III/*Not*I digestion of pB (lane 3). Undigested pB (lane 2), pB-EGFP (lane 4) and pB-NLS^{mSTI1}-EGFP (lane 6) were included. The red lines represent mSTI1 cDNA and the green lines, GFP cDNA.

3.3.1.2 pB-NLS^{mSTI1}EGFP

The NLS^{mSTI1}EGFP cDNA PCR amplification reaction successfully yielded an expected 815-bp fragment (D.4) which was ligated into pGEM(T) (D.4). The NLS^{mSTI1}EGFP cDNA was inserted into pB to produce pB-NLS^{mSTI1}EGFP (Figure 3.1C). *Hind*III digestion of pB-NLS^{mSTI1}EGFP produced the expected 7700-bp, 4100-bp and 3260-bp fragments (Figure 3.1F, lane 7). Sequencing of pGEM(T)NLS^{mSTI1}EGFP[*Xho*I/*Not*I] confirmed the sequence and in-frame fusion of the NLS^{mSTI1} with the EGFP cDNA.

3.3.2 mSTI1 is cytoplasmic and co-localizes with mSTI1-EGFP

Normal NIH 3T3 fibroblasts were analyzed for mSTI1 localization by immunostaining and confocal laser fluorescence microscopy. Endogenous mSTI1 was mainly localized in the cytoplasm of NIH 3T3 cells (incidence of 77%), in a perinuclear pattern (Figure 3.2A), confirming previous reports (Lässle *et al.,* 1997). A small fraction of fluorescence was noted in the nucleus. To determine if the EGFP moiety affected the subcellular distribution of mSTI1, co-localization of endogenous mSTI1 with mSTI1-EGFP, using an anti-mSTI1 antibody was performed on both transfected and untransfected cells. The exogenous mSTI1-EGFP as detected by both EGFP fluorescence and Cy3 immunofluorescence had a nonoverlapping staining pattern with endogenous mSTI1 (Figure 3.2B). This suggested that the fusion of EGFP to the C-terminal of mSTI1 had no significant effect on its subcellular distribution.

3.3.3 mSTI1-EGFP is predominantly cytoplasmic

Mouse NIH 3T3 fibroblasts, stably expressing mSTI1-EGFP and EGFP, were analyzed by confocal laser fluorescence microscopy. mSTI1-EGFP was mainly localized in the cytoplasm of NIH 3T3 cells (incidence of 87%), in a perinuclear pattern, whereas EGFP

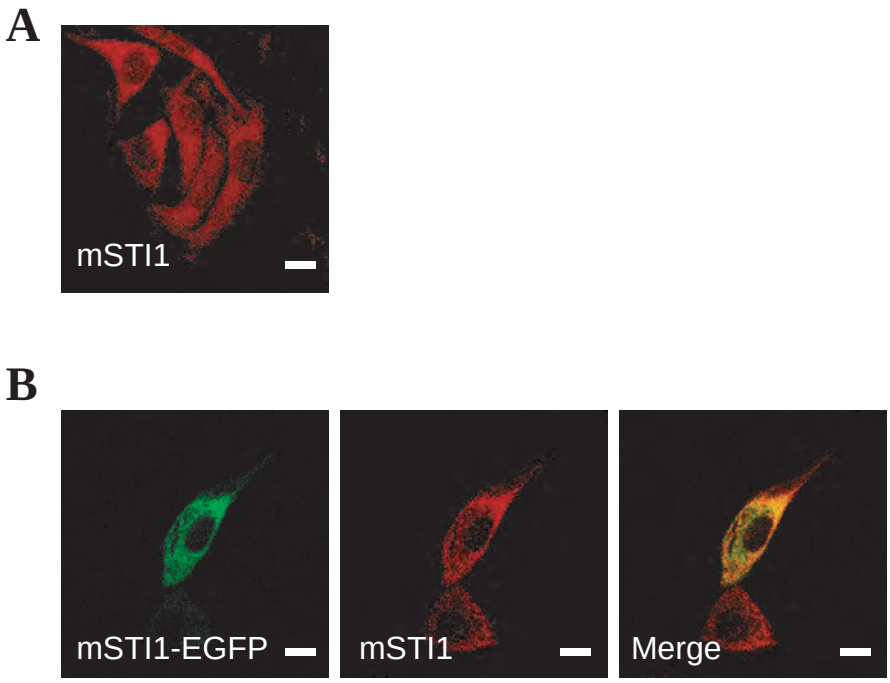

Figure 3.2: mSTI1 was cytoplasmic and co-localized with mSTI1-EGFP

(A) Mouse NIH 3T3 fibroblasts were fixed in 3.7% paraformaldehyde, immunostained with SF1 polyclonal rabbit anti-mSTI1 and Cy3-conjugated donkey anti-rabbit and visualized by confocal laser fluorescence microscopy. Scale bars represent 10 micrometers. (B) Mouse NIH 3T3 fibroblasts transiently transfected with pB-mSTI1-EGFP were fixed in 3.7% paraformaldehyde, permeabilized in 0.1% saponin, immunostained with SF1 polyclonal rabbit anti-mSTI1 and Cy3-conjugated donkey anti-rabbit. Cells were visualized by confocal laser fluorescence microscopy. Scale bars represent 10 micrometers.

was found to localize throughout the cell in all cells (Figure 3.3). A small fraction of fluorescence was noted in the nucleus, while the plasma membrane was negative. This pattern may suggest expression at, or close to, the microtubule-organizing centre. Similar observations of GFP-mSTI1 chimeric proteins have been made previously by our group (Metcalf, 1998).

The cytoplasmic localization of mSTI1 could be as a result of cytoplasmic retention or a dynamic nucleocytoplasmic shuttling process. mSTI1 may be anchored in the cytoplasm through binding to a cytoplasmic retention factor. This may imply that nuclear import of mSTI1 does not occur, and the proposed NLS is non-functional. Conversely, this cytoplasmic localization may be the result of a dynamic nucleocytoplasmic shuttling process in which nuclear export of mSTI1 is more efficient than nuclear import. Nucleocytoplasmic shuttling of mSTI1 would require the presence of a functional NLS driving nuclear import. The basis of mSTI1 cytoplasmic localization was further elucidated by establishing the functionality of the mSTI1 NLS and the occurrence of nuclear export of the mSTI1 protein.

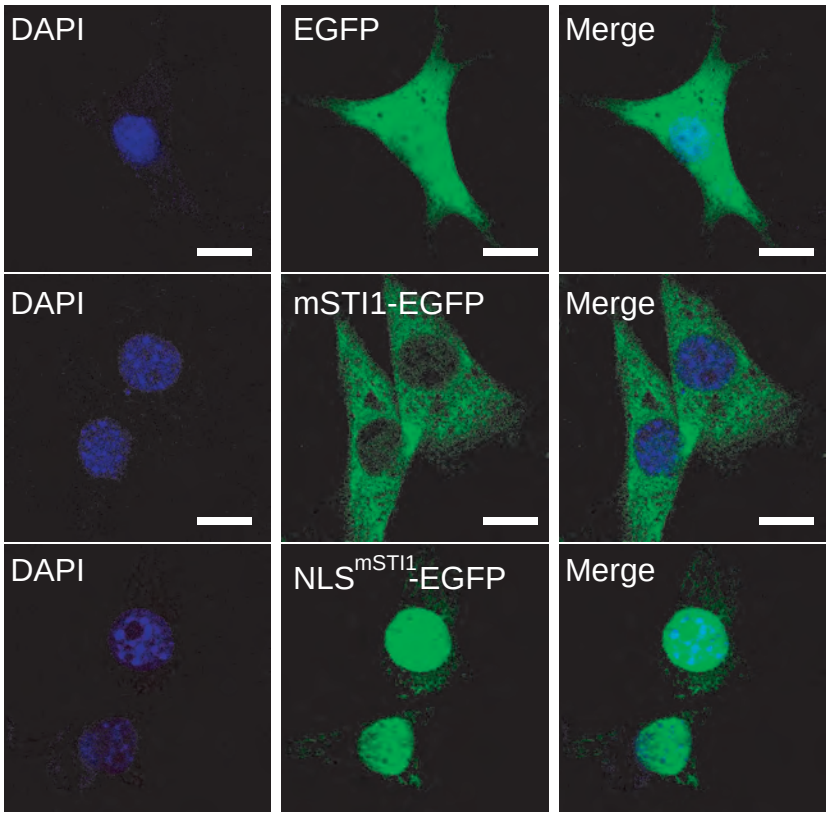

Figure 3.3: mSTI1-EGFP is cytoplasmic and amino acids 222-239 functioned as an NLS

(A) Mouse NIH 3T3 fibroblasts were stably transfected with pB-EGFP (top), pB-mSTI1-EGFP (middle) and pB-NLS^{mSTI1}-EGFP(bottom). Cells were subcultured, fixed in 3.7% paraformaldehyde, stained with DAPI and visualized by confocal laser fluorescence microscopy. Scale bars represent 10 micrometers.

3.3.4 Amino acids 222-239 function as an NLS

μProteins larger than 40-60 kDa cannot enter into the nucleus through the nuclear pore complex by passive diffusion (Okuno *et al*. 1993). Since mSTI1-EGFP (89 kDa) is too large, and endogenous mSTI1 (63 kDa) is of borderline mass, to diffuse into the nucleus, a functional nuclear localization signal (NLS) would be required for the active transport of mSTI1 into the nucleus. Yet, we observed a small amount of fluorescence in the nucleus of all cells immunostained for endogenous mSTI1 (Figure 3.3C) while mSTI1-EGFP was nuclear in 13% of the cells under normal growth conditions (Chapter 4). To assess the potential of the proposed mSTI1 NLS to direct nuclear import, a construct encoding amino acids 222-239 fused to the N-terminus of EGFP was expressed in NIH 3T3 cells. The expressed protein, denoted NLS^{mSTI1}-EGFP, localized strongly to the nucleus in all cells, compared to the EGFP control, which was localized diffusely throughout the cytoplasm and nucleus in all cells (Figure 3.3A). According to the theoretical size of NLS^{mSTI1}-EGFP (about 30 kDa), it would be expected that it could diffuse freely between the nucleus and the cytoplasm by diffusion. A negligible fraction of the NLS^{mSTI1}-EGFP was observed in the cytoplasm suggesting a constitutively active nuclear import process. These data therefore clearly suggested that amino acids 222-239 of mSTI1 contain a functional NLS.

3.4 CONCLUSIONS

The exogenous EGFP fusion expression system was an appropriate system for localization studies of mSTI1, and mSTI1-EGFP and EGFP were successfully expressed in NIH 3T3 fibroblasts. Transfectants of these constructs exhibited bright fluorescence, indicating the correct translation in-frame as well as correct folding of the EGFP moiety at least, since the GFP chromophore is fluorescent only when encapsulated inside the correctly folded protein (Cubitt *et al.*, 1995). Both mSTI1-EGFP and mSTI1 were cytoplasmically localized in all cells, although a small nuclear fraction was observed, correlating with reported mSTI1 localization studies (Lässle *et al.*, 1997). The EGFP tag did not therefore affect mSTI1 localization compared to endogenous mSTI1.

The nuclear fraction of mSTI1 implied the existence of a nuclear import process for mSTI1. NLS^{mSTI1}-EGFP localized strongly to the nucleus, indicating the constitutively active nuclear import of NLS^{mSTI1}-EGFP. Novel evidence presented here suggests amino acids 222-239 function as an NLS in mSTI1. The cytoplasmic localization of mSTI1 could therefore be as a result of cytoplasmic retention or a dynamic nucleocytoplasmic shuttling process. A dynamic nucleocytoplasmic shuttling process would require the presence of a functional NLS driving nuclear import, as well as a nuclear export system of mSTI1. Conditions favouring the nuclear import of mSTI1 were therefore investigated, as well as the existence of a nuclear export process of mSTI1 (Chapter 4).

CHAPTER 4

MECHANISTIC AND INHIBITION STUDIES ON THE SUBCELLULAR LOCALIZATION OF mSTI1

SUMMARY: mSTI1 is cytoplasmic under normal and heat shock conditions, implying a similar regulation of localization under these conditions. This localization differs from the nuclear accumulation reported for Hsp70 under heat shock conditions (Welch, 1987), and therefore the heat shock localization of mSTI1 may be Hsp70-independent. mSTI1 accumulates under leptomycin B conditions, implying either indirect recruitment of mSTI1 under these conditions or possible exportation from the nucleus by a CRM1-dependent mechanism. Although mSTI1-EGFP contains a functional NLS, it remains predominantly cytoplasmic, possibly, by a dynamic equilibrium of a nuclear import system and a dominating nuclear export system. mSTI1 localization did not change under CKII inhibition (DRB) conditions, implying mSTI1 may not be phosphorylated by CKII. However, mSTI1 nuclear localization increased under cdc2 kinase inhibition (olomoucine) and cdc2 kinase inactivation (hydroxyurea-induced G1/S phase arrest). These data imply mSTI1 to be phosphorylated by cdc2 kinase under normal conditions and active cdc2 kinase to be required for the cytoplasmic localization of mSTI1. The percentage of cells arrested in G1/S was similar to the incidence of mSTI1 nuclear localization under these conditions, suggesting an increase in nuclear localization of mSTI1 in the G1/S stage of the cell cycle.

4.1 INTRODUCTION

4.1.1 Inhibition of CRM1-mediated nuclear export by Leptomycin B

Leptomycin B is a *Streptomyces* metabolite causing growth arrest of *Saccharomyces pombe* and mammalian cells at G1 and G2 phases, and is considered to be a clinically important anti-tumor drug (Yoshida *et al.,* 1990). Leptomycin B, at nanomolar concentrations, had been shown to completely block the G1/S transition and partially inhibit the G2/M transition in the mammalian cell cycle (Yoshida *et al.,* 1990). The CRM1-dependent translocation of human immunodeficiency virus type 1 Rev from the nucleus to the cytoplasm was blocked by leptomycin B (Wolff *et al.,* 1997) indicating the inhibition of nuclear export by this antibiotic.

The target of leptomycin B is CRM1, a multifunctional nuclear protein essential for proliferation and chromosome region maintenance (Kudo *et al.,* 1997). CRM1 is required for maintaining chromosome structures during the cell cycle (Adachi and Yanagida, 1989). CRM1's localization in the nucleus or its periphery has allowed it to be proposed as a negative regulator of interphase chromosome condensation (Kudo *et al.,* 1997). CRM1 is conserved in eukaryotes (Adachi and Yanagida, 1989) and is a cell cycle regulated component of the nuclear export apparatus in the nuclear envelope (Kudo *et al.,* 1997). A variety of phenotypes observed in eukaryotes, upon gain or loss of function of CRM1, can be ascribed to the alteration of nuclear export of proteins (Kudo *et al.,* 1997). Several groups have demonstrated the usefulness of leptomycin B in nucleocytoplasmic shuttling studies using GFP fusions (Shulga *et al.,* 1999; Engel *et al.,* 1998; Brennan *et al.,* 2002; Yagita *et al.,* 2002; Hishino *et al.,* 2002; Perander *et al.,* 2001; Rodier *et al.,* 2001)

4.1.2 The inhibition of cyclin-dependent kinases by the purine analogue, olomoucine

Phosphorylation of serine, threonine and tyrosine residues by protein kinases represents one of the most common post-translational regulatory modifications of proteins. The importance of protein kinases in physiological processes has stimulated an active search for specific inhibitors with potential pharmalogical interest. Several classes of compounds have been identified: staurosporine; naphthalene sulfonamides (W7, ML-9, SC-9); isoquinoline derivatives (H-7, H-8, KN-62); sphingosine; tyrophostins; and others, but in most cases these inhibitors display broad specificity (Veselý *et al.,* 1994).

An active search for chemical inhibitors of cdk proteins has been stimulated by the frequent deregulation of cdk proteins in cancer and the discovery of natural inhibitors. Such cdk inhibitors could act by various mechanisms i.e. by interfering with the binding of substrates (ATP or protein); by affecting the binding of regulatory subunits (cyclins or $p9^{ckShs}$); by interacting with some sites involved in the activation (Thr161 in cdc2); by interacting with the nuclear/cytoplasmic localization signals or by mimicking the natural inhibitor/cdk interactions (Veselý *et al.,* 1994). Inhibitors of cdc2 kinase/cyclin B kinase include the non-specific N^6-(Δ^2)-isopentenyl adenine (Sherr, 1993); staurosporine (Gadbois *et al.,* 1992); butyrolactone-I (Someya *et al.,* 1994); and the flavone L86-8275 (Losiewicz *et al.,* 1994). These compounds appear to act as competitive inhibitors for ATP binding. Olomoucine and other C2, N6 and N9-substituted purines have been found to exert strong inhibitory effects on the cdc2, cdk2, cdk5 and ERK1 kinases, but not on cdk4 and cdk6 (among 35 kinases tested) (Veselý *et al.,* 1994). Olomoucine inhibits both *in vitro* M-phase promoting factor activity and *in vitro* DNA synthesis in *Xenopus* egg extracts, as well as the starfish oocyte G2/M transition *in vivo*. Olomoucine acts as a competitive inhibitor for ATP and as a non-competitive inhibitor for histone H1 (linear inhibition for both substrates). Olomoucine also inhibited autophosphorylation on the cyclin B (Veselý *et al.,* 1994). Thus olomoucine inhibits G1/S transition in unicellular algae, mesophyl protoplasts, interleukin-2-stimulated T lymphocytes (CTLL-2 cells) and the non-small cell lung cancer cell line MR65 (Abraham *et al.,* 1995).

4.1.3 The inhibition of CKII by DRB

Protein kinase CKII is a serine/threonine protein kinase, ubiquitous and highly conserved among eukaryotic organisms (Allende and Allende, 1995). It is composed of two catalytic subunits (α) and of two regulatory subunits (β), which tetramerize to adopt a $\alpha_2\beta_2$ structure (Allende and Allende, 1995). CKII localizes both in the nucleus and in the cytoplasmic compartment, where it phosphorylates a variety of substrates involved in different cellular functions. Although its precise role remains elusive, CKII has been involved in the major cellular processes, including control of cell division and proliferation (Pinna and Meggio, 1997), development and differentiation. In addition to being necessary for cell viability in yeast (Padmanabha *et al*., 1990), the human homologue of CKIIβ was shown to increase resistance to UV irradiation (Teitz *et al*., 1990), raising the question of whether CKII may play a role in the response to stress. Among all the CKII substrates described so far, it is striking to note that many are proteins involved in the response to heat shock, including chaperone proteins Hsp56 (Miyata, 1997) and Hsp90 (Miyata and Yahara, 1992), stress related transcription factors HSF-1 and EGR-1 (Jain, 1996), the DNA repair machinery i.e. topoisomerase II (Redwood *et al*.,1998), DNA ligase (Prigent *et al*., 1998) and APE/REF-1 (Fritz and Kaina, 1999), or in the control of transcription (Pinna and Meggio, 1997).

CKII has been found to relocalize in a particular nuclear fraction, after stress, and its activity is increased up to three fold in the nucleolus (Gerber *et al*., 2000). 5, 6-dichloro-1-beta-D-ribofuranosylbenzimidazole (DRB) is a classic inhibitor of CDK7 TFIIH-associated kinase, CKI and CKII kinases (te Poele *et al*., 1999, David-Pfeuty *et al*., 2001).

4.1.4 The G1/S transition and the inhibitor hydroxyurea

Cell division is controlled by way of a complex network of biochemical signals that are similar in all eukaryotic cells. Together, these signals regulate specific transitions in the cell cycle (Van den Heuvel and Harlow, 1993). The best-characterized transitions are

those from G1 to S phase and from G2 to mitosis. The dependency of late events in the cell cycle on the completion of early events occurs through control mechanism checkpoints that appear to have the role of checking that prerequisites have been properly satisfied (Hartwell and Weinert, 1989). In mammalian tissue culture cells, arrest of DNA synthesis by specific inhibitors or by mutational inactivation of replication enzymes prevents continuation of the cell cycle to mitosis and arrests cells at the G1/S transition (Hartwell and Weinert, 1989). Temperature-sensitive mutants defective in some DNA replication functions (DNA polymerase I, *cdc17*; DNA polymerase III, *cdc2*; and DNA ligase, *cdc9*) do not normally undergo mitosis at the restrictive temperature. In yeast, the *RAD9* gene specifies a component of this checkpoint control system (Hartwell and Weinert, 1989). Dependency of mitosis on the completion of DNA synthesis is relieved, however, by a complete deficiency of *RAD9*; as cells with a *RAD9* gene defect then continue through mitosis into the next cell cycle at the restrictive temperature (Johnston and Nasmyth, 1978). Chromosome condensation, elaboration of the mitotic spindle, and cytokinesis are all prevented when DNA synthesis is inhibited (Hartwell and Weinert, 1989).

The classic inhibitor hydroxyurea arrests cells in the G1/S phase and is often used in G1/S arrest studies (Choy and Kron, 2002). The mechanism by which hydroxyurea acts is through the inactivation of ribonucleoside reductase by the formation of a free radical nitroxide that binds to a tyrosyl free radical in the active site of the enzyme (Lassman, *et al.,* 1992). This blocks the synthesis of deoxynucleotides (Hendriks and Matthews, 1998, Lu *et al.,* 2002), which inhibits DNA synthesis and thus induces synchronization at the G1/S transition.

4.1.5 Heat Shock effects on the cell

Under normal conditions of cell growth, quality control over protein structure and function is maintained by the activities of molecular chaperones and proteases. Under stress conditions, such as heat shock, the amount of unfolded proteins increases dramatically and the balance between chaperones, proteases, and unfolded proteins is

disturbed, which can lead to the formation of protein aggregates (Nollen *et al.,* 2001). Chaperone localization would therefore correlate with the localization of unfolded proteins. Little is known about where exactly in the cell unfolded proteins are processed by chaperones. Hsp70 has been shown to co-localize to the nucleoli with thermally unfolded nuclear proteins, and is in addition, required for the translocation event (Nollen *et al.,* 2001). Stress, such as heat shock or oxidative stress, disturbs numerous cellular processes including those involved in the cell cycle, leading to an arrest in the G1/S and G2/M phases (Kühl and Rensing, 2000). After the initial response to stress, namely the upregulation of Hsps, a state of acquired thermotolerance is reached, ensuring a lower sensitivity to further stress exposures. This includes the effects on the cell cycle (Kühl *et al.*, 2000), allowing the cell to return to a proliferating cycle with a thermotolerant advantage.

4.1.6 Specific hypothesis, aims and objectives

It is hypothesized that nuclear import and export of mSTI1 occurs, and that this is affected by cell cycle kinases.

mSTI1, the murine homolog of STI1, is a stress inducible phosphoprotein implicated in mediating the heat shock response in *Saccharomyces cerevisiae* (Blatch *et al.*, 1997; Nicolet and Craig, 1989). Hsp70 binds with high affinity to Hop in the presence of Hsp90 (Hernández *et al.,* 2002). Hsp70 is normally cytoplasmically localized, but during heat shock, has been shown to translocate to the nucleus and in particular the nucleolus, from which it withdraws during recovery (Welch, 1987). Therefore it was proposed that the subcellular localization of mSTI1 under heat shock conditions would involve translocation to the nucleus.

The target of leptomycin B is CRM1, a multifunctional nuclear protein essential for proliferation and chromosome region maintenance (Kudo *et al.,* 1997). mSTI1 has been shown to be mostly cytoplasmic with a small nuclear fraction (Chapter 3). However, since a nuclear fraction of mSTI1 exists and mSTI1 has been shown to contain a

functional NLS (Chapter 3), this cytoplasmic localization of mSTI1 may be a result of a dominant nuclear export process. Therefore, we hypothesize that inhibition of CRM1-dependent nuclear export in mSTI1-EGFP transfectants using leptomycin B will result in accumulation of mSTI1 in the nucleus.

CKII and cdc2 kinases phosphorylate mSTI1 *in vitro*, proximal to the NLS, at positions S189 and T198 respectively (Longshaw *et al.,* 2000). This phosphorylation supports a predicted CcN motif in mSTI1. The CcN motif is a phosphorylation regulated NLS module (Jans *et al*., 1991). The cdc2 kinase and CKII sites in the T-antigen CcN motif appear to function independently of one another in terms of both regulating T-antigen nuclear transport and influencing phosphorylation at the other site (Jans *et al*., 1991). Therefore, it is hypothesized that mSTI1 is phosphorylated by either CKII or cdc2 kinase *in vivo*. The mechanism of cdc2 kinase-mediated inhibition of nuclear localization appears to be through cytoplasmic retention (Jans and Jans, 1994), while that of CKII phosphorylation-mediated enhancement of nuclear localization may be by increasing the affinity of association with the karyopherin complex (Jans and Jans, 1994), enhancing the docking rate at the NPC. DRB is a classic inhibitor of CKII kinase and olomoucine exerts strong inhibitory effects on cdc2 kinase (Veselý *et al.,* 1994). Therefore, we hypothesize that olomoucine exposure will increase the nuclear localization of mSTI1, while DRB exposure will decrease the nuclear localization of mSTI1.

We hypothesize that exposure of mSTI1-EGFP expressing cells to hydroxyurea, when cdc2 kinase is inactive, will increase the nuclear localization of mSTI1. cdc2 kinase phosphorylates mSTI1 *in vitro* at position T198 (Longshaw *et al.,* 2000). The classic inhibitor hydroxyurea arrests cells in the G1/S phase by blocking the synthesis of deoxynucleotides (Hendriks and Matthews, 1998), which inhibits DNA synthesis and thus induces synchronization at the G1/S transition. The mechanism of cdc2 kinase-mediated inhibition of nuclear localization appears to be through cytoplasmic retention (Jans and Jans, 1994). Cdc2 kinase is inactive at the G1/S transition (Alberts *et al.*, 1994).

4.2 EXPERIMENTAL PROCEDURES

4.2.1 The localization of mSTI1 during heat shock, and kinase, cell cycle and nuclear export inhibition

NIH 3T3 mouse fibroblasts transfected with pB-mSTI1-EGFP (B.12) were subcultured into 8 well chamber slides 24 hours prior to each treatment. For stress conditions: slides were incubated at 42ºC for 15 minutes (Lässle *et al*., 1997). Greater than 15 minutes exposure, or exposure to temperatures higher than 42 ºC, resulted in cell death. pB-mSTI1-EGFP transfectants were exposed to 0.3 mM DRB for 8 hours, to inhibit CKII. Similarly, pB-mSTI1-EGFP transfectants were exposed to 0.3 mM olomoucine for 8 hours, to inhibit cdc2 kinase. pB-mSTI1-EGFP transfectants were exposed to 10 mM hydroxyurea for 8 hours, to arrest cells in the G1/S phase. pB-mSTI1-EGFP transfectants were exposed to 10 ng/ml leptomycin B for 3 hours, to inhibit nuclear export. No initial arrest in G_0 (by incubation of cells in serum-free media) was performed, as this would produce a stressed cellular state, inappropriate conditions for the study of a chaperone protein. Slides were visualized by confocal laser scanning fluorescent microscopy (B.14).

4.2.2 Establishing the percentage of G1/S arrested cells

5-bromodeoxyuridine is an artificial thymidine analogue. It can be added to the media in which proliferating cells are growing, and will be taken up and selectively incorporated into the synthesizing DNA during S-phase, instead of thymidine (Boccadora *et al.,* 1986). Subsequent probing with antibodies specific to bromodeoxyuridine will reveal any localization in the nucleus, which only occurs in cells synthesizing DNA, and thus at the G1/S transition. NIH 3T3 fibroblasts were subcultured into 8 well chamber slides 24 hours prior to treatment with hydroxyurea (B.12). Cells were incubated in the presence of 100 μM bromodeoxyuridine monophosphate and 10 mM hydroxyurea (B.12). Cells were immunostained using the bromodeoxyuridine-specific antibody (B.15) and visualized by confocal laser scanning fluorescence microscopy (B14) for nuclear staining.

4.3 RESULTS AND DISCUSSION

4.3.1 Heat shock does not change mSTI1 distribution

Since mSTI1 associates with Hsc/Hsp70, and Hsp70's localization changes from cytoplasmic to nuclear under heat shock (Welch *et al.,* 1987), we investigated whether the localization of mSTI1 changed in response to heat shock. mSTI1-EGFP expressing NIH 3T3 fibroblasts were incubated at 42°C for 15 minutes (Lässle *et al.,* 1997) (Figure 4.1). Similarly, NIH 3T3 fibroblasts were incubated at 42 °C for 15 minutes and immunostained against endogenous mSTI1. The distribution of mSTI1 after these heat shock conditions did not change (Figure 4.1), suggesting the nuclear import of mSTI1 to be similar under both normal and these heat shock conditions. Additional experiments using increasing severe heat shock conditions, including those from which the cells were unable to recover, also had no effect on mSTI1-EGFP localization (data not shown). When cells were exposed to pre-heated 42°C media a nuclear localization of endogenous mSTI1 was observed. However, this nuclear localization was not reproducible, and it is proposed that any potential nuclear localization under heat shock conditions may only occur due to specifically induced changes in the kinetics of mSTI1 cellular distribution.

4.3.2 mSTI1 enters and is exported from the nucleus

Although mSTI1-EGFP contains a functional NLS at positions 222-239, it remains predominantly cytoplasmic under normal growth conditions (87% of cells had a cytoplasmic only staining pattern with no nuclear component) (Figure 4.2). This may be caused by the presence of a nuclear export system, which predominates over nuclear import. To assess the potential nuclear export of mSTI1, mSTI1-EGFP expressing NIH 3T3 fibroblasts, and normal NIH 3T3 fibroblasts, were treated with leptomycin B. Treatment with leptomycin B for 3 hours induced nuclear accumulation in the majority of cells of mSTI1-EGFP and mSTI1 (Figure 4.2A and B). For most EGFP-expressing cells, EGFP demonstrated ubiquitous cytoplasmic and nuclear localization, before and after leptomycin B treatment (Figure 4.2A). These data should be carefully interpreted.

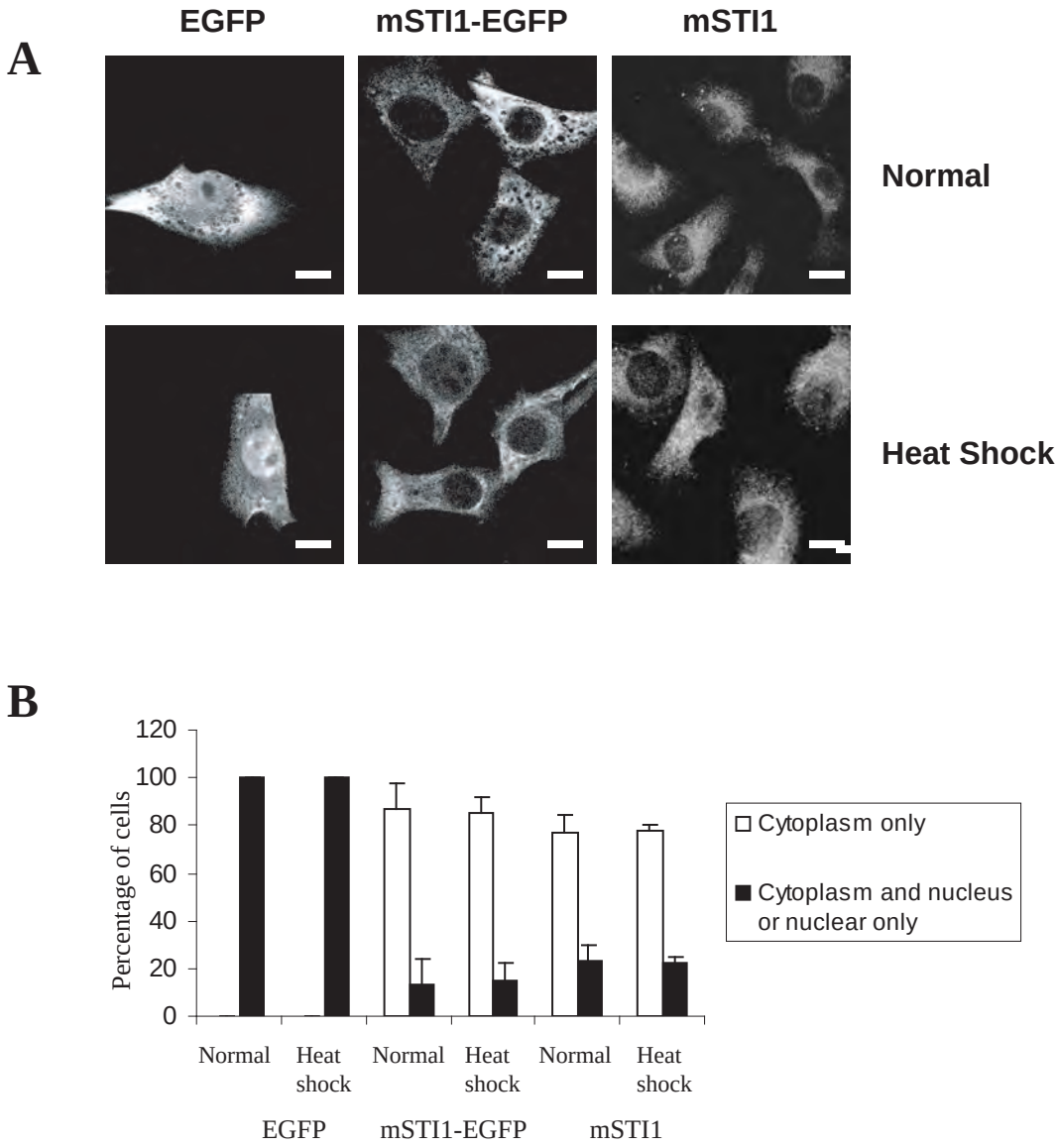

Figure 4.1: The subcellular localization of mSTI1 is not affected by heat shock.

(A) Mouse NIH 3T3 fibroblasts were stably transfected with pB-EGFP (left), pB-mSTI1-EGFP (right) and heat shocked (42℃) for 15 mins. Cells were fixed in 3.7% paraformaldehyde and visualized by confocal laser fluorescence microscopy. Similarly, normal NIH 3T3 fibroblasts were heat shocked, immunostained with SF1 polyclonal rabbit anti-mSTI1 and Cy3-conjugated donkey anti-rabbit and visualized by confocal laser fluorescence microscopy. Scale bars represent 10 micrometers. (B) Cells were transfected as described in (A). Cells demonstrating cytoplasmic fluorescence or nuclear and cytoplasmic fluorescence were scored from 5 fields.

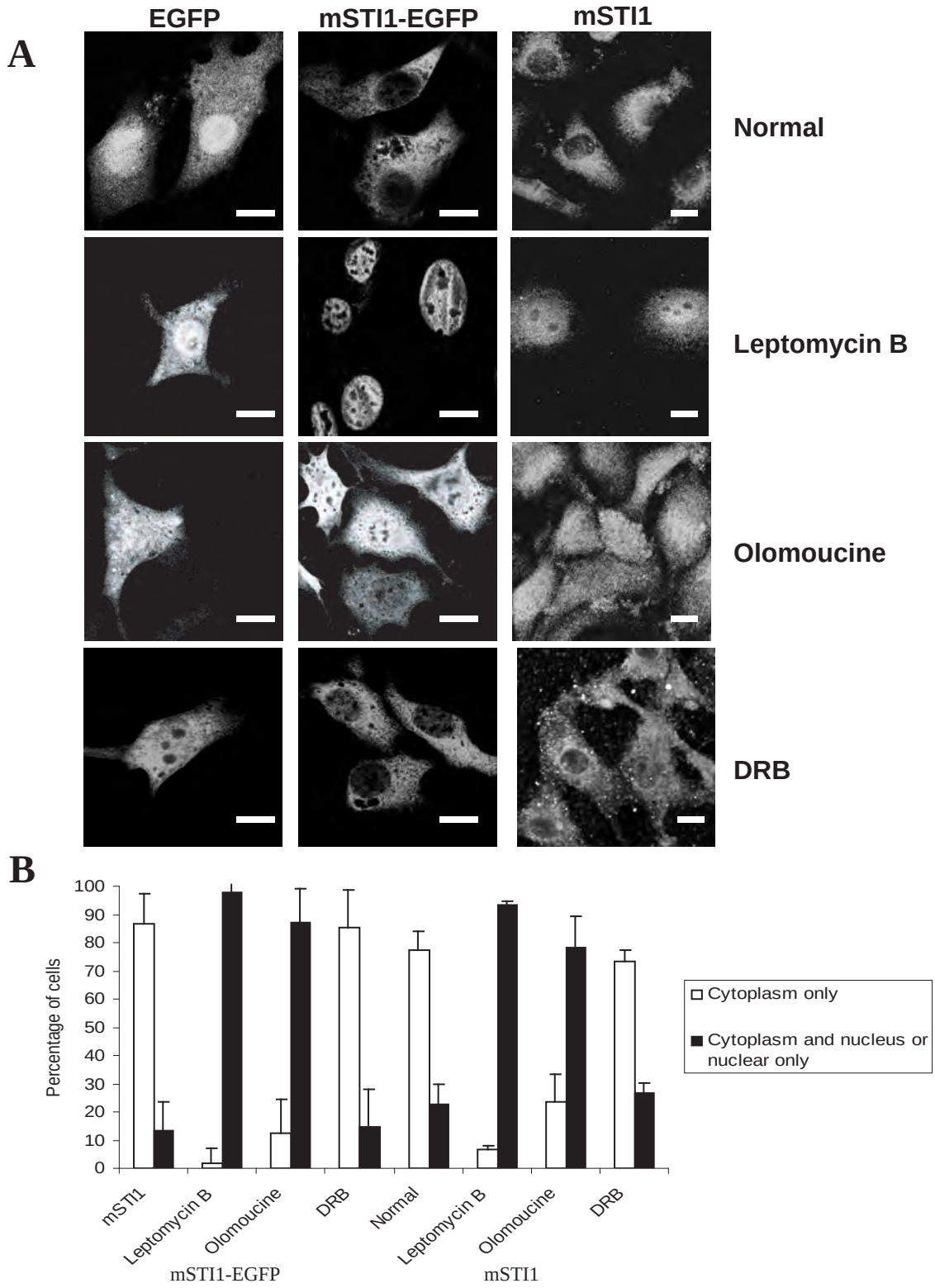

Figure 4.2: The nuclear localization of mSTI1-EGFP is enhanced by inhibition of nuclear export and of cdc2 kinase, but not by inhibition of CKII

(A) Mouse NIH 3T3 fibroblasts were stably transfected with pB-EGFP (left), pB-mSTI1-EGFP (middle) and exposed to leptomycin B (10 ng/ml), olomoucine (0.1 mM) or DRB (0.3 mM) for 3, 8 and 8 hours respectively. Cells were fixed in 3.7% paraformaldehyde, and visualized by confocal laser fluorescence microscopy. ixed in 3.7% paraformaldehyde, permeabilized in 0.1% saponin, immunostained with SF1 polyclonal rabbit anti-mSTI1 and Cy3-conjugated donkey anti-rabbit. Cells were visualized by confocal laser fluorescence microscopy. Scale bars represent 10 micrometers. (B) Cells were exposed to leptomycin B, olomoucine and DRB as described in (A). Cells demonstrating cytoplasmic fluorescence or nuclear and cytoplasmic fluorescence were scored from 5 fields.

This nuclear localization under leptomycin B conditions was noted as accumulation in the nucleus rather than simply nuclear entry. Accumulation of mSTI1 in the nucleus after leptomycin B treatment may result in conditions indirectly leading to the recruitment of mSTI1 to the nucleus for its co-chaperone function. Alternatively, these data may have demonstrated that mSTI1 was exported from the nucleus by a mechanism either involving a functional *cis*-acting, leptomycin B-sensitive nuclear export signal (NES) or via an NES-containing interaction partner of mSTI1 (Fukuda *et al.,* 1997; Fornerod *et al*., 1997; Stade *et al*., 1997; Ossareh-Nazari *et al*., 1997; Kudo *et al*., 2000). The predominant cytoplasmic distribution of mSTI1 under normal conditions may, therefore, result from a dynamic equilibrium between nuclear import and export, where in the majority of cells the rate of export was the greater. An attempt was made to examine the mSTI1 sequence for an NES, however any putative NES signals reported in the literature are described as merely "leucine rich" and as yet no consensus sequence has been reported (Fischer *et al.,* 1995; Wen *et al.,* 1995; Fukuda *et al*., 1996; Engel *et al*., 1998; Toyoshima *et al*., 1998; Yamaga *et al.,* 1999). Therefore the sequence for an NES may vary between proteins and have few conserved residues. Such a putative "leucine rich" NES could not be found in the primary amino acid sequence of mSTI1, and therefore any NES potentially present in mSTI1 may be structurally different to reported NESs. Future work could include a continued search for this predicted NES in mSTI1.

4.3.3 Kinase inhibition affects mSTI1 localization

The presence of a CcN motif in mSTI1 could be capable of directing nuclear import under cell cycle control (Longshaw, *et al*. 2000). The proposed CcN motif would comprise the NLS at position 222-239, together with the *in vitro* recognized CKII (S^{189}) and cdc2 kinase (T^{198}) sites located upstream from the NLS. To assess any effect of specific inhibition of cdc2 kinase and CKII in cells on the cytoplasmic distribution of mSTI1-EGFP, we exposed mSTI1-EGFP expressing NIH 3T3 fibroblasts, and normal NIH 3T3 fibroblasts, to olomoucine, a specific inhibitor of cdc2 kinase, and DRB, a specific inhibitor of CKII. The incidence of cells with a cytoplasmic distribution of mSTI1-EGFP or mSTI1 was unchanged after DRB treatment (Figure 4.2). This suggested

that inactivation of CKII did not change the distribution of mSTI1. For all EGFP-expressing cells, EGFP demonstrated ubiquitous cytoplasmic and nuclear localization before and after both DRB and olomoucine treatments (Figure 4.2). In contrast, olomoucine treatment resulted in a marked increase in the incidence of nuclear localization of mSTI1-EGFP and endogenous mSTI1 (Figure 4.2), suggesting that active cdc2 kinase was required for the nuclear exclusion of mSTI1.

4.3.4 Arrest at the G1/S transition promotes a nuclear localization of mSTI1

A cdc2 kinase site in mSTI1 was previously identified and was recognized by cdc2 kinase *in vitro* (Longshaw *et al.,* 2000). Furthermore, the inhibition of cdc2 kinase led to an increase in the incidence of nuclear localization of mSTI1-EGFP and mSTI1 (Figure 4.2). The arrest of the cell at the G1/S transition, when cdc2 kinase was inactive, could therefore have an effect on the cytoplasmic distribution of mSTI1. After hydroxyurea treatment, a marked increase in the incidence of nuclear localization of mSTI1-EGFP and of endogenous mSTI1 was observed (Figure 4.3A and B), suggesting again that active cdc2 kinase was required for the nuclear exclusion of mSTI1. Exposure of NIH 3T3 cells to hydroxyurea for 10 hours resulted in the arrest of 71% of NIH 3T3 cells in the G1/S phase, as determined by bromodeoxyuridine (BrdU) incorporation (Figure 4.4A). This was in contrast to cells under normal growth conditions when approximately 10% of cells were in G1/S (Figure 4.4B). Interestingly, the percentage of cells in G1/S was, under both normal growth conditions and following hydroxyurea treatment, very similar to the incidence of mSTI1-EGFP and mSTI1 nuclear localization (Figure 4.3B and 4.4 B). These data suggested that the nuclear localization of mSTI1 was increased when the cells were in the G1/S stage of the cell cycle.

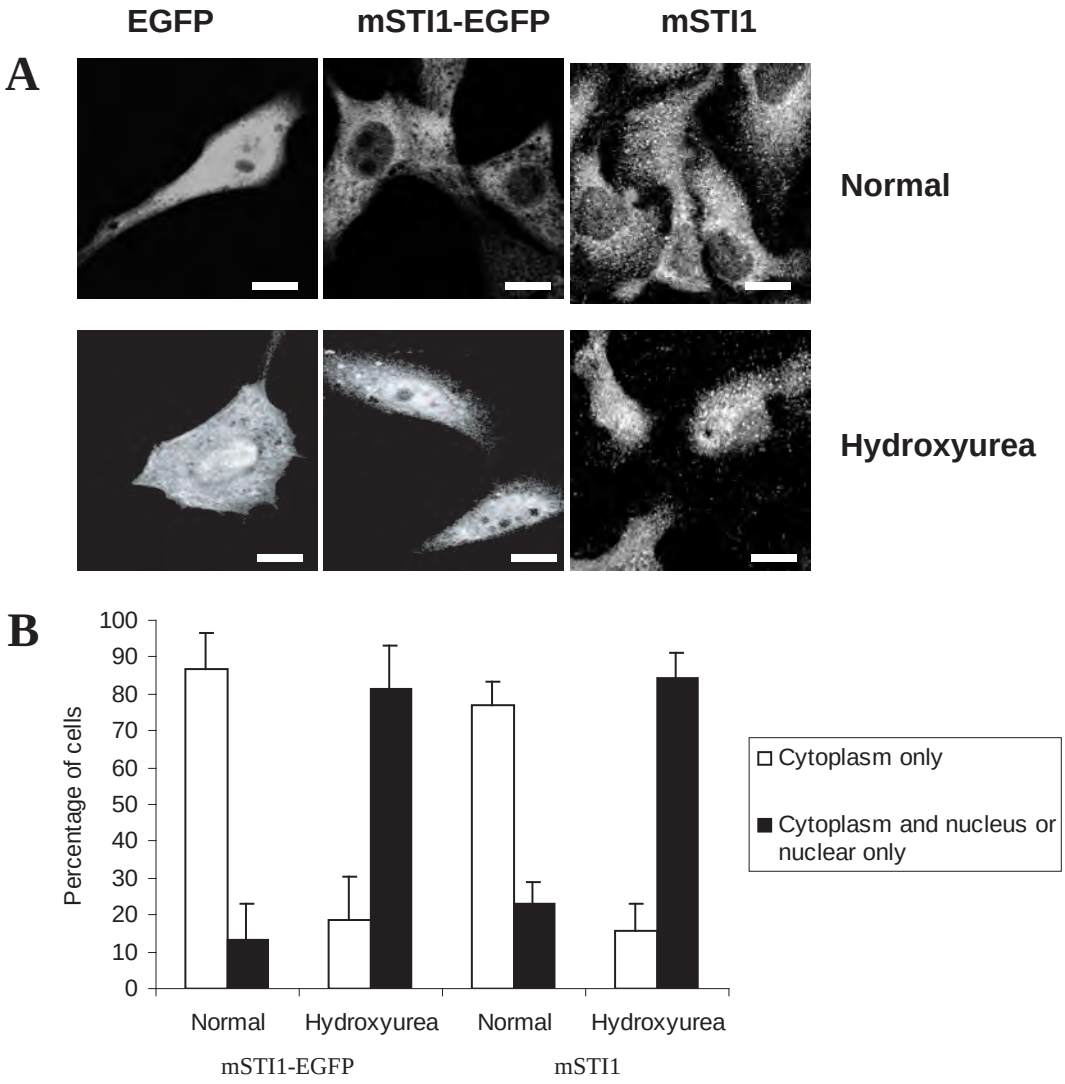

Figure 4.3: The nuclear localization of mSTI1 is enhanced by G1/S phase arrest.

(A) Mouse NIH 3T3 fibroblasts were stably transfected with pB-EGFP (left) and pB-mSTI1-EGFP (middle) and exposed to hydroxyurea (10 mM) for 10 hours. Cells were fixed in 3.7% paraformaldehyde and visualized by confocal laser fluorescence microscopy. Mouse NIH 3T3 fibroblasts were fixed in 3.7% paraformaldehyde, permeabilized in 0.1% saponin, immunostained with SF1 polyclonal rabbit anti-mSTI1 and Cy3-conjugated donkey anti-rabbit. Cells were visualized by confocal laser fluorescence microscopy. Scale bars represent 10 micrometers. (B) Cells were exposed to hydroxyurea as described in (A). Cells demonstrating cytoplasmic fluorescence or nuclear and cytoplasmic fluorescence were cscored from 5 fields.

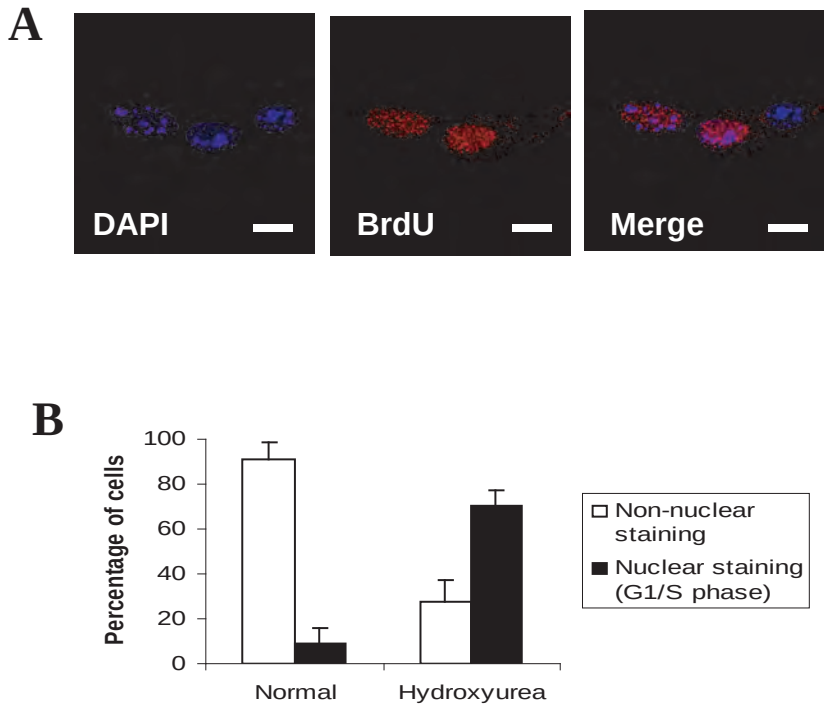

Figure 4.4: The population of cells in G1/S phase was assessed using bromodeoxyuridine staining

(A) Mouse NIH 3T3 fibroblasts were exposed to hydroxyurea (10 mM) and bromodeoxyuridine (100 mM) for 10 hours. Cells were fixed in 3.7% paraformaldehyde, permeabilized in 0.1% saponin, stained with DAPI, and probed for bromodeoxyuridine incorporation with mouse anti-bromodeoxyuridine primary antibody, and donkey anti-mouse Cy3-conjugated secondary antibody. Cells were visualized by confocal laser fluorescence microscopy. (B) Cells were treated as in (A) and nuclear or non-nuclear fluorescencing cells were scored from 5 fields.

4.3 CONCLUSIONS

mSTI1 is induced during stress (Blatch *et al*., 1997) and associates with Hsp70 (Hernández *et al*., 2002) which localizes to the nucleus under stress conditions (Welch, 1987). However, mSTI1 is cytoplasmic under both normal and heat shock conditions. The NLS-dependent nuclear import of mSTI1 may thus be similar under both normal and the heat shock conditions used, and Hsp70-independent. Stress, such as starvation, ethanol, heat or oxidants have been shown to inhibit specific NLS-dependent nuclear import (Stochaj *et al.,* 2000).

Novel evidence shown here suggests that mSTI1 may be indirectly recruited to the nucleus under export-inhibition conditions or is exported from the nucleus by a mechanism either involving a functional *cis*-acting, leptomycin B-sensitive nuclear export signal (NES) or via an NES-containing interaction partner of mSTI1. Although mSTI1-EGFP contains a functional NLS, it remains predominantly cytoplasmic. This may be caused by the presence of a nuclear export system, which predominates over nuclear import.

Inactivation of CKII by DRB did not change the distribution of mSTI1 under our conditions. mSTI1 may therefore not be phosphorylated by CKII under normal conditions. CKII phosphorylation of mSTI1 may therefore not have a role in cell cycle-regulated localization of mSTI1. Inactivation of cdc2 kinase by olomoucine increased the nuclear localization of mSTI1. mSTI1 may therefore be phosphorylated by cdc2 kinase under normal conditions and active cdc2 kinase may be required for the cytoplasmic localization of mSTI1.

Arrest in the G1/S transition by hydroxyurea treatment, when cdc2 kinase is inactive, increased the nuclear localization of mSTI1. This evidence further supports the idea that mSTI1 is phosphorylated by cdc2 kinase under normal conditions. The percentage of cells in G1/S, under both normal growth conditions and following hydroxyurea treatment,

was very similar to the incidence of mSTI1-EGFP and mSTI1 nuclear localization. These data suggested that the nuclear localization of mSTI1-EGFP was increased when the cells were in the G1/S stage of the cell cycle. Evidence is presented here of a *in vivo* link between mSTI1 and the cell cycle machinery. Recently, it was shown that STI1 interacts directly with cdc37 (Abbas-Terki *et al.*, 2002). Furthermore, cdc37 has been found to interact with cdc28 in *Saccharomyces cerevisiae* (Mort-Bontemps-Soret *et al.*, 2002). Therefore STI1, cdc37 and cdc28 may interact together in a cell cycle dependent manner to regulate both the chaperoning and localization of client proteins. These data provide the first evidence of regulated nuclear import/export of a major Hsp70/Hsp90 co-chaperone, and the regulation of this nuclear import by cell cycle status and cell cycle kinases.

CHAPTER 5

IN VIVO ANALYSIS OF THE POTENTIAL CKII AND CDC2 KINASE PHOSPHORYLATION SITES OF mSTI1

SUMMARY: The removal of the potential *in vivo* CKII phosphorylation site at S189 did not affect the localization of mSTI1 under normal, heat shock, G1/S arrest conditions, or nuclear export inhibition conditions. mSTI1 may therefore not be modified at S189 *in vivo*. However, the introduction of negative charge at this site promoted nuclear localization of mSTI1. This site may therefore be functional under conditions that are as yet unknown. The removal of the potential *in vivo* cdc2 kinase phosphorylation site at T198 did not affect the localization of mSTI1 under normal conditions, heat shock or nuclear export inhibition conditions. However, under G1/S arrest conditions, removal of this site increased nuclear accumulation qualitatively, while the introduction of negative charge at this site decreased the incidence of nuclear accumulation of mSTI1, implying a nuclear localization inhibitory role for this site at the G1/S transition. Heat shock and G1/S arrest may affect the phosphorylation status of mSTI1, as the isoform composition of mSTI1 changed under these conditions. This status of mSTI1 may be determined by *in vivo* modifications at S189 and T198, as *in vitro* modifications at these sites decreased the number of isoforms of mSTI1-EGFP under normal conditions. Therefore, taken together, these results imply that modifications at S189 and T198 may occur *in vivo*, however although the effects of such modifications may not extend to the final equilibrium of mSTI1 localization.

5.1 INTRODUCTION

5.1.1 Assessing the regulation of NLS signals by amino-acid substitution at phosphorylation sites

Nuclear localization signals are short peptide sequences that are necessary and sufficient for nuclear localization of their respective proteins (Jans and Hűbner, 1996). NLSs are regarded as functioning via receptor/ligand receptor-like interactions with nuclear transport machinery. Previous studies of the classical SV40 large T-antigen CcN motif have shown that negative charge at the CKII site flanking the nuclear localization signal, is mechanistically important for enhanced nuclear import (Jans and Jans, 1994). The mechanism of CKII phosphorylation-mediated enhancement is through increasing the affinity of association with the karyopherin complex (Jans and Jans, 1994), enhancing the docking rate at the NPC. Flanking sequences and phosphorylation at the CKII site are mechanistically important in NLS recognition by karyopherin α in both T-antigen (Hübner *et al*., 1997) and Dorsal transcription factor from Drosophila (Briggs *et al*., 1998). On removal of the CKII site, either by substitution of $S^{111/112}$ by non-phosphorylatable amino-acid residues, or mutation of the Asp-Asp-$Glu^{113/115}$ CKII recognition sequence to Asn-Asn-Gln, nuclear import rates less than 4% wild type resulted (Jans and Jans, 1994). Conversely, the substitution of Asp for Ser^{112}, the serine preferentially phosphorylated by purified CKII, enhanced nuclear import to about 45% maximal wild type rates (Jans and Jans, 1994). Mutations of the NLS-containing yeast transcription factor SW15 at cdk site serines Ser^{646} and Ser^{664} to alanine resulted in constitutive nuclear localization (Jans *et al*., 1995). In mammalian cells, the SW15 fusion proteins were similarly transported to the nucleus in an NLS-dependent fashion, while the mutation to Ala of the cdk site serines increased the maximal level of nuclear accumulation from 1- to over 8-fold (Jans *et al*., 1995). Phosphorylation sites have also been mimicked by the site-directed amino-acid substitution to a negatively charged residue such as glutamic acid (Maciejewski *et al*., 1995). Alanine substitution at the PKA site (Ser^{266}) N-terminal to the NLS in the *c*-rel proto-oncogene, abolishes its nuclear localization whereas aspartic acid at the site simulates PKA phosphorylation in inducing

nuclear translocation (Gilmore and Temin, 1988). T^{124} phosphorylation at the cdc2 kinase site of the SV40 T-antigen protein, which could be functionally simulated by a T-to-D substitution, was found to reduce the maximal extent of nuclear accumulation whilst negligibly affecting the import rate. Thus, amino-acid substitution has been demonstrated to be a useful tool in the removal or simulation of phosphorylation sites, especially with respect to their regulatory role in nucleocytoplasmic transport.

5.1.2 Specific hypothesis, aims and objectives

CcN motifs comprise both enhancing and inhibitory phosphorylation sites proximal to the NLS. The CKII site increases the rate of NLS-dependent nuclear import, whereas cdc2 kinase site inhibits transport, markedly reducing the level of maximal nuclear accumulation. The cdc2 kinase and CKII sites appear to function independently of one another in terms of both regulating T-antigen nuclear transport and influencing phosphorylation at the other site. (Jans *et al*., 1991). The mechanism of cdc2 kinase-mediated inhibition appears to be through cytoplasmic retention, while that of CKII phosphorylation-mediated enhancement may be increasing the affinity of association with the karyopherin complex, enhancing the docking rate at the NPC (Jans and Jans, 1994). Furthermore, CKII and cdc2 kinases have been shown to phosphorylate mSTI1 *in vitro*, proximal to the NLS, supporting a predicted CcN motif (Longshaw *et al.,* 2000).

It is hypothesized that the modification of residues phosphorylated by cdc2 kinase or CKII kinase will change the localization of mSTI1.

Since the cytoplasmic localization of mSTI1 is not affected by inhibition of CKII during exposure to DRB (Chapter 4), it can be concluded either that mSTI1 may not be phosphorylated by CKII *in vivo* under normal conditions, or that such phosphorylation of mSTI1 affects the kinetics of mSTI1 nuclear import or export. The similar mSTI1 distribution under normal and DRB conditions may be explained if any potential phosphorylation of mSTI1 by CKII may be subject to removal by phosphatases under normal conditions. It is therefore hypothesized that substitution of the potential *in vivo*

CKII phosphorylation site at S189 with a non-phosphorylatable alanine residue will not affect the nuclear accumulation of mSTI1. However, substitution of this S189 residue with a non-removable negatively charged residue such as glutamic acid will functionally simulate phosphorylation at this site and promote nuclear accumulation of mSTI1.
Nuclear localization of mSTI1 was promoted by inhibition of cdc2 kinase during exposure to olomoucine, implying that mSTI1 was phosphorylated by cdc2 kinase *in vivo* and that active cdc2 kinase was required for the cytoplasmic retention of mSTI1. It is therefore hypothesized that substitution of the potential *in vivo* cdc2 kinase phosphorylation site at T198 with a non-phosphorylatable alanine residue will increase the nuclear accumulation of mSTI1. However, substitution of this S189 residue with a negatively charged residues such as glutamic acid will functionally simulate phosphorylation at this site. Since nuclear accumulation of mSTI1 is promoted at G1/S phase (Chapter 4), when cdc2 kinase is inactive, functional simulation of the T198 site is proposed to inhibit this nuclear accumulation of mSTI1.

A shift in the *in vivo* isoform composition of Hop, to more acidic (and therefore possibly more phosphorylated) forms, occurs after viral transformation as well as after heat shock, suggesting the stress-induced phosphorylation of a Hop subpopulation (Honoré *et al*., 1992). It is hypothesized that a number of endogenous mSTI1 isoforms exist in vivo, and that these isoforms are different under normal and stress, even though there is no change in mSTI1 localization. Furthermore, the increase in nuclear localization of mSTI1 under G1/S arrest leads to the prediction of different endogenous mSTI1 isoforms under hydroxyurea conditions. Since *in vitro* phosphorylation of mSTI1 by CKII and cdc2 kinases occurs at S189 and T198 respectively (Longshaw *et al.,* 2000) it is hypothesized that modification at these points will affect the isoform composition of mSTI1 qualitatively and quantitatively.

5.2 EXPERIMENTAL PROCEDURES

5.2.1 Preparation of transfectants expressing mSTI1-EGFP derivatives

Purified preparations of template pSK-mSTI1-EGFP (B.11) were prepared. Plasmids encoding mSTI1-EGFP(S189A), mSTI1-EGFP(T198A), mSTI1-EGFP(S189E) and mSTI1-EGFP(T198E), were prepared by site-directed mutagenesis (B.16) using a double stranded whole plasmid linear amplification (Jung *et al*., 1992). Mutagenesis was performed on the pSK-mSTI1-EGFP construct instead of the pB-mSTI1-EGFP as it was smaller and therefore easier to amplify by whole plasmid linear amplification. Derivative plasmids were screened by restriction endonuclease digestion with diagnostic enzymes (B.16), and fragments resolved by agarose gel electrophoresis (B.2). The mSTI1-EGFP derivative fragments were inserted into pB (B.7, E.5). pSK-mSTI1-EGFP derivative plasmids were sequenced (B.10) to confirm amino acid substitutions. Mouse NIH 3T3 fibroblasts were stably transfected with pB-mSTI1-EGFP derivative plasmids (B.13), and visualized by confocal laser scanning fluorescent microscopy (B.14).

5.2.2 The treatment of cells with heat shock, and kinase, cell cycle and nuclear export inhibitors

Episomally stable transfectants expressing mSTI1-EGFP(S189A); mSTI1EGFP(T198A); mSTI1-EGFP(S189E) and mSTI1-EGFP(T198E) were subcultured into 8 well chamber slides, and exposed to heat shock, hydroxyurea and leptomycin B conditions as before (section 4.2.1). For stress conditions, slides were incubated at 42ºC for 15 minutes. Transfectants were exposed to 10 mM hydroxyurea for 8 hours, to arrest cells in the G1/S phase. Similarly, transfectants were exposed to 10 ng/ml leptomycin B for 3 hours to inhibit nuclear export. Slides were visualized by confocal laser scanning fluorescence microscopy (B.14).

5.2.3 The separation of endogenous mSTI1 isoforms

Three 175-cm^2 flasks of attached NIH 3T3 fibroblasts were cultured (B.12) until 90% confluency was reached. One 175-cm^2 flask was then exposed to heat shock conditions at 42 °C for 15 minutes and one to hydroxyurea conditions at 10 mM for 8 hours. The cells were harvested, the total protein separated by two-dimensional electrophoresis (B.19), and transferred to a nitrocellulose membrane by Western blotting (B.20). mSTI1 isoforms were detected by chemiluminescence-based immunodetection (B.21) using the membrane with primary SF1 Antibody (Lässle *et al.*, 1997) diluted to 1:500 in blocking solution.

5.2.4 The separation of mSTI1-EGFP isoforms and of derivative isoforms

Transfectants expressing mSTI1-EGFP, mSTI1-EGFP(S189A) and mSTI1-EGFP(T198A) were cultured in 175-cm^2 flasks (B.12), before preparing a total protein extract for separation by 2D electrophoresis (B.19) and chemiluminescence-based Western analysis (B.20). The primary antibody used was an anti-GFP antibody, diluted 1:100 in block solution.

5.3 RESULTS AND DISCUSSION

5.3.1 Mammalian constructs encoding mSTI1-EGFP and its modified derivatives are successfully produced.

E. coli transformants containing putative pSK-mSTI1-EGFP mutated plasmids were screened (B.5) by restriction endonuclease digestion (B.6) and the resultant DNA fragments resolved by agarose gel electrophoresis (B.2). Digestion of pSK-mSTI1-EGFP with *Nco*I (Figure 5.1A and F, lane 3) produced the expected 5170-bp fragment, compared to digestion of the putative pSK-mSTI1-EGFP(S189A) with *Nco*I (Figure 5.1B and F, lane 4) which generated the expected 4396 and 774-bp fragments. Digestion of pSK-mSTI1-EGFP with *Ban*I (Figure 5.1A and F, lane 7) produced, among others, the 1723-bp fragment, compared to digestion of the putative pSK-mSTI1-EGFP(T198A) with *Ban*I (Figure 5.1C and F, lane 8), which generated the expected 1080 and 643-bp fragments. Digestion of pSK-mSTI1-EGFP with *Acc*I (Figure 5.1A and G, lane 3) produced the 5296-bp fragments as expected, whereas digestion of the putative pSK-mSTI1-EGFP(S189E) with *Acc*I (Figure 5.1D and G, lane 4) generated the expected 4712 and 584-bp fragments. Digestion of pSK-mSTI1-EGFP with *BSi*EI (Figure 5.1A and G, lane 7) produced the 1835-bp fragments as expected, whereas digestion of the putative pSK-mSTI1-EGFP(T198E) with *BSi*EI (Figure 5.1E and G, lane 8) generated the expected 1040 and 795-bp fragments. The mutations were confirmed by sequencing. The coding regions for mSTI1-EGFP and its mutant derivatives were inserted into pB (B.7, D5).

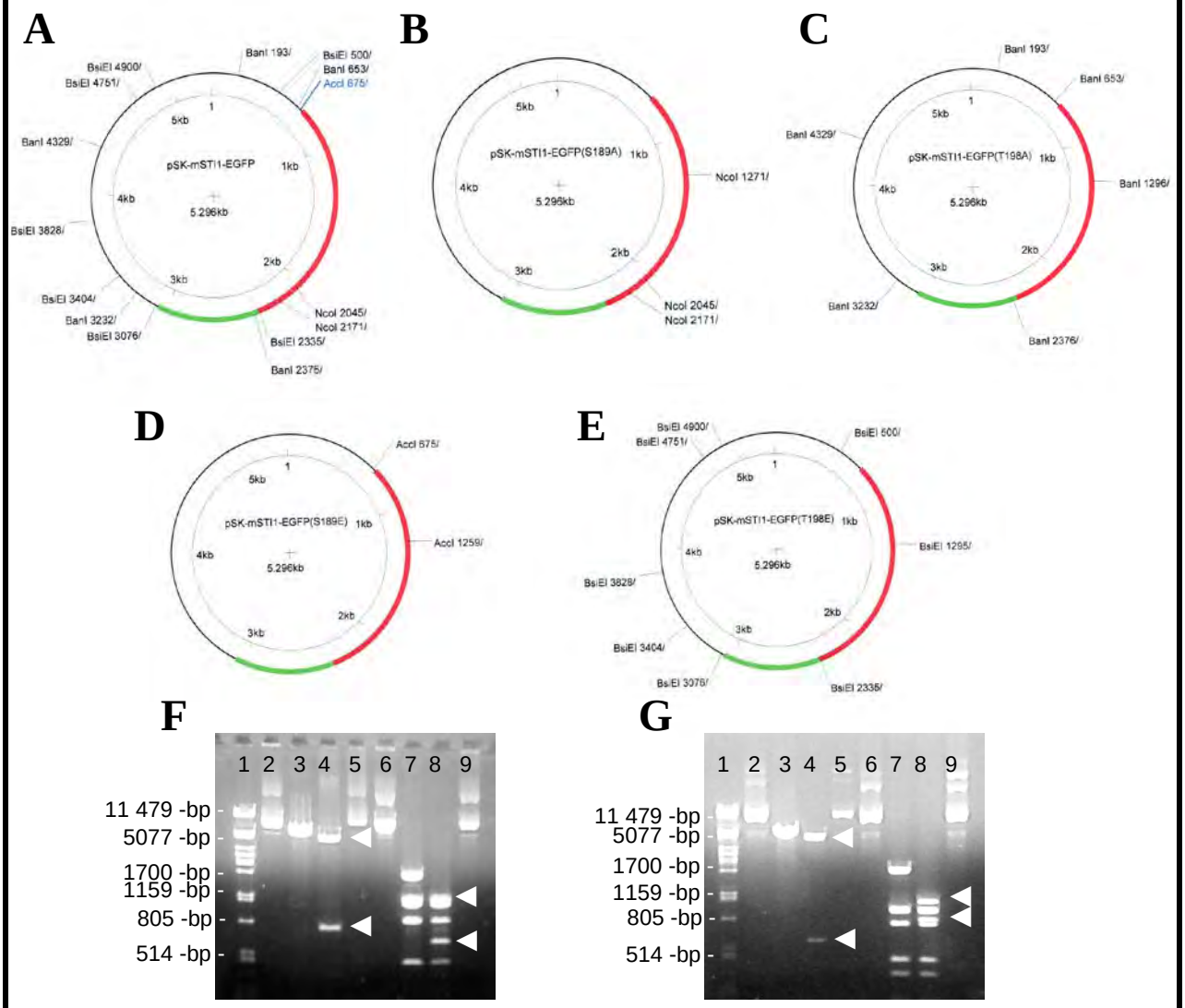

Figure 5.1: The pSK-mSTI1-EGFP constructs and its derivatives are successfully produced

Site directed mutagenesis of pSK-mSTI1-EGFP (A) produced pSK-mSTI1-EGFP(S189A) (B), pSK-mSTI1-EGFP(T198A) (C), pSK-mSTI1-EGFP(S189E) (D) and pSK-mSTI1-EGFP(T198E) (E). The red and green lines represent cDNA of mSTI1 and EGFP respectively. Digestion of pSK-mSTI1-EGFP(S189A) with *Nco*I produced the expected fragments of 4396-bp and 774-bp (F, lane 4), compared to that of pSK-mSTI1-EGFP, which produced the expected 5170 -bp fragment (F, lane 3). The undigested DNA of pSK-mSTI1-EGFP (F, lane 2) and pSK-mSTI1-EGFP(S189A) (F, lane 5) was also resolved. Digestion of pSK-mSTI1-EGFP(T198A) with *Ban*I produced the expected fragments of 1080, and 643 -bp (F, lane 8), compared to that of pSK-mSTI1-EGFP, which produced the expected 1723 -bp fragment (F, lane 7). The undigested DNA of pSK-mSTI1-EGFP (F, lane 6) and pSK-mSTI1-EGFP(T198A) (F, lane 9) was also resolved. Digestion of pSK-mSTI1-EGFP(S189E) with *Acc*I produced the expected fragments of 4712, and 584 -bp (G, lane 4), compared to that of pSK-mSTI1-EGFP, which produced the expected 5296 -bp fragment (G, lane 3). The undigested DNA of pSK-mSTI1-EGFP (G, lane 2) and pSK-mSTI1-EGFP(S189E) (G, lane 5) was also resolved. Digestion of pSK-mSTI1-EGFP(T198E) with *BSi*EI produced the expected fragments of 1040 and 795 -bp (G, lane 8), compared to that of pSK-mSTI1-EGFP, which produced the expected 1835 fragment (G, lane 7). The undigested DNA of pSK-mSTI1-EGFP (G, lane 6) and pSK-mSTI1-EGFP(T198E) (G, lane 9) was also resolved.

5.3.2 Mimicking of phosphorylation at the CKII site (S189) promotes a nuclear localization of mSTI1-EGFP

Studies of the CcN motif in SV40 T-antigen have shown simulation of phosphorylation by replacement of the serine phosphorylation site with a negatively charged amino acid, have resulted in an enhancement of transport of the SV40 T-antigen (Jans and Jans, 1994). Therefore, to assess the effect of phosphorylation at the CKII site on nuclear import of mSTI1-EGFP, the serine at position 189 was replaced with a glutamic acid. The percentage of cells that demonstrated an increased nuclear localization of expressed protein was found to be greater in mSTI1-EGFP(S189E) (44 %) expressing cells than in mSTI1-EGFP expressing cells (13 %) (Figure 5.2). This suggested an enhancing effect of a negative charge at the S189 site on mSTI1-EGFP nuclear import under normal conditions. The nuclear accumulation of mSTI1-EGFP (97%) and mSTI1-EGFP(S189E) (96%) were found to be similar under conditions of nuclear import inhibition (leptomycin B) (Figure 5.3), suggesting that nuclear import cannot be further enhanced by this substitution under these conditions. The S189E mutation therefore does not have an effect on the nuclear accumulation of mSTI1-EGFP under leptomycin B conditions. We removed the potential *in vivo* CKII site, S189, by replacement with an alanine residue. The percentage of cells that demonstrated nuclear localization of expressed protein was found to be similar in mSTI1-EGFP(S189A) (18 %) expressing cells and mSTI1-EGFP expressing cells (13%) under normal conditions (Figure 5.2). Similar localization of mSTI1-EGFP (97%) and mSTI1-EGFP(S189A) (98%) occurred under conditions of nuclear export inhibition (leptomycin B) (Figure 5.3). The S189A mutation therefore does not have an effect on the nuclear accumulation of mSTI1-EGFP under leptomycin B conditions. Under conditions of heat shock (Figure 5.3) and G1/S phase arrest (Figure 5.4), neither removal of phosphorylation sites, nor mimicking of phosphorylation at the S189 site affected the cytoplasmic localization of mSTI1.

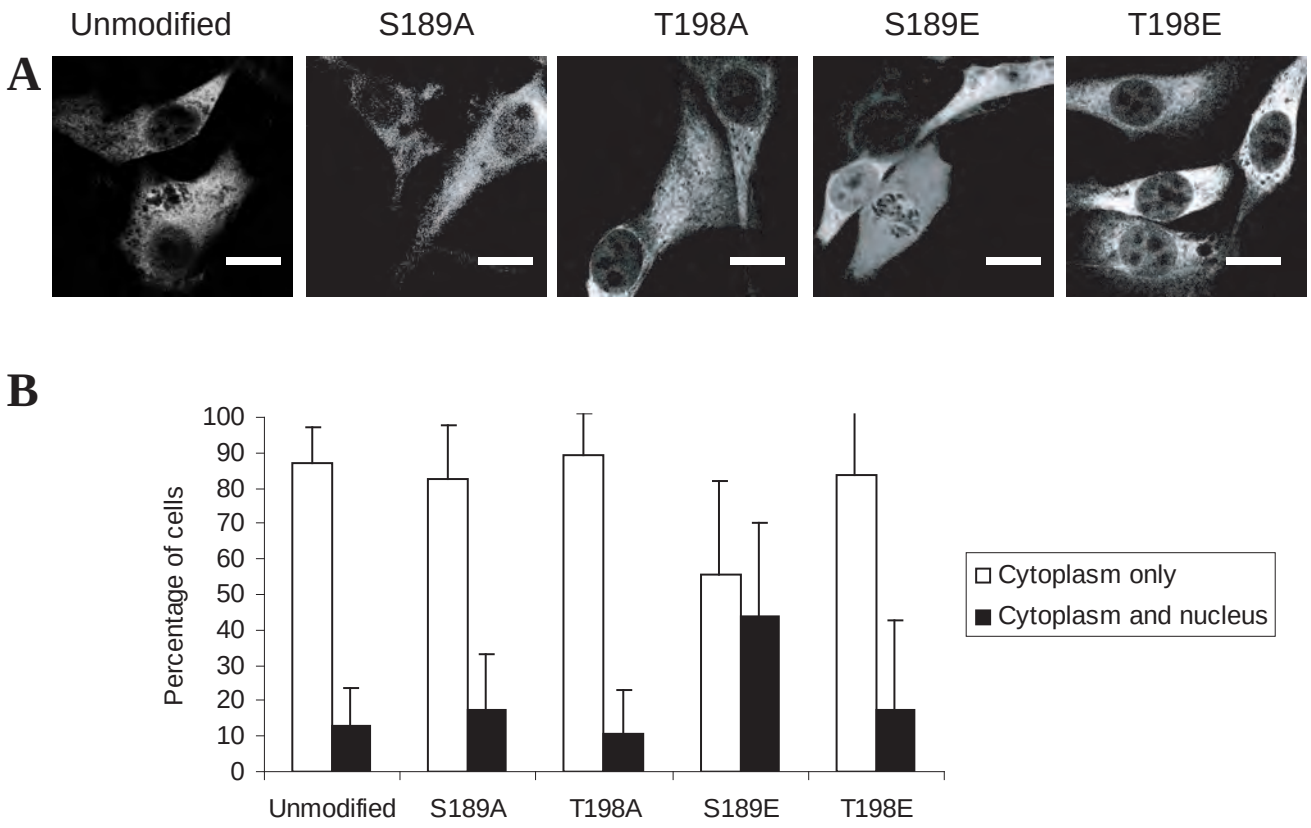

Figure 5.2: Phosphorylation mimic at S189 and not T198 affects the localization of mSTI1-EGFP in resting cells.

(A) Mouse NIH 3T3 fibroblasts were stably transfected with pB-mSTI1-EGFP and its derivatives pB-mSTI1-EGFP(S189A), pB-mSTI1-EGFP(T198A), pB-mSTI1-EGFP(S189E) and pB-mSTI1-EGFP(T198E). Cells were fixed in 3.7% paraformaldehyde and visualized by confocal laser fluorescence microscopy. Scale bars represent 10 micrometers. (B) Cells were transfected as described in (A). Cells demonstrating cytoplasmic fluorescence or nuclear and cytoplasmic fluorescence were scored from 5 fields.

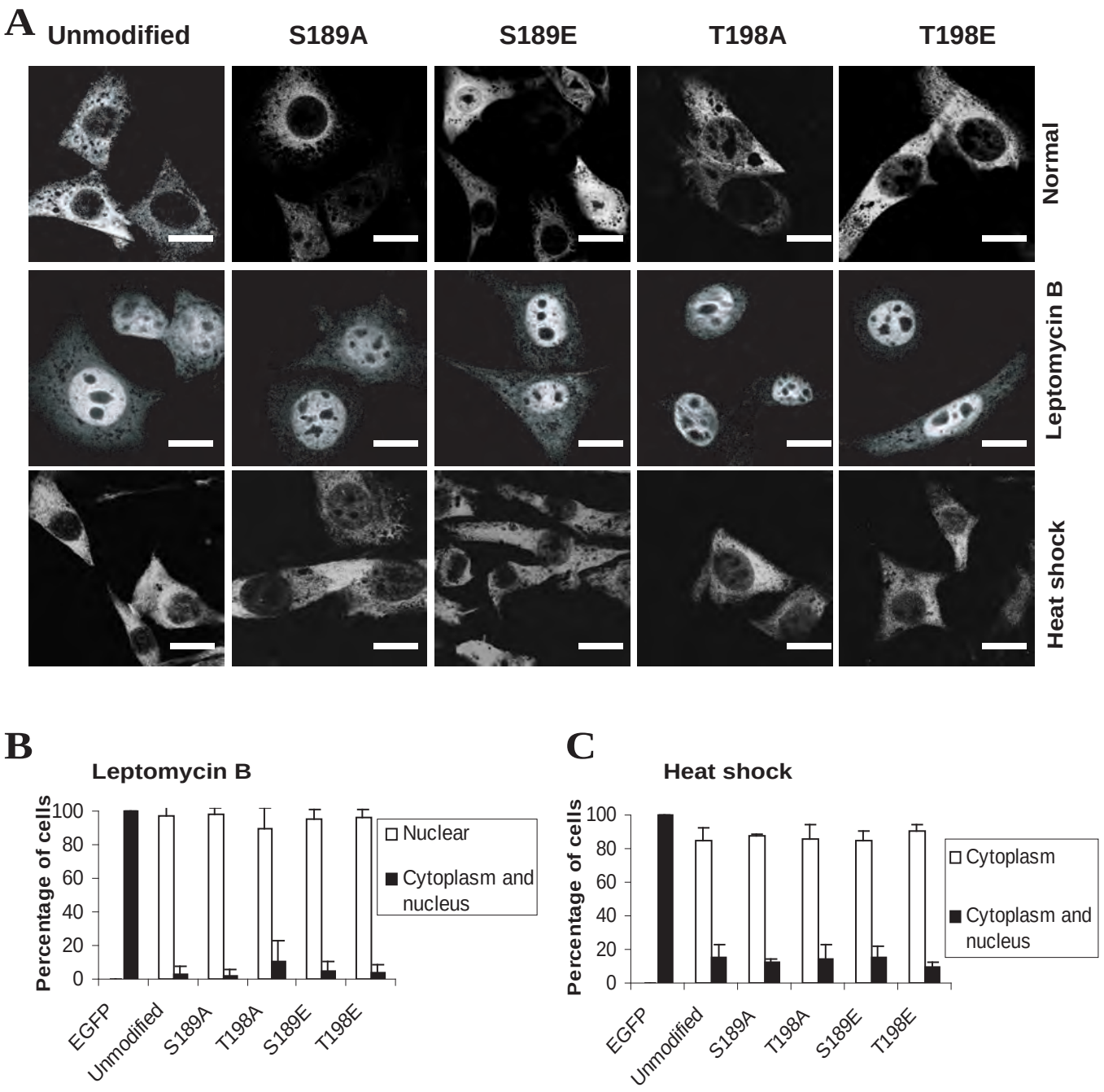

Figure 5.3: Mutations at sites S189 and T198 did not affect final nuclear import under normal or heat shock conditions

(A) Mouse NIH 3T3 fibroblasts were stably transfected with pB-mSTI1-EGFP and its derivatives pB-mSTI1-EGFP(S189A), pB-mSTI1-EGFP(T198A), pB-mSTI1-EGFP(S189E) and pB-mSTI1-EGFP(T198E). Cells were exposed to 10 ng/ml leptomycin B or 15 minutes heat shock at 42C, fixed in 3.7% paraformaldehyde and visualized by confocal laser fluorescence microscopy. Scale bars represent 10 micrometers. (B) Cells were transfected and treated as described in (A). Cells demonstrating cytoplasmic fluorescence or nuclear and cytoplasmic fluorescence were scored from 5 fields

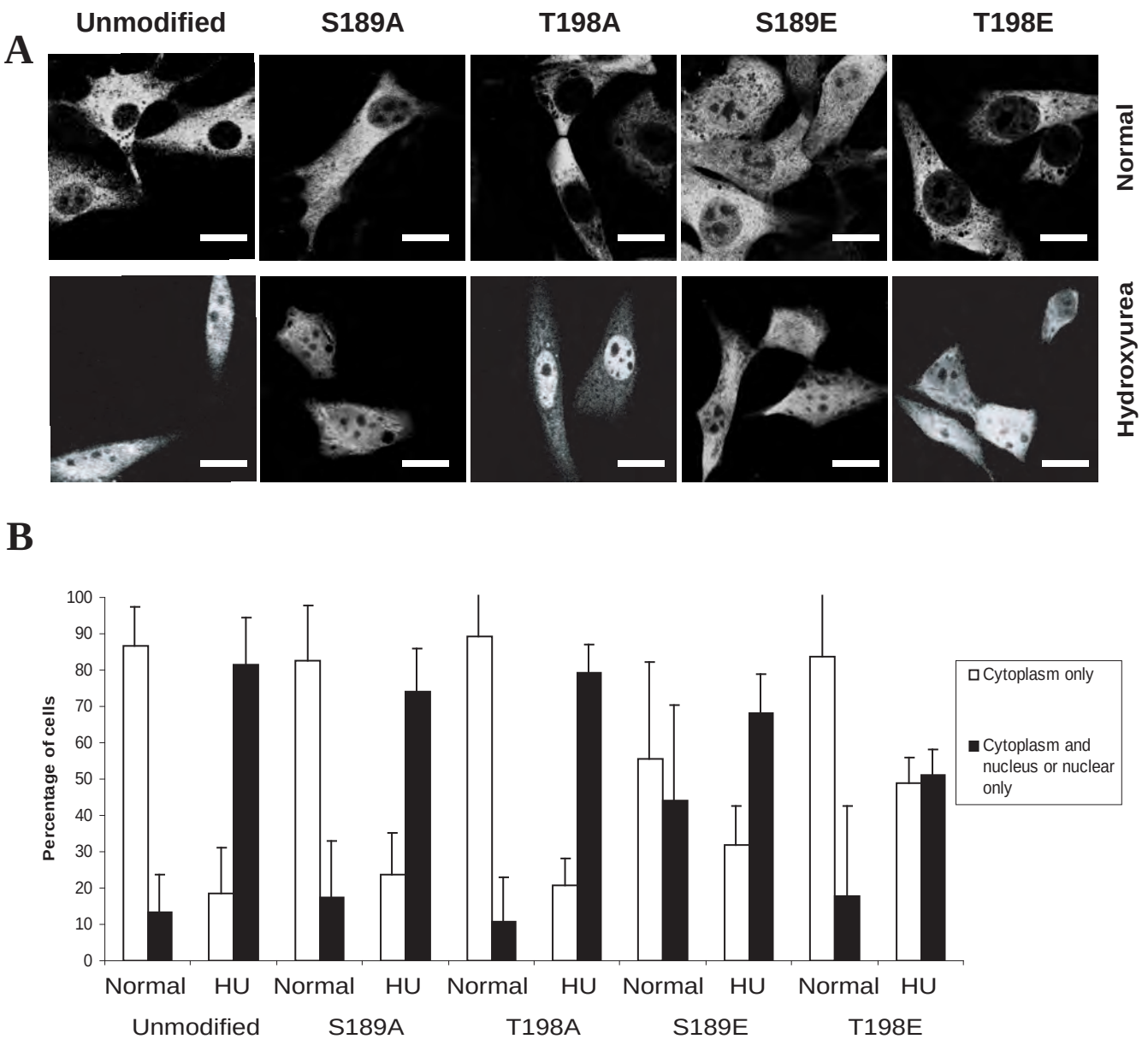

Figure 5.4: Phosphorylation mimic and phosphorylation site removal at T198 affects the localization of mSTI1-EGFP under G1/S phase arrest.

(A) Mouse NIH 3T3 fibroblasts were stably transfected with pB-mSTI1-EGFP and its derivatives pB-mSTI1-EGFP(S189A), pB-mSTI1-EGFP(T198A), pB-mSTI1-EGFP(S189E) and pB-mSTI1-EGFP(T198E). Cells were treated with hydroxyurea (10 mM) for 10 hours, fixed in 3.7% paraformaldehyde and visualized by confocal laser fluorescence microscopy. Scale bars represent 10 micrometers. (B) Cells were transfected as described in (A). Cells demonstrating cytoplasmic fluorescence or nuclear and cytoplasmic fluorescence were scored from 5 fields.

5.3.3 Removal of the cdc2 kinase site (T198A) promotes a nuclear localization of mSTI1-EGFP at the G1/S transition

Since specific inhibition of cdc2 kinase increased the nuclear localization of mSTI1, we assessed the importance of the potential *in vivo* cdc2 kinase phosphorylation site, T198, by replacement with an alanine residue. The percentage of cells demonstrating cytoplasmic and nuclear localization of fluorescence was found to be similar in mSTI1-EGFP(T198A) (11%) expressing cells and in mSTI1-EGFP expressing cells (13%) under normal conditions (Figure 5.2). Similarly, there was no difference in nuclear localization of mSTI1-EGFP (98%) and mSTI1-EGFP(T198A) (90%) under leptomycin inhibition of nuclear export (Figure 5.3). The T198A mutation therefore does not have an effect on the nuclear accumulation of mSTI1-EGFP under leptomycin B conditions. Under conditions of heat shock, neither removal of phosphorylation sites, nor mimicking of phosphorylation at the T198 site affected the cytoplasmic localization of mSTI1 (Figure 5.4). These data suggest that mSTI1 may not be phosphorylated at this site *in vivo,* or that this site does not function to regulate mSTI1 localization under heat shock conditions.

However, following hydroxyurea treatment, although the percentage mSTI1-EGFP and mSTI1-EGFP(T198A) expressing cells with cytoplasmic and nuclear localization of expressed protein was similar, a greater degree of nuclear accumulation of mSTI1-EGFP(T198A) occurred (Figure 5.4). The removal of this cdc2 kinase site, therefore, significantly promoted nuclear localization of mSTI1-EGFP under G1/S phase arrest conditions. The incidence of cells demonstrating cytoplasmic and nuclear localization of fluorescence was found to be similar in mSTI1-EGFP(T198E) (18%) expressing cells as in mSTI1-EGFP expressing cells (13%), under normal conditions (Figure 5.2). Similarly, there was no difference in the incidence of cells demonstrating nuclear localization of mSTI1-EGFP (98%) and mSTI1-EGFP(T198E) (96%) under leptomycin B inhibition of nuclear export (Figure 5.3). The T198E mutation therefore does not have an effect on the nuclear accumulation of mSTI1-EGFP under leptomycin B conditions. However,

following hydroxyurea treatment a lesser incidence of nuclear accumulation of mSTI1-EGFP(T198E) (51%) than mSTI1-EGFP (81%) occurred (Figure 5.4). Therefore, either mSTI1 may not be phosphorylated at this site *in vivo,* or removal of the cdc2 kinase site may have no effect on localization of mSTI1 under normal conditions, but may increase nuclear localization at the G1/S transition.

5.3.4 The isoform composition of mSTI1 changes after heat shock and at the G1/S transition

To investigate the potential presence of different isoforms of mSTI1 in cells under different conditions, we separated NIH 3T3 cell lysates obtained from cells after heat shock and hydroxyurea treatment by 2D gel electrophoresis, and detected mSTI1 by Western analysis (Figure 5.5A). Previously, the levels and types of mSTI1 isoforms have been shown to change after heat shock (Lässle *et al.,* 1997). We found a similar change in endogenous mSTI1 isoform levels under these heat shock conditions, in that the levels of the major isoform present under normal conditions was decreased, with a simultaneous increase in more acidic isoforms and hence potentially more phosphorylated forms of mSTI1 (Figure 5.5A). We noticed no change in the subcellular distribution of mSTI1-EGFP or mSTI1 after heat shock, suggesting that the change in mSTI1 isoform levels that occurred after heat shock did not mediate a change in cellular localization. Endogenous mSTI1 isoform composition also changed after hydroxyurea exposure, to a pattern that differed from that observed under heat shock conditions. Levels of the major isoform present under normal growth conditions were decreased, with a simultaneous increase in more acidic and hence potentially more phosphorylated isoforms (Figure 5.5A). In particular, a new acidic isoform at position –3 was observed. These data provided evidence of different isoforms of mSTI1 in the cell under G1/S phase arrest. The extent to which these changes in mSTI1 isoform composition correlate with changes in mSTI1 localization remains to be determined.

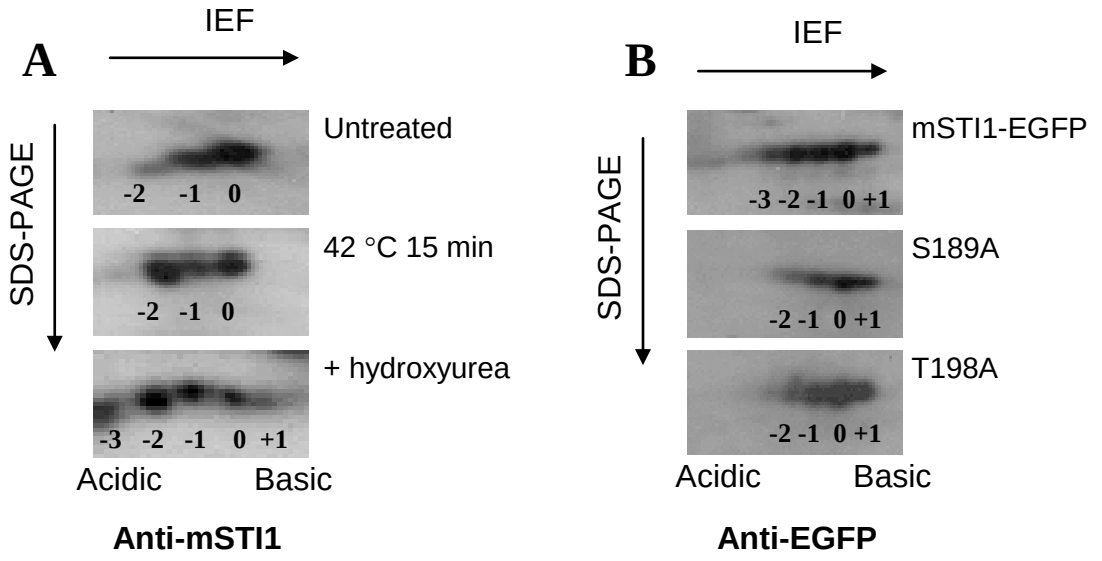

Figure 5.5: mSTI1 demonstrates acidic isoforms *in vivo*

(A) 100 μg total NIH 3T3 fibroblast lysate prepared from cells under normal (*top*), heat shock (*middle*) and 10 mM hydroxyurea (*bottom*) was focused on IEF pH 3-10 strips in the first dimension, then separated on a (0.1%) SDS (12%) PAGE gel in the second dimension. SDS PAGE gels were transferred to nitrocellulose membranes and probed with SF1 anti-mSTI1 antibody. After aligning the blots, the most prominent spots were labeled, with the most abundant spot under non-treatment conditions labeled 0, and spots located towards the more acidic region of the gel labeled increasing negative numbers. (B) Cell extracts of mouse NIH 3T3 fibroblasts that were transfected with pB-mSTI1-EGFP (*top*), pB-mSTI1-EGFP(S189A) (*middle*) and pB-mSTI1-EGFP(T198A) (*bottom*) were analyzed as described in (A). After aligning the blots, the most prominent spots were labelled, with the most abundant spot under non-treatment conditions labeled 0, and spots located towards the more acidic region of the gel labeled increasing negative numbers. Spots located towards the more basic region of the gel labeled increasing positive numbers

5.3.5 Modification at the S189 and T198 positions affects the isoform composition of mSTI1

To investigate whether substitutions at the potential phosphorylation sites S189 and T198, affect isoform composition, lysates from NIH 3T3 cells expressing the chimeric proteins mSTI1-EGFP, mSTI1-EGFP(S189A) and mSTI1-EGFP(T198A) were separated by 2D gel electrophoresis and the EGFP moiety detected by Western analysis (Figure 5.5B). Interestingly, five isoforms were detected for mSTI1-EGFP while three isoforms were detected for endogenous mSTI1 under normal conditions (Figure). Therefore, although the fusion of the EGFP to the C-terminus of mSTI1 did not affect the subcellular localization of mSTI1, it did increase the number of mSTI1 isoforms. The

fusion of the EGFP may reveal additional modifications on mSTI1, or EGFP may itself be modified *in vivo*, producing additional isoforms. While five isoforms were detected for mSTI1-EGFP (Figure 5.5B, top), four isoforms were detected for mSTI1-EGFP(S189A) and for mSTI1-EGFP(T198A) (Figure 5.5B, middle and bottom). These results imply that the modification at S189 and T198 under normal conditions could account for some of the different isoforms of mSTI1-EGFP. There are more than two different isoforms of mSTI1-EGFP(S189A) and mSTI1-EGFP(T198A) implying additional sites of modification must be present in addition to S189 and T198. In previous studies of CcN motifs, phosphorylation at either the CKII or the cdc2 kinase site was found to occur but never at both sites simultaneously. These data are consistent with the results for endogenous mSTI1 isoforms in that they also suggest the existence of phosphorylated mSTI1 isoforms. In addition, these data suggest that there may be additional sites of modification/phosphorylation in mSTI1 that are located outside the CcN motif. We have used in an *in vitro* assay with recombinant mSTI1 protein to investigate this possibility (Chapter 6).

5.3 CONCLUSIONS

Substitution of the potential *in vivo* CKII phosphorylation site at S189 with a non-phosphorylatable alanine residue did not affect the localization of mSTI1 under normal conditions. However, substitution of this S189 residue with a negatively charged residue, such as glutamic acid, promoted the incidence of a nuclear localization of mSTI1. These modifications of mSTI1 did not affect the functionality of nuclear import as they accumulated in the nucleus under leptomycin B inhibition of nuclear export. These data imply that mSTI1 may not be phosphorylated at the potential *in vivo* CKII phosphorylation site at S189 under normal conditions. However, the presence of negative charge at this site may serve to increase nuclear accumulation of mSTI1. Therefore, this potential *in vivo* CKII phosphorylation site may function to promote nuclear localization of mSTI1 under conditions that are as yet unknown. These substitutions affected neither the cytoplasmic localization of mSTI1 under heat shock conditions, nor the cytoplasmic and nuclear localization of mSTI1 under G1/S arrest conditions, implying no role for this site in the regulation of mSTI1 localization under these conditions.

Substitution of the potential *in vivo* cdc2 kinase phosphorylation site at T198 with a non-phosphorylatable alanine residue did not affect the localization of mSTI1 under normal conditions. Similarly, substitution of this S189 residue with the negatively charged residue glutamic acid did not affect the localization of mSTI1. This data implies that mSTI1 is not modified at this T198 site *in vivo* under normal conditions. These substitution modifications of mSTI1 did not affect the functionality of nuclear import as they accumulated in the nucleus under leptomycin B inhibition of nuclear export. However, under G1/S phase arrest, when nuclear accumulation of mSTI1 is promoted (Chapter 4) and cdc2 kinase is inhibited, removal of the potential *in vivo* cdc2 kinase phosphorylation site at T198 increased nuclear accumulation qualitatively. Furthermore, the presence of negative charge at this site decreased the incidence of nuclear accumulation of mSTI1 under G1/S arrest conditions. Therefore, the presence of this potential *in vivo* cdc2 kinase phosphorylation site may function to inhibit nuclear localization of mSTI1 under G1/S arrest conditions, implying a role for this site in cell-

cycle regulation of mSTI1 localization. These substitutions did not affect the cytoplasmic localization of mSTI1 under heat shock conditions, implying no role for this site in the regulation of mSTI1 under heat shock conditions.

A shift in the *in vivo* isoform composition of Hop, to more acidic (and therefore possibly more phosphorylated) forms, occurs after heat shock, suggesting the stress-induced phosphorylation of a Hop subpopulation (Chen *et al*., 1996). The isoform compositions of endogenous mSTI1 changed qualitatively after heat shock, and both qualitatively and quantitatively under G1/S arrest conditions. These different isoforms may be various phosphorylated forms of mSTI1. Heat shock and G1/S arrest may therefore affect the phosphorylation status of mSTI1. Fusion of EGFP to mSTI1 affected the isoform composition of mSTI1. Nevertheless, modification at the S189 and T198 positions decreased the number of isoforms of mSTI1-EGFP under normal conditions, suggesting that these sites in mSTI1-EGFP are modified *in vivo*. Therefore, taken together, these results imply that modifications at S189 and T198 may occur *in vivo*, however although the effects of such modifications may potentially extend to the kinetics of subcellular distribution, they do not affect the final equilibrium of mSTI1 localization.

It is possible that other kinases may phosphorylate the CcN motif sites, although no other kinase phosphorylation consensus sequences were identified in the CcN motif. In this way kinase specific phosphorylation data was obtained. Previously, it was reported that *in vitro* CKII and cdc2 kinase phosphorylate mSTI1 at S189 and T198 only (Longshaw *et al.,* 2000). However, this work was limited to GST-tagged mSTI1, and in light of the presence of multiple isoforms of endogenous mSTI1 under G1/S arrest conditions, further *in vitro* kinetic phosphorylation studies on untagged mSTI1 were required for characterization of the phosphorylation of mSTI1 by CKII and cdc2 kinase (Chapter 6).

CHAPTER 6

IN VITRO ANALYSIS OF THE POTENTIAL CKII AND CDC2 KINASE PHOSPHORYLATION SITES OF mSTI1

SUMMARY: Recombinant GST-mSTI1 and untagged mSTI1, and derivatives, were produced and purified. CKII specifically phosphorylated GST-mSTI1 and mSTI1, but negligible phosphorylation by CKII was detected for the no-enzyme autophosphorylation control, GST-mSTI1(S189A) and mSTI1(S189A) derivatives. This provides strong evidence that S189 is the specific CKII phosphorylation site recognised *in vitro*. Cdc2 kinase phosphorylated mSTI1 to higher levels than mSTI1(T198A), implying that the T198 phosphorylation site was recognised by cdc2 kinase *in vitro*. A similar level of phosphorylation was observed for mSTI1(T198A) and mSTI1(T198A,T332A) phosphorylation reactions, indicating that another, as yet unidentified, cdc2 recognized phosphorylation site, which did not map to T198 or T332, may exist in mSTI1. There may therefore be multiple *in vitro* cdc2 kinase phosphorylation sites in mSTI1, which may explain the spectrum of mSTI1 isoforms observed *in vivo*. T198, however, appears to be the major *in vitro* cdc2 kinase site. mSTI1 did not form a detectable stable complex with cdc2 kinase, suggesting that the interaction between mSTI1 and cdc2 kinase may only be transitory.

6.1 INTRODUCTION

6.1.1 Phosphorylation of mSTI1 and its homologs

Previously, little information on potential phosphorylation of mSTI1 or its homologs was available. The first data that suggested phosphorylation of a homolog of mSTI1 was reported by Chen *et al.* (1996) when its was found that the *in vivo* isoform composition of Hop shifted to more acidic (and therefore possibly more phosphorylated) forms, after viral transformation as well as after heat shock. This implied the stress-induced phosphorylation of a Hop subpopulation (Honoré *et al*., 1992). This work similarly reports a shift in the *in vivo* isoform composition of mSTI1 to more acidic forms after heat shock (Chapter 4). Preliminary investigations into the possible phosphorylation of mSTI1 have shown that MAP kinase-activated protein kinase 2 (MAPKAP kinase 2), a heat activated kinase, does not phosphorylate mSTI1 to detectable levels (Lässle *et al*., 1997). The heat-activated S6 kinase $pp90^{rsk}$, however, has been shown to phosphorylate an N-terminal peptide of mSTI1 with low activity (Lässle *et al*., 1997). The cell cycle kinases CKII and cdc2 kinase have been found to phosphorylate mSTI1 *in vitro*. More specifically CKII and cdc2 kinase have been shown to phosphorylate mSTI1 at S189 and T198 respectively (Longshaw *et al*., 2000). However, the investigation of phosphorylation of mSTI1 by CKII and cdc2 kinase has to date been carried out on GST- and His-tagged mSTI1 protein, such that these tags may have affected the phosphorylation of mSTI1. Furthermore, the numerous isoforms of mSTI1 (Chapter 5) imply that more than one phosphorylation site exists in mSTI1. A more accurate characterization of this phosphorylation of mSTI1 therefore needs to be performed on untagged mSTI1 protein. In order to maintain continuity with previous work and confirm these results on a more accurate untagged system, phosphorylation studies were carried out on GST-mSTI1 and mSTI1 proteins respectively. Recently, it was shown that STI1 interacts directly with cdc37 (Abbas-Terki *et al*., 2002). Furthermore, cdc37 has been found to interact with cdc28 in *Saccharomyces cerevisiae* (Mort-Bontemps-Soret *et al*., 2002). Therefore STI1, cdc37 and cdc28 may interact together in a cell cycle dependent manner to regulate both the chaperoning and localization of client proteins.

6.1.2 Specific hypothesis, aims and objectives

The main function of mSTI1 appears to be its association with Hsp70 and Hsp90 via the TPR motifs in mSTI1 (van der Spuy *et al.,* 2000). The rate-limiting ATP-dependent opening of the steroid binding cleft after Hsp90 binding (Kanelakis *et al.,* 2002) may be regulated by the co-chaperone Hop. mSTI1 is a homolog of Hop (Lässle *et al.*, 1997). The assembly and regulation of the GR-Hsp90 chaperone system by mSTI1 may therefore be affected by potential phosphorylation of mSTI1. Furthermore, CKII and cdc2 kinases phosphorylate mSTI1, proximal to the NLS, supporting a predicted CcN motif (Longshaw *et al.,* 2000) (Figure 1.5). The localization of the GR-Hsp90 chaperone system by mSTI1 may therefore be affected by potential phosphorylation of mSTI1.

Untagged mSTI1 is hypothesized to be phosphorylated by CKII and cdc2 kinase at the CcN motif, and interact with cdc2 kinase in a complex.

In order to characterize the phosphorylation of mSTI1 by CKII and cdc2 kinase, recombinant mSTI1 was produced and enriched to sufficient purity such that *in vitro* phosphorylation studies could be carried out. The phosphorylation data previously reported for mSTI1 (Longshaw *et al.*, 2000) was performed using GST- and His- tagged mSTI1. The large nature of the GST-tag and the highly charged nature of the His-tag may affect the phosphorylation of mSTI1. Furthermore, the numerous isoforms of mSTI1 (Chapter 5) imply that more than one phosphorylation site exists in mSTI1. Therefore, mSTI1 was produced and purified in an untagged system, and the phosphorylation of mSTI1 by CKII and cdc2 kinase characterized. Amino acid replacement was carried out at position S189 for CKII phosphorylation (Longshaw *et al.,* 2000) and at T198 and T332 for cdc2 kinase phosphorylation (Longshaw *et al.,* 2000 and by bioinformatic analysis in Chapter 2). T332 was the only other position in mSTI1 that conformed to the cdc2 kinase consensus site that was also in close proximity to a potential NLS. The association of cdc2 kinase and mSTI1 in a complex was also investigated, using a GST-mSTI1 binding assay (van der Spuy *et al.,* 2000, Longshaw *et al.,* 2000).

6.2 EXPERIMENTAL PROCEDURES

The vendors of the materials used are described in Appendix A (A) and the general procedures used are described in Appendix B (B). The identity and characteristics of the primers used are described in Appendix C (C) and subcloning steps are described in Appendix D (D). The maps of the plasmid vectors used are shown in Appendix E (E).

6.2.1 Preparation of pGEX3X2000 and derivative plasmids

The pGEX3X2000 plasmid (constructed by Prof. Blatch, Rhodes University, vector map E.1), expressing GST-mSTI1 was a kind gift of J acquiva n der S puy (UCL). pGEX3X2000 was transformed into *E. coli* XL1Blue competent cells (B.8). Purified preparations of pGEX3X2000 DNA were prepared (B.11). Plasmids encoding GST-mSTI1(S189A), GST-mSTI1(T198A) and GST-mSTI1(T198A, T332A), were prepared by site-directed mutagenesis (B.16) and transformed into *E. coli* XL1Blue supercompetent cells (B.4). Derivative plasmids were screened by restriction endonuclease digestion with diagnostic enzymes (B.16), and fragments resolved by agarose gel electrophoresis (B.2). pGEX3X2000 derivative plasmids were sequenced (B.10) to confirm amino acid substitutions.

6.2.2 Purification of GST-mSTI1 and derivative proteins

The induction of GST-mSTI1 proteins was optimized: single colonies of *E. coli* XL1Blue transformants expressing GST, GST-mSTI1, GST-mSTI1(S189A), GST-mSTI1(T198A) and GST-mSTI1(T198A,T332A) from freshly streaked 0.1 mg/ml ampicillin 2 x YT broth plates were cultured overnight at 37 °C in 2 x YT broth [25 ml] containing 0.1 mg/ml ampicillin. These overnight cultures were each diluted 1: 10 into fresh 2 x YT broth [225 ml] and incubated for a further 3 hours until logarithmic phase was reached (A_{600}=0.6-1). Samples [2 x 1 ml] were taken. The production of recombinant proteins was induced by the addition of iso-propyl-β-D-galactopyranoside (IPTG) to a final

concentration of 1 mM. Samples [2 x 1 ml] were taken hourly: the A_{600} of the one sample was measured and the cells of the other sample collected by centrifugation at 6000 x g for 1 minute. The cell pellets were resuspended in phosphate buffered saline (PBS) (137 mM NaCl, 2.7 mM KCl, 4.3 mM Na_2HPO_4, 1.4 mM KH_2PO_4; pH 7.4) in a ratio of 50 µl PBS per 0.5 A_{600} unit, in order to achieve comparable concentrations of cell suspensions. The samples pre- and post- induction were resolved by SDS PAGE (B.18) to assess the optimum induction period. Similarly, induced cultures were prepared and induced for 4 hours. Typically each protein purification was carried out from a 250 ml induced culture. The cell pellets were resuspended in PBS [5 ml] containing 100 µg/ml phenylmethylsulfonyl fluoride (PMSF), aliquoted [1 ml] into eppendorfs, and lysed on ice by sonication (set at 40%) for 5 x 30 seconds. The extract was centrifuged at 12 000 x g for 20 minutes, and the soluble cell extract incubated with 50 % slurry of glutathione agarose beads [250 µl] in PBS, at 4°C with gentle agitation, for 45 minutes. The beads were washed three times with ice-cold PBS, followed by elution of bound GST-fusion proteins in elution buffer [500 µl] (50 mM Tris-HCl, pH 8.0, 5 mM reduced glutathione). The concentration of purified GST-mSTI1 proteins was measured using the Lowry method (B.22). Purified protein preparations were used immediately or stored in aliquots [20-100 µl] at -80°C.

6.2.3 The PCR amplification of mSTI1 and insertion into pGEM(T)

In order to produce a construct expressing untagged mSTI1, the mSTI1 open reading frame (ORF) was amplified from the pGEX3X2000 template DNA plasmid by PCR (B.1) using the mSTI1-specific forward primer PCRmSTI1pET5aF and the reverse primer PCRmSTI1pET5aR (C). The cycling parameters were as described in B.1, except that an annealing temperature of 50°C was used. The resultant PCR product encompassed the mSTI1 open reading frame, including the authentic mSTI1 start methionine (…ATGGAGCAG…), immediately preceded by an *Nde*I site and followed by an *Nhe*I site downstream of the mSTI1 stop codon. The PCR product [5 µl] was resolved by

agarose gel electrophoresis (B.2), ligated to pGEM(T) (B.3, E.2), and transformed into supercompetent *E. coli* XL1Blue cells (B.4). Transformants were screened for putative pGEM(T)mSTI1[*Nde*I/*Nhe*I] plasmid DNA (B.5). Plasmid DNA was extracted from *E. coli* cultures of transformants forming white colonies, by a modified alkaline lysis method (Birnboim and Doly, 1979; Joly, 1996) and using the High Pure Plasmid Isolation Kit (B.5). Putative pGEM(T)mSTI1[*Nde*I/*Nhe*I] plasmid DNA was restricted separately with *Nde*I, in high salt buffer, and with *Nhe*I in medium salt buffer (B.6). Plasmid DNA *Nde*I and *Nhe*I restriction fragments were resolved by agarose gel electrophoresis (B.2) and those plasmid digestions containing fragments migrating expected distances corresponding to sizes of 3015-bp and 1600-bp were regarded as pGEM(T)mSTI1[*Nde*I/*Nhe*I] (D.6).

6.2.4 The directional ligation of mSTI1 cDNA into the pET5a vector and the preparation of derivative plasmids

Bulk pGEM(T)mSTI1[*Nde*I/*Nhe*I] and pET5a vector (5 µg) were each first restricted with *Nhe*I in medium salt buffer and then with *Nde*I in high salt buffer, ethanol precipitated and resolved by agarose gel electrophoresis (B.7). The appropriate bands (1600-bp and 4134-bp for pGEM(T)mSTI1[*Nde*I/*Nhe*I] and pET5a digests respectively), were excised and extracted from the agarose gel (B.2). The gel-purified 1600-bp mSTI1 cDNA insert was ligated to the restricted and gel-purified 4134-bp pET5a vector (B.7, E.6). Ligation reactions were transformed into *E. coli* XL1Blue (B.8). Putative pET5a2000 plasmid DNA was screened by *Pst*I restriction, in high salt buffer (B.5), and resolved by agarose gel electrophoresis (B.2). Those plasmid digestions containing fragments migrating expected distances corresponding to the sizes of 3500-bp and 1950-bp were regarded as pET5a2000. The integrity of the mSTI1 cDNA insert in pET5a2000 was confirmed by sequencing (B.10) and it included the authentic mSTI1 start methionine (…ATGGAGCAG…).

Purified preparations of template pET5a2000 (B.11) were prepared. Plasmids encoding mSTI1(S189A), mSTI1(T198A) and mSTI1(T198A, T332A), were prepared by site-

directed mutagenesis (B.16) and transformed into *E. coli* XL1Blue supercompetent cells (B.4). Derivative plasmids were screened by restriction endonuclease digestion with diagnostic enzymes (B.16), and fragments resolved by agarose gel electrophoresis (B.2). pET5a2000 derivative plasmids were sequenced (B.10) to confirm amino acid substitutions.

6.2.5 Purification of mSTI1 and derivative proteins

pET5a2000 and derivative plasmids were transformed into competent *E. coli* BL21 (DE3) (B.8). The induction of mSTI1 proteins was optimized as described in section 5.2.2. Similarly, log phase cultures were prepared at 37 °C and induced for 3 hours at 25°C. Typically, each protein purification was carried out from a 250 ml induced culture. The cell pellets were resuspended in PBS [5 ml] containing 100 µg/ml PMSF, aliquoted [1 ml] into eppendorfs, and lysed on ice by sonication (set at 40%) for 5 x 30 seconds. The extract was centrifuged at 12 000 x g for 20 minutes, and the soluble cell extract was then loaded onto a chromatofocussing column [30 ml] which was pre-equilibrated in Start buffer (20 mM Tris-HCl, pH 8.0). Fractions [1.5 ml] were collected at a flow rate of 30 ml/hr. The column was washed with Start buffer [50 ml], followed by Wash buffer [50 ml] (20 mM Tris-HCl, 0.1 M NaCl). Protein bound to the column was eluted using an elution gradient of 0.1-0.3 M NaCl in which Wash buffer [50 ml] was set against Elution buffer [50ml] (20 mM Tris-HCl, 0.3 M NaCl). The A_{280} of all fractions was measured, and samples [80 µl] of peaks added to SDS PAGE gel loading buffer [20 µl]. These samples were resolved by SDS PAGE (B.18). The concentration of peaks exhibiting a large amount of 60 kDa protein was measured using the Lowry method (B.22). Purified protein preparations were used immediately or stored in aliquots [20-100 µl] at -80°C.

6.2.6 CKII phosphorylation of mSTI1

CKII phosphorylation assays were performed according to Lässle *et al* (1997). A radioactive cocktail was prepared containing sterile deionised triple-distilled water [55

µl], 10x CKII buffer [16 µl] (200 mM Tris-HCl pH 7.5, 500 mM KCl, 100 mM $MgCl_2$), ATP [6.4 µl] (100 mM) and [γ-^{32}ATP] (to a final specific activity of 400 µCi/µmol). Reactions were set up containing the substrates GST, GST-mSTI1, GST-mSTI1(S189A), mSTI1 and mSTI1(S189A), each to 5 µM in a final volume of 10 µl. Control reactions to which no substrate was added, and to which no enzyme was added, were also included. The radioactive cocktail [10 µl] was added to the no-enzyme control containing GST-mSTI1. CKII [25 U] was added to the radioactive cocktail and aliquots [10 µl] of the radioactive cocktail containing CKII added to all other reactions. The final volume was 20 µl and reactions were incubated for 1 hour at 30°C. The reactions were stopped by the addition of SDS PAGE loading buffer [5 µl], and resolved by SDS PAGE (B.18). The gel was dried and radioactive phosphorylation detected by autoradiography: the dried gel was placed against X-ray film in a screen-containing cassette, and incubated at 37°C for 1-5 days. The X-ray film was developed (B.21) and photographs of autoradiograms were taken over a light box.

6.2.7 cdc2 kinase phosphorylation of mSTI1

A radioactive cocktail was prepared containing sterile deionised triple-distilled water [55 µl], 10x cdc2 kinase buffer [16 µl] (50 mM Tris-HCl pH 7.5, 10 mM $MgCl_2$, 1 mM EDTA, 1 mM DTT), ATP [6.4 µl] (100 mM) and [γ-^{32}ATP] (to a final specific activity of 400 µCi/µmol). Reactions were set up containing the substrates GST, GST-mSTI1, GST-mSTI1(T198A), GST-mSTI1(T198A, T332A), mSTI1, mSTI1(T198A), and mSTI1(T198A, T332A), each to 5 µM in a final volume of 10 µl. Control reactions to which no substrate was added, and to which no enzyme was added, were also included. The radioactive cocktail [10 µl] was added to the no-enzyme control containing GST-mSTI1. cdc2 kinase [120 U] was added to the radioactive cocktail and aliquots [10 µl] of the radioactive cocktail containing cdc2 kinase added to all other reactions. The final volume was 20 µl and reactions were incubated for 3 or 9 hours at 30°C. The reactions were stopped by the addition of SDS PAGE loading buffer [5 µl], and resolved by SDS PAGE (B.18). The gel was dried and radioactive phosphorylation detected by

autoradiography: the dried gel was placed against X-ray film in a screen-containing cassette, and incubated at 37°C for 1-5 days. The X-ray film was developed (B.21) and photographs of autoradiograms were taken over a light box.

6.2.8 GST-mSTI1 co-precipitation assay for the detection of mSTI1-cdc2 kinase binding

Mouse NIH 3T3 fibroblast extract was prepared from a 90% confluent 75 cm^2 flask (B.12) by harvesting the cells (B.12) and resuspending the cell pellet in lysis buffer [0.5 ml per T75 flask cultured] (50 mM Tris-HCl, pH 8.0, 150 mM NaCl, 0.02% sodium azide, 100 µg/ml PMSF, 1 µg/ml aprotinin, 1% Triton X-100). Lysis was allowed to occur at 4°C with inversion for 10 minutes, and the cell debris removed by centrifugation ay 12 000 x g. The extracts were used immediately.

Recombinant GST-mSTI1 [1 mg] in PBS [1 ml] was coupled to glutathione agarose beads [80 µl] (50% slurry) in PBS at 4°C, with inversion for 45 minutes. The beads were centrifuged at 6000 x g for 30 seconds, the supernatent aspirated and discarded, and the beads resuspended in PBS [1 ml]. This wash step was repeated three times. Mouse NIH 3T3 cell extract [1 mg] was added to the beads and the volume made up to 1 ml with PBS. The binding assays were incubated at 4°C, with inversion for 16 hours to allow equilibration of binding. The beads were washed twice in PBS as before, and resuspended in 80 µl SDS PAGE loading buffer. Co-precipitating proteins were resolved by SDS PAGE (B.18), and analyzed by Western analysis by chemiluminescence-based immunodetection (B.21) using an anti-Hsc70 or anti-cdc2 antibody.

6.3 RESULTS AND DISCUSSION

6.3.1 Constructs for heterologous production of mSTI1 are successfully prepared

The mSTI1 cDNA PCR amplification reaction successfully yielded a 1600-bp DNA product, which was ligated into pGEM(T). The mSTI1 cDNA from pGEM(T)mSTI1[*Nde*I/*Nhe*I] was inserted into the vector pET5a to produce pET5a2000 (Figure 6.1A), which, upon *Pst*I digestion, yielded the expected 3500-bp and 1950-bp fragments (Figure 6.1B, lane 3). Sequencing of the pET5a2000 plasmid insert confirmed the faithful amplification of the mSTI1 cDNA (data not shown).

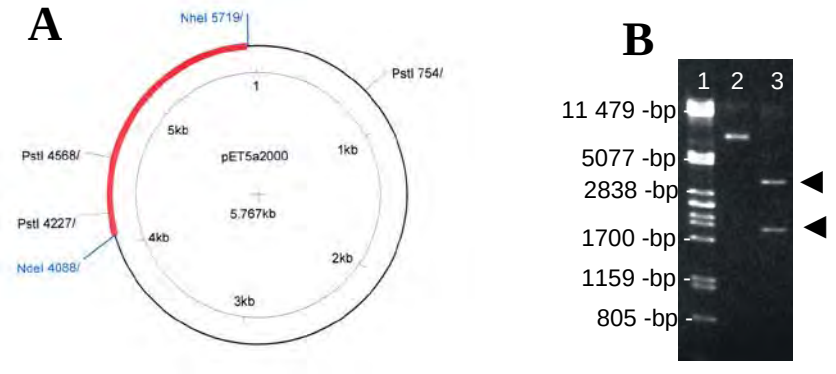

Figure 6.1: mSTI1 cDNA was successfully inserted into the pET5a vector

mSTI1 cDNA from pGEM(T)mSTI1[*Nde*I/*Nhe*I] was successfully inserted into the vector pET5a, to produce pET5a2000(A), which upon *Pst*I digestion, yielded the expected 3500 -bp and 1950 -bp fragments (B, Lane 3). *Pst*I digested λ DNA molecular weight standards (B, lane 1) and undigested DNA were included (B, lane 2). The red line represents mSTI1 cDNA.

6.3.2 Constructs for the heterologous production of mSTI1 derivative proteins are successfully prepared

E. coli transformants containing putative mutated plasmids of pGEX3X2000 and pET5a2000 were screened by restriction endonuclease digestion, and the resultant DNA

fragments resolved by agarose gel electrophoresis. Digestion of pGEX3X2000 with *Nco*I (Figure 6.2A and E, lane 3) produced the expected 1341-bp fragment, whereas digestion of the putative pGEX3X2000(S189A) with *Nco*I (Figure 6.2B and E, lane 4) generated the expected 777, and 565-bp fragments. Digestion of pGEX3X2000 with *Ban*I (Figure 6.2A and E, lane 7) produced the 4499-bp fragments as expected, whereas digestion of the putative pGEX3X2000(T198A) with *Ban*I (Figure 6.2C and E, lane 8) generated the expected 2706, and 1793-bp fragments. Digestion of pGEX3X2000 with *Eco*O1091 (Figure 6.2A and F, lane 3) produced the 810-bp fragments as expected, whereas digestion of the putative pGEX3X2000(T198A,T332A) with *Eco*O1091 (Figure 6.2D and F, lane 4) generated the expected 546-bp and 264-bp fragments. Similarly, the derivative plasmids of pET5a2000 were screened and identified (Figure 6.3). The mutations were confirmed with sequencing (data not shown).

6.3.3 Recombinant GST-mSTI1 and its derivatives are successfully produced and purified

A 26 kDa protein, corresponding to GST subunit was produced after IPTG induction of a *E. coli* XL1Blue[pGEX3X] log phase culture (Figure 6.4A). Similarly, a 89 kDa protein corresponding to GST-mSTI1 subunit, was produced after IPTG induction of *E. coli* XL1Blue[pGEX3X2000] (Figure 6.4B). These proteins were present at maximal levels after 4 hours of induction (Figure 6.4A and B, lanes 5) and were soluble (Figure 6.4C and D, lanes 2). These produced proteins bound to glutathione agarose beads and were successfully eluted with glutathione (Figure 6.4C and D, lanes 8). The identity of GST-mSTI1 was confirmed by Western analysis (Figure 6.4D, inset). Total protein concentrations of elutions containing GST-mSTI1 were typically 25-42 μM, and estimated to be 80 % pure, while that of GST was typically 150–200 μM and estimated to be 90-100 % pure. Similarly, purifications of GST-mSTI1(S189A), GST-mSTI1(T198A) and GST-mSTI1(T198A,T332A) were successful (D.7)

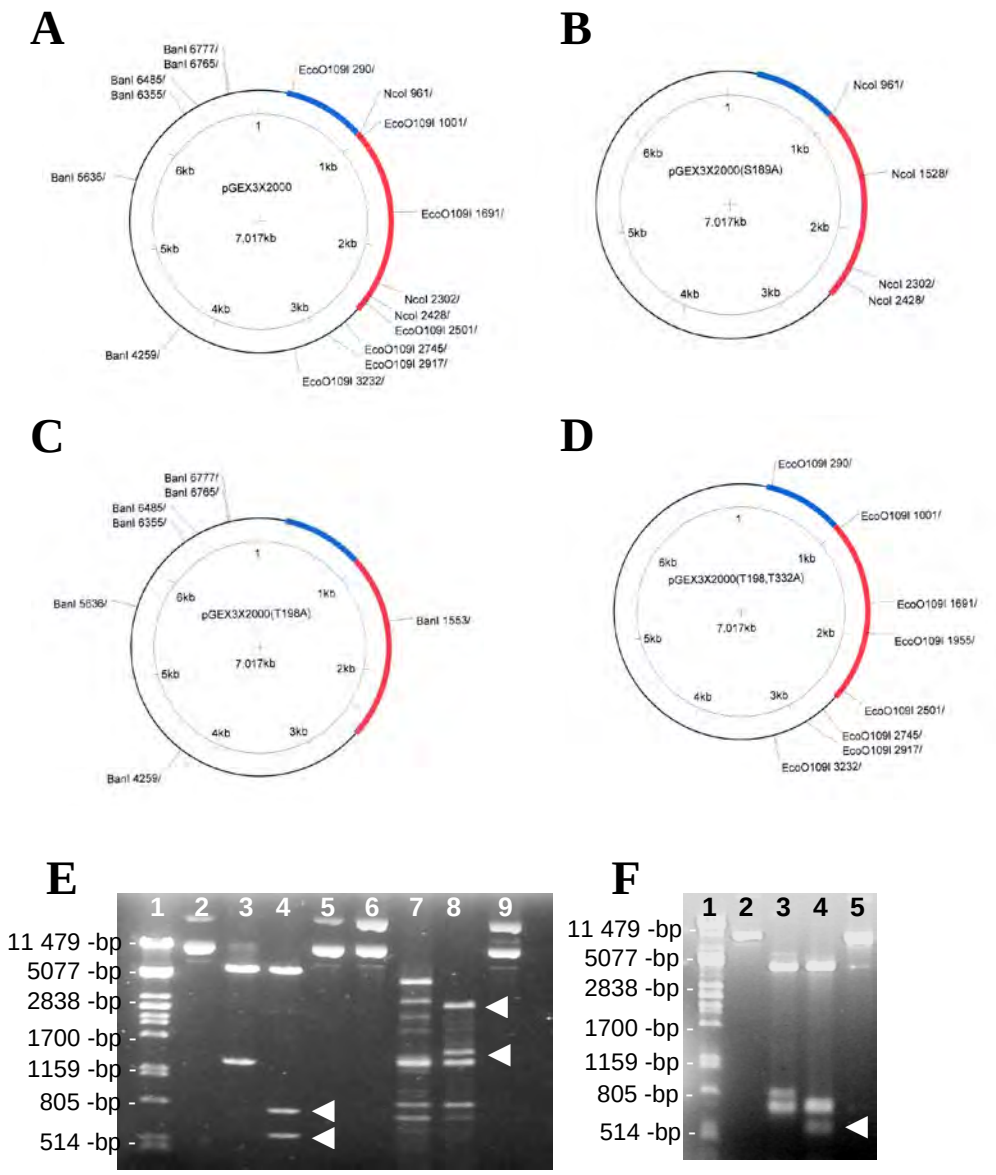

Figure 6.2: The plasmid pGEX3X2000 and its derivatives

pGEX3X2000 (A) was mutated by site-directed mutagenesis to produce its derivatives pGEX3X2000(S189A) (B), pGEX3X2000(T198A) (C) and pGEX3X2000(T198A,T332A) (D). The red lines represent mSTi1 cDNA, and the blue lines, GST cDNA. When digested with *Nco*I, pGEX3X2000 produced the expected 1341-bp fragment (E, lane 3) while pGEX3X2000(S189A) produced the expected 777-bp and 565-bp fragments (E, lane 4). *Pst*I digested λ DNA molecular weight standards (E, lane 1) and undigested pGEX3X2000 and pGEX3X2000(S189A) were included (E, lanes 2 and 5 respectively). When digested with *Ban*I, pGEX3X2000 produced the expected 4499-bp fragment (E, lane 7), while pGEX3X2000(T198A) produced the expected 2706-bp and 1793-bp fragments (E, lane 8). Undigested pGEX3X2000 and pGEX3X2000(T198A) were included (E, lanes 6 and 9 respectively). When digested with *Eco*01091, pGEX3X2000(T198A) produced the expected 810-bp fragment (F, lane 3) while pGEX3X2000(T198A,T332A) produced the expected 546-bp (shown) and 264-bp (not shown) fragments (F, lane 4). *Pst*I digested λ DNA molecular weight standards (F, lane 1) and undigested pGEX3X2000(T198A) and pGEX3X2000(T198A,T332A) were included (F, lanes 2 and 5 respectively). Blue and red lines represent GST and mSTI1 cDNA respectively.

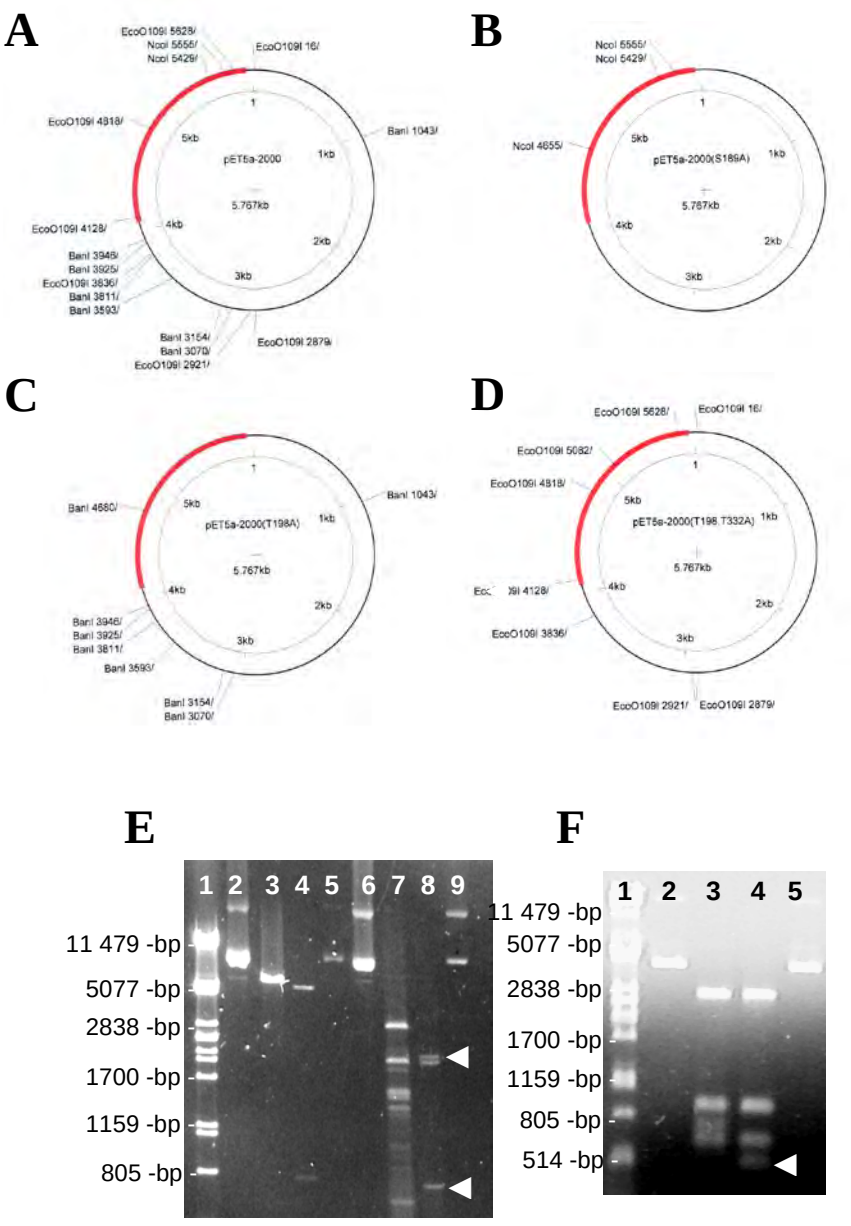

Figure 6.3: The plasmid pET5a2000 and its derivatives

pET5a2000 (A) was mutated by site-directed mutagenesis to produce its derivatives pET5a2000(S189A) (B), pET5a2000(T198A) (C) and pET5a2000(T198A,T332A) (D). The red lines represent mSTI1 cDNA. When digested with *Nco*I, pET5a2000 produced the expected 5767-bp fragment (E, lane 3) while pET5a2000(S189A) produced the expected 4867-bp and 777-bp fragments (E, lane 4). *Pst*I digested λ DNA molecular weight standards (E, lane 1) and undigested pET5a2000 and pET5a2000(S189A) were included (E, lanes 2 and 5 respectively). When digested with *Ban*I, pET5a2000 produced the expected 4499-bp fragment (E, lane 7), while pET5a2000(T198A) produced the expected 2706-bp and 1793-bp fragments (E, lane 8). Undigested pET5a2000 and pET5a2000(T198A) were included (E, lanes 6 and 9 respectively). When digested with *Eco*01091, pET5a2000(T198A) produced the expected 810-bp fragment (F, lane 3) while pET5a2000(T198A,T332A) produced the expected 546-bp (shown) and 264-bp (not shown) fragments (F, lane 4). *Pst*I digested λ DNA molecular weight standards (F, lane 1) and undigested pET5a2000(T198A) and pET5a2000(T198A,T332A) were included (F, lanes 2 and 5 respectively).

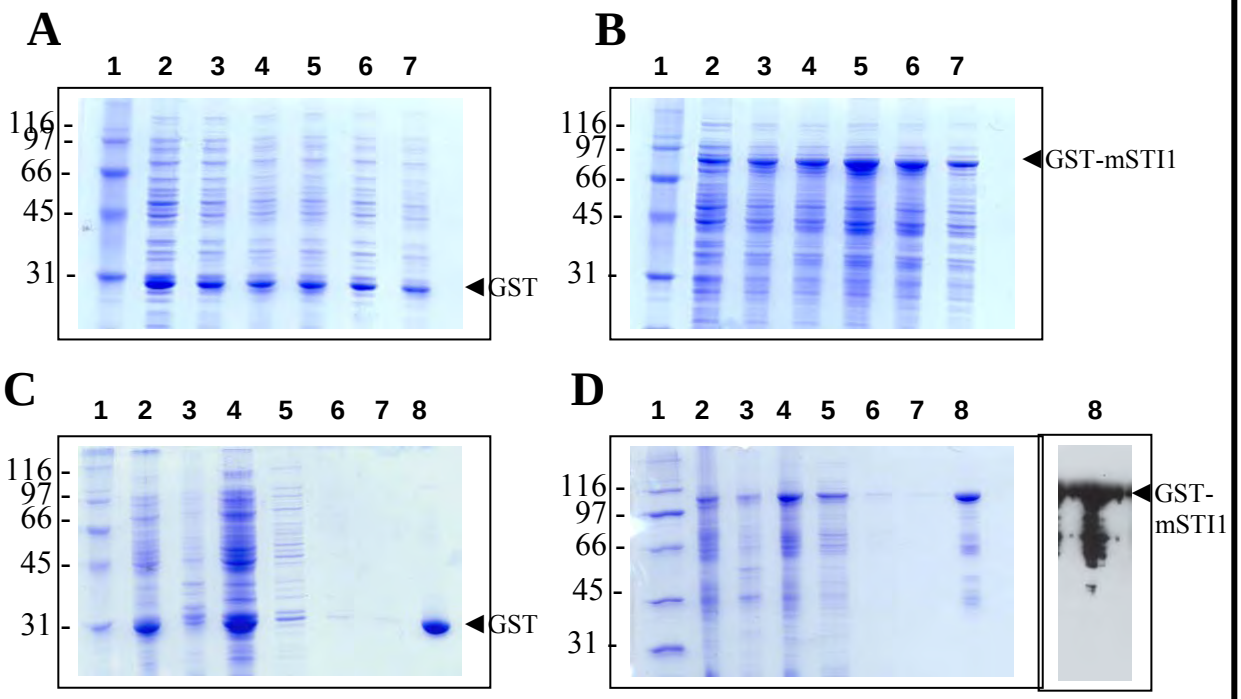

Figure 6.4: Recombinant GST and GST-mSTI1 is produced and purified

A (0.1%) SDS (12%) PAGE gel of whole IPTG induced logarithmic phase *E. coli* cells XL1Blue transformed with pGEX3X confirmed the presence of an overproduced 26 kDa protein. Samples were taken of the culture before induction (A, lane 2) and 1 hour (A, lane 3), 2 hours (A, lane 4), 3 hours (A, lane 5), 4 hours (A, lane 6) and 5 hours (A, lane7) post-induction. GST was produced at maximal levels 3-4 hours after induction (A, lanes 5 and 6). A (0.1%) SDS (12%) PAGE gel of whole IPTG induced logarithmic phase *E. coli* XL1Blue cells transformed with pGEX3X2000 confirmed the presence of an overproduced 89 kDa protein. Samples were taken of the culture before induction (B, lane 2) and 1 hour (B, lane 3), 2 hours (B, lane 4), 3 hours (B, lane 5), 4 hours (B, lane 6) and 5 hours (B, lane7) post-induction. GST-mSTI1 was produced at maximal levels 3-4 hours after induction (B, lanes 5 and 6). Produced GST proteins were purified using glutathione agarose affinity chromatography.

A (0.1%) SDS (12%) PAGE gel of the purification of GST from IPTG induced logarithmic phase *E. coli* XL1Blue cells confirmed the presence of a purified 26 kDa protein. Soluble extract (C, lane 2) was separated from insoluble extract (C, lane 3) by centrifugation. Soluble extract was bound to the glutathione agarose beads and then discarded (C, lane 4). The beads were washed three times in PBS (C, lanes 5-7) and bound protein eluted with 5 mM glutathione (C, lane 8). A (0.1%) SDS (12%) PAGE gel of the purification of GST-mSTI1 from IPTG induced logarithmic phase *E. coli* XL1Blue cells confirmed the presence of a purified 89 kDa protein. Soluble extract (D, lane 2) was separated from insoluble extract (D, lane 3) by centrifugation. Soluble extract was bound to the glutathione agarose beads and then discarded (D, lane 4). The beads were washed three times in PBS (D, lanes 5-7) and bound protein eluted with 5 mM glutathione (D, lane 8). The eluted protein in lane 8 was probed for GST-mSTI1 using Western Analysis (inset). Lanes 1 of all gels contains separated Bio-Rad Molecular weight markers in kDa.

6.3.4 Recombinant mSTI1 and its derivatives are successfully produced and purified

A 63 kDa protein corresponding to mSTI1, was overexpressed after IPTG induction of *E. coli* XL1Blue[pET5a2000]. This protein were present at maximal levels after 4 hours of induction (Figure 6.5A, lane 6), was soluble, and bound to a PBE polybuffer exchanger column at pH 8.0 (Figure 6.5 B). The 63 kDa protein was successfully eluted with a 0.1M-0.3M NaCl gradient elution (Figure 6.5C) into 2 peaks, and was completely removed from the column before regeneration. The identity of mSTI1 was confirmed by Western analysis (Figure 6.5D, inset). Total protein concentrations of elutions containing mSTI1 (Figure 6.5C and D), and derivatives, were typically 200 μM, and estimated to be 80% pure. Similarly, purifications of mSTI1(S189A), mSTI1(T198A) and mSTI1(T198A,T332A) were successful.

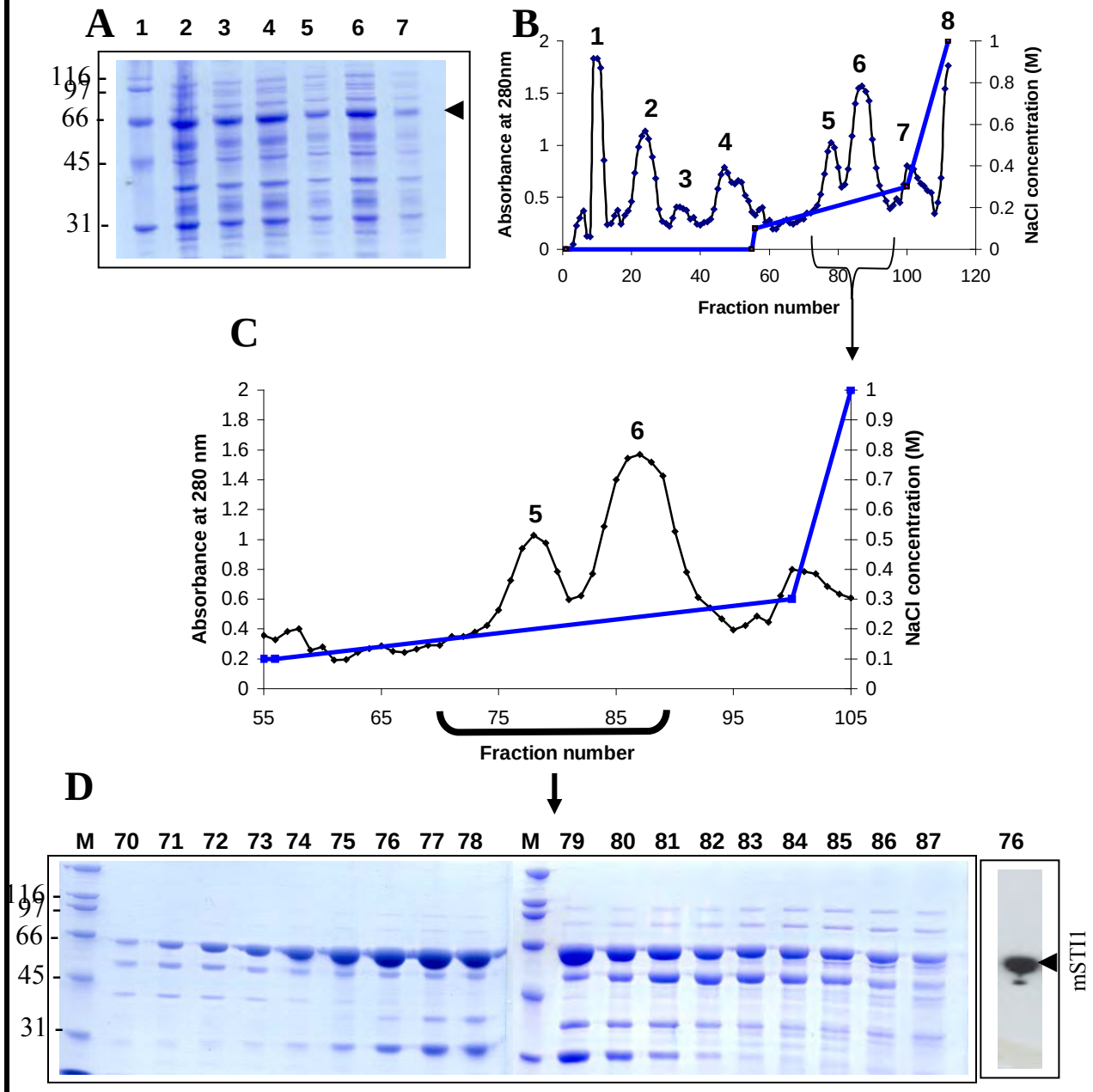

Figure 6.5: Recombinant mSTI1 are produced and purified

A (0.1%) SDS (12%) PAGE gel of whole IPTG induced logarithmic phase *E. coli* BL21(DE3) cells transformed with pET5a2000 confirmed the presence of an overproduced 63 kDa protein. Samples were taken of the culture before induction (A, lane 2) and 1 hour (A, lane 3), 2 hours (A, lane 4), 3 hours (A, lane 5), 4 hours (A, lane 6) and 5 hours (A, lane 7) post-induction. mSTI1 was produced at maximal levels 3-4 hours after induction (A, lanes 5 and 6). IPTG induced logarithmic phase *E. coli* BL21(DE3)[pET5a2000] cell lysate, the column was separated through a PBE exchanger column. The column was washed stepwise with start buffer, followed by start buffer containing 0.1 M NaCl. An gradient elution of start buffer containing 0.1 M and 0.3 M NaCl was used to elute mSTI1, and the column stripped with start buffer containing 1 M NaCl. The 280 nm absorbance profile of eluted proteins was measured (B) and the peaks collected were resolved by SDS PAGE (C, lanes correspond to peaks). mSTI1 was enriched in peaks 5-6 (C and D). The eluted protein in peaks 5 and 6 (fractions 70 to 87) was resolved by SDS PAGE. Fraction 76 was used for further phosphorylation assays and was probed for mSTI1 using Western Analysis (inset). Lanes 1 of both gels contain separated Bio-Rad Molecular weight markers in kDa.

5.3.5 CKII phosphorylates serine 189

Previously we showed S189 of tagged mSTI1 to be phosphorylated *in vitro* (Longshaw *et al.,* 2000, Longshaw, 1999). In order to more fully characterize CKII phosphorylation here, untagged mSTI1 has been used and the incubation period for CKII phosphorylation has been extended to 9 hours. GST-mSTI1 and mSTI showed specific incorporation of [^{32}P] after CKII phosphorylation (Figure 6.6A, lanes 3,4,7 and 8), while no specific incorporation of [^{32}P] was detected for the no-enzyme autophosphorylation and no-substrate controls (Figure 6.6A, lanes 1 and 2), GST-mSTI1(S189A) or mSTI1(S189A) derivatives (Figure 6.6A, lanes 5 and 9) after 3 hours. A relatively low incorporation of [^{32}P] by GST-mSTI1(S189A) and mSTI1(S189A) after extended CKII phosphorylation for 9 hours occurred (Figure 6.6 A, lanes 6 and 10). Since GST-mSTI1(S189A) and mSTI1(S189A) showed negligible CKII phosphorylation after extended incubation, these data provide strong evidence that S189 is the major specific CKII phosphorylation site recognised *in vitro*.

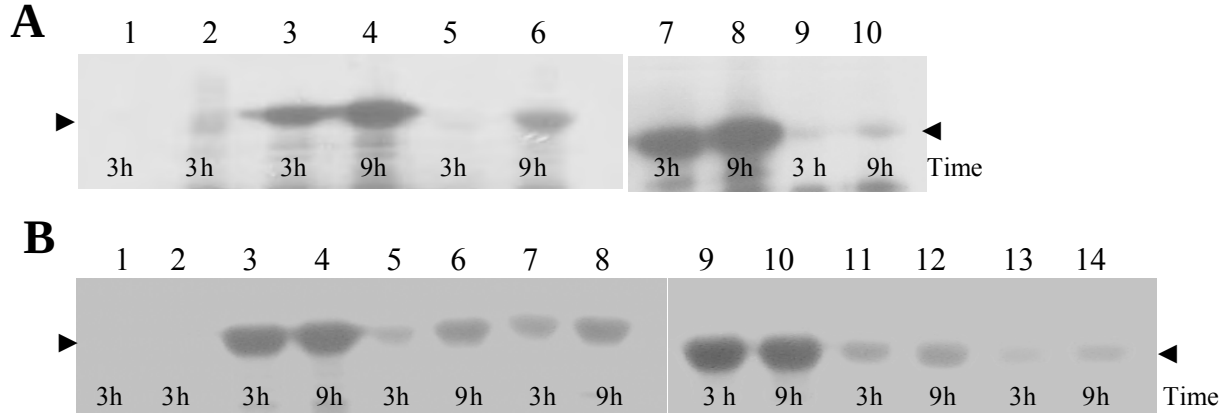

Figure 6.6: The *in vitro* phosphorylation of mSTI1

In vitro kinase assays with substrates [5 µM] were analyzed by (0.1%) SDS (12 %) PAGE. CKII assays and p34^{cdc2} assays were incubated for 3 and 9 hours. The gel was dried and radioactive phosphorylation detected by autoradiography. (**A**) CKII phosphorylation: Lane 1, GST-mSTI1 (no-enzyme control); lane 2, no-substrate control; lane 3, GST-mSTI1 (3 hours); lane 4, GST-mSTI1 (9 hours); lane 5, GST-mSTI1(S189A) (3 hours); lane 6, GST-mSTI1(S189A) (9 hours); lane 7, mSTI1 (3 hours); lane 8, mSTI1 (9 hours); lane 9, mSTI1(S189A) (3 hours); lane 10, mSTI1(S189A) (9 hours). (**B**) p34^{cdc2} phosphorylation: Lane 1, GST-mSTI1 (no-enzyme control); lane 2, no-substrate control; lane 3, GST-mSTI1 (3 hrs); lane 4, GST-mSTI1 (9 hrs); lane 5, GST-mSTI1(T198A) (3 hrs); lane 6, GST-mSTI1(T198A) (9 hrs); lane 7, GST-mSTI1(T198A,T332A) (3 hrs); lane 8, GST-mSTI1(T198A,T332A) (9 hrs); lane 9, mSTI1 (3 hrs); lane 10, mSTI1 (9 hrs); lane 11, mSTI1(T198A) (3 hrs); lane 12, mSTI1(T198A) (9 hrs); lane 13, mSTI1(T198A,T332A) (3 hrs); lane 14, mSTI1(T198A,T332A) (9 hrs).

6.3.6 Threonine 198 is not the only site recognized by cdc2 kinase

Previously we reported the *in vitro* phosphorylation of mSTI1 by cdc2 kinase at T198 using GST-mSTI1 recombinant protein in radioactive cdc2 kinase assays (Longshaw *et al.,* 2000). Here untagged mSTI1 has been used in radioactive cdc2 kinase assays for 3 hours and 9 hours in order to investigate any low levels of phosphorylation at sites other than T198 with extended incubation. To ensure that phosphorylation experiments of the CcN motif were not contaminated with murine Hsp90, which may inhibit phosphorylation at these mSTI1 sites by binding to mSTI1, purified kinases and not cell extract were used. In this way kinase specific phosphorylation data was obtained. GST-mSTI1(T198A) and mSTI1(T198A) showed greatly reduced phosphorylation levels compared to unmodified protein, suggesting that T198 was the major *in vitro* cdc2 kinase phosphorylation site in mSTI1 (Figure 6.6B, lanes 6 and 12 compared to lanes 4 and 10). The 9 hour incubations detected a low level of phosphorylation in the GST-mSTI1(T198A) and mSTI1(T198A) reactions that was significantly above that detected for the auto-phosphorylation control (Figure 6.6B, lanes 6 and 12). Therefore, cdc2 kinase was phosphorylating another site, which we speculated to be T332, the only other site in mSTI1 that conforms to the cdc2 kinase consensus sequence and is associated within a potential CcN motif. However, the physiological significance of this is probably low due to the long incubation time required to achieve phosphorylation at this site. Nevertheless, this region resembles another putative CcN motif (amino acids 326-351) with a putative CKII site at position S326, a putative cdc2 kinase site at position T332, and a putative bipartite NLS at positions 337-351. Removal of the T332 site was performed to produce GST-mSTI1(T198A,T332A) and mSTI1(T198A,T332A). A similar level of phosphorylation was observed for the GST-mSTI1(T198A,T332A) phosphorylation reaction (Figure 6.6B, lanes 7 and 8), as for GST-mSTI1(T198A), indicating that another, as yet unidentified, cdc2 recognized phosphorylation site, which did not map to T198 or T332, may exist in mSTI1. The level of phosphorylation was, however, reduced between mSTI1(T198A) and mSTI1(T198A,T332A) (Figure 6.6B, lanes 12 and 14), suggesting that T332 was a minor phosphorylation site in mSTI1. The

presence of multiple *in vitro* cdc2 kinase phosphorylation sites may explain the spectrum of mSTI1 isoforms observed *in vivo*, although T198 appears to be the major *in vitro* cdc2 kinase site.

6.3.7 mSTI1 does not associate stably with cdc2 kinase

GST-mSTI1 has been shown to specifically interact with Hsc70 using glutathione agarose co-precipitation assays (Van der Spuy *et al.,* 2000; Longshaw *et al.,* 2000). This interaction was therefore used as a binding assay control during the detection of cdc2 kinase interaction with mSTI1 (Figure 6.7A, lane 3). mSTI1 co-precipitating proteins did not contain cdc2 kinase, even when high levels (1 mg) of GST-mSTI1 protein were incorporated in the binding assay (Figure 6.7B, lane 3). This may indicate that although an *in vitro* interaction between mSTI1 and cdc2 kinase has been shown (section 6.3.6), this interaction may not occur *in vivo* or mSTI1 may not form a stable complex with cdc2 kinase. The mSTI1-cdc2 kinase interaction may be of a transient nature.

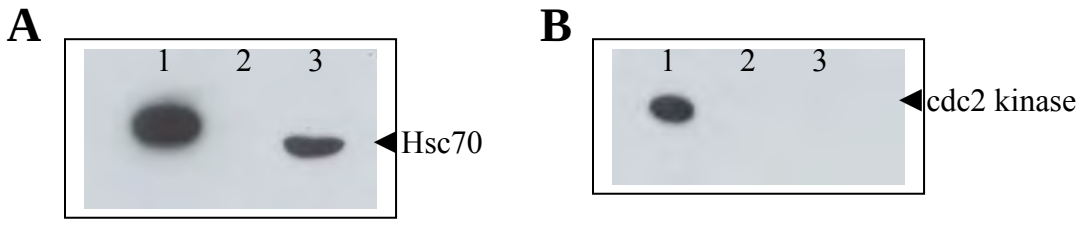

Figure 6.7: mSTI1 does not associate stably with cdc2 kinase

1 mg recombinant GST or GST-mSTI1 was coupled to glutathione agarose beads [80 µl] (50% slurry) in PBS at 4°C, with inversion for 45 minutes. The beads were washed in PBS 3 times. 1 mg mouse NIH 3T3 cell extract was added to beads and the volume made up to 1 ml with PBS. The binding assays were incubated at 4°C, with inversion for 16 hours to allow equilibration of binding then washed twice in PBS. Co-precipitating proteins were resolved by SDS PAGE, and analyzed by Western analysis by chemiluminescence-based immunodetection using an anti-Hsc70 (A) or anti-cdc2 kinase antibody (B). 15 µg NIH 3T3 extract was used as a positive control (lanes 1), and GST co-precipitating proteins (lanes 2) and GST-mSTI1 co-precipitating proteins (lanes 3) probed for the presence of Hsc70 (A) and cdc2 kinase (B).

6.4 CONCLUSIONS

The recombinant GST-mSTI1 and untagged mSTI1 proteins were successfully produced and enriched to sufficient purity for use for the investigation of phosphorylation of mSTI1. Similarly, the derivatives of GST-mSTI1 and mSTI1 were successfully produced.

CKII specifically phosphorylated GST-mSTI1 and mSTI1, but negligible phosphorylation by CKII was detected for the no-enzyme autophosphorylation control, GST-mSTI1(S189A) and mSTI1(S189A) derivatives. This provides strong evidence that S189 is the specific CKII phosphorylation site recognised *in vitro*. The extended incubations detected a low level of cdc2 kinase phosphorylation in the mSTI1(T198A) reaction that was above that detected for the auto-phosphorylation control. This suggests that mSTI1 was phosphorylated by cdc2 kinase at a position other than T198. The only other potential cdc2 kinase phosphorylation site that was in the proximity of an NLS was T332, and this site was therefore removed by amino acid replacement. A similar level of phosphorylation was observed for mSTI1(T198A) and mSTI1(T198A,T332A) phosphorylation reactions, indicating that another, as yet unidentified, cdc2 recognized phosphorylation site, which did not map to T198 or T332, may exist in mSTI1. There may therefore be multiple *in vitro* cdc2 kinase phosphorylation sites in mSTI1, which may explain the spectrum of mSTI1 isoforms observed *in vivo*. T198, however, appears to be the major *in vitro* cdc2 kinase site.

In this work, evidence for the presence of *in vivo* cdc2 kinase phosphorylation sites in mSTI1 has been shown. Inactivation of cdc2 kinase by olomoucine increased the nuclear localization of mSTI1 (Chapter 4) suggesting that the cytoplasmic localization of mSTI1 may require active cdc2 kinase. Recently, it was shown that yeast STI1 interacts directly and stably with cdc37 (Abbas-Terki *et al.*, 2002). However, this interaction, although detectable, was of a relatively low level. On investigation of the interaction between mSTI1 and cdc2 kinase using a GST-mSTI1 binding assay, it was shown here that this potential interaction in a mammalian system was not stable, since mSTI1 did not form a detectable stable complex with cdc2 kinase. The interaction of mSTI1 and cdc2 kinase

may have implications for the formation of the Hsp70/mSTI1/Hsp90 chaperone heterocomplex, and for the Hsp90-independent chaperoning of protein kinases. In the Hsp70/mSTI1/Hsp90 chaperone heterocomplex, the NLS of mSTI1 may not be assessable to NLS-binding machinery. However, in an alternate mSTI1 complex, potentially involving cdc37 and cdc2, the NLS of mSTI1 may be accessible to NLS-binding machinery.

CHAPTER 7

DISCUSSION AND CONCLUSION

7.1 THE IMPORTANCE OF CELL CYCLE-REGULATED NUCLEAR ACCUMULATION OF mSTI1

Chaperones and heat shock proteins are being recognised as increasingly important in cell signalling events, because of their association with cell cycle components, regulatory proteins and members of the mitogenic signal casade (Helmbrecht *et al.,* 2000). Recently, a direct interaction of the *Candida albicans* STI1 and cdc2 kinase has been reported (Ni *et al .,* 2001). Here evidence is shown for the first time that the Hsp70/Hsp90 co-chaperone, mSTI1, has a functional NLS, and that the localization of mSTI1 is affected by cdc2 kinase and is cell cycle dependent. The incidence of nuclear localization of mSTI1 was increased in cells in the G1/S phase arrest, by inhibition of the cdc2 kinase with olomoucine and by point inactivation of the putative cdc2 kinase phosphorylation site.

The T-antigen CcN motif function is affected by phosphorylation: the mechanism of cdc2 kinase-mediated inhibition is through cytoplasmic retention (Jans and Jans, 1994), while that of CKII phosphorylation-mediated enhancement is through increasing the affinity of association with the karyopherin complex (Jans and Jans, 1994), enhancing the docking rate at the NPC. Flanking sequences and phosphorylation at the CKII site are mechanistically important in NLS recognition by karyopherin α in both T-antigen (Hübner *et al*., 1997) and Dorsal transcription factor from Drosophila (Briggs *et al .,* 1998). The phosphorylation of mSTI1-EGFP, particularly in the region of its putative NLS, is therefore significant as many reports show that phosphorylation regulates NLSs (Jans and Hübner, 1996). The recognition of these phosphorylation sites by cell cycle kinases is also significant, indicating both a connection to the cell cycle, and nuclear

import that is under cell cycle control. Studies of cell cycle expression of proteins did not report the expression of Hop to be regulated by the cell cycle (Whitfield *et al.,* 2002). Furthermore, although cdc2 kinase recognizes and phosphorylates mSTI1 *in vitro* there seems to be no stable interaction of mSTI1 and cdc2 kinase. However, mSTI1 localization and hence function within the cell appears to be cell cycle dependent. Such cell cycle regulation, in the case of mSTI1, implies a role for this co-chaperone in the cell cycle. Future experiments should focus on analysis of a predicted mSTI1-cdc2 interaction *in vivo*, possibly using a glutaldehyde fixation of mouse fibroblast cells, subsequent isolation of mSTI1 and mSTI1 complexes, and immuno-chemiluminescent probing for cdc2 kinase. Further characterization of this cdc2 kinase-mSTI1 interaction may be achieved by investigation of the kinetics of the cdc2 kinase phosphorylation of mSTI1 *in vitro* using purified cdc2 kinase and mSTI1.

The marked accumulation of NLS^{mSTI1}EGFP in the nucleus compared to EGFP, suggests that mSTI1's putative NLS is functional, supporting the prediction of a CcN motif in this region of mSTI1 *in vivo.* The accumulation of mSTI1 under nuclear export inhibition conditions demonstrates not only a functional import signal in mSTI1, here proposed to be the predicted CcN motif at positions 189-239, but also a CRM-1 recognized, as yet unidentified, nuclear export signal (NES) in mSTI1 for nuclear export. The subcellular distribution of mSTI1 may not, therefore, be static, but rather a dynamic balance of nuclear import and export processes, the fulcrum of which may be shifted under different conditions.

The proposed CcN motif may be regulated by the cell cycle as mSTI1 is observed in the nucleus at G1/S phase arrest when cdc2 kinase is inactive, and negative charge at the predicted cdc2 kinase phosphorylation site inhibits nuclear accumulation under these conditions. A cell cycle role, as has been suggested (Longshaw *et al.,* 2000), may require transport of the mSTI1 protein into the nucleus at this transition in the cell cycle. One explanation may be that assembly of protein machinery at G1/S, in order to carry out DNA synthesis, demands an increased requirement for chaperone activity in the nucleus for the maintenance of functional proteins and facilitation of conformational changes during this process. An enhanced requirement for nuclear transport also occurs during S-

phase, and the nuclear import rate in proliferating cells is higher than that in quiescent cells (Csérmèly *et al.,* 1995, Feldherr and Akin, 1993). A translocation of Hsc70 into the nucleus occurs during S-phase (Helmbrecht *et al.,* 2000; Milarski and Morimoto, 1986; Zeise *et al.,* 1998). A close interaction between mSTI1 and Hsc70 has been reported (Lässle *et al.,* 1997.). Therefore, a change of mSTI1 distribution to the nucleus at the G1/S transition would not be unexpected. mSTI1 could possibly function as an import partner, allowing Hsc70 to "piggy-back" into the nucleus (Pratt, 1998.). The Hsc70/mSTI1/Hsp90 chaperone heterocomplex may then be assembled in the nucleus for increased nuclear chaperone activity. In some cell lines the production of Hsc70 is cell cycle-dependent and suppressed by treatment with the inhibitor of DNA synthesis Ara C (Hang and Fox, 1995; Milarski and Morimoto, 1986), indicating a potential involvement of Hsc70 in DNA replication. Thus the Hsc70/mSTI1/Hsp90 chaperone heterocomplex may play a role in stabilization of cell cycle components in the nucleus during S-phase. Alternatively, the chaperone heterocomplex may function in the degradation of G1 cyclins, such that G1 cyclins are targeted for degradation at appropriate protein degradation locations in the cell at G1/S checkpoints. Thus, the balance of functional *versus* degraded cell cycle components may be assisted by the chaperone activity of the Hsc70/mSTI1 complex.

7.2 THE NUCLEAR ACCUMULATION OF mSTI1 APPEARS TO BE CELL CYCLE RELATED BUT NOT HEAT SHOCK RELATED

The nuclear accumulation of mSTI1 is proposed to have an important role in cell cycle progression under normal growth conditions, but was apparently not important or necessary under our heat shock conditions. These heat shock conditions, although producing a change in isoform composition of mSTI1, did not affect the cytoplasmic distribution of mSTI1. Future experiments should be focussed towards the optimisation of the heat shock treatment of mSTI1-EGFP expressing cells such that the heat shock is achieved with maximum efficiency (e.g. exposure to pre-heated media). The kinetics of

heat shock may then be determined over time and the localization of mSTI1-EGFP more rigorously d etermined. The m odifications m ade a t t he C KII (S189) a nd c dc2 ki nase (T198) s ites di d not e ffect a ny change i n l ocalization of m STI1 und er he at s hock conditions, s uggesting t hat ne ither of t hese s ites operate a s functional r egulators of t he NLS unde r s tress c onditions. T he C KII s ite a t S 189 m ay ha ve a n e ffect on m STI1 localization under conditions that are as yet unknown.

Stress, such as starvation, ethanol, heat or oxidant treatments, have been shown to inhibit specific N LS-dependent nuc lear i mport (Stochaj *et al*., 2000). T his i nhibition of t he classical nuclear protein import under stress conditions has been attributed to the collapse of t he nu cleocytoplasmic gradient of t he s mall G TPase Gsp1p (Ran) (Stochaj *et al*., 2000), a nuc lear t ransport f actor. Interestingly, Hsp70 is nor mally c ytoplasmically localized, but dur ing he at s hock, has be en s hown t o t ranslocate t o t he nuc leus and i n particular t he nuc leolus, from w hich i t w ithdraws dur ing recovery (Welch, 1987). T his movement of Hsp70 in and out of the nucleolus has been proposed to be associated with repair of h eat-induced nuc leolar damage (Nollen *et al*., 2001). T he i ncreased nu clear import of Hsc/Hsp70 during heat shock, when classical nuclear import rates are generally decreased, is thought to be due to a novel NLS-independent import mechanism (Lamian *et al.,* 1996). Taken together with these data, this suggests Hsc70 and mSTI1 co-localize and co-operate du ring e ntry of the c ell int o S-phase, but do not ne cessarily c o-localize and co-operate under heat shock.

7.3 THE IMPORTANCE OF THE PHOSPHORYLATION STATE OF mSTI1

Phosphorylation i s he re proposed t o ha ve a s ignificant r ole i n t he r egulation of nuc lear localization in the context of mSTI1in its role in chaperone complexes. The association of mSTI1 with other chaperones i n the c ytoplasm has be en well cha racterized especially with respect to its role in the chaperoning of steroid hormone receptors (Murphy *et al*., 2001; Dittmar and Pratt, 1997; Johnson *et al.,* 2000; Kaul *et al.,* 2002). However, mSTI1 may be r ecruited t o t he nuc leus a nd f unction i n t he r econstitution of c haperone complexes i n t he nuc leus. T hese r econstituted c haperone c omplexes c ould pl ay an

important role in the chaperoning of telomerase complexes (Forsythe *et al.,* 2001) and other cell cycle components (Aligue *et al.,* 1994; Nakamura *et al.,* 1999) such as cdc kinases (Zhu *et* al, 1997) and cyclins. Thus the Hsc70/mSTI1/Hsp90 chaperone heterocomplex may have an important function in the stabilization of enzymes such as telomerase and polymerase as well as the transport of cyclins out of the nucleus for degradation during S-phase. The observation that the mSTI1-EGFP(T198A) mutant qualitatively accumulated in the nucleus to a greater degree than mSTI1-EGFP under G1/S phase arrest conditions provides striking evidence of the role of phosphorylation regulation of mSTI1 by cdc2 kinase (at this mSTI1 T198 site) in the nuclear localization of mSTI1 in S-phase.

The presence of a large number of isoforms of mSTI1 suggests that different populations of post-translationally modified mSTI1 protein are present at any one time. The decrease in isoform number observed on removal of either the S189 or T198 site supports the presence of modifying phosphates at these sites under normal growth conditions *in vivo*. The presence of multiple *in vitro* cdc2 kinase phosphorylation sites may explain the spectrum of mSTI1 isoforms observed *in vivo*, although T198 appears to be the major *in vitro* cdc2 kinase site. The finding of increased nuclear accumulation of mSTI1-EGFP(T198A) under hydroxyurea conditions suggests that mSTI1 modification at this site inhibits nuclear accumulation and promotes the presence of a cytoplasmic localization.

Furthermore, mSTI1 has been proposed to exist as a dimer (Van der Spuy *et al.,* 2000, Van der Spuy *et al.,* 2001). Therefore, for the mSTI1-EGFP studies, there is the potential in this experimental paradigm, that endogenous mSTI1 subunits have formed heterodimers with their recombinant chimeric proteins, thereby moderating any localization effects of the introduced amino acid substitutions (such as S189A, S189E, T198A, and T198E). The phosphorylation of one subunit in such heterodimers may be sufficient to mediate the translocation of the protein, and therefore the removal of one kinase site will not prevent this. Similarly, the phosphorylation of dimer subunits could be co-operative and add an extra level of complexity to the regulation of mSTI1

localization. The effects of substitution on localization of mSTI1 may have to be investigated further in cells not expressing endogenous mSTI1.

7.4 THE INTERACTIONS OF mSTI1

Bioinformatic analysis of mSTI1 indicated that the NLS, but not the CcN motif phosphorylation sites, was conserved in STI1 proteins. Sequence analysis limits predictions of residue interactions as it cannot include three-dimensional data, but can be positively used to assess possible conservation of residues and therefore their possible mechanistic importance. Residues in the mSTI1 homologue Hop NLS spacer region and CcN motif CKII phosphorylation site, that were highly conserved, were involved in binding to Hsp90. Thus the binding sites for import machinery and Hsp90 may overlap, such that these residues mediate both the binding of Hsp90 to the TPR2 domain of STI1 proteins and karyopherin-α to the bipartite NLS. Although a direct interaction between mSTI1 and karyopherin-α remains to be shown, the simultaneous binding of karyopherin-α and Hsp90 may be sterically impossible. This alternate binding of Hsp90 or karyopherin-α would probably have mechanistic implications. Furthermore, the cdc2 kinase site T198 in mSTI1 is proposed to stabilize the highly conserved K229 residue in the mSTI1 NLS spacer region. Phosphorylation at this cdc2 kinase site would therefore disrupt the T198-K229 contact, and affect the local protein conformation. Conformational changes induced by phosphorylation at this site, may allow preferential binding of either Hsp90 or karyopherin-α, and add an extra level of complexity to the regulation of mSTI1 interactions. Further experiments on a potential karyopherin-α-mSTI1 interaction *in vivo* could prove advantageous in determining the kinetics and specificity of mSTI1 nuclear import. This direction of experiments may include FRET studies of co-expressed karyopherin-α and mSTI1 as well as *in vitro* binding studies of the specificity and kinetics of potential karyopherin-α and mSTI1 interaction.

mSTI1 has been shown here to be recognised and phosphorylated by cdc2 kinase *in vitro*. Recently, it was shown that STI1 interacts directly with cdc37 (Abbas-Terki *et al.,* 2002). Furthermore, cdc37 has been found to interact with cdc28 in *Saccharomyces cerevisiae*

(Mort-Bontemps-Soret *et al*., 2002). Therefore STI1, cdc37 and cdc28 may interact together in a cell cycle dependent manner to regulate both the chaperoning and localization of client protein kinases. However, the interaction between mSTI1 and cdc2 kinase in a mammalian system was not stable or not that of a detectable stable protein complex, as detected by the co-precipitation assays. This interaction may therefore simply be of a transitory nature, such as for that of an enzyme-substrate interaction.

In conclusion, the work presented here may be regarded as novel data in the investigation of the localization of mSTI1 *in vivo* under normal conditions and the control of mSTI1 localization, and therefore function, by the cell cycle. In order to better understand this role, the mechanisms of the predicted *in vivo* karyopherin-α-mSTI1 and cdc2 kinase-mSTI1 interactions require more detailed investigation. The mSTI1 protein may prove to be a key protein in the localization and assembly of the Hsp90/mSTI1/Hsp70 chaperone heterocomplex, and/or in an alternative potential cdc37/cdc2/mSTI1complex. The interactions of mSTI1 between Hsp90 or NLS-binding partner proteins like karyopherin-α, predicted by this work to be influenced by cell cycle kinase phosphorylation, may be integral to the mechanisms of mSTI1 function *in vivo*.

APPENDIX A

MATERIALS

Table A.1: Experimental materials were obtained from commercial suppliers

Material	Catalogue number	Supplier
QIAprep Spin Miniprep Kit (50)	27104	QIAGEN, U.S.A.
DNA Clean and Concentrator-5	D4005	Zymo research, U.S.A.
T4 DNA polymerase	E2040Y	Amersham Pharmacia Biotech
PCR Nucleotide Mix	1 581 295	Roche Molecular Biochemicals, Germany
pGEM-T easy vector system I	A1360	Promega Corporation, U.S.A.
Anti-Hsp70	SPA-810	Stressgen, Canada
Quikchange Site-Directed Mutagenesis kit (30)	200518	Stratagene, U.S.A.
Glutathione Agarose	G4510	Sigma-Aldrich Inc., U.S.A.
High Pure Plasmid Isolation Kit (250)	1 754 785	Roche Molecular Biochemicals, Germany
BM Chemiluminescence Western Blotting Kit (mouse/rabbit)	1 520 709	Boehringer Mannheim, Germany
Cdc2 protein kinase (human)	P6020S	New England Biolabs, U.S.A.
Anti-cdk1 (cdc2)	KAM-CC101	Stressgen Biotechnologies Corporation, Canada
Anti-GFP Living Colours A.v. peptide Antibody (Anti-GFP)	8367-1	Clontech laboratories, Inc. U.S.A.
SDS-PAGE Molecular weight Standards, Broad range	161-0312	Bio-Rad Laboratories, U.S.A.
Bradford Reagent	B6916	Sigma-Aldrich Inc., U.S.A.
Albumin, Fraction V	735 078	Roche Molecular Biochemicals, Germany

Hybond-C extra supported nictrocellulose membrane		Amersham International, U.K.
NucleoSpin Extract 2 in 1		Macherey-Nagel, Germany
Expand High Fidelity PCR System	1 732 641	Roche Molecular Biochemicals, Germany
Agarose type D-1 LE low electroendosmosis		Hispanagar, Spain
Phosphatase, alkaline, shrimp	1 758 250	Roche Molecular Biochemicals, Germany
*Acc*I	E1001Y	Amersham Pharmacia Biotech
*Bam*HI	E1010V	Amersham Pharmacia Biotech
*Eco*RI	E1040W	Amersham Pharmacia Biotech
*Eco*RV	E1042Y	Amersham Pharmacia Biotech
*Hind*III	E1060Y	Amersham Pharmacia Biotech
*Nco*I	E1160Y	Amersham Pharmacia Biotech
*Nde*I	E1161V	Amersham Pharmacia Biotech
*Nhe*I	E1162Y	Amersham Pharmacia Biotech
*Not*I	E0304Y	Amersham Pharmacia Biotech
*Pst*I	E1073Y	Amersham Pharmacia Biotech
*Sac*II	E1079V	Amersham Pharmacia Biotech
*Xho*I	E1094Y	Amersham Pharmacia Biotech
Lamda DNA	D1501	Promega Corporation, U.S.A.
*Bse*EI	R05545	New England Biolabs, U.S.A.
IPTG	V3951	Promega Corporation, U.S.A.
T4 DNA ligase	M1801	Promega Corporation, U.S.A.
Kodak BioMax M R Film		Kodak
Lipofectamine Plus Transfection reagent	10964-013	Invitrogen Life Technologies, U.S.A

APPENDIX B

GENERAL PROCEDURES

B.1 The PCR amplification of cDNA

The required open reading frame (ORF) was amplified from the plasmid template DNA by a polymerase chain reaction (PCR), using the engineered forward and reverse primers. The PCR reaction included final concentrations of the template plasmid DNA (2 ng/µl), forward primer (300 mM), reverse primer (300 mM), dNTPs (200 µM each) and Expand High Fidelity PCR enzyme mix (2.6 U) in 1 x Expand HF buffer with $MgCl_2$ (1.5 mM) to a final volume of 50 µl. The cycling parameters were such that the PCR reaction was incubated at 94°C for 2 minutes, followed by a 3-step cycle of 94°C for 30 seconds, 55°C for 1 minute and 72°C for 2.5 minutes, repeated a total of 30 times. A final elongation step of 10 minutes at 72°C was included.

B.2 Agarose gel electrophoresis

The DNA sample [20 µl] was added to agarose gel loading buffer [5 µl] (30 % glycerol v/v, 0.25 % w/v bromophenol blue) and resolved on an agarose gel [50 ml] (0.7% w/v) gel containing ethidium bromide (0.5 µg/ml), in TBE buffer (45 mM Tris, 45 mM Borate, 1 mM EDTA, pH8.3) at 100 V for 2 hours. *Pst*I-digested lamda DNA was resolved as a molecular marker. For gel purification: upon confirmation of the resolution of the DNA sample to the expected size, the reaction was similarly resolved on an agarose (0.8 %) gel and the approximate DNA band excised under long wave ultraviolet (UV) radiation. The PCR product was extracted from the agarose gel using the Nucleospin kit. Buffer BT1 [300 µl] was added and the agarose sample incubated at 50ºC for 10 minutes with frequent inversion. The melted agarose sample was loaded onto a nucleospin column and centrifuged at 12 000 x g for 30 seconds. The nucleospin column was then washed twice

with buffer NT3 [700 µl] by centrifugation at 12 000 x g for 1 minute and any residual buffer NT3 removed by an additional centrifugation. The bound nucleic acids were eluted by the addition of elution buffer NE [50 µl] (5 mM Tris-HCl, pH 8.5), followed by centrifugation at 12 000 x g for 1 minute.

B.3 The ligation of a PCR product into pGEM(T)

The PCR product [1.5 µl] was ligated to pGEM(T) plasmid DNA [0.5 µl] in 1 x ligase buffer (30 mM Tris-HCl, pH 7.8, 10 mM $MgCl_2$, 10 mM dithiothreitol, 10 mM ATP) using T4 ligase [0.5 µl] (1.5 U) at 25ºC for 1 hour and then at 4ºC for 16 hours. Controls containing no insert DNA, containing insert DNA, as well as negative controls of all reactions to which no ligase was added, were similarly incubated. Such controls demonstrated whether pGEM(T) plasmid T-overhangs were intact, the functionality of the T4 ligase, and the presence of circular DNA pre-ligation respectively.

B.4 The transformation of supercompetent cells

Separate aliquots of *E. coli* XL1Blue supercompetent cells [50 µl] were incubated with aliquots of the ligation products [2 µl], as well as with pGEX3X2000 [2 µl] (50 ng/µl) as a positive transformation control, and sterile deionized triple-distilled water [2 µl] as a negative transformation control. Transformation reactions were incubated on ice for 30 minutes. The transformation reactions were then heat pulsed for 30 seconds at 42ºC in a dry heating block, and placed on ice for 2 minutes. Sterile 2 x YT broth [500 µl] (1.6 % tryptone, 1 % yeast extract, 0.5 % NaCl), preheated to 42 ºC, was added to each transformation reaction, before incubation at 37ºC for 1 hour. The transformation reactions were then centrifuged at 5000 x g for 1 minute, the supernatent partially removed [500 µl], and the cell pellets resuspended in the remaining supernatent [100 µl] and plated out onto 2 x YT broth agar plates containing 0.1 mg/ml ampicillin. The plates were incubated at 37°C for 16 hours.

B.5 The screening of transformants

Putative plasmid DNA was extracted from *E. coli* cultures of transformants forming white colonies, by a modified alkaline lysis method (Birnboim and Doly, 1979; Joly, 1996) and using the High Pure Plasmid Isolation kit. Single colonies of *E. coli* XL1Blue potentially transformed with pGEM(T)mSTI1[*Nhe*I/*Sac*II] were separately cultured overnight at 37°C with shaking, in 2 x YT broth [4 ml] containing 0.1 mg/ml ampicillin. An aliquot [500 µl] of the overnight culture was removed and added to sterile glycerol [500 µl] (30 % v/v) and stored at –80°C as a glycerol stock. The bacterial cells [2 ml] were collected by centrifugation at 5000 x g for 1 minute, the supernatent discarded and the cell pellet resuspended in Suspension buffer [250 µl] (50 mM Tris-HCl; 10 mM EDTA, 1 mg/ml RNase A, pH 8.0). Lysis buffer [250 µl] (200 mM NaOH, 1% SDS) was then added, the suspension mixed gently by inversion and incubated at room temperature for 5 minutes. Binding buffer [350 µl] (4.0 M guanidine hydrochloride, 0.5 M potassium acetate, pH 4.2) was added, the solution mixed gently by inversion, incubated on ice for 5 minutes, and centrifuged at 13 000 x g for 10 minutes at 4 °C. The resultant plasmid–containing supernatent was transferred into the upper reservoir of a High Pure filter column (Vogelstein and Gillespie, 1979; Chen and Thomas, 1980), inserted into a collection tube, and centrifuged at 13 000 x g for 1 minute. The High Pure filter column was washed by the addition of Wash Buffer II [700 µl] (20 mM NaCl, 2 mM Tris-HCl, pH 7.5, 80 % ethanol) and centrifuged as before. The Wash Buffer was discarded from the collection tube and the centrifugation repeated in order to remove residual Wash Buffer quantitatively. The bound plasmid DNA was then eluted into a sterile eppendorf tube by the application of Elution Buffer [50 µl] (10 mM Tris-HCl, pH 8.5) to the column, followed by centrifugation as before. The A_{260} of a 20X (in water) dilution of the eluted plasmid DNA was measured for quantification, and the DNA preparation stored at -20°C.

B.6 The restriction of DNA by endonuclease digestion

Plasmid DNA [300 ng] was restricted with 5 U of the required restriction endonuclease, in the buffer provided by the manufacturer [2 µl] (10x).

Table B.1: Composition of the various restriction enzyme buffers

Buffer	Final composition
Medium Salt buffer	10 mM Tris-HCl, pH 7.5, 10 mM $MgCl_2$, 1 mM DTT, 50 mM NaCl
High salt buffer	50 mM Tris-HCl, pH 7.5, 10 mM $MgCl_2$, 10 mM dithiothreitol and 100 mM NaCl.
Tris-acetate buffer	330 mM Tris-acetate, pH 7.9, 100 mM Mg-acetate, 5 mM DTT, 660 mM K acetate, 0.01% BSA
Potassium buffer	20 mM Tris-HCl, pH 8.5, 10 mM $MgCl_2$, 1 mM DTT, 100 mM KCl

Restriction reactions were carried out in a total volume of 20 µl, at 37°C for 8 hours. An uncut plasmid DNA control whereby no restriction enzyme was added was similarly incubated. For a double digest, the DNA digestions were first incubated in the lower salt buffer and then salt added such that the restriction solution was made up to the higher salt buffer. The DNA digestions were resolved by agarose gel electrophoresis (B.2).

B.7 The directional ligation of cDNA into vector DNA

Bulk plasmid DNA containing the insert required (~5 µg) and vector DNA [10 µl] (~5 µg) were separately restricted in double digests, such that 10 µl of the restriction buffers and 20 U enzyme were used in a total volume of 100 µl. The restricted plasmid DNA was ethanol precipitated by the addition of sodium acetate [10 µl] (3.0 M) and absolute ethanol [200 µl] (-20ºC), incubation at –20ºC for 4 hours and centrifugation at 12 000 x g for 1 hour. The precipitated restricted DNA pellet was washed in ethanol [200 µl] (70%, –20ºC) and centrifuged at 12 000 x g for 20 minutes. After removal of the supernatent, the plasmid DNA pellet was air dried, and resuspended in sterile triple-distilled deionized water [10 µl]. Agarose gel loading buffer [5 µl] was added and the restricted DNA fragments resolved by agarose gel electrophoresis. The appropriate bands were excised

and extracted from the agarose gel. The insert cDNA [3 µl] was ligated to the vector DNA [1 µl] with T4 ligase [1 µl] (10 U) by incubation in 1 x ligase buffer [10 µl total](300 mM Tris-HCl, 100 mM $MgCl_2$, 100 mM dithiothreitol, 10 mM ATP, pH 7.8) at 4 ºC for 16 hours. Similarly, two vector-only ligation control reactions were prepared, one to which no insert DNA was added, and one to which no ligase was added, in order to determine the efficiency of the vector digestion and dephosphorylation respectively.

B.8 The preparation and transformation of competent *E. coli* cells

E. coli XL1Blue or BL21 competent cells were cultured from a separate overnight culture incubated in 2 x YT broth [100 ml], with shaking at 37ºC. The overnight culture was first separately diluted 1:10 into fresh 2 x YT broth [100 ml], then incubated with shaking at 37 ºC as before, for a further 3 hours, such that the culture reached log phase (A_{600} = 0.6-1). *E. coli* cells were collected by centrifugation at 5000 x g for 15 minutes at 4 ºC, in sterile centrifuge tubes and the cell pellet resuspended in ice cold $MgCl_2$ [100 ml] (0.1 M). The cell suspension was incubated on ice for 20 minutes before the cells were collected by centrifugation as before, and resuspended in ice-cold $CaCl_2$ [50 ml] (0.1 M). The suspensions were incubated on ice for 2 hours, and the cells collected by centrifugation as before and resuspended in ice-cold $CaCl_2$ [5 ml] (0.1 M). Sterile glycerol [5 ml] (30 % w/v) was added and the competent cells stored in 300 µl aliquots at –80 ºC. Ligation reactions [2 µl] were transformed into *E. coli* XL1Blue according to B.4, except that transformation reactions were heat pulsed for 2 minutes instead of 30 seconds.

B.9 The filling in of DNA overhangs using T4 polymerase

The restricted DNA was resuspended in sterile deionized triple-distilled water [10 µl], and overhangs filled in by the addition of dNTPs [1µl] (330 µM each), T4 polymerase (8 U) and 10 x T4 polymerase buffer [2 µl] (67 mM Tris-HCl, 6.7 mM $MgCl_2$, 16.6 mM

$(NH_4)_2SO_4$, 10 mM 2-mercaptoethanol, 6.7 μM EDTA, 0.167% BSA). The reaction was carried out at room temperature for 10 minutes, in a final volume of 20 μl. T4 polymerase was inactivated by incubation of the reaction at 75°C for 10 minutes.

B.10 The sequencing of plasmid constructs

The insert regions of plasmid constructs were sequenced according to the chain termination method (Fangan *et al.*, 1999), using the Big Dye™ ready reaction kit. Plasmid DNA (200-500 ng) was added to 3.2 pmol sequencing primer, and the volume made up to 12 μl with sterile deionized triple-distilled water. Big Dye [4μl] was added, and the sequencing reactions PCR amplified, according to the following parameters: a 96ºC pre-incubation step for 1 second was followed by a 3 step cycle of 96ºC for 10 seconds, 50ºC (or 5ºC below the T_m of the sequencing primer, Appendix C) for 5 seconds, and 60º C for 4 minutes, repeated a total of 25 times. Reactions were subsequently cooled at 4ºC for 45 minutes. Cycle sequencing products were cleaned before sequencing using the Zymo DNA Clean and Concentrator™-5 kit. DNA binding buffer [100 μl] was added to the cycled reaction, and the resulting solution loaded onto a Zymo-spin column, placed in a collection tube, and centrifuged at 13 000 x g for 10 seconds. The flow-through was discarded, wash buffer [200 μl] applied, and the column centrifuged as before. This wash step was repeated, with an additional centrifugation step to remove residual buffer quantitatively. The column was transferred to a sterile eppendorf tube, sterile deionized triple-distilled water [8 μl] was added to the column matrix, and centrifuged at 13 000 x g for 10 seconds. The DNA elution was air dried at 37ºC for 16 hours. The dried pellet was submitted for sequencing on a Applied Biosystems ABI3100 Prism DNA sequencer at the Rhodes University DNA sequencing facility.

B.11 The preparation of plasmid DNA for mammalian transfection reactions and site-directed mutagenesis

Purified preparations of plasmid DNA were prepared using a modified alkaline lysis procedure (Birnboim and Doly, 1979; Joly, 1996) and the QIAGEN Maxiprep kit. A single colony of each of *E. coli XL1Blue*[pB-EGFP] and *E. coli XL1Blue*[pB-mSTI1-EGFP] were separately cultured overnight as before, in 2 x YT broth [500 ml] containing 0.1 mg/ml ampicillin. An aliquot [500 µl] of each of the overnight cultures was removed, added to sterile glycerol [500 µl] (30 % v/v) and stored at –80°C as a glycerol stock. The bacterial cells were collected by centrifugation at 5000 x g for 1 minute, the supernatent discarded and the cell pellet resuspended in Buffer P1 [10 ml] (50 mM Tris-HCl, 10 mM EDTA, 100 µg/ml RNase A, pH 8.0) and transferred to sterile centrifuge tubes. Buffer P2 [10 ml] (200 mM NaOH, 1% SDS) was then added, the suspension mixed gently by inversion and incubated at room temperature for 5 minutes. Buffer P3 [10 ml] (3.0 M CH_3COOK, pH 5.5) was added, the solution mixed gently by inversion, incubated on ice for 20 minutes, and centrifuged at 13 000 x g for 30 minutes at 4 °C. The resultant supernatent was decanted into a new sterile centrifuge tube and centrifuged again as before. The QIAGEN Maxiprep column was pre-equilibrated by the application of Buffer QBT [10 ml] (750 mM NaCl, 50 mM MOPS, pH 7.0, 15% isopropanol, 0.15 % Triton X-100), and the column emptied by gravity flow. The final plasmid–containing supernatent was then transferred into the upper reservoir of a QIAGEN Maxiprep column, and allowed to enter the resin by gravity flow. The QIAGEN Maxiprep column was washed with Buffer QC [60 ml] (1.0 M NaCl, 50 mM MOPS, pH 7.0, 15 % isopropanol). The bound plasmid DNA was then eluted into a sterile 50 ml falcon tube by the application of Buffer QF [15 ml] (1.25 M NaCl, 50 mM Tris-HCl, pH 8.5, 15 % isopropanol) to the column, and the eluant aliquoted [625 µl] into sterile eppendorfs. Isopropanol [438 µl] was added to each aliquot, followed by centrifugation at 15 000 x g for 30 minutes at 4°C. The supernatent was carefully removed and the plasmid DNA pellets washed by the addition of ethanol [100 µl] (70 %), recentrifuged and the supernatents discarded. The pellets were allowed to air dry in an inverted position before resuspension in TE Buffer

[100 µl] (10 mM Tris-HCl, 1 mM EDTA, pH 8.0). The A_{260} of a 20X (in water) dilution of the eluted plasmid DNA was measured for quantification, and the DNA preparation stored at -20°C.

B.12 The culturing of mouse NIH 3T3 fibroblasts

Mouse NIH 3T3 fibroblasts were cultured from glycerol stocks and maintained in Dulbecco's modified Eagle's medium supplemented with 10% calf serum and penicillin (100 U/ml) / streptomycin (100 U/ml) (complete media) in a humidified atmosphere, at 37°C with 10% CO_2 until 90% confluency was reached. The cells were trypsinized with 0.25% trypsin / 0.1% versene for 2-10 min, collected by centrifugation at 5000 x g for 5 min at 4°C, and washed twice with in ice-cold phosphate buffered saline (PBS) (137 mM NaCl, 2.7 KCl, 4.3 mM Na_2HPO_4, 1.4 mM KH_2PO_4).

For subculturing, the final cell pellet was resuspended in 5 ml complete media and the cell concentration determined using a haemocytometer. For 8 well chamber slides: a total of 1 x 10^5 cells was added to 300 µl media per well. For 3.2 cm^2 transfection petri dishes and 25 cm^2 flasks: a total of 1 x 10^6 cells was added to 3 ml and 5 ml complete media, respectively. For 75 cm^2 flasks: a total of 3 x 10^6 cells was added to 4 ml media in the flask, and the volume made up to 5 ml using complete media. The 25 cm^2 and 75 cm^2 flasks were incubated as before until 90 % confluency was reached. The 3.2 cm^2 petri dishes were typically incubated 24 hours, in preparation for transfection reactions.

B.13 The transfection of mouse NIH 3T3 fibroblasts and selection of episomally stable transfectants

For transient transfections: NIH 3T3 fibroblasts were subcultured into 8 well chamber slides 24 hours prior to transfection such that a 30-50% confluency was reached. Plasmid DNA [100 ng] was added to serum-free media [12.5 µl], followed by the addition of Lipofectamine Plus reagent [1 µl], and incubation at room temperature for 15 minutes.

Separately, Lipofectamine reagent [0.5 µl] was added to serum-free media [100µl], then this solution was added to the DNA/Plus reagent solution, and incubated at room temperature for 15 minutes. 8 well chamber slides to be transfected were first washed in PBS before the addition of the transfection mixture [114 µl] to each well containing NIH 3T3 fibroblasts. Transfection reactions were incubated for 3 hours as per B.12. 2 x media [200 µl] (complete media containing 20% calf serum) was added and the cells incubated for 20 hours as per B.12.

For episomally stable transfectants, NIH 3T3 fibroblasts were subcultured into 3.2 cm^2 petri dishes as described in B.12, 24 hours prior to transfection such that a confluency of 30-50% was reached. For each 3.2 cm^2 petri dish, plasmid DNA [55 µl](40 µg/ml) was added to 2 x HBS buffer [62.5 µl](280 mM NaCl, 10 mM KCl, 1.5 mM $Na_2HPO_4.2H_20$, 12 mM dextrose, 50 m M HEPES, pH 7.05) and mixed well by vortexing. $CaCl_2$ [8.25 µl](2.0 M) was added and the reaction immediately vortexed well for 20 seconds. Similarly, a negative transfection control was prepared in which water was used instead of plasmid DNA solution. The DNA in transfection reactions was allowed to precipitate at room temperature for 20 minutes, before the whole reaction was added directly to the 3 ml media in the 3.2 cm^2 petri dish containing the overnight culture of NIH 3T3 fibroblasts. The media was replaced after 20 hours, and the culture incubated for a further 8 hours before replacing the media with selection media [3 ml](complete media containing 0.5 mg/ml geneticin). The selection media was subsequently replaced every 2 days, for 3 weeks, until 90 % confluency was reached. Geneticin selected NIH 3T3 fibroblasts were considered to be episomally stable pB-mSTI1-EGFP transfectants since negative controls did not survive selection, and were subcultured according to B.12, and maintained in selection media. Thus the episomally stable pB-mSTI1-EGFP transfectants were prepare from a pool of clones. For visualization by fluorescence microscopy, episomally stable pB-mSTI1-EGFP transfectants were subcultured into 8 well chamber slides as in B.12.

B.14 The visualization of pB-mSTI1-EGFP transfectants by confocal laser scanning fluorescence microscopy

8 well chamber slide cultures were used for visualization by fluorescence microscopy. Wells were washed 3 times in PBS, and incubated in formaldehyde [100 µl] (3.7% in PBS) for 10-15 minutes. Wells were washed twice with PBS, then incubated in 4',6'-diamidino-2-phenylindole (DAPI) staining solution [100 µl] (2 µg/ml DAPI in PBS) for 5 minutes before a final PBS wash. Chamber slides were dismantled, the gasket removed, and slides mounted in DAKO fluorescent mounting solution. Slides were visualized on an LSM510 confocal laser scanning fluorescence microscope. Conditions for visualization of all further experiments were identical.

B.15 Immunostaining of endogenous mSTI1 in mouse NIH 3T3 fibroblasts

Transient pB-mSTI1-EGFP transfectants, or untransfected cells, were prepared in 8 well chamber slides. Wells were washed 3 times in PBS and fixed in formaldehyde[100 µl] (3.7% in PBS) for 10-15 minutes. Wells were washed twice with wash buffer I [200 µl] (0.5% BSA, 20 mM glycine, 0.1% saponin, 0.1% NaN_3), and permeabilized by incubation in wash buffer I for 5 minutes on the second wash. Non-specific binding was blocked by the addition of block solution [100 µl] (3% BSA, 0.1% saponin, 10% normal donkey serum) to each well, and incubated for 30 minutes at room temperature. Wells were incubated in primary antibody solution [100 µl] (block solution, rabbit anti-mSTI1 SF1 antibody diluted 1:250, Lässle *et al*., 1997) for 1 hour at room temperature, and washed in wash buffer II (0.5% BSA, 0.1% saponin) twice. Secondary antibody solution [100 µl] (block solution, donkey anti-rabbit Cy3 conjugated antibody diluted 1:200) was added to each well and incubated for 1 hour at room temperature. Slides were washed twice in PBS, stained with DAPI staining solution, mounted and visualized by normal fluorescence microscopy. Pictures were taken with a digital camera under low light conditions.

B.16 The preparation of mSTI1 derivatives by site-directed mutagenesis

A purified preparation of template plasmid DNA was prepared (B.11). Plasmids encoding derivative mSTI1 proteins, were prepared by site-directed mutagenesis using a double stranded whole plasmid linear amplification (Jung *et al.*, 1992).

Table B.2: Site-directed mutagenesis was used to substitute amino acids

Engineered change	**Primers used**	**Diagnostic enzyme**	**Diagnostic fragments expected for unmodified plasmid (bp)**	**Diagnostic fragments expected for modified plasmid (bp)**
Serine to alanine at 189	S189AF S189AR	*Nco*I	pSKmSTI1-EGFP: 5170 pGEX3X2000: 1341, pET5a2000: 5767	 4396 and 774 771, 565 4867 and 777
Threonine to alanine at 198	T198AF T198AR	*Ban*I	pSKmSTI1-EGFP: 1723 pGEX3X2000: 4499 pET5a2000: 4499	 1080 and 643 2706, 1793 2706 and 1793
Threonine to alanine at 332	T332AF T332AR	*Eco*O1091	pGEX3X2000(T198A): 810 pET5a2000(T198A): 810	 546 and 264 546 and 264
Serine to glutamic acid at 189	S189EF S189ER	*Acc*I	pSKmSTI1-EGFP: 5296	 4712 and 584
Threonine to glutamic acid at 198	T198EF T198ER	*BSi*EI	pSKmSTI1-EGFP: 1835	 1040 and 795

The reactions were prepared under sterile conditions in 0.2 ml thin walled polypropylene microcentrifuge tubes. The linear amplification reactions included final concentrations of the template plasmid DNA (4 ng/µl), forward primer (8 ng/µl), reverse primer (8 ng/µl), dNTPs (200 µM each) and Pfu™ DNA polymerase (25 U) in 1 x reaction buffer (100 mM KCl, 100 mM $(NH_4)SO_4$, 200 mM Tris-HCl, pH 8.8, 20 mM $MgSO_4$, 1% Triton X-100, 1 mg/ml nuclease-free BSA) to a final volume of 50 µl. The cycling parameters were such that the linear amplification reaction was incubated at 95 °C for 1 minute, followed by a 3-step cycle of 95°C for 30 seconds, 52°C for 30 seconds, and 68°C for 14 minutes, repeated a total of 18 times. A final incubation step was performed at 78°C for 7 minutes.

A positive control reaction was prepared for the mutagenesis of pWhitescript™. pWhitescript™ positive control plasmid (10 ng), primer number 1 (125 ng), primer number 2 (125 ng), dNTP mix (200 µM each) was made up to 50 µl with sterile deionized triple-distilled water and Pfu™ DNA polymerase (25 U) added. The control reaction was cycled as described above.

To digest the template DNA, *Dpn*I [1 µl](10U) was added directly to each amplification reaction and the reaction mixtures incubated for 16 hours at 37°C. Agarose gel loading buffer [5 µl] was added to the amplification products [15 µl] and the products resolved by agarose gel electrophoresis (B.2). Aliquots of *E. coli* XL1Blue supercompetent cells were transformed with amplification products as described. The pWhitescript™ positive control transformation reaction was, however, plated onto MacConkey agar plates (5%) containing ampicillin (0.1 mg/ml). The mutagenesis efficiency (ME) for the pWhitescript™ positive control transformation reaction was calculated according to the following formula:

$$ME = \frac{\text{Number of red cfu}}{\text{Number of total cfu}} \times 100\%$$

B.17 Screening of putative derivative plasmids

Putative preparations of derivative plasmid were prepared (B.5). Aliquots of template DNA [2 µl] and putative derivative plasmid [2 µl] were restricted with diagnostic enzyme (table, B.16). The DNA digestions were resolved by agarose gel electrophoresis (B.2) and plasmid DNA exhibiting fragments migrating as expected (Table B.2) were regarded as putative mutants. DNA regions of mutation were sequenced for confirmation as described.

B.18 SDS PAGE

SDS PAG electrophoresis was carried out according to Laemmli (ref). A (0.1%) SDS (4%) PAGE stacking gel was pre-cast on top of a (0.1%) SDS (12%) PAGE resolving gel in a Bio-Rad minigel electrophoresis set. Protein samples were added to SDS PAGE gel denaturing loading buffer [4 µl of a 5x buffer] (62.5 mM Tris-HCl, pH 6.8, 10 % (v/v) glycerol, 2% (w/v) SDS, 5% (v/v) β-mercaptoethanol, 0.05% (w/v) bromophenol blue) and heated to 95 °C for 5 minutes. The protein samples were loaded onto the gel and resolved at 200 V for 45 minutes in SDS PAGE running buffer (0.025 M Tris, 0.0192 M glycine, 1% (w/v) SDS). The gel was removed and incubated with shaking for 1 hour in Coomassie blue stain (0.1% (w/v) Coomassie Brilliant Blue R-250, 40% (v/v) methanol, 10% (v/v) glacial acetic acid) and 3 hours in destain (40% (v/v) methanol, 10% (v/v) glacial acetic acid).

B.19 Two dimensional electrophoresis

A 175 cm^2 flask of NIH 3T3 fibroblasts was cultured (B.12) until 90% confluency was reached. The cells were harvested by trypsinization (B.12) and washed once with PBS and once with 0.5 x PBS to remove as much salt as possible. The cell pellets were resuspended directly in 2D gel electrophoresis rehydration buffer [250 µl] (9.8 M urea, 4% CHAPS, 100 mM DTT, 0.2% (w/v) Bio-Lytes, 0.001 % bromophenol blue), and

centrifuged at 13 000 rpm for 20 minutes on a desk-top microfuge to remove insoluble cell debris. The total protein concentration was determined according to the Bradford method, using the Bio-Rad Bradford concentrate [200 µl] added to a sample dilution [1 µl sample into 800 µl water] and the absorbance measured at 550 nm. A standard protein curve of BSA amount (range: 0-20 µg) was constructed from similarly prepared BSA standards.

For the first dimension separation by IEF, the sample was first diluted in rehydration buffer to a final concentration of 100 µg total protein in 250 µl buffer, then loaded onto a Bio-Rad Protean IEF cell machine. The strips were kept moist by the loading of mineral oil [250 µl] over both strip and sample. Rehydration was carried out for 12 hours at 20°C, followed by isoelectric focusing (IEF) at 250V for 1 hour, 500V for 1 hour, 4000V for 35 000 volt hours and maintained at 500V for 2 hours. After focusing, the strip was equilibrated in Equilibation Buffer I [2 ml] (6 M urea, 2% SDS, 0.375 M Tris-HCl, pH 8.8, 20% glycerol, 130 mM DTT) for 30 minutes, followed by incubation in Equilibation Buffer II [2 ml] (6 M urea, 2% SDS, 0.375 M Tris-HCl, pH 8.8, 20% glycerol, 135 mM iodoacetamide) for 30 minutes. For the second dimension, the strip was loaded on a (0.1%) SDS (4%) PAGE stacking gel with melted agarose (1%) gel. This stacking gel was pre-cast on top of a (0.1%) SDS (12%) PAGE resolving gel in a Bio-Rad minigel eletrophoresis set. The focused proteins on the strip were resolved through the second dimension at 200 V for 45 minutes in SDS PAGE running buffer (0.025 M Tris, 0.0192 M glycine, 1% (w/v) SDS).

B.20 Western transfer of proteins

Following electrophoresis, the SDS PAGE gel was equilibrated in ice-cold Transfer Buffer (25 mM Tris, 192 mM glycine, 20% (w/v) methanol), along with nitrocellulose membrane and 3MM Whatman filter paper. The pre-equilibrated SDS PAGE gel was placed against the nitrocellulose membrane, excluding air bubbles, between pieces of equilibrated 3MM Whatman filter paper, and the proteins transferred from the gel to the membrane in a small scale Bio-Rad Western transfer set, in chilled Transfer Buffer at

100V for 1 hour. The transfer was kept chilled by the insertion of the cooling unit containing ice, and continual stirring on a magnetic stirrer. Following completion of the transfer, the nitrocellulose membrane was stained with Ponsceau stain (0.5% (w/v) Ponsceau S, 1% (v/v) glacial acetic acid) for 1 minute and rinsed with distilled water, to determine whether transfer was successful.

B.21 Chemiluminescence-based immunodetection of Western blots

Following Western transfer, the membrane was washed twice in TBS (50 mM Tris-HCl, pH 7.5, 150 mM NaCl) and blocked overnight in blocking solution (5% w/v non-fat milk powder in TBS) at 4°C. Proteins were specifically detected by incubating the membrane with primary antibody diluted in blocking solution (according to manufacturers instructions), for 1 hour at room temperature with shaking. The primary antibody was removed and stored at 4°C with sodium azide (1%) for repeated use. The membrane was then washed for 20 minutes in TBST (0.1% (v/v) Tween-20 in TBS) four times at room temperature with shaking. The secondary antibody, goat horseradish peroxidase, anti-rabbit conjugate, was diluted 1: 20 000 in blocking solution, and incubated with the membrane for 1 hour at room temperature with shaking. The membrane was washed in TBST as before, and then incubated with luminol-based detection reagents in the dark. The membrane was exposed to X-ray film for various time intervals (30 seconds to 5 minutes) and the film developed in developer solution, rinsed in stop solution, fixed in fixer solution and rinsed in water before air-drying.

B.22 The determination of protein concentration by the Lowry method

The concentration of purified proteins was determined by a standard Lowry assay (Lowry, 1951),. A 1-20 μg range of standard BSA concentrations was prepared in water to a final volume of 1 ml. Sample proteins [2 μl] were added to deionised water [798 μl].

Freshly prepared alkaline copper reagent [5 ml] (0.01 % $CuSO_4$, 0.02 % Na tartrate, 4 % $NaCO_3$, 0.1 N aOH) was added, the samples incubated at room temperature for 20 minutes, and the A_{500} measured. A standard curve of BSA amounts (µg) versus A_{500} readings was constructed and the protein concentrations of the unknowns calculated from a fitted linear regression line.

APPENDIX C

PRIMERS

Table C.1: Primers were used for site-directed mutagenesis and PCR amplification of DNA

Name of primer	Sequence (5'-3')	Length	Tm (°c)
PCRmSTI1pCineoF	ATCGGCTAGCAGAATGGAGCAGGTGAATGAG	31	66.8
PCRmSTI1pCineoF	ATTACCGCGGCCGAATTGCGATGAGCA	27	66.7
PCRmSTI1pET5aF	GATCCATATGGAGCAGGTGAATGAG	25	59
PCRmSTI1pET5aR	GAGCGCTAGCTTACCGAATTGCGATGAGAC	30	66
S189AF	GTTGATCTGGGCGCCATGGATGAAGAGG	28	85
S189AR	CCTCTTCATCCATGGCGCCCAGATCAAC	28	85
T198AF	GAGGAAGAGGCAGCGGCACCCCCACC	26	88
T198AR	GGTGGGGGTGCCGCTGCCTCTTCCTC	26	88
T332AF	GCAGAGCACCGGGCCCCAGATGTG	24	69.6
T332AR	CACATCTGGGGCCCGGTGCTCTGC	24	69.6
S189EF	CCTCCTTGGGGTAGACCTGGGCGAAATGGATGAAG	35	83.6
S189ER	CTTCATCCATTTCGCCCAGGTCTACCCCAAGGAGG	35	83.6
T198EF	GAGGAAGAGGCGGCCGAACCCCCACCCCCAC	31	84
T198ER	GTGGGGGTGGGGGTTCGGCCGCCTCTTCCTC	31	84
EGFP-NLSmSTI1F	ATTACTCGAGCGGATGGAGAATAAGAAACAGGCA CTGAAAGAGAAGGAGCTGGGAAATGATGCCTACA AGAAGAAAATGGTGAGCAAGGGCGAGG	95	77.9
VLEGFP1R	ACGCCGTAGGTCAGG	15	53.4
EGFP-NLS-R	ATTAGCGGCCGCTTACTTGTACAGCTCGTCCATGCC	36	71.7
210NEW	CTCTGTCATAATGCTTCAGGG	21	54.0

APPENDIX D

SUPPLEMENTARY RESULTS

D.1 The preparation of pGEM(T)mSTI1[*Nhe*I/*Sac*II]

The mSTI1 cDNA PCR amplification reaction successfully yielded a 1600 bp DNA product (Figure D.1B, lane 2), which was subcloned into pGEM(T). The digestion of pGEM(T)mSTI1[*Nhe*I/*Sac*II] with *Nhe*I yielded the expected linearized 4615 bp fragment (Figure D.1A and B, lane 4), while *Sac*II (Figure D.1B, lane 5) and *Nhe*I/*Sac*II double digestion (Figure D.1B, lane 6) yielded the expected 3015 bp and 1600 bp fragments.

D.2 The preparation of pCineo-mSTI1-EGFP

The mSTI1 cDNA from pGEM(T)mSTI1[*Nhe*I/*Sac*II] was successfully subcloned into pCineo-EGFP (Figure D.1C). pCineo-mSTI1-EGFP was found to extract poorly due to its low copy number (characteristics typical of a mammalian construct). However, *Hind*III digestion of pCineo-mSTI1-EGFP preparations successfully produced fragments that migrated distances corresponding to 3815 bp, 2748 bp and 1239 bp on an agarose (0.8%) gel (Figure D.1D and 30E, lane 3), as expected. Similarly, *Nhe*I and *Sac*II double digestion of pCineo-mSTI1-EGFP (Figure D.1D and E, lane 4) successfully produced fragments migrating distances corresponding to 6027 bp and 1600 bp on an agarose (0.8%) gel, as expected.

D.3 The preparation of pSK-mSTI1-EGFP and pSK-EGFP

The EGFP and mSTI1-EGFP cDNA from pCineo-EGFP and pCineo-mSTI1-EGFP were subcloned into the vector pSK to introduce the *Xho*I restriction site, so that further cloning into pB was possible (Karasuyama and Melchers, 1988). Digestion of pSK-EGFP

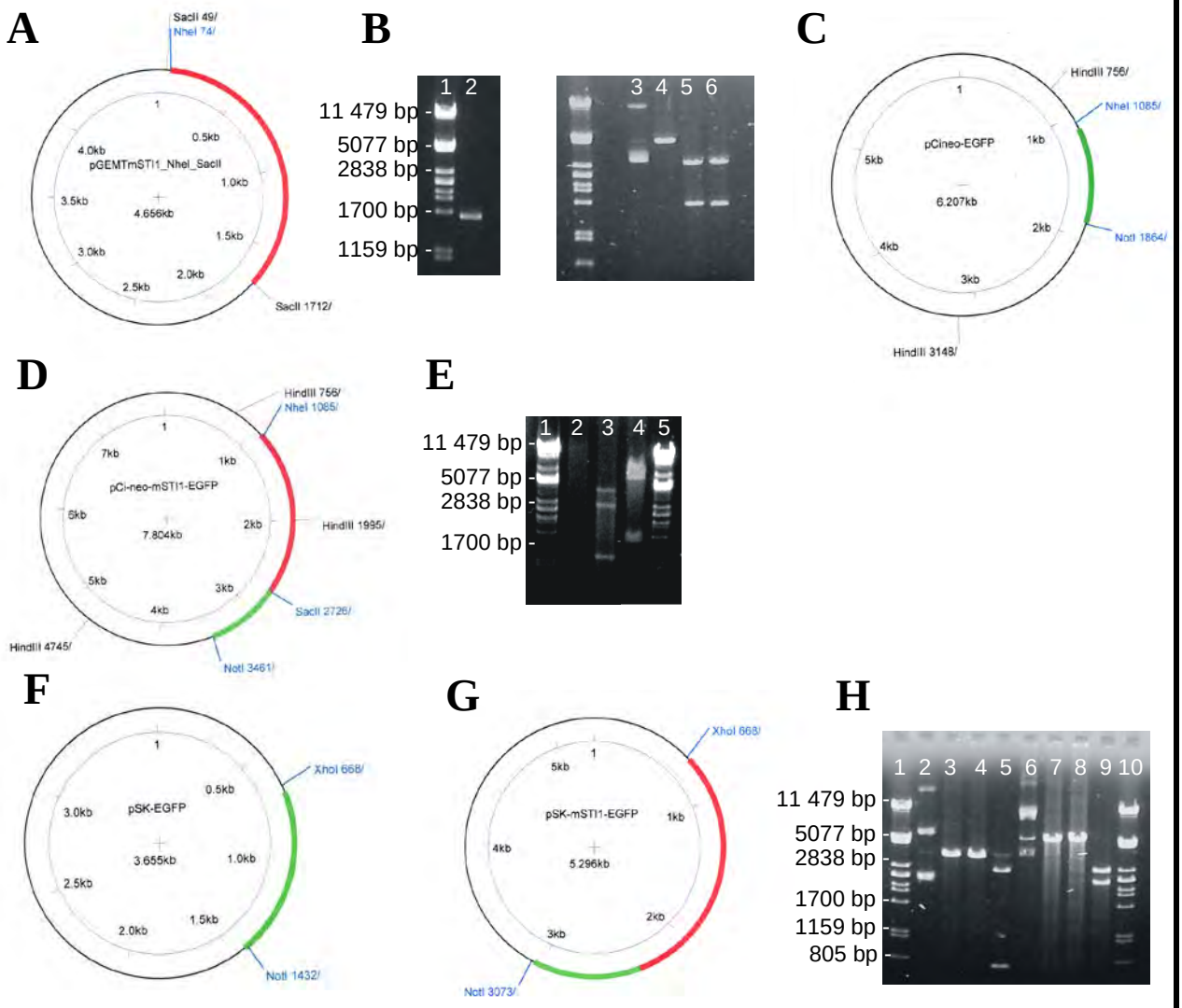

Figure D.1:The plasmid constructs pGEM(T)mSTI1[NheI/SacII], pCineo-mSTI1-EGFP, pSK-EGFP and pSK-mSTI1-EGFP were successfully generated

pGEM(T)mSTI1[*Nhe*I/*Sac*II] (A) containing the 1600 bp mSTI1 PCR amplified ORF (B, lane 2) was digested with NheI (B, lane 4) to linearize the 4615 bp contruct. SacII (B, lane 5); or both NheI and SacII (B, lane 6) digestion of pGEM(T)mSTI1[*Nhe*I/*Sac*II] produced the expected 3015 bp and 1600 bp fragments compared to undigested DNA (B, lane 3). The 1600 bp mSTI1 cDNA was inserted into the *Nhe*I and *Sac*II sites of pCineo-EGFP (C) to produce pCineo-mSTI1-EGFP (D). *Hind*III digestion of pCineo-mSTI1-EGFP produced the expected 3815 bp, 2748 bp and 1239 bp fragments (E, lane 3), while *Nhe*I and *Sac*II double digestion produced the expected 6027 bp and 1600 bp fragments (E, lane 4) compared to undigested DNA (E, lane 2). The 764 bp EGFP cDNA was ligated into the *Eco*RV and *Not*I sites of pSK to produce pSK-EGFP (F), while the 2378 bp mSTI1-EGFP cDNA was ligated into the *Eco*RV and *Not*I sites of pSK to produce pSK-mSTI1-EGFP (G). Digestion of pSK-EGFP with either *Xho*I (H, lane 3) or *Not*I (H, lane 4) linearized the contruct and produced an expected 3764 fragment. Digestion of pSK-EGFP with both *Xho*I and *Not*I (H, lane 5) produced the expected 3000 bp and 764 bp fragments compared to undigested pSK-EGFP (H, lane 2). Digestion of pSK-mSTI1-EGFP with either *Xho*I (H, lane 7) or *Not*I (H, lane 8) linearized the contruct and produced an expected 5378 fragment. Digestion of pSK-mSTI1-EGFP with both *Xho*I and *Not*I (H, lane 9) produced the expected 3000 bp and 2378 bp fragments compared to undigested pSK-mSTI1-EGFP (H, lane 6). The red lines represent the mSTI1 coding region, and the green lines represent the GFP coding region.

with *Xho*I or *Not*I (Figure D.1F and 30H, lanes 3 and 4), linearized the construct, producing the expected 3764 bp fragment. Digestion of pSK-EGFP with both *Xho*I and *Not*I (Figure 32H, lane 5), released the insert, producing 764 bp and 3000 bp fragments. Digestion of pSK-mSTI1-EGFP with either *Xho*I or *Not*I (Figure D.1G and H, lanes 7 and 8), linearized the construct and produced a 5378 bp fragment. Digestion of pSK-mSTI1-EGFP with both *Xho*I and *Not*I, released the insert as expected, producing 2378 bp and 3000 bp fragments (Figure D.1H, lane 9). Sequencing of pSK-mSTI1-EGFP confirmed the mSTI1 cDNA sequence and in frame fusion of the mSTI1 with the EGFP cDNA.

D.4 The preparation of pGEM(T)NLS^{mSTI1}EGFP[*Xho*I/*Not*I]

The NLS^{mSTI1}EGFP cDNA PCR amplification reaction successfully yielded an expected 815 bp fragment on an agarose (0.8%) gel (Figure D.2B, lane 3). Ligation of this PCR product with pGEM(T) plasmid DNA resulted in pGEM(T)NLS^{mSTI1}EGFP[*Xho*I/*Not*I]. Digestion of pGEM(T)NLS^{mSTI1}EGFP[*Xho*I/*Not*I] with *Xho*I and *Not*I, yielded the expected 3015 bp and 815 bp fragments (Figure D.2A and B, lane 4).

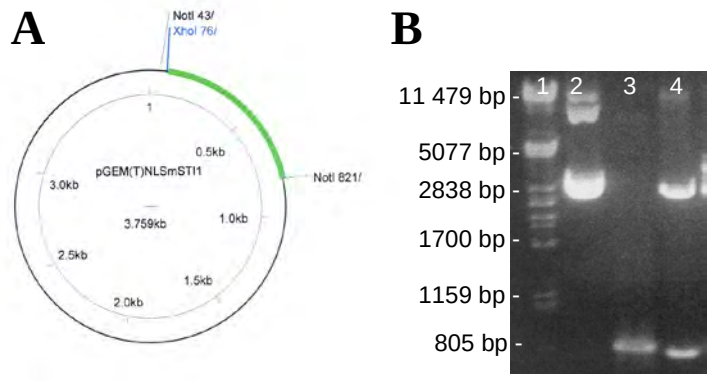

Figure D.2: NLS^{mSTI1}EGFP cDNA was successfully ligated into pGEM(T)

NLS^{mSTI1}EGFP was successfully amplified (B, lane 3) and ligated into pGEM(T) to produce pGEM(T)NLS^{mSTI1}[*Xho*I/*Not*I] (A). *Xho*I/*Not*I digestion of pGEM(T)NLS^{mSTI1}[*Xho*I/*Not*I] (B, lane 4) produced the expected fragments of 815 bp (NLS^{mSTI1}EGFP cDNA) and 3015 bp (pGEM(T) vector). Undigested DNA was included (B, lane 2). The green lines represents NLS^{mSTI1}-EGFP cDNA.

D.5 The insertion of pSK-mSTI1-EGFP derivatives into pB

Digestion of pSK-mSTI1-EGFP derivative plasmids: pSK-mSTI1-EGFP(S189A), pSK-mSTI1-EGFP(T198A), pSK-mSTI1-EGFP(S189E) and pSK-mSTI1-EGFP(T198E) with *Xho*I and *Not*I, released the 2378 bp mSTI1-EGFP insert for all constructs (data not shown). The mSTI1-EGFP cDNA from pSK-mSTI1-EGFP derivative plasmids were subcloned into the vector pB to produce pB-mSTI1-EGFP derivative plasmids which, upon *Hind*III digestion resulted in 7700 bp, 5000 bp, 3790 bp and 902 bp fragments for pSK-mSTI1-EGFP(S189A) (Figure D.3A, lane 5), pSK-mSTI1-EGFP(T198A) (Figure 34A, lane 7), pSK-mSTI1-EGFP(S189E) (Figure D.3B, lane 3) and pSK-mSTI1-EGFP(T198E) (Figure D.3C, lane 3).

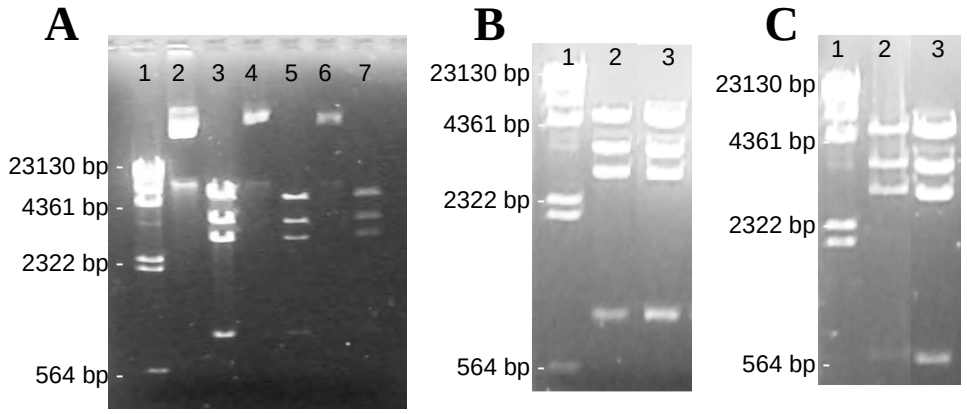

Figure D.3: The successful preparation of pB-mSTI1-EGFP derivative plasmids

The mSTI1-EGFP cDNA from pSK-mSTI1-EGFP derivative plasmids was were subcloned into the vector pB to produce pB-mSTI1-EGFP derivative plasmids which, upon *Hind*III digestion resulted in 7700 bp, 5000 bp, 3790 bp and 902 bp fragments for pSK-mSTI1-EGFP(S189A) (A, lane 5), pSK-mSTI1-EGFP(T198A) (A, lane 7), pSK-mSTI1-EGFP(S189E) (B, lane 3) and pSK-mSTI1-EGFP(T198E) (C, lane 3).

D.6 The preparation of pGEM(T)mSTI1[*Nde*I/*Nhe*I]

Putative pGEM(T)mSTI1[*Nde*I/*Nhe*I] plasmid DNA was extracted from *E. coli* cultures of transformants forming white colonies by a modified alkaline lysis method. Putative pGEM(T)mSTI1[*Nde*I/*Nhe*I] plasmids were restricted with *Nhe*I and *Nde*I. The DNA digestions were resolved by agarose gel electrophoresis. Plasmid DNA migrated expected distances corresponding to sizes of 3015 bp and 1600 bp, and were regarded as pGEM(T)mSTI1[*Nde*I/*Nhe*I] (Figure D.4A and B, lane 7).

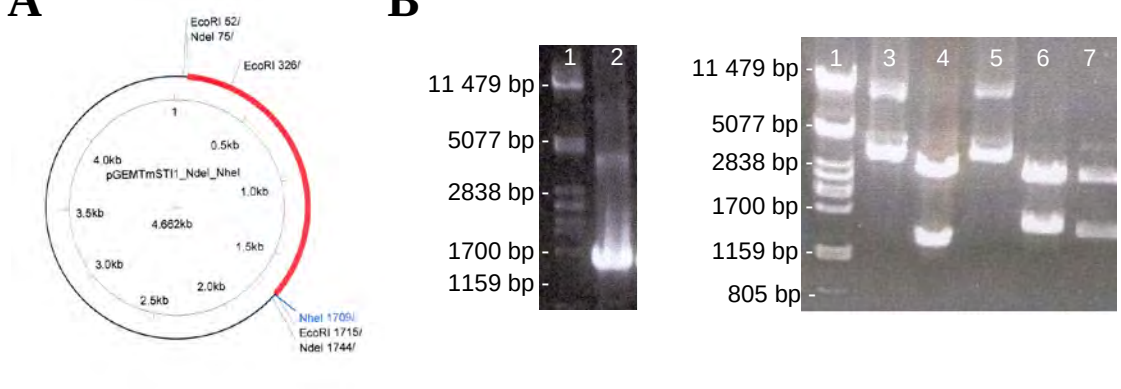

Figure D.4: mSTI1 cDNA was successfully inserted into pGEM(T)

mSTI1 cDNA was successfully amplified (B, lane 2) and inserted into pGEM(T) to produce pGEM(T)mSTI1[*Nde*I/*Nhe*I] (A). *Eco*RI digestion of pGEM(T)mSTI1[*Nde*I/*Nhe*I] (B, lane 4) produced the expected fragments of 1600 bp (mSTI1 cDNA) and 3015 bp (pGEM(T) vector). *Nde*I digestion of pGEM(T)mSTI1[*Nde*I/*Nhe*I] (B, lane 6) and *Nde*I/*Nhe*I digestion (B, lane 7) produced the expected fragments of 1600 bp (mSTI1 cDNA) and 3015 bp (pGEM(T) vector). Undigested DNA was included (B, lane 3 and 5)

D.7 The production of GST-mSTI1 derivative proteins

A 89 kDa protein corresponding to GST-mSTI1, was overexpressed after IPTG induction of *E. coli* XL1Blue transformants containing pGEX3X2000(S189A), pGEX3X2000(T198A) and pGEX3X2000(T198A,T332A). These proteins were present at maximal levels after 4 hours of induction (Figure D.5A,B,C, lanes 6) and were soluble (Figure D.5D,E,F, lanes 2). These overexpressed proteins bound to glutathione agarose beads and were successfully eluted with glutathione (Figure D.5D,E,F, lanes 8).

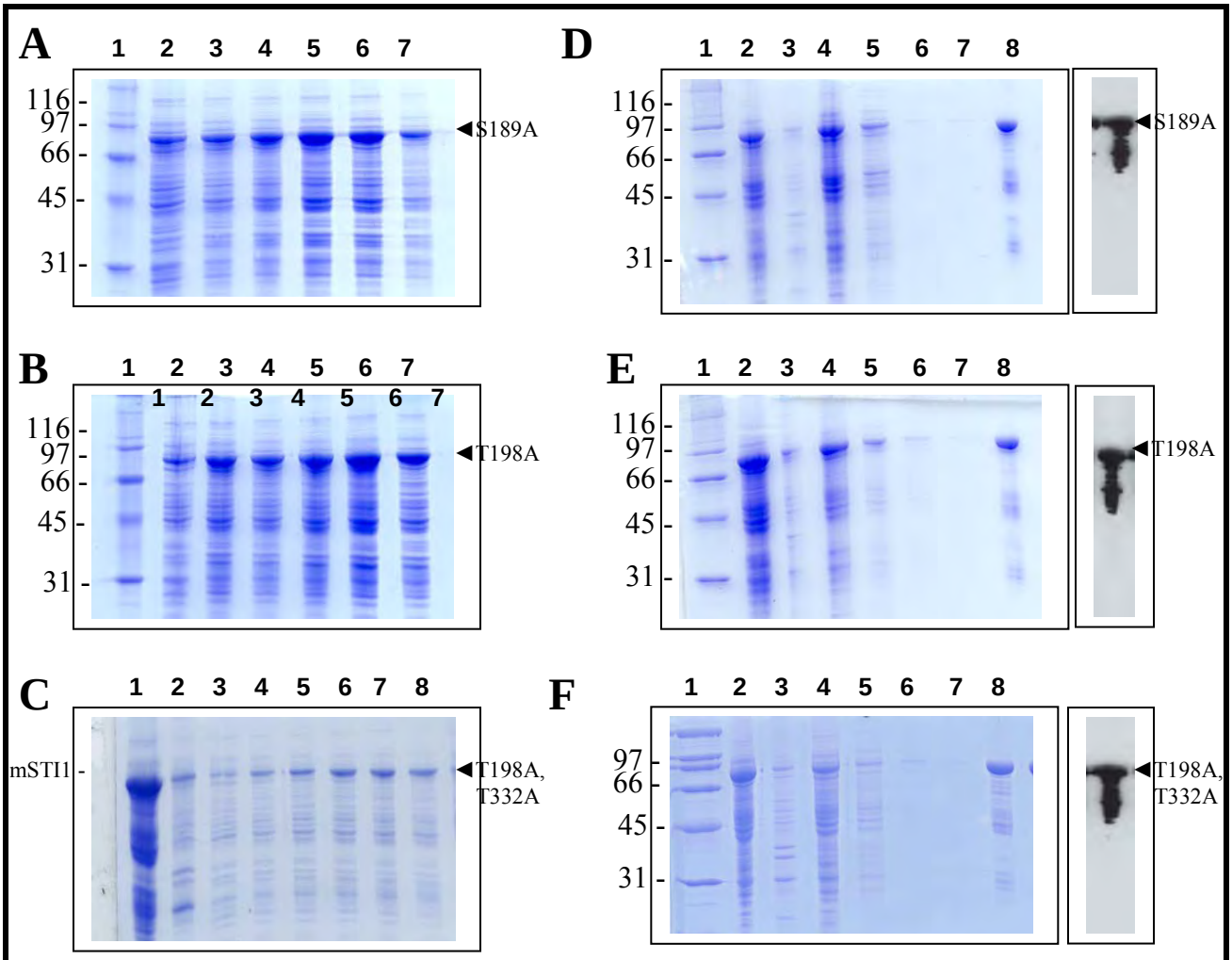

Figure D.5: Recombinant GST-mSTI1 derivatives were produced and purified

A (0.1%) SDS (12%) PAGE gel of whole IPTG induced logarithmic phase XL1Blue *E.coli* cells transformed with pGEX3X2000(S189A) (A), pG EX3X2000(T198A) (B) and pG EX3X2000(T198A,T332A) (c) c onfirmed t he presence of an overproduced 89 kDa protein. Samples were taken of the culture before induction (A, lane 2) and 1 hour (A, lane 3), 2 hours (A, lane 4), 3 hours (A, lane 5), 4 hours (A, lane 6) and 5 hours (A, lane 7) post-induction. GST-mSTI1 d erivative p rotein was p roduced at maximal l evels 3 -4 ho urs a fter induction (A, l anes 5 a nd 6). Overexpressed GST-mSTI1 derivative proteins were purified using glutathione agarose beads.
A (0.1%) SDS (12%) PAGE gel of the purification of GST from IPTG induced logarithmic phase XL1Blue *E.coli* cells transformed with pGEX3X2000(S189A) (D), pGEX3X2000(T198A) (E) and pGEX3X2000(T198A,T332A) (F) confirmed the presence of a purified 89 kDa protein. Soluble extract (lanes 2) was separated from insoluble extract (lanes 3) by centrifugation. Soluble extract was bound to the glutathione agarose beads and then discarded (C, lane 4). The beads were washed three times in PBS (lanes 5-7) and bound protein eluted with 5 mM glutathione (lanes 8). Lanes 1 of gels A, B, D, E and F contains separated Biorad Molecular weight markers. Lane 1 of gel C contains soluble extract with overexpressed mSTI1 as a marker.

The identity of GST-mSTI1 derivatives was confirmed by Western analysis (Figure D.5, insets). Total protein concentrations of elutions containing GST-mSTI1 was typically 25-42 μM, and estimated to be 80 % pure, while that of GST was typically 150 – 200 μM and estimated to be 90-100 % pure.

D.8 The production of mSTI1 derivative proteins

A 63 kDa protein corresponding to mSTI1, was overexpressed after IPTG induction of *E. coli* BL21[pET5a2000]. This protein were present at maximal levels after 4 hours of induction (Figure D.6A,B.C lanes 6), was soluble (Figure D.6E,F,G, lanes 2), and bound to a PBE polybuffer exchanger column at pH 8.0 (Figure D.6G). The 63 kDa proteins were successfully eluted with a 0.1M-0.3M NaCl gradient elution (Figure D.6), having been completely removed from the column as the regeneration fractions did not contain this 63 kDa protein. The identity of mSTI1 was confirmed by Western analysis (Figure D.6A, B , C insets). Total protein concentrations of elutions containing mSTI1, and derivatives, were typically 200 μM, and estimated to be 80 % pure.

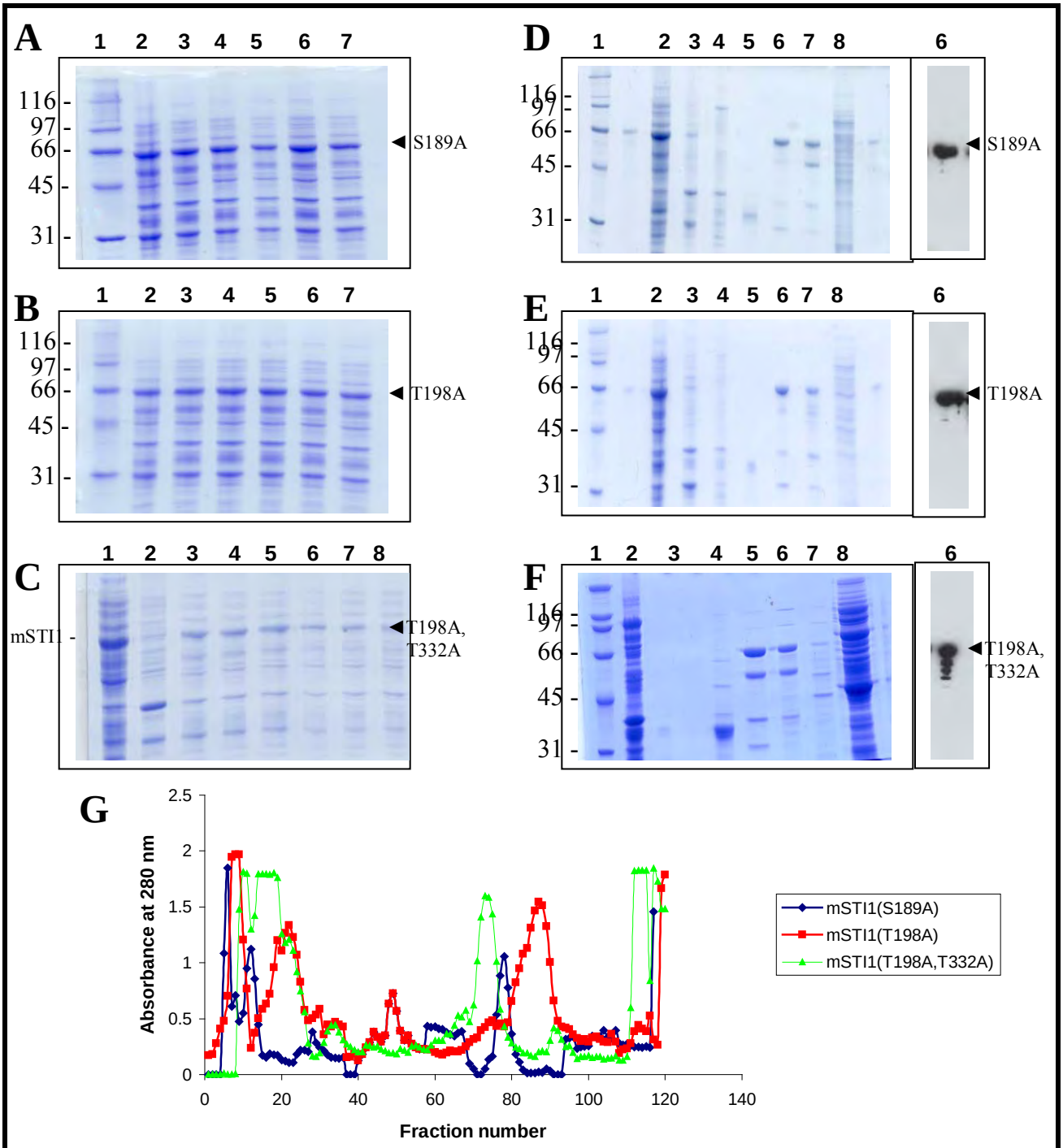

Figure D.6: Recombinant mSTI1 derivatives were produced and purified

A (0.1%) SDS (12%) PAGE gel of whole IPTG induced logarithmic phase XL1Blue *E.coli* cells transformed with pET5a2000 confirmed the presence of an overproduced 63 kDa protein. Samples were taken of the culture before induction (A, lane 2) and 1 hour (A, lane 3), 2 hours (A, lane 4), 3 hours (A, lane 5), 4 hours (A, lane 6) and 5 hours (A, lane 7) post-induction. mSTI1 was produced at maximal levels 3-4 hours after induction (A, lanes 5 and 6). IPTG induced logarithmic phase BL21 *E.coli*[pET5a2000] cell lysate, the column was separated through a PBE exchanger column.The column was washed stepwise with start buffer, followed by start buffer containing 0.1 M NaCl. An gradient elution of start buffer containing 0.1 M and 0.3 M NaCl was used to elute mSTI1, and the column stripped with start buffer containing 1 M NaCl. The 280 nm absorbance profile of eluted proteins was measured (B) and the 8 peaks collected were resolved by SDS PAG electrophoresis (C, lanes correspond to peaks). mSTI1 was enriched in peaks 5-6 (C, lane 7). Lanes 1 of both gels contain separated Biorad Molecular weight markers.

APPENDIX E

PLASMID VECTORS

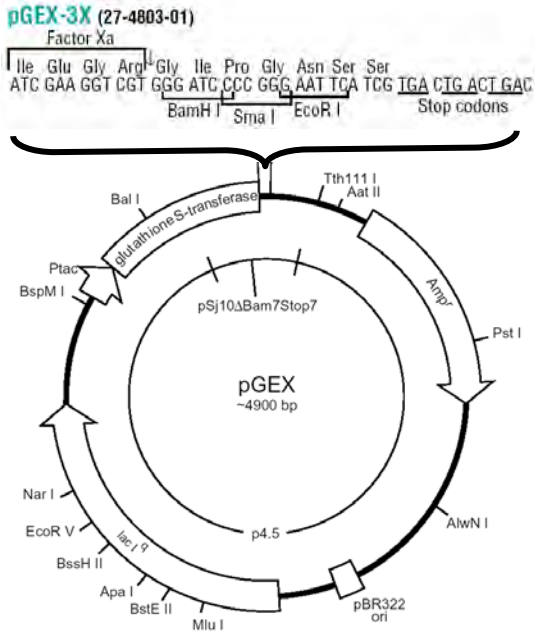

Figure E.1: The plasmid map of the plasmid vector pGEX3X from Amersham

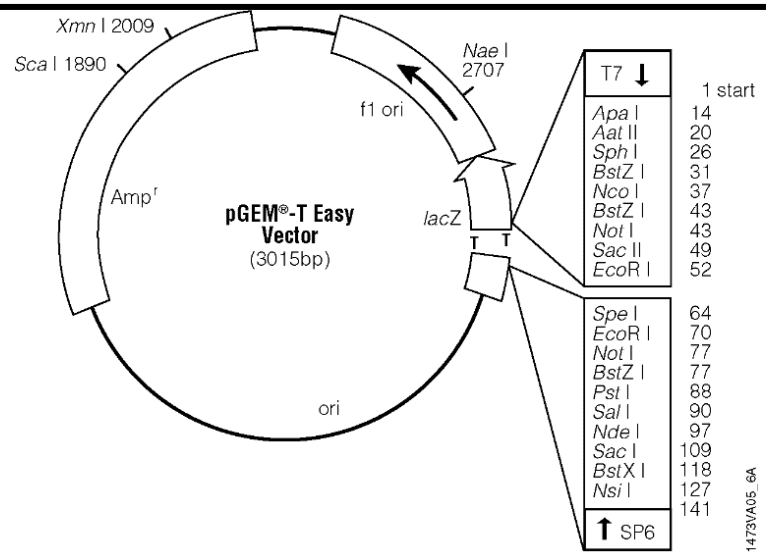

Figure E.2: The plasmid map of the plasmid vector pGEM(T)Easy from Promega

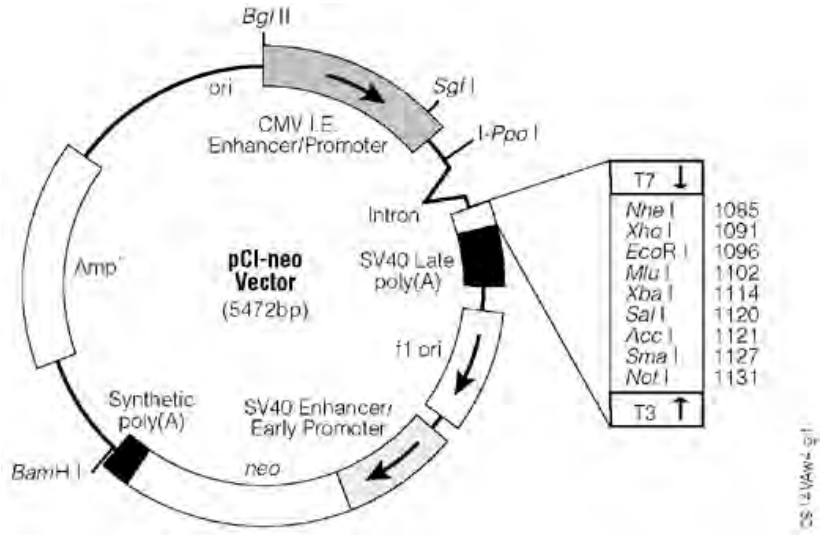

Figure E.3: The plasmid map of the plasmid vector pCineo from Promega

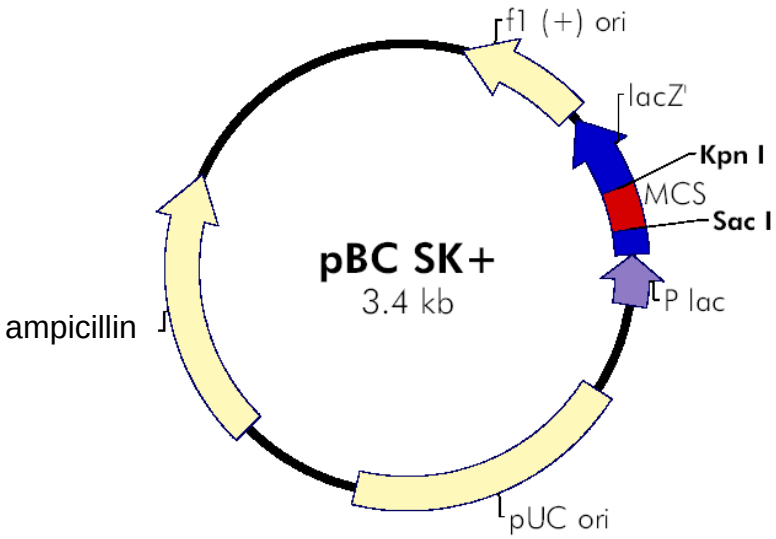

Figure E.4: The plasmid map of the plasmid vector pSK from Stratagene

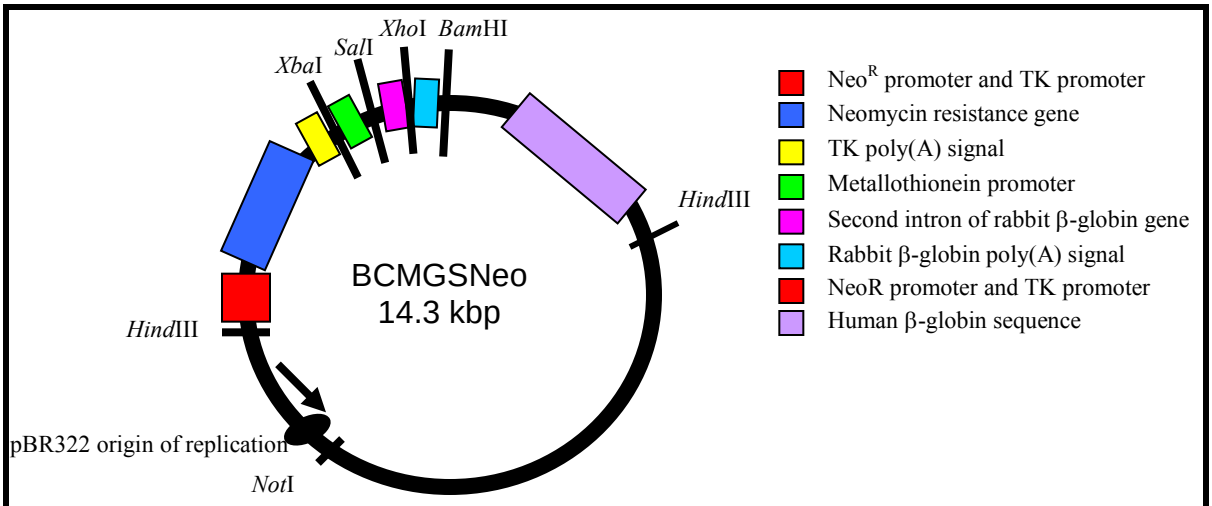

Figure E.5: The plasmid map of the plasmid vector BCMGSNeo (Karasuyama and Melchers, 1988)

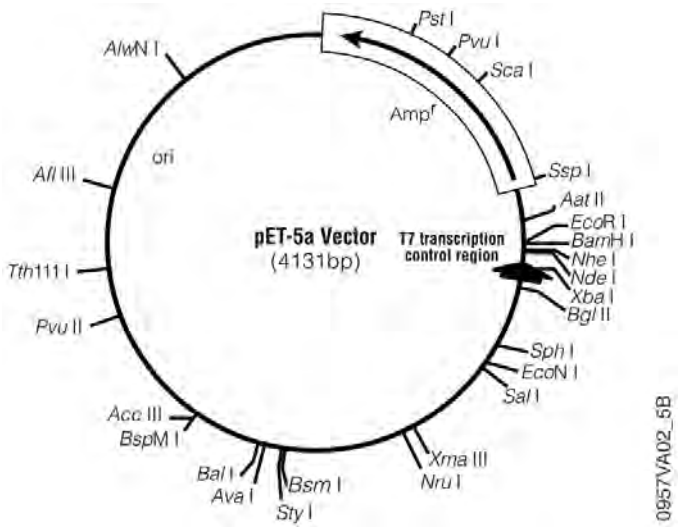

Figure E.6: The plasmid map of the plasmid vector pET5a from Promega

REFERENCES

Abbas-Terki, T., Briand, P.A., Donzé, O. and Picard, D. (2002) The Hsp90 co-chaperones cdc37 and STI1 interact physically and genetically. *Biol. Chem.* 383: 1335-1342

Abbas-Terki, T., Donz, O. and Picard, D. (2000) The molecular chaperone cdc37 is required for Ste11 function and pheromone-induced cell cycle arrest. *Febbs. Lett.* 467: 111-116

Abe, H., Nagaoka, R. and Obinata, T. (1993) Cytoplasmic localization and nuclear transport of cofilin in cultured myotubes. *Exp. Cell Res.* 206: 1-10

Abraham, R.T., Acquarone, M., Anderson, A., Asensi, A., Bellé, R., Berger, F., Bergounioux, C., Brunn, G., Buquet-Fagot, C., Glab, N., Goudeau, H., Goudeau, M., Guerrier, P., Houghton, P., Hendriks, H., Kloareg, B., Lippai, M., Marie, D., Maro, B., Meijer, L., Mester, J., Mulner-Lorillon, O., Poulet, S.A., Schierenberg, E., Schutte, B., Vaulot, D. and Verlhac, M.H. (1995) Cellular effects of olomoucine, an inhibitor of cyclin-dependent kinases. *Biol. Cell.* 83: 105-120

Adachi, Y. and Yanagida, D.G. (1989) Higher order chromosome structure is affected by cold-sensitive mutations in a Schizosaccharomyces pombe gene crm1+ which encodes a 115-kD protein preferentially localized in the nucleus and its periphery *J. Cell Biol.* 108: 1195-1207

Adam, S.A. (1999) Transport pathways of macromolecules between the nucleus and the cytoplasm. *Curr. Opin. Cell. Biol.* 11: 402-406

Adam, S.A., Sterne-Marr, R. and Gerace, L. (1990) Nuclear import in permeabilized mammalian cells requires soluble cytoplasmic factors. *J. Cell. Biol.* 111: 807-816

Adam, S.A., Sterne-Marr, R. and Gerace, L. (1991) *In vitro* nuclear protein import using permeabilized mammalian cells. *Methods Cell. Biol.* 35: 469-482

Agarraberes, F.A. and Dice, J.F. (2001) A molecular chaperone complex at the lysosomal membrane is required for protein translocation. *J. Cell Sci*. 114:2491-2499.

Aghdasi, B., Ye, K., Resnick, A., Huang, A., Ha, H.C., Guo, X., Dawson, T.M., Dawson, V.L. and Snyder, S.H. (2001) FKBP12, the 12-kDa FK506-binding protein, is a physiologic regulator of the cell cycle. *Proc. Natl. Acad. Sci. U.S.A.* 98: 2425-2430

Agutter, P.S. and Prochnow, D. (1994) Nucleocytoplasmic transport. *Biochem J.* 300: 609-618

Alam, J. and Cook, J.L. (1990) Reporter genes: application to the study of mammalian gene transcription. *Anal. Biochem.* 188: 245-254

Alberts, B., Bray, D., Lewis, J., Raff, M., Roberts, K. and Watson, J.D. (1994) Molecular Biology of the Cell (3rd edition), pp 860 - 892. Garland Publishing, Inc., New York.

Aligue, R., Akhavan-Niak, H. and Russell, P. (1994) A role for Hsp90 in cell cycle control: Wee-1 tyrosine kinase activity requires interaction with Hsp90. *EMBO J.* 13: 6099-6106

Allende, J.E. and Allende, C.C. (1995) Protein kinases. 4. Protein kinase CK2: an enzyme with multiple substrates and a puzzling regulation. *FASEB J.* 9:313-23.

Altschul, S.F., Gish, W., Miller, W., Myers, E.W., and Lipman, D. J. (1990) Basic local alignment search tool. *J. Mol. Biol.* 215: 403-410

Ananthan, J., Goldberg, A.L. and Voellmy, R. (1986) Abnormal proteins serve as eukaryotic stress signals and trigger the activation of heat shock genes. *Science* 232: 252-254

Ausubel, F.M., Brent, R., Kingston, R.E., Moore, D.D., Seidman, J.G., Smith, J.A. and Struhl, K. (1987-1999) Current protocols in Molecular Biology. pp 16.1.1-16.4.5, 16.7.1-16.7.7. John Wiley and Sons Inc. U.S.A

Bar-sagi, D. (2001) A Ras by any other name. *Mol. Cell. Biol.* 21: 1441-1443

Basso, A.D., Solit, D.B., Chiosis, G., Giri, B., Tsichlis, P. and Rosen, N. (2002) Akt forms an intracellular complex with heat shock protein 90 (Hsp90) and Cdc37 and is destabilized by inhibitors of Hsp90 function. *J. Biol. Chem.* 277: 39858-39866

Becker, J. and Craig, E.A. (1994) Heat-shock proteins as molecular chaperones. *Eur. J. Biochem.* 219: 11-23

Beckmann, R.P. Mizzen, L.A. and Welch, W.J. (1990) Interaction of hsp70 with newly synthesized proteins: implication for protein folding and assembly. *Science* 248: 850-853.

Beissinger, M. and Buchner, J. (1998) How chaperones fold proteins. *Biol. Chem.* 79: 245-259

Bercovich, B., Stancovski, I., Mayer, A., Blumenfeld, N., Laszlo, A., Schwartz, A.L. and Ciechanover, A. (1997) Ubiquitin-dependent degradation of certain protein substrates in vitro requires the molecular chaperone Hsc70. *J. Biol. Chem.* 272: 9002-9010.

Berger, J. Hauber, R., Gieger, R., and Cullen, B. R. (1988) Secreted placental alkaline phosphatase: a powerful new quantitative indicator of gene expression in eukaryotic cells. *Gene* 66: 1-10

Berra, E., Diaz-Meco, M.T., Dominguez, I., Municio, M.M., Sanz, L., Lozano, J., Chapkin, R.S. and Moscat, J. (1993) Protein kinase C zeta isoform is critical for mitogenic signal transduction. *Cell* 74: 555-563

Birnboim, H.C. and Doly, J. (1979) A rapid alkaline extraction procedure for screening recombinant plasmid DNA. *Nucleic Acids Res.* 7:1513-23.

Bischoff, F.R and Ponstingl, H. (1991) Catalysis of guanine nucleotide exchange on Ran by the mitotic regulator RCCI. *Nature* 354: 80-82

Bischoff, F.R., Klebe, C., Kretchmer, J., Wittinghofer, A. and ponstingl, H. (1994) RanGAPI induces GTPase activity of nuclear ras-related Ran. *Proc. Natl. Acad. Sci. U.S.A.* 91: 2587-2591

Bischoff, J.R., Friedman, P.N., Marshak, D.R., Prives, C. and Beach, D. (1990) Human p53 is phosphorylated by p60-cdc2 and cyclin B-cdc2. *Proc. Natl. Acad. Sci. U.S.A.* 87: 4766-4770

Blatch, G.L. and Lässle, M. (1999) The tetratricopeptide repeat: a structural motif mediating protein-protein interactions. *Bioessays* 21: 932-939

Blatch, G.L., Lässle, M., Zetter, B.R. and Kundra, V. (1997) Isolation of a mouse cDNA encoding mSTI1, a stress-inducible protein containing the TPR motif. *Gene* 194: 277-282

Blond-Elguindi, S., Cwirla, S.E., Dower, W.J., Lipshutz, R.J., Sprang, S.R., Sambrook, J.K. and Gething, M.J.H. (1993) Affinity panning of a library of peptides displayed on bacteriophages reveals the binding specificity of BiP. *Cell* 75: 717-728

Bloom, G.S. and Goldstein, L.S.B. (1998)Cruising along microtubule highways: how membranes move through the secretory pathway. *J. Biol. Chem.* 140: 1277-1280

Boguski, M.S., Sikorski, R.S., Hieter, P., and Goebl, M. (1990) Expanding family. *Nature* 346: 114

Bole, D.G., Hendershot, L.M. and Kearney, J.F. (1986) Post-translational association of immunoglobulin heavy chain binding protein with nascent heavy chains in non-secreting and secreting hybridomas. *J. Cell Biol.* 102: 1558-1566.

Bonifaci, N., Moroianu, J., Radu, A. and Blobel, G. (1997) Karyopherin beta2 mediates nuclear import of a mRNA binding protein. *Proc. Natl. Acad. Sci. USA* 94: 5055

Boone, A.N., Ducouret, B. and Vijayan, M.M. (2002) Glucocorticoid-induced glucose release is abolished in trout hepatocytes with elevated Hsp70 content. *J. Endocrinol.* 172: R1-5

Borkovich, K.A., Farrelly, F.W., Finkelstein, D.B., Taulien, J. and Lindquist, S. (1989) Hsp82 is an essential protein that is required in higher concentrations for growth of cells at higher temperatures. *Mol. Cell Biol.* 9: 3919-3930

Bose, S., Weikl, W., Bugl, H., and Buchner, J. (1996) Chaperone function of Hsp90 associated proteins. *Science* 274: 1715-1717

Bowie, J.U., Luthy, R. and Eisenberg, D. (1991) A method to identify protein sequences that fold into a known three-dimensional structure. *Science* 253:164-170

Bradford, M. (1976) A rapid and sensitive method for the quantification of microgram quantities of protein untilizing the principle of protein-dye binding. *Anal. Biochem.* 72: 248

Breeuwer, M. and Goldfarb, D.S. (1990) Facilitated nuclear transport of histone H1 and other small nucleophilic proteins. *Cell* 60: 999-1008

Brennan, J.A., Volle, D.J., Chaika, O.V. and Lewis, R.E. (2002) Phosphorylation regulates the nucleocytoplasmic distribution of kinase suppressor of Ras. *J. Biol. Chem.* 277: 5369-5377

Brewer, J., Hendershot, L.M., Sherr, C.J. and Diehl, J.A. (1999) Mammalian unfolded protein response inhibits cyclin D1 translation and cell cycle progression. *Proc. Natl. Acad. Sci. USA* 96: 8505-8510

Briggs, L.J., Johnstone, R.W., Elliot, R.M., Xiao, C.Y., Dawson, M., Trapani, J.A. and Jans, D.A. (2001) Novel properties of the protein kinase CK2-site-regulated nuclear-localization sequence of the interferon-induced nuclear factor IFI 16. *Biochem. J.* 353: 69-77

Briggs, L.J., Stein, D., Goltz, J., Corrigan, V.C., Efthymiadis, A., Hübner, S. and Jans, D.A. (1998) The camp-dependent protein Kinase Site (Ser312) enhances dorsal nuclear import through facilitating nuclear localization sequence/importin interaction. *J. Biol. Chem.* 273: 22745-22752

Brinker, A., Scheuffler, C., von der Mülbe, F., Fleckenstein, B., Herrmann, C., Jung, G., Moarefi, I. and Hartl, U. (2002) Ligand discrimination by TPR domains. *J. Biol. Chem.* 277: 19265-19275

Bronstein, I., Fortin, J., Stanley, P.E., Stewart, G.S. and Kricka, L.J. (1994) Chemiluminescent reporter gene assays. *Anal. Biochem.* 219: 169-181

Buchner, J. (1999) Hsp90 and co-a holding for folding. *TIBS* 24: 136 - 141

Bunnell, S.C., Hong, D.I., Kardon, J.R., Yanazaki, T., Mc Glade, C.J., Barr, V.A. and Samelson, L.E. (2002) T cell receptor ligation induces the formation of dynamically regulated signalling assemblies. *J. Cell Biol.* 158: 1263-1275

Cai, B., Tomida, A., Mikami, K., Nagata, K. and Tsuruo, T. (1998) Down regulation of epidermal growth factor receptor-signalling pathway by binding of Grp78 / BiP to the receptor under glucose starved stress conditions. *J. Cell Physiol.* 177: 282-288

Carey, K.L., Richards, S.A., Lounsbury, K.M. and Macara, I.G. (1996) Evidence using a green fluorescent protein-glucocorticoid receptor chimera that the RAN/TC4GTPase mediates an essential function independent of nuclear protein import. J. Cell Biol. *133: 985-996*

Castoria, G., Barone, M.V., Domenico, M.D., Bilancio, A., Ametrano, D., Migliaccio, A. and Auricchio, F. (1999) Non-transcriptional action of oestradiol and progestin triggers DNA synthesis. *EMBO J.* 18: 2500-2510

Cato, A.C. and Mink, S. (2001) Bag1 family of cochaperones in the modulation of nuclear receptor action. *J. Steroid Biochem. Mol. Biol.* 78: 379-388

Chalfie, M., Tu, Y., Euskirchen, G., Ward, W.W. and Prasher, D.C. (1994) Green fluorescent protein as a marker for gene expression. *Science* 263, 802-805

Chatterjee, S. and Stochaj, U. (1996) Monitoring nuclear transport in HeLa cells using the green fluorescent protein. *Biotechniques* 21: 62-63

Chatterjee, S., Javier, M. and Stochaj, U. (1997) *In vivo* analysis of nuclear protein traffic in mammalian cells. *Exp. Cell Res.* 236: 346

Chaufour, S., Mehlen, P. and Arrigo, A.P. (1996) Transient accumulation, phosphorylation and changes in the oligomerization of Hsp27 during retinoic acid-induced differentiation of Hl-60 cells: possible role in the control of cellular growth and differentiation. *Cell Stress Chap.*1: 225-235.

Chen, C.F., Chen, Y. and Dai, K., Chen, P.L., Riley, D.J. and Lee, W.H. (1996a) A new member of the Hsp90 family of molecular chaperones interacts with the retinoblastoma protein during mitosis and after heat shock. *Mol. Cell. Biol.* 16: 4691-4699

Chen, C.W. and Thomas, C.A. Jr. (1980) Recovery of DNA segments from agarose gels. *Anal. Biochem.* 101: 339-41

Chen, S., Prapapanich, V., Rimerman, R.A. Honoré, B., and Smith, D.F. (1996b) Interactions of p60, a mediator of progesterone receptor assembly, with heat shock proteins hsp90 and hsp70. *Mol. Endocrinol.* 10: 682-693

Cheng, L., Fu, J., Tsukamoto, A. and Hawley, R.G. (1996) Use of the green fluorescent protein variants to monitor gene transfer and expression in mammalian cells. *Nature Biotechnology* 14: 606-609

Chevalier, M., Rhee, H., Elguindi, C. and Blond, S.Y. (2000) Interaction of murine BiP/GRP78 with the DnaJ homologue MTJ1. *J. Biol. Chem.* 275: 19620-19627

Chiang, H.L., Terlecky, S.R., C.P. Plant, and Dice, J.F. (1989) A role for a 70 kDa heat shock protein in lysosomal degradation of intracellular proteins. *Science* 24: 382-385

Chiocchetti, A., Tolosano, E., Hirsch, E., Silengo, L. and Altruda, F. (1996) Green fluorescent protein as a reporter of gene expression in transgenic mice. *Biochim Biophys Acta* 1352: 193-202

Chiu, W.L., Niwa, Y., Zeng, W., Hirano, T., Kobayashi, H., and Sheen, J. (1996) Engineered GFP as a vital reporter in plants. *Current Biology* 6: 325-330

Chook, Y. and Blobel, G. (2001) Karyopherins and nuclear import. *Curr. Opin. Struc. Biol.* 11: 703-715

Chou, P.Y. and Fasman, G.D. (1974) Prediction of protein conformation. *Biochemistry* 13: 222-245

Chou, P.Y. and Fasman, G.D. (1978) Empirical predictions of protein conformation. *Ann. Rev. Biochemistry* 47: 251-276

Choy, J.S. and Kron, S.J. (2002) NuA4 subunit Yng2 function in intra-S-phase DNA damage response. *Mol. Cell Biol.* 22: 8215-8225

Clothia, A.B. (1992) Proteins. One thousand families for the molecular biologist. *Nature* 357: 543-544

Conti, E. and Izaurralde, E. (2001) Nucleocytoplasmic transport enters the atomic age. *Curr. Opin. Cell Biol.* 13: 310-319

Cormack, B.P., Bertram, G., Egerton, M., Gow, N.A.R., Falkow, S. and brown, A.J.P. (1997) Yeast-enhanced green fluorescent protein (yEGFP): a reporter of gene expression in *Candida albicans*. *Microbiology* 143: 3.3-311

Cormack, B.P., Valdivia, R.H. and Falkow, S. (1996) FACS-optimized mutants of the green fluorescent protein (GFP). *Gene.*173: 33-38

Corpet, F. (1988) Multiple sequence alignment with heirarchical clustering. *Nucl. Acids. Res*. 16 10881-10890

Creighton, T.E. (1988) Towards a better understanding of protein folding pathways. *Proc. Natl. Acad. Sci. U.S.A.* 85: 5082-5086

Critchfield, J.W., Coligan, J.E., Folks, T.M. and Butera, S.T. (1997) Casein kinase II is a selective target for HIV-1 transcriptional inhibitors. *Proc. Natl. Acad. Sci. USA* 94: 6110-6115

Csermely, P., Schaider, T. and Szántó, I. (1995) Signalling and transport through the nuclear membrane. *Biochim. Biophys. Acta* 1241: 425

Cubitt, A.B., Heim, R., Adams, S.R., Boyd, A.E., Gross, L.A. and Tsien, R.Y. (1995) Understanding, improving and using green fluorescent proteins. *TIBS* 20: 448-455

Cvoro, A. and Matic, G. (2002) Hyperthermic stress stimulates the association of both constitutive and inducible isoforms of 70 kDa heat shock protein with rat liver glucocorticoid receptor. *Int. J. Biochem. Cell Biol.* 34: 279-285

Cyr, D.M., Lu, X. and Douglas, M.G. (1992) Regulation of Hsp70 function by a eukaryotic DnaJ homologue. *J. Biol. Chem.* 267: 20927-20931

Das, A.K., Cohen, P.T.W. and Barford, D. (1998) The structure of the tetratricopeptide repeats of protein phosphatase 5: implications for TPR-mediated protein-protein interactions. *EMBO J.* 17: 1192-1199

David-Pfeuty, T., Nouvian-Dooghe, Y., Sirri, V., Roussel, P., Hernandez-Verdun, D. (2002) Common and reversible regulation of wild-type p53 function and of ribosomal biogenesis by protein kinases in human cells. *Oncogene* 20: 5951-5963

Davies, T.H., Ning, Y.M. and Sanchez, E.R. (2002) A new first step in activation of steroid receptors. *J. Biol. Chem.* 277; 4597-4600

Davis, L.I. (1995) The nuclear pore complex. *Ann. Rev. Biochem.* 64: 865-896

De Bondt, H.L., Rosenblatt, J., Jancarik, H.D., Morgan, D.O. and Kim, S.H. (1993) Crystal structure of cyclin - dependent kinase 2. *Nature* 363: 595-602

De Wet, J.R., Wood, K.V., DeLuca, M., Helinski, D.R. and Subramani, S. (1987) Firefly luciferase gene: structure and expression in mammalian cells. *Mol. Cell Biol.* 7: 725-737

DeFranco, D.B. (2000) Role of molecular chaperones in subcellular trafficking of glucocorticoid receptors. *Kidney Int.* 57: 1241-1249

DeFranco, D.B. (2002) Navigating steroid hormone receptors through the nuclear compartment. *Mol. Endocrinol.* 16: 1449-1455

DeFranco, D.B., Madan, A.P., Tang, Y., Chandran, U.R., Xiao, N. and Yang, J. (1995) Nucleocytoplasmic shuttling of steroid receptors. *Vitam. Horm.* 51: 315-338

Dingwall, C. and Laskey, R.A. (1991) Nuclear targeting sequences-a consensus? *Trends Biochem. Sci.* 16: 478-481

Dingwall, C., Robbins, J., Dilworth, S.M., Roberts, B. and Richardson, W.D. (1988) The nucleoplasmin nuclear localization sequence is larger and more complex than that of SV40 large T-antigen. *J. Cell Biol.* 107: 841-849

Dingwall, C., Sharnick, S.V. and Laskey, R.A. (1982) A polypeptide domain that specifies migration of nucleoplasmin into the nucleus. *Cell* 30: 449-458

Dittmar, K.D. and Pratt, W.B. (1997) Folding of the glucocorticoid receptor by the reconstituted Hsp90-based chaperone machinery. *J. Biol. Chem.* 272: 13047-13054

Dittmar, K.D., Demady, D.R., Stancato, L.F., Krishna, P. and Pratt, W.B. (1997) Folding of the glucocorticoid receptor by the heat shock protein (hsp) 90-based chaperone machinery. The role of p23 is to stabilise receptor.hsp90 heterocomplexes formed by hsp90.p60.hsp70. *J. Biol. Chem.* 272: 21213-21220

Dobson, S.P., Livingstone, C., Gould, G.W. and Tavaré, J.M. (1996) Dynamics of insulin-strimulated translocation of GLUT4 in single living cells visualized using green fluorescent protein. *FEBS Lett* 393:179-184

Drubin, D.G. and Nelson, W.J. (1996) Origin of cell polarity. *Cell* 84: 335-344

Dunphy, W.G. and Newport, J.W. (1988) Unraveling of mitotic control mechanisms. *Cell* 55: 925-928

Duverger, E., Carpentier, V., Roche, A.C. and Monsigny, M. (1993) Sugar-dependent nuclear import of glycoconjugates is distinct from the classical NLS pathway. *Exp. Cell Res.* 207: 197-201

Edington, B.V., Whelan, S.A., Hightower, L.E. (1989) Inhibition of heat shock (stress) protein induction by deuterium oxide and glycerol: Additional support for the abnormal protein hypothesis of induction. *J. Cell Physiol.* 139: 219-228.

Efthymiadis, A., Shao, H., Hubner, S. and Jans, D.A. (1997) Kinetic characterization of the human retinoblastoma protein bipartite nuclear localization sequence *in vivo* and *in vitro*: a comparison with the SV40 large T-antigen NLS. *J. Biol. Chem.* 272: 22134-22139

Ellis, R.J. and van der Vies, S.M. (1991) Molecular chaperones. *Ann. Rev. Biochem.* 60: 321-347

Emini, E., Hughes, J.V., Perlow, D.S., and Boger, J. (1985) Induction of hepatitis A virus-neutralizing antibody by a virus specific synthetic peptide. *J. Virol.* 55: 836-839

Engel, K., Kotlyarov, A. and Gaestel, M. (1998) Leptomycin B-sensitive nuclear export of MAPKAP 2 kinase 2 is regulated by phosphorylation. *EMBO J.* 17: 3363-3371

Fabre, E. and Hurt, E.C. (1994) Nuclear transport. *Curr. Opin. Cell Biol.* 6: 335-342

Falk, M. (2002) Genetic tags for labelling live cells: gap junctions and beyond. *Trends Cell Biol.* 12: 399

Fangan, B.M., Dahlberg, O.J., Deggerdal, A.H., Bosnes, M. and Larsen, F. (1999) Automated system for purification of dye-terminator sequencing products eliminates up-stream purification of templates. *Biotechniques*. 26: 980-983

Feldherr, C.M. and Akin, D. (1990) The permeability of the nuclear envelope in dividing and non-dividing cell cultures. *J. Cell Biol.* 111: 1-8

Feldherr, C.M. and Akin, D. (1993) Regulation of nuclear transport in proliferating and quiescent cells. *Exp. Cell Res.* 205: 179-186

Feldherr, C.M., Kallenbach, E. and Schultz, N. (1984) Movement of a karyophilic protein through the nuclear pores of oocytes. *J.Cell Biol.* 99: 2216-2222

Fischer, U., Huber, J., Boelens, W.C., Mattaj, I.W. and Luhrmann, R. (1995) The HIV-1 Rev activation domain is a nuclear export signal that accesses and export pathway used by specific cellular RNAs. *Cell* 82: 475-483

Fischer-Fantuzzi, L. and Vesco, C. (1988) Cell-dependant efficiency of reiterated nuclear signals in a mutant simian virus 40 oncoprotein targeted to the nucleus. *Mol. Cell Biol.* 8: 5495-5503

Flaherty, K.M., DeLuca, C. and McKay, D.B. (1990) Three-dimensional structure of the ATPase fragment of a 70 kDa heat-shock cognate protein. *Nature* 346: 623 - 628

Flynn, G.S., Rohl, J., Flocco, M.T., and Rothman, J.E. (1991) Peptide binding specificity of the molecular chaperone BiP. *Nature* 353: 726-730

Fontes, M.R., Teh, T. and Kobe, B. (2000) Structural basis of recognition of monopartite and bipartite nuclear localization sequences by mammalian importin-alpha. *J. Mol. Biol.* 297: 1183-1194

Fornerod, M., Ohno, M., Yoshida, M., Mattaj, I.W. (1997) CRM1 is an export receptor for leucine-rich nuclear export signals. *Cell* 90: 1051-1060

Forsythe, H.L., Jarvis, J.L., Turner, J.W., Elmore, L.W. and Holt, S.E. (2001) Stable association of Hsp90 and p23, but not Hsp70, with active human telomerase. *J. Biol. Chem.* 276: 15571-15574

Freeman, B.C. and Yamamoto, K.R. (2002) Disassembly of transcriptional regulatory complexes by molecular chaperones. *Science* 296: 2232-2235

Freeman, B.C., Toft, D.O., Morimoto, R.I., (1996) Molecular chaperone machines: chaperone activities of the cyclophilin CyP40 and the steroid aporeceptor - associated protein p23. *Science* 274: 1718-1720

Fridell, R.A., Truant, R., Thorne, L., Benson, R.E. and Cullen, B.R. (1997) Nuclear import of hnRNP A1 is mediated by a novel cellular cofactor related to karyopherin-beta. *J. Cell Sci.* 110: 1325

Fritz, G. and Kaina, B. (1999) Phosphorylation of the DNA repair protein APE/REF-1 by CKII affects redox regulation of AP-1. *Oncogene* 18: 1033-1040

Frydman, J. (2001) Folding of newly translated proteins *in vivo*: The role of molecular chaperones. *Annu. Rev. Biochem.* 70: 603-47

Fujii, G., Tsuchiya, R., Ezoe, E. and Hirohashi, S. (1999) Analysis of nuclear localization signals using a green fluorescent protein-fusion protein library. *Exp. Cell Res.* 251: 299-306

Fukuda, M., Asano, S., Nakamura, T., Adachi, M., Yashinda, M. and Yanagida, M. (1997) CRM1 is responsible for intracellular transport mediated by the nuclear export signal. *Nature* 390: 308-311

Fukuda, M., Gotoh, I., Gotoh, Y. and Nishida, E. (1996) Cytoplasmic localization of mitogen-activated protein kinase kinase directed by its NH_2-terminal, leucine rich short amino acid sequence, which acts as a nuclear export signal. *J. Biol. Chem.* 271: 20024-20028

Gadbois, D.M., Hamaguchi, J.R., Swank, R.A. and Bradbury, E.M. (1992) Staurosporine is a potent inhibitor of p34cdc2 and p34cdc2-like kinases.*Biochem. Biophys. Res. Commun.* 184:80-85

Galea-Lauri, J., Latchman, D.S. and Katz, D.R. (1996) The role of the 90 kDa heat shocl protein in cell cycle control and differentiation of the monoblastoid cell line U937. *Exp. Cell Res.* 226: 243-254

Galigniana, M.D., Radanyi, C., Renoir, J.M., Housley, P.R. and Pratt, W.B. (2001) Evidence that the peptidylprolyl isomerase domain of the hsp90-binding immunophilins FKBP52 is involved in both dynein interaction and glucocorticoid receptor movement to the nucleus. *J. Biol. Chem.* 276: 14884-14889

Galigniana, M.D., Scruggs, J.L., Herrington, J., Welsh, M.J., Carter-Su, C., Housley, P.R. and Pratt, W.B. (1998) Heat shock-protein 90-dependent (geldamycin-inhibited) movement of the glucocorticoid receptor through the cytoplasm to the nucleus requires intact cytoskeleton. *Mol. Endocrinol.* 12: 1908-1913

Garcia-Bustos, J., Heitman, J. and Hall, M.N. (1991) Nuclear protein translocation. *Biochem. Biophys. Acta* 1071: 83-101

Garcia-Mata, R., Bebok, Z.Sorscher, E.J., Sztul, E.S. (1999) Characterization and dynamics of aggresome formation by a cytosolic GFP-chimera. *J. Cell Biol.* 146: 1239-1254

Garnier, J., Osguthorpe, D.J., and Robson, B. (1978) Analysis of the accuracy and implications of simple methods for predicting the secondary structure of globular proteins. *J. Mol. Biol.* 120: 97-120

GeneTools version 1.0, Biotools Incorporated (2002) (Canada)

Georgopoulos, C. and Welch, W.J. (1993) Role of the major heat shock proteins as molecular chaperones. *Ann. Rev. Cell Biol.* 9: 601-634

Gerace, L. (1995) Nuclear export signals and the fast track to the cytoplasm. *Cell* 82: 341-344

Gerber, D.A., Souquere-Besse, S., Purion, F., Dubois, M.F., Bensuade, O. and Cochett, C. (2000) Heat-induced relocalization of protein kinase CK2. 275: 23919-23926

Gibbs, A.J., and McIntyre, G.A. (1970) The diagram, a method for comparing sequences. Its use with amino acid and nucleotide sequences. *Eur. J. Biochem*. 16:1-11

Gibrat, J.F., Garnier, J. and Robson, B. (1987) Further developments of protein secondary structure prediction using information theory. New parameters and consideration of residue pairs. *J. Mol. Biol.* 198: 425-443

Gibrat, J.F., Madej, T., and Bryant, S.H. (1996) Surprising similarity in structure comparison. *Curr Opin. Struc, Biol*. 6: 377-385

Gilmore, T.D. and Temin, H.M. (1988) v-Rel oncoproteins in the nucleus and cytoplasm of transformed chicken spleen cells. *J. Virol.* 62: 733-741

Goldberg, M.W. and Allen, T.D. (1995) Structural and functional organization of the nuclear envelope. *Curr. Opin. Cell Biol.* 7: 301-309

Goldfarb, D.S., Gariépy, J., Schoolnik, G. and Kornberg, R.D. (1986) Synthetic peptides as nuclear localization signals. *Nature* 322: 641-644

Görlich, D. and Kutay, U. (1999) Transport between the cell nucleus and the cytoplasm. *Ann. Rev. cell Dev. Biol.* 15: 607-660

Görlich, D. and Mattaj, I.W. (1996) Nucleocytoplasmic transport. *Science* 271:1513-1518

Gorman, C.M., Moffat, L.G. and Howard, B.H. (1982) Recombinant genomes which express chloramphenicol acetyltransferase in mammalian cells. *Mol. Cell Biol.* 2: 1044-1051

Greene, L.E., Zinners, R., Naficy, S. and Eisenberg, E. (1995) Effect of nucleotide on the binding of peptides to the 70 kDa heat shock protein. *J. Biol. Chem.* 270: 2967-2973

Guex, N. and Peitsch, M.C. (1997) Swiss-model and the swiss-pdbviewer: An environment for comparative protein modeling. *Electrophoresis* 18: 2714-2723

Haas, J., Park, E.C. and Seed, B. (1996) Codon usage limitation in the expression of HIV-1 envelope glycoprotein. *Current Biology* 6: 315-325

Hall, N.M., Hereford, L. and Herskowitz, I. (1984) Targeting of *E. coli* beta-galactosidase to the nucleus in yeast. *Cell* 36: 1057-1065

Hanaka, H., Shimizu, T. and Izumi, T. (2002) Nuclear-localization-signal-dependent and nuclear-export-signal-dependent mechanisms determine the localization of 5-lipoxygenase. *Biochem J.* 361: 505-514

Hang, H. and Fox, M.H. (1995) Cell cycle variations of Hsp70 levels in HeLa cells. *J. Cell Physiol.* 165: 367-375

Hang, H. and Fox, M.H. (1995) Expression of hsp70 induced in CHO cells by 45.0C hyperthermia is cell cycle associated and DNA synthesis dependent. *Cytometry*. 19:119.

Harootunian, A.T., Adams, S.R., Wen, W., Meinkoth, J.L., Taylor, S.S. and Tsien, R.Y. (1993) Movement of the free catalytic subunit of cAMP-dependent protein kinase into and out of the nucleus can be explained by diffusion. Mol. Biol. *Cell* 4: 993-1002

Hartl, F.U. (1996) Molecular chaperones in cellular protein folding. *Nature* 381: 571-580

Hartwell, L.H. and Weinert, T.A. (1989) Checkpoints: Controls that ensure the order of cell cycle events. *Science* 246: 629-634

Heim, R., Cubitt, A.B. and Tsien, R.Y. (1995) Improved green fluorescence. *Nature* 373: 663-664

Helmbrecht, K. and Rensing, L. (1999) Differential constitutive heat shock protein 70 expression during proliferation and differentiation of rat C6-glioma cells. *Neurochem. Res.* 24: 1293

Helmbrecht, K. Zeise, E. and Rensing, L. (2000) Chaperones in cell cycle regulation and mitogenic signal transduction: a review. *Cell Prolif.* 33:341-365.

Hendriks and Matthews (1998) *JBC* 273: 29519-29523

Henikoff, S. and Henikoff J.G (1992) Amino acid substitution matrices from protein blocks. *Proc. Natl. Acad. Sci. U.S.A*, 89: 10915-10919

Hennekes, H., Peter, M., Weber, K. and Nigg, E.A. (1993) Phosphorylation of protein kinase C sites inhibits nuclear import of Lamin B2. *J. Cell Biol.* 120: 1293-1304

Hernández, M.P., Sullivan, W.P. and Toft, D.O. (2002) The assembly and intermolecular properties of the hsp70-Hop-Hsp90 molecular complex. *J. Biol. Chem.* 277: 38294-38304

Heyduk, T. (2002) Measuring protein conformational changes by FRET/LRET. *Curr. Opin. Biotechnol.* 13: 292

Higgins, D.G. and Sharp, P.M. (1988) CLUSTAL: A package for performing multiple sequence alignment on a microcomputer. *Gene* 73:237-244

Higgins, D.G. Thompson, J.D., and Gibson, T.J. (1996) Using CLUSTAL for multiple sequence alignments. *Methods Enzymol.* 266: 383-402

Hightower, L.E. (1980) Cultured cells exposed to amino acid analogues or puomycin rapidly synthesize several polypeptides. *J. Cell Physiol.*, 102: 407-24

Hightower, L.E. (1991) Heat shock, stress proteins, chaperones, and proteotoxicity. *Cell* 66: 191-197

Hishino, H., Kobayashi, A., Yoshida, M., Kudo, N., Oyake, T., Motohashi, H., Hayashi, N., Yamamoto, M. and Igarashi, K. (2000) Oxidative stress abolishes leptomycin B-sensitive nuclear export of transcription repressor Bach2 that counteracts activation of Maf recognition element. *J. Biol. Chem.* 275: 15370-15376

Höfeld, J. Minami, Y. and Hartl, F.U. (1995) Hip, a new co-chaperone involved in the eukaryotic Hsc70/Hsp40 reaction cycle. *Cell* 83: 589-598

Höhfeld, J. (1998) Regulation of the heat shock cognate Hsc70 in the mammalian cell: the characterization of the anti-apoptotic protein BAG-1 provides novel insights. *Biol. Chem.* 379: 269-274

Honoré, B., Leffers, H., Madsen, P., Rasmussen, H.H., Vandekerekhove, J. and Celis, J.E. (1992) Molecular cloning and expression of a transformation-sensitive human protein containing the TPR motif and sharing identity to the stress-inducible yeast protein STI1. *J. Biol. Chem.* 267: 8485-8491

Hood, J.K. and Silver, P.A. (1999) In or out? Regulating nuclear transport. *Curr. Opin. Cell Biol.* 11: 241-247

Htun, H., Barsony, J., Renyi, I., Gould, D.I. and Hager, G.L. (1996) Visualization of glucocorticoid receptor translocation and intranuclear organization in living cells with a green fluorescent protein chimera. *Proc. Natl. Acad. Sci. USA* 93: 4845-4850

Hübner, S., Xiao, C.Y. and Jans, D.A. (1997) The protein kinase C K2 site (Ser111/112) enhances recognition of the simian virus 40 large T-antigen nuclear localization sequence by importin. *J. Biol. Chem.* 272: 17191-17195

Hunt, C. and Calderwood, S. (1990) Characterization and sequence of a mouse *Hsp70* gene and its expression in mouse cell lines. *Gene* 87:199-204.

Hunt, C., Parsian, A.J., Goswami, P.C. and Kozak, C.A. (1999) Characterization and expression of the mouse Hsc70 gene. *Biochim. Biophys. Acta* 1444: 315-325

Hunter, T. (1991) Protein kinase classification. *Methods Enzymol.* 200: 3-37

Imamoto, N., Matsuoka, Y., and Kurihara, T. (1992) Antibodies against 70-kDa heat shock cognate protein inhibit mediated nuclear import of karyopheric proteins. *J. Cell Biol.* 119: 1047 (check)

Imamoto, N., Shimaoto, T., Kose, S., Takao, T., Tachibana, T., Matsybae, M., Sekimoto, T., Shimonishi, Y. and Yoneda, Y. (1995) The nuclear pore-targeting complex binds to nuclear pores after association with a karyophile. *FEBS Lett.* 368: 415-419

Imamoto-Sonobe, N., Matsuoka, Y., Kurihara, T., Kohno, K., Miyagi, M., Sakiyama, F., Okada, Y., Tsunasawa, S. and Yoneda, Y. (1992) Antibodies to 70 kDa heat shock cognate protein inhibit mediated nuclear import of karyophilic proteins. *J. Cell Biol.* 119: 1047-1061

Inoue, A., Torigoe, T. and Sogahata, K., Kamiguchi, K., Takahashi, S., Sawada, Y., Saijo, M., Taya, Y., Ishii, S., Sato, N. *et al.* (1995) 70 kDa heat shock cognate protein interacts directly with the N-terminal region of the retinoblastoma gene product pRb. *J. Biol. Chem.* 270: 22571-22576

Inouye, S. and Tsuji, F.I. (1994) *Aequorea* green fluorescent protein: expression of the gene and fluorescence characteristics if the recombinant protein. *FEBS Lett* 341: 211-214

Izaurralde, E., Kutay, U., von Kobbe, C., Mattaj, I.W. and Görlich, D. (1997) The asymmetric distribution of the constituents of the Ran system is essential for transport into and out of the nucleus. *EMBO J.* 16: 6535-6547

Jaenicke, R. (1991) Protein folding: local structures, domains, subunits, and assemblies. *Biochemistry*, 30: 3147-3161

Jain, N., Mahendran, R., Philp, R., Guy, G.R., Tan, Y.H. and Cao, X. (1996) Casein kinase II associates with Egr-1 and acts as a negative modulator of its DNA binding and transcription activities in NIH 3T3 cells. *J Biol Chem* 271:13530-6.

Jakob, U., Gaestel, M., Engel, K., Buchner, J. (1993) Small heat shock proteins are molecular chaperones. *J. Biol Chem* 268: 1517-1520

James, P., Pfund, C. and Craig, E.A. (1997) Functional specificity among Hsp70 molecular chaperones. *Science* 275: 387 - 389

Janin, J., Wodak, S., Levitt, M. and Maigret, B. (1978) Conformation of amino acid side-chains in proteins. *J. Mol Biol.* 125: 357-386

Jans, D. A. and Hübner, S. (1996) Regulation of protein transport to the nucleus: central role of phosphorylation. *Physiol. Rev.* 76: 651-685

Jans, D.A. Ackermann, M., Bischoff, J.R., Beach, D.H. and Peters, R. (1991) p34cdc2 mediated phosphorylation at T124 inhibits nuclear import of SV40 T-antigen proteins. *J. Cell Biol.* 115: 1203-1212

Jans, D.A. and Jans, P. (1994) Negative charge at the casein kinase II site flanking the nuclear localization signal of the SV40 T-antigen is mechanistically important for enhanced nuclear import. *Oncogene* 9: 2961-2968

Jans, D.A., Ackermann, M., Bischoff, J.R., Beach, D.H. and Peters, R. (1991) $p34^{cdc2}$ mediated phosphorylation at T^{124} inhibits nuclear import of SV40 T-antigen proteins. *J. Cell Biol.* 115: 1203-1212

Jans, D.A., Moll, T., Nasmyth, K. and Jans, P. (1995) Cyclin-dependent kinase site-regulated signal-dependent nuclear localization of the SW15 yeast transcription factor in mammalian cells. *J. Biol. Chem.* 270: 17064-17067

Jans, D.A., Xiao, C.Y. and Lam, M.H. (2000) Nuclear targeting signal recognition: a key control point in nuclear transport? *Bioessays* 22: 532-544

Jefferson, R.A., Kavanagh, T.A. and Bevan, M.W. (1987)GUS fusions: beta-glucuronidase as a sensitive and versatile gene fusion marker in higher plants. *EMBO J.* 6: 3901-3907

Jeffry, P.D., Russo, A.A., Polyak, K., Gibbs, E., Hurwitz, J., Massague, J. and Pavletich, N.P. (1995) Mechanism of cdk activation revealed by the struture of a cyclin a - cdk2 complex. *Nature* 376: 313-320

Jérôme, Y., Vourc'h, C., Baulieu, E.E., Catelli, M.G. (1993) Cell cycle regulation of the chicken Hsp90a expression. *Exp. Cell Res.* 205: 44

Jin, P., Hardy, S. and Morgan, D.O. (1998) Nuclear localization of cyclin B1 controls mitotic entry after DNA damage. *J. Cell. Biol.* 141: 875-885

Johnson, B.D., Chadli, A., Felts, S.J., Bouhouche, I., Catelli, M.G. and Toft, D.O. (2000) Hsp90 chaperone activity requires the full-length protein and interaction among its multiple domains. *J. Biol. Chem.* 275: 32499-32507

Johnson, B.D., Schumacher, R.J., Ross, E.D., and Toft, D.O. (1998) Hop modulates Hsp70/Hsp90 interactions in protein folding. *J. Biol. Chem.* 273: 3679-3686

Johnson, J.L., and Toft, D.O. (1994) A novel chaperone complex for steroid receptors involving heat shock proteins, immunophilins and p23. *J. Biol. Chem.* 269: 24989-24993

Johnson, J.L., and Toft, D.O. (1995) Binding of p23 and hsp90 during assembly with the progesterone receptor. *Mol. Endocrinol.* 9: 670-678

Johnston, J.A., Ward, C.L. and Kopito, R.R. (1998) Aggresomes: a cellular response to misfolded proteins. *J. Cell Biol.* 143: 1883-1898

Johnston, L.H and Nasmyth, K.A. (1978) Saccharomyces cerevisiae cell cycle mutant cdc9 is defective in DNA ligase. *Nature* 274: 891

Joly, E. (1996) Preparation of plasmid DNA using alkaline lysis. *Methods Mol. Biol*. 58: 257-263

Jung, R., Scott, M.P., Olivera, L.O. and Nielsen, N.C. (1992) A simple and efficient method for the oligodeoxy ribo nucleotide-directed mutagenesis of double stranded DNA. *Gene* 121: 17-24

Kain, S.R., Adams, A., Kondepudi, T.T., Yang, T., Ward, W.W. and Kitts, P. (1995) Green fluorescent protein as a reporter of gene expression and protein localization. *Biotechniques*. 19: 650-655

Kakinoki, Y., Somers, J., Brautigan, D.L. (1997) Multisite phosphorylation and the nuclear localization of phosphatase inhibitor 2-green fluorescent protein fusion protein during S-phase of the cell growth cycle. *J. Biol. Chem.* 272: 32308-32314

Kalderon, D., Roberts, B.L., Richardson, W.D. and Smith, A.E. (1984) A short amino acid sequence able to specify nuclear location. *Cell* 39: 499-509

Kambach, C. and Mattaj, I.W. (1992) Intracellular distribution of the U1A protein depends on active transport and nuclear binding to U1 snRNA. *J. Cell Biol.* 118: 11-21

Kanelakis, K.C., Shewach, D.S. and Pratt, W.B. (2002) Nucleotide binding states of Hsp70 and hsp90 during sequential steps in the process of glutocorticoid receptor-Hsp90 heterocomplex assembly. *J. Biol. Chem.* 277: 33698-33703

Kang, K.I., Devin, D.J., Cadepond, F., Gibard, N., Guiochon-Mantel, A., Baulieu E.E. and Catelli, M.G. (1994) *In vivo* functional protein-protein interaction: nuclear targetted hsp90 shifts cytoplasmic steriod receptor mutants into the nucleus. *Proc. Natl. Acad. Sci. USA* 91: 340-344

Karasuyama, H. and Melchers, F. (1988) Establishment of mouse cell lines which constitutively secrete large quantities of interleukin 2, 3, 4 or 5, using modified cDNA expression vectors. *Eur. J. Immunol.* 18: 97-104

Kaul, S., Murphy, P.J.M., Chen, J., Brown, L., Pratt, W.B. and Simons, S.S. Jr. (2002) Mutations at positions 547-553 of rat glucocorticoid receptors reveal that Hsp90 binding requires the presence, but not defined composition, of a seven-amino acid sequence at the amino terminus of the ligand binding domain. *J. Biol. Chem.* 277: 36223-36232

Kawamura, H., Tomozoe, Y., Akagi, T., Kamei, D., Ochiai, M. and Yamada, M. (2002) Identification of the nucleocytoplasmic shuttling sequence of heterologous nuclear riconuceloprotein D-like protein JKTBP and its interaction with mRNA. *J. Biol. Chem.* 277: 2732-2739

Kelly, W.L. and Georgopoulos, C. (1992) Chaperones and protein folding, *Curr. Opin Cell Biol*. 4: 984-91

Kemp, B.E. and Pearson, R.B. (1990) Protein kinase recognition sequence motifs. *TIBS* 15: 342-346

Kiefer, P., Acland, P., Pappin, D., Peters, G. and Dickson, C. (1994) Competition between nuclear localization and secretory signals determines the subcellular fate of a single CUG-initiated form of FGF3. *EMBO J.* 13: 4126-4136

Kimura, Y., Rutherford, S.L., Miyata, Y., Yahara, I., Freeman, B.C., Yue, L., Morimoto, R.I. and Lindquist, S. (1997) Cdc37 is a molecular chaperone with specific functions in signal transduction. *Genes Dev*. 11: 1775-1785

King, F.W., Wawrzynow, A., Höfeld, J. and Zylicz, M. (2001) Co-chaperones Bag-1, Hop and hsp40 regulate hsc70 and Hsp90 interactions with wild-type or mutant p53. *EMBO J.* 20: 6297-6305

King, W.J. and Greene, G.L. (1984) Monoclonal antibodies localize oestrogen receptor in the nucleus of target cells. *Nature* 307: 745-747

Klonis, N., Rug, M., Harper, I., Wickham, M., Cowman, A. and Tilley, L. (2002) Fluorescence photobleaching analysis for the study of cellular dynamics. *Eur. Biophys. J.* 31: 36-51

Kneller, D.G., Cohen, F.E., and Langridge, R. (1990) Improvements in protein secondary structure prediction by an enhanced neural network. *J. Mol. Biol*. 214: 171-182

Knudsen, K.E., Knudsen, E.S., Wang, J.Y. and Subramani, S. (1996) p34cdc2 kinase activity is maintained upon activation of the replication checkpoint in *Schizosaccharomyces pombe*. *Proc. Natl. Acad. Sci. U.S.A.* 93: 8278-8283

Koike, M., Ikuta, T., Miyasaka, T. and Shiomi, T. (1999) The nuclear localization signal of the human Ku70 is a variant bipartite type recognized by the two components of nuclear pore-targeting complex. *Exp. Cell Res.* 250: 401-413

Kozak, M. (1983) Comparison if initiation of protein synthesis in prokaryotes, eukaryotes, and organelles. *Microbiological reviews*. 47: 1-45

Kraulis, P.J. (1991) MOLSCRIPT: A program to produce both detailed and schematic plots of protein structures. *J. App. Crystal.* 24: 946-950

Krebber, H. and Silver, P.A. (2000) Directing proteins to the nucleus by fusion to nuclear localization signal tags. 283-297

Kriegler, M.P. (1990) Gene transfer and expression: A laboratory manual: W.H. Freeman and company, New York.

Krone, P.H. and Sass, J.B. (1994) Hsp90α and Hsp90β are present in the zebrafish and are differentially regulated in developing embryos. *Biochem. Biophys. Res. Commun.* 204: 746-752

Kudo, K., Khochbin, S., Nishi, K., Kitano, K., Yanagida, M., Yoshida, M. and Horinouchi, S. (1997) Molecular cloning and cell-cycle dependent expression of mammalian CRM1, a protein involved in nuclear export of proteins. *J. Biol. Chem.* 272: 29742-29751

Kudo, N., Matsumori, N., Taoka, H., Fujiwara, D., Schreiner, E.P., Wolff, B., Yoshida, M. and Horinouchi, S. (1999) Leptomycin B inactivates CRM1/exportin 1 by covalent modification at a cysteine residue in the central conserved region. *Proc. Natl. Acad. Sci. U.S.A.* 96: 9112-9117

Kühl, N.M. and Rensing, L. (2000) Heat shock effects on cell cycle progression. *C.M.L.S.*: 57: 450

Kühl, N.M., Kunz, J. and Rensing, L. (2000) Heat shock-induced arrests in different cell cycle phases of rat C6-glioma cells are attenuated in heat shock-primed thermotolerant cells. *Cell Prolif.* 33: 147

Kurihara, T., Hori, M., Takeda, H., Inoue, M. and Yoneda. Y. (1996) Partial purification and characterization of a protein kinase that is activated by nuclear localization signal peptides. *FEBS Lett*. 380: 241-245

Labbé, J.C., Capony, J.P., Caput, D., Cavadore, J.C., Derancourt, J., Kaghad, M., Lalias, J.M., Picard, A. and Dorée, M. (1989) MPF from starfish oocytes at first meiotic metaphase as a heterodimer containing one molecule of cdc2 and one molecule of cyclin B. *EMBO J* 8: 2275-2282

Laemmli, U.K. (1970) Cleavage of structural proteins during the assembly of the head of bacteriophage T4. *Nature* 227: 680-685

Lamian, V., Small, G.M. and Feldherr, C.M. (1996) Evidence for the existence of a novel mechanism for the nuclear import of Hsc70. *Exp. Cell Res.* 228: 84-91

Lanford, R.E. and Butel, J.S. (1984) Construction and characterization of an SV40 mutant defective in nuclear transport of T-antigen. *Cell* 37: 801-813

Lanford, R.E., Kanda, P. and Kennedy, R.C. (1986) Induction of nuclear transport with a synthetic peptide homologous to the SV40 T antigen transport signal. *Cell* 46; 575

Lange, B M, Rebollo, E., Herold, A. and Gonzalez, C. (2002) Cdc37 is essential for chromosome segregation and cytokinesis in higher eukaryotes. *EMBO J.* 21: 5364-5374

Lässle, M., Blatch, G.L., Kundra, V., Takatori, T. and Zetter, B.R. (1997) Stress-inducible murine protein mSTI1. *J. Biol. Chem.* 272: 1876 - 84

Lassman, G., Thelander, L. and Graslund, A. (1992) EPR stopped flow studies of the reaction of the tyrosyl radical of protein R2 from ribonucleotide reductase with hydroxyurea. *Biochem. Biophys. Res. Commun.* 188: 879-887

Lau, J.F., Parisien, J.P. and Horvath, C.M. (2000) Interferon regulator factor subcellular localization is determined by a bipartite nuclear localization signal in the DNA-binding domain and interaction with cytoplasmic retention factors. *Proc. Natl. Acad. Sci.* 97: 7278-7283

Lebeau, M.C., Massol, N., Herrick, J., Faber, L.E., Renoir, J.M., Radanyi, C., and Baulieu, E.E. (1992) p59, an hsp90 binding protein. Cloning and sequencing of its cDNA and preparation of a peptide directed polyclonal antibody. *J. Biol. Chem.* 267: 4281-4284

Lees-Miller, S.P. and Anderson, C.W. (1989) Two human 90-kDa heat shock proteins are phosphorylated *in vivo* at conserved serines that are phosphorylated *in vitro* by casein kinase II. *J. Biol. Chem.* 264:2431-2437.

Lef, J. and Lam, K.B. (1976) Bromodeoxyuridine 5'-monophosphate incorporation into yeast nuclear and mitochondrial deoxyribonucleic acid. *J. Bacteriol.*127:354-361

Levin, J.M.; Robson, B. and Garnier, J. (1986) An algorithm for secondary structure determination in proteins based on sequence similarity. *FEBS Lett* 205: 303-308

Li, J., Meyer, A.N. and Donoghue, D.J. (1997) Nuclear localization of cyclin B1 mediates its biological activity and is regulated by phosphorylation. *Proc. Natl. Acad. Sci.* 94: 502-507

Liberek, K., Marszalek, J., Ang, D., Georgopoulos, C. and Zylicz, M. (1991) *Escherichia coli* DnaJ and GrpE heat shock proteins jointly stimulate ATPase activity of DnaK. *Proc. Natl. Acad. Sci. U.S.A.* 88: 2874-2878

Lindquist, S. and Craig, E.A. (1988) The heat-shock proteins. *Annu. Rev. Genet.* 22: 631-677

Loewinger, L. and McKeon, F. (1988) Mutations in the nuclear lamin proteins resulting in their aberrant assembly in the cytoplasm. *EMBO J.* 7: 2301-2309

Longshaw, V.M. (1999) MSc thesis, University of the Witwatersrand, South Africa

Longshaw, V.M., Dirr, H.W., Blatch, G.L. and Lässle, M. (2000) The *in vitro* phosphorylation of the co-chaperone mSTI1 by cell cycle kinases substantiates a predicted casein kinase II-p34^{cdc2}-NLS (CcN) motif. Biol. Chem. 381:1133-1138.

Losiewicz, M.D., Carlson, B.A., Kaur, G., Sausville, E.A. and Worland, P.J. (1994) Potent inhibition of CDC2 kinase activity by the flavonoid L86-8275. *Proc. Am. Assoc. Cancer Res.* 35: 27

Louvion, J.K., Warth, R. and Picard, D. (1996) Two eukaryote-specific regions of Hsp82 are indespensable for its viability and signal transduction functions in yeast. *Proc. Natl. Acad. Sci. U.S.A* .93: 13937-13942

Loveland, K.L., Herszfed, D., Chu, B., Rames, E., Briggs, L.J., Shakri, R., de Kretser, D.M. and Jans, D.A. (1999) A novel low molecular weight microtubule-associated protein-2 (MAP-2) isoform containing a functional nuclear localization sequence in testis. *J. Biol. Chem.* 274: 19261-19268

Lowry, D.H., Rosebrough, N.J., Fan, A.,L., and Randall, R.J. (1951) Protein measurement with the Folin-phenol reagent. *J. Biol. Chem.* 193: 265-275

Lu, X., Gong, S., Monks, A., Zaharevitz, D. and Moscow, J.A. (2002) Correlation of nucleoside and nucleobase transporter gene expression with antimetabolite drug cytotoxicity. *J. Exp. Ther. Oncol.* 2: 200-212

Ludin, B., Doll, T., Meili, R., Kaech, S. and Matus, A. (1996) Application of novel vectors for GFP-tagging of proteins to study microtubule-associated proteins. *Gene* 173: 107-111

Lui, X.L., Xiao, B., Yu, Z.C., Guo, J.C., Zhao, Q.C., Xu, L., Shi, Y.Q. and Fan, D.M. (1999) Down-regulation of hsp90 could change cell cycle distribution and increase drug sensitivity of tumor cells. *World J. Gastroenterol.* 5: 199-208

Lusky, M., Berg, L., Weiher, H. and Botchan, M. (1983) Bovine papilloma virus contains an activator of gene expression at the distal end of the early transcription unit. Mol. Cell Biol. 3: 1108

Lyons, R.H., Ferguson, B.Q. and Rosenberg, M. (1987) Pentapeptide nuclear localization signal in adenovirus E1A. *Mol. Cell Biochem.* 7: 2451-2456

Maciejewski, P.M., Peterson, F.C., Anderson, P.J. and Brooks, C.L. (1995) Mutation of serine 90 to glutamic acid mimics phosphorylation of bovine prolactin. *J. Biol. Chem.* 270: 27661-27665

Mandell, R.B. and Feldherr, C.M. (1992) The effect of carboxy terminal deletions on the nuclear transport rate of Hsc70. *Exp. Cell Res.* 198: 164-169

Matheny, C., Day, M.C., Milbrandt, J. (1994) The nuclear localization signal of NGF1-A is located within the zinc finger binding domain, *J. Biol. Chem.* 269: 8176-8181

Matsumoto, M. and Fujimoto, H. (1990) Cloning of hsp70-related gene expressed in mouse spermatids. *Biochim. Biophys. Res. Commun*. 166:43-49. 9

McCann, R. and Glover, C.V.C. (1995) Evidence for the physiological interaction of yeast cdc37 and casein kinase II (CKII). *Mol. Cell. Biol.* 6: 133a

McLaughlin, S.H., Smith, H.W. and Jackson, S.E. (2002) Stimulation of the weak ATPase activity of human Hsp90 by a client protein. *J. Mol. Biol.* 315: 787-798

McShan, G.D. and Wilson, V.G. (1997) Casein kinase II phosphorylates bovine papillomavirus type (E) *in vitro* at a conserved motif. *J. Gen. Virol.* 78: 171-177

Melchior, F., Gerace, L. (1995) Mechanism of nuclear protein import. *Curr. Opin. Cell Biol.* 7: 310-318

Metcalf, D. (1999) MSc thesis, University of the Wiwatersrand, South Africa

Michael, W.M., Choi, M. and Dreyfuss, G. (1995) A nuclear export signal in hnRNP A1: a signal-mediated, temperature-dependent nuclear protein export pathway. *Cell* 83: 415

Michikawa, Y., Baba, T., Arai, Y., Sakakura, R. and Kusakabe, M. (1993) Structure and organization of the gene encoding a mouse mitochondrial stress-70 protein. *FEBS Lett* 336:27-33.

Milarski, K.L. and Morimoto, R.I. (1986) Expression of human HSP70 during the synthetic phase of the cell cycle. *Proc. Natl. Acad. Sci. USA*. 83:9517.

Milarski, K.L., Welch, W.J. and Morimoto, R.I. (1989) Cell cycle-dependent association of Hsp70 with specific cellular proteins. *J. Cell Biol.* 108: 413

Mishra, K. and Parnaik, V.K. (1995) Essential role of protein phosphorylation in nuclear transport. *Exp. Cell Res.* 216: 124-134

Mishra, K., Divi, K. and Parnaik, V.K. (1994) A conserved epitope on nuclear pore phosphoproteins reflects cell division status. *Ind. J. Biochem. Biophys.* 31: 243-248

Miyata, Y. and Yahara, I. (1992) The 90-kDa heat shock protein, HSP90, binds and protects casein kinase II from self-aggregation and enhances its kinase activity. *J. Biol. Chem.* 267: 7042-7047

Miyata, Y., Chambraud, B., Radanyo, C., Leclerc, J., Lebeau, M.C., Renoir, J.M., Shirai, R., Catelli, M.G., Yahara, I. And Baulieu, E.E. (1997) Phosphorylation of the immunosuppressant FK506-binding protein FKBP52 by casein kinase II: regulation of Hsp90 binding activity of FKBP52. *Proc. Natl. Acad. Sci. U.S.A.* 94: 14500-14505

Moore, J.D., Yang, J., Truant, R. and Kornbluth (1999) Nuclear import of cdk/cyclin complexes: Identification of distinct mechanisms for import of cdk2/cyclin E and cdc2/cyclin B1. *J. Cell Biol.* 144: 213-224

Moore, M.S. and Blobel, G. (1992) The two steps of nuclear import, targeting to the nuclear envelope and translocation through the nuclear pore require different cytosolic factors. *Cell.* 69: 939-950

Moore, M.S. and Blobel, G. (1994) Purification of a Rad-interacting protein that is required for protein import into the nucleus. *Proc. Natl. Acad. Sci. USA* 91: 10212-10216

Morgan, D.O. (1997) Cyclin-dependent kinases: engines, clocks, and microprocessors. *Annu. Rev. Cell Dev. Biol.* 13:261-291.

Morianu, J., Hijikata, M., Blobel, G. and Radu, A. (1995) Mammalian karyopherin α1β and α2β heterodimers: α1or α2 subunit binds nuclear localization signal and β subunit interacts with peptide repeat-containing nucleoporins. *Proc. Natl. Acad. Sci. U.S.A.* 92: 6532-6536

Morishima, Y., Kanelakis, K.C., Silverstein, A.M., Ditmmar, K.D., Estrada, L. and Pratt, W.B. (2000a) The Hsp organiser protein Hop enhances the rate of but is not essential for glucocorticoid receptor folding by the multiprotein Hsp90-based chaperone system. *J. Biol. Chem.* 275; 6894-6900

Morishima, Y., Murphy, P.J.M., Li, D.P., Sanchez, E.R. and Pratt, W.B. (2000b) Stepwise assembly of a glucocorticoid receptor-Hsp90 heterocomplex resolves two sequential ATP-dependent events involving first Hsp70 and then Hsp90 in opening of the steroid binding pocket. *J. Biol. Chem.* 275; 18054-18060

Moroianu, J., Blobel, G. and Radu, A. (1995) Previously identified protein of uncertain function is karyopherin alpha together with karyopherin beta docks import substrates at nuclear pore complexes. *Proc. Natl. Acad. Sci. USA* 92: 2008-2011

Moroianu, J., Blobel, G. and Radu, A. (1996) The binding site of karyopherin α for karyopherin β overlaps with a nuclear localization sequence. *Proc. Natl. Acad. Sci. USA* 93: 6572-6576

Mort-Bontemps-Soret, M., Facca, C. and Faye, G. (2002) Physical interaction of cdc28 with cdc37 in *Saccharomyces cerevisiae*. *Mol. Genet. Genomics* 267: 447-458

Mosialos, G., Hamer, P., Capobianco, A.J., Laursen, R.A. and Gilmore, T.D. (1991) A protein-kinase-A recognition sequence is structurally linked to transformation by $p59^{v\text{-}rel}$ and cytoplasmic retention of $p68^{c\text{-}rel}$. *Mol. Cell Biol.* 11: 5867-5877

Mount, D.W. (2001) Bioinformatics. Sequence and genome analysis. Cold Spring Harbour Press, Cold Spring Harbour, New York, U.S.A.

Mulner-Lorillon, O., Cormier, P., Labbé, J.C., Dorée, M., Poulhe, R., Osborne, H., Bellé, R. (1990) M-phase-specific cdc2 protein kinase phosphorylates the β subunit of casein kinase II and increases casein kinase II activity. *Eur. J. Biochem*. 193: 529-534

Mulner-Lorillon, O., Marot, J., Cayla, X., Pouhle, R. and Bellé, R. (1988) Purification and characterization of a casein kinase II type enzyme from *Xenopus laevis* ovary: Biological effects on the meiotic cell division of full - grown oocytes. *Eur. J. Biochem.* 171: 107-117

Muňoz, M.J. and Jimenez, J. (1999) Genetic interactions between Hsp90 and the cdc2 mitotic machinery in the fission yeast *Schizosaccharomyces pombe*. *Mol. Gen. Genet.*261: 242-250

Murphy, P.J.M., Kanelakis, K.C., Galigniana, M.D., Morishima, Y. and Pratt, W.B. (2001) Stoichiometry, abundance, and functional significance of the Hsp90/Hsp70-based multiprotein chaperone machinery in reticulocyte lysate. *J. Biol. Chem.* 276: 30092-30098

Nachury, M.V. and Weiss, K. (1999) The direction of transport through the nuclear pore can be inverted. *Proc. Natl. Acad. Aci. U.S.A.* 96: 9622-9627

Nakai, A., Satoh, M.; Hirayoshi, K., Nagata, K. (1992) Involvement of the stress protein Hsp47 in procollagen processing in the endoplasmic reticulum, *J Cell Biol*, 117: 904-914

Nakamura, S., Tatuno, I., Noguchi, Y., Kitagawa, M. Kohn, L.D., Saito, Y. and Hirai, A. (1999) 73 kDa heat shock cognate protein interacts directly with $p27^{Kip1}$, a cyclin-dependent kinase inhibitor, during G_1/S transition. *Biochem. Biophys. Res.Commun.* 257: 340-343

Nakielny, S. and Dreyfuss, G. (1999) Transport of proteins and RNAs in and out of the nucleus. *Cell* 99: 677-690

Ni, J., Chen, X., Yang, T. and Chen, J.Y. (2001) Construction of *Candida albicans* Two-hybrid Library and screening for proteins interacting with Crk1. 33:198-204

Nicolet, C.M. and Craig, E.A. (1989) Isolation and characterization of STI1, a stress inducible gene from *Saccharomyces cerevisiae*. *Mol. Cell Biol.*9: 3638-3646

Nishikawa, K. and Oi, T. (1986) Amino acid sequence homology applied to the prediction of protein secondary structures, and joint prediction with existing methods. *Biochim. Biophys Acta* 871: 45-54

Nollen, E.A.A., Salomons, F.A., Brunsting, J.F., Van der Want, J.J.L., Sibon, O.C.M. and Kampinga, H.H. (2001) Dynamic changes in the localization of thermally unfolded nuclear proteins associated with chaperone-dependent protection. *Proc. Natl. Acad. Sci. USA* 98: 12038-12043

Norbury, C.J. and Nurse, P. (1989) Control of the higher eukaryote cell cycle by $p34^{cdc2}$ homologues. *Biochim. Biophys. Acta* 989: 85-95

Nylandsted, J., Rohde, M., Brand, K., Bastholm, L., Elling, F. and Jäättela, M. (2000) Selective depletion of heat shock protein 70 (Hsp70) activates a tumor-specific death program that is independent of caspases and bypasses Bcl-2. *Proc. Natl. Acad. Sci. U.S.A.* 97: 7871-7876

O'Farrell, P.H. (1975) High resolution two-dimensional electrophoresis of proteins. *J. Biol. Chem.*250: 4007-4021

Odunuga, O.O., Hornby, J.A., Bies, C., Zimmerman, R., Pugh, D.J. and Blatch, G.L. (2003) Tetratricopeptide repeat motif-mediated Hsc70-mSTI1 interaction. Molecular characterization of the critical contacts for successful binding and specificity. *J. Biol. Chem.* 278: 6896-6904

Ogawa, H., Inouye, S., Tsuji, F.I., Yasuda, K. and Umesono, K. (1995) Localization, trafficking, and temperature-dependence of the *Aequorea* green fluorescent protein in cultured vertebrate cells. *Proc. Natl. Acad. Sci. USA* 92: 11899-11903

Okuda, M., Horn, H.F., Tarapore, P., Tokuyama, Y., Smulian, A.G., Chan, P.K. Knudsen, E.S., Hofman, I.A., Snyder, J.D., Bove, K.E. and Fukasawa, K. (2000) Nucleophosmin/B23 is a target of cdk2/cyclin E in centrosome duplication. *Cell* 103: 127-140

Okuno, Y., Imamoto, N. and Yoneda, Y. (1993) 70-kda heat-shock protein cognate colocalizes with karyophilic proteins into the nucleus during their transport *in vitro*. *Exp. Cell Res.* 206: 134-142

Ookata, K., Hisanaga, S., Bulinski, J.C., Murofushi, H., Aizawa, H., Itoh, T.J., Hotani, H., Okumura, E., Tachibana, K. and Kishimoto, T. (1995) Cyclin B interaction with microtubule-associated protein 4 (MAP4) targets p34c dc2 kinase to microtubules and is a potential regulator of M-phase microtubule dynamics. *J. Cell Biol.* 128: 849-862

Ossareh-Nazari, B., Bachelerie, F. and Dargemont, C. (1997) Evidence for the role of CRM1 in signal-mediated nuclear protein export. *Science* 278: 141-144

Ou, W.J., Thomas, D.Y., Bell, A.W. and Bergeron, J.J. (1992) Casein kinase II phosphorylation of signal sequence receptor alpha and the associated membrane chaperone calnexin. *J. Biol. Chem.* 267: 23789-23796

Overton, M. and Blumer, K. (2002) Use of fluorescence resonance energy transfer to analyze oligomerization of G-protein-coupled receptors expressed in yeast. *Methods* 27: 324

Owens-Grillo, J.K., Czar, M.J., Hutchison, K.A., Hoffmann, K., Perdew, G.H., and Pratt, W.B. (1996) A model of protein targeting mediated by immunophilins and other proteins that bind to Hsp90 via tetratricopeptide repeat domains. *J. Biol. Chem.* 271: 13468-13475

Owens-Grillo, J.K., Hoffman, K., Hutchison, K.A., Yem, A.W., Deibel, M.R., Jr., Handschumacher, R.E., and Pratt, W.B. (1995) The cyclosporin A-binding immunophilin CyP40 and the FK506-binding immunophilin hsp56 bind to a common site on hsp90 and exist in independent cytosolic heterocomplexes with the untransformed glucocorticoid receptor. *J. Biol. Chem.* 270: 20479-20484

Padmanabha, R., Chen-Wu, J.L., Hanna, D.E. and Glover, C.V. (1990) Isolation, sequencing, and disruption of the yeast CKA2 gene: casein kinase II is essential for viability in *Saccharomyces cerevisiae*. *Mol. Cell Biol.* 10: 4089-4099

Paine, P.L. (1975) Nucleocytoplasmic movement of fluorescent tracers microinjected into living salivary gland cells. *J. Cell Biol.* 66: 652-657

Paine, P.L., Moore, L.C. and Horowitz, S.B. (1975) Nuclear envelope permeability. *Nature* 254: 109-114

Panté, N. and Aebi, U. (1995) Exploring nuclear pore complex structure and function in molecular detail. *J. Cell Sci. Supplement* 19: 1-11

Pascarella S. and Argos, P. (1992) Analysis of insertions/deletions in protein sequences. *J. Mol. Biol.* 224: 461-471

Pearson, W.R. and Lipman, D.R. (1988) Improved tools for biological sequence comparison. *Proc. Natl. Acad. Sci. U.S.A.* 85: 2444-2448

Pelham, H.R. (1984) Hsp70 accelerates the recovery of nucleolar morphology after heat shock. *EMBO J.* 3: 3095-3100

PepTool version1.1, Biotools Incorporated (1998) (Canada)

Perander, M., Bøgrkøy, G. and Johansen, T. (2001) Nuclear import and export signals enable rapid nucleocytoplasmic shuttling of the atypical protein kinase C λ. *J. Bio. Chem.* 276: 13015-13024

Perrot-Applanat, M., Logeat, F., Groyer-Picard, M.T., and Milgrom, E. (1985) Immunocytochemical study of mammalian progesterone receptor using monoclonal antibodies. *Endocrinol.* 116: 1473-1484

Perry, M.D., Aujame, L., Shtang, S. and Moran, L.A. (1994) Structure and expression of an inducible HSP-70 encoding gene from *Mus musculus*. *Gene*. 146:273-278.

Picard, D. and Yamamoto, K.R. (1987) Two signals mediate hormone dependent nuclear localization of the glucocorticoid receptor. *EMBO J.* 6: 3333-3340

Picard, D., Kumar, V., Chambon, P., and Yamamoto, K.R. (1990) Signal transduction by steroid hormones: nuclear localization is differentially regulated in estrogen and glucocorticoid receptors. *Cell. Regul.* 1: 291-299

Pines, J. (1995) GFP in mammalian cells. *Trends Genet*. 11: 326-327

Pinna, L.A. and Meggio, F. (1997) Protein kinase CK2 ("casein kinase-2") and its implication in cell division and proliferation. *Prog. Cell Cycle Res.* 3: 77-97

Planas-Silver, M.D. and Weinberg, R.A. (1997) Estrogen-dependent cyclin E-cdk2 activation through p21 redistribution. *Mol. Cell. Biol.* 17: 4059-4069

Plautz, J.D., Day, R,N., Dailey, G.M., Welsh, S.B., Hall, J.C., Halpain, S. and Kay, S. A. (1996) Green fluorescent protein and its derivatives as versatile markers of gene expression in living *Drosophila melangaster*, plant and mammalian cells. *Gene* 173-83-87

Pollard, V.W., Michael, W.M., Nakielny, S., Siomi, M. C., Wang, F. and Dreyfuss, G. (1996) A novel receptor-mediated nuclear protein import pathway. c*ell* 86: 985

Pratt, W.B. (1997) The role of the Hsp90-based chaperone system in signal transduction by nuclear receptors and receptors signaling via MAP kinase. *Annu. Rev. Pharmacol. Toxicol.* 37: 297-326

Pratt, W.B. (1998) The HSP90-based chaperone system: involvement in signal transduction from a variety of hormone and growth factor receptors. *Proc. Soc. Exp. Biol. Med*. 217:420.

Pratt, W.B. and Toft, D.O. (1997) Steroid receptor interactions with heat shock protein and immunophilin chaperones. *Endo. Rev*. 18:306-360.

Pratt, W.B., Krishna, P. and Olsen, L.J. (2001) Hsp90-binding immunophilins in plants: the protein movers. *Trends in Plant Science* 6: 54-58

Pratt, W.B., Silverstein, A.M. and Galigniana, M.D. (1999) A model for the cytoplasmic trafficking of signalling proteins involving the hsp90-binding immunophilins and p50cdc37. *Cell. Signal.* 11: 839-851

Prigent, C., Lasko, D.D., Kodama, K., Woodgett, J.R. and Lindahl, T. (1992) Activation of mammalian DNA ligase I through phosphorylation by casein kinase II. *EMBO J.* 11: 2925-2933

Prima, V., Depoix, C., Masselot, B., Formstecher, P. and Lefebvre, P. (2000) Alteration of the glutocorticoid receptor subcellular localization by non steroidal compounds. *J. Steroid Biochem. Mol. Biol.* 72: 1-12

Prodomou, C. Roe, S.M., O'Brien, R., Ladbury, J.E., Piper, P.W. and Pearl, L.H. (1997) Identification and structural characterization of the ATP / ADP - binding site in the Hsp90 molecular chaperone. *Cell* 90: 65-75

Pyerin, W. (1994) Human casein kinase II: structures, genes, expression and requirement in cell growth stimulation. *Advan. Enzyme Regul.* 34:225-246.

QIAexpressionist, The (1997) pp 11 - 89.

Queitsch, C., Sangster, T.A. and Lindquist, S. (2002) Hsp90 as a capacitor of phenotypic variation. *Nature* 417: 618-624

Radanyi, C., Chambraud, B., and Baulieu, E.E. (1994) The ability of the immunophilin FKBP59-HBI to interact with the 90-kDa heat shock protein is encoded by its tetratricopeptide repeat domain. *Proc. Natl. Acad. Sci. U.S.A.* 91: 11197-11201

Rajapandi, T., Greene, L.E. and Eisenberg, E. (2000) The molecular chaperones Hsp90 and Hsc70 are both necessary and sufficient to activate hormone binding by glucocorticoid receptor. *J. Biol. Chem.* 275: 22597-22604

Rani, C.S.S., Abe, A., Chang, Y., Rosenzweig, N., Saltiel, A.R., Radin, N.S. and Shayman, J.A. (1995) Cell cycle arrest induced by an inhibitor of glucosylceramide synthase: correlation with cyclin-dependent kinases. *J. Biol. Chem.* 270: 2859-2867

Ratajczak, T. and Carrello, A. (1996) Cyclophilin 40 (CyP40), mapping of its hsp90 binding domain and evidence that FKBP52 competes with CyP40 for Hsp90 binding. *J. Biol. Chem.* 271: 2961- 65

Ratajczak, T., Carrello, A., Mark, P.J., Warner, B.J., Simpson, R.J., Moritz, R.L., and House, A.K. (1993) The cyclophilin component of the unactivated estrogen receptor contains a tetratricopeptide repeat domain and shares identity with p59 (FKBP59). *J. Biol. Chem.* 268: 13187- 13192

Ratner, V., Kahana, E., Eichler, M. and Haas, E. (2002) A general strategy for site-specific double labelling of globular proteins for kinetic FRET studies. *Bioconjug. Chem.* 13: 1163-1170

Redwood, C., Davies, S.L., Wells, N.J., Fry, A.M. and Hickson, I.D. (1998) Casein kinase II stabilizes the activity of human topoisomerase I Ialpha in a phosphorylation-independent manner. *J. Biol. Chem.*273: 3635-3642

Reed, S.I. (1980) The selection of *S. cerevisiae* mutants defective in the start event of cell division. *Genetics* 95; 561-577

Reindl, A., Schoffl, F., Schell, J. Koucz, C. and Bako, L. (1997) Phosphorylation by a cyclin dependent kinase modulates DNA binding of the *Arabidopsis* heat shock transcription factor HSF1 *in vitro*. *Plant Physiol.* 115: 93-100

Ribbeck, K. and Görlich, D. (2001) Kinetic analysis of translocation through nuclear pore complexes. *EMBO J.* 20: 1320-1330

Rihs, H.P. and Peters, R. (1989) Nuclear transport kinetics depend on phosphorylation-site-containing sequences flanking the karyophilic signal of the Simian virus 40 T-antigen. *EMBO J.* 8: 1479-1484

Rihs, H.P., Jans, D.A., Fan, H. and Peters, R. (1991) The rate of nuclear cytoplasmic protein transport is determined by the casein kinase II site flanking the nuclear localization sequence of the SV40 T-antigen. *EMBO J.* 10: 633-639

Rizzuto, R., Brini, M., Pizzo, P, Murgia, M. and Pozzan, T. (1995) Chimeric green fluorescent protein as a tool for visualizing subcellular organelles in living cells. *Curr. Biol.* 5: 635-642

Robbins, J., Dilworth, S.M. Laskey, R.A. and Dingwall, C. (1991) Two interdependent basic domains in nucleoplasmin nuclear targeting sequence: identification of a class of bipartite nuclear targeting sequence. *Cell* 64: 615-623

Roberts, B. (1989) Nuclear location signal-mediated protein transport. *Biochim. Biophys. Acta* 1008: 263-280

Roberts, B., Richardson, W.D. and Smith, A.E. (1987) The effect of protein context on nuclear location signal function. *Cell* 50: 465-475

Rodier, G., Montagnoli, A., Di Marcotullio, L., Coulombe, P., Draetta, G.F., Pagano, M. and Meloche, S. (2001) p27 cytoplasmic localization is regulated by phosphorylation on Ser10 and is not a prerequisite for its proteolysis. *EMBO J.* 20: 6672-6682

Rost and Sander, (1996) Bridging the protein sequence-structure gap by structure predictions. *Annu Rev Biophys Biomol Struct.* 1996;25:113-36. Review.

Rost, B. and Sander, C. (1993) Improved prediction of protein secondary structure by use of sequence profiles and neural networks. *Proc. Natl. Acad. Sci.* 90: 7558-7562

Sainis, I., Angelidis, C., Pagoulatos, G. and Lazaridis, I. (1994) The hsc70 gene which is slightly induced by heat is the main virus inducible member of the hsp70 gene family. *FEBS Lett.* 335:282-286.

Sambrook, J. and Russell, D.W. (2001) *In* Argentine, J. (ed.) Molecular cloning, a laboratory manual, vols 1-3, 3rd ed. Cold Spring Harbour Laboratory Press, Cold Spring Harbour, New York.

Sanders, S.L., Whitfield, K.M., Vogel, J.P., Rose, M.D. and Schekman, R. (1992) Sec61p and BiP directly facilitate polypeptide translocation into the ER. *Cell* 69: 353-365

Sanger, F. and Tuppy, H. (1951) the amino acid sequence of the phenylalanyl chain of insulin. *Biochem J* 49: 481-490

Sarver, N., Gruss, P., Law, M.F., Khoury, G. and Howley, P.M., (1981) Bovine papilloma virus deoxyribonucleic acid: a novel eucaryotic cloning vector. *Mol. Cell. Biol.* 1: 486

Sato, N. and Torigoe (1998) The molecular chaperones in cell cycle control in "stress of life from molecules to man". *Ann. NY Acad. Sci.* 851: 61

Scheibel, T. and Buchner, J. (1997a) Guidebook to molecular chaperones and protein catalysts (Ed. Gething, M.) pp 147-151. Oxford University Press, Oxford

Scheibel, T. and Buchner, J. (1997b) The HSP90 family-an overview. M.J. Gething ed. Oxford. Oxford University Press, pp. 147151.

Scheibel, T., Weikl, T. and Buchner, J. (1998) Two chaperone sites in Hsp90 differing in substrate specificity and ATP - dependence. *Proc.Natl. Acad. Sci. U.S.A.* 95: 1495-1499

Scheufler, C., Brinker, A., Bourenkov, G., Pegoraro, S., Moroder, L., Bartunik, H., Hartl, F.U. and Moarefi, I. (2000) Structure of TPR domain-peptide complexes: critical elements in the assembly of the hsp70/hsp90 multichaperone machine. *Cell* 101:199-210.

Schlenstedt, G. (1996) Protein import into the nucleus. *FEBS Lett.* 389: 75-79

Schmidt-Zachmann, M.S., Dargemont, C., Kühn, L.C. and Nigg, E.A. (1993) Nuclear export of proteins: the role of nuclear retention. *Cell* 74: 493-504

Schreibel, T. and Buchner, J. (1997) Guidebook to molecular chaperones and protein catalysts (ed Gething, M.) Oxford University Press, Oxford, U.K.

Shackleford, G.M., Ganguly, A. and MacArthur, C.A. (2001) Cloning, expression and nuclear localization of human NPM3, a member of the nucleophosmin/nucleoplasmin family of nuclear chaperones. *BCM Genomics* 2: 8. http://www.biomedcentral.com/1471-2164/2/8

Shaulsky, G., Goldfinger, N., Ben-Ze'ev, A. and Rotter, V. (1990) Nuclear localization of p53 is mediated by several nuclear localization signals and plays a role in tumorigenesis. *Mol. Cell Biol.* 10: 6565-6577

Sheffield, W.P., Shore, G.C. and Randall, S.K. (1990) Mitochondrial precursor protein. Effects pf 70 kDa heat shock protein on polypeptide folding, aggregation, and import competence. *J. Biol. Chem.* 265: 11069-11076

Sheih, M.W., Wesser, S.R. and raikhel, N.V. (1993) Nuclear targeting of the maize R protein requires two nuclear localization sequences. *Plant Physiol.* 101: 353-361

Sherr, C.J. and Roberts, J.M. (1995) Inhibitors of mammalian G1 cyclin - dependent kinases. *Genes Dev*. 9: 1149-1163

Sherr, C.S. (1993) Mammalian G1 cyclins, *Cell* 73: 1059-1065

Shi, Y. and Thomas, J.O. (1992) The transport of proteins into the nucleus requires the 70-kilodalton heat shock protein or its cytosolic cognate. *Mol. Cell Biol.* 12: 2186-2192

Shi, Y., Brown, E.D. and Walsh, C.T. (1994) Expression of recombinant human casein kinase II and recombinant heat shock protein 90 in E scherichia coli and characterization of their interactions.*Proc Natl Acad Sci U S A.* 91: 2767-71.

Shibanuma, M., Kuroki, T. and Nose, K. (1992) Cell-cycle dependent phosphorylation of Hsp28 by TGF beta 1 and H 202 in normal mouse osteoblastic cells (MC3T3-E1), but not in their ras-transformants. *Biochem. Biophys. Res. Commun.* 187: 1418-1425

Shiying, C., Prapapanich, V., Rimerman, R.A., Honoré, B., and Smith, D.F. (1996) Interactions of p60, a mediator of progesterone receptor assembly, with heat shock proteins Hsp90 and Hsp70. *Mol. Endocrinol.* 10: 682-693

Shulga, N., James, P., Craig, E. A. and Goldfarb, D.S. (1999) A nuclear export signal prevents *Saccharomyces cerevisiae* Hsp70 Ssb1p from stimulating nuclear localization signal-directed nuclear transport. *J. Biol. Chem.* 274: 16501-16507

Shulga, N., Roberts, P., Gu, Z.Y. (1996) *In vivo* nuclear transport kinetics in *Saccharomyces cerevisiae*: a role for heat shock protein 70 during targeting and translocation. *J. Cell Biol.* 135: 329

Siligard, G., Panaretou, B., Meyer, P., Singh, S., Woolfson, D.N., Piper, P.W., Pearl, L.H. and Prodomou, C. (2002) Regulation of Hsp90 ATPase activity by the co-chaperone cdc37p/p50^{cdc37}. *J. Biol. Chem.* 277:20151-20159

Silver, P.A., Sadler, I. and Osborne, M. A. (1989) Yeast proteins that recognize nuclear localization sequences. *J. Cell Biol.* 109: 983

Siomi, H. and dreyfuss, G. (1995) Yeast proteins that recognize nuclear localization sequences. *J. Cell Biol.* 129: 551

Skowyra, D., Georgopolous, C. and Zylicz, M. (1990) The *E. coli* DnaK product, the Hsp70 homologue, can reactivate heat inactivated RNA polymerase in an ATP hydrolysis-dependent manner. *Cell* 62: 939-944

Smith, D. F., Stensgard, B.A., Welch, W.J., and Toft, D.O. (1992) Assembly of progesterone receptor with heat shock proteins and receptor activation are ATP mediated events. *J. Biol. Chem.* 267: 1350-1356

Smith, D.F. (1993) Dynamics of heat shock protein 90-progesterone receptor binding and the disactivation loop model for steroid receptor complexes. *Mol. Endocrinol.* 7: 1418-1429

Smith, D.F., Sullivan, W.P., Marion, T.N., Zaitsu, K., Madden, B., McCormick, D.J., and Toft, D.O. (1993) Identification of a 60 kDa stress-related protein, p60, which interacts with Hsp90 and Hsp70. *Mol. Cell. Biol.* 13: 869-876

Smith, M.R. and Greene, W.C. (1992) Characterization of a novel nuclear localization sequence in the HTLV-I tax transactivator protein. *Virology* 187: 316-320

Someya, A., Tanaka, N. and Okuyama, A. (1994) Inhibition of cell cycle oscillation of DNA replication by a selective inhibitor of the cdc2 kinase family, butyrolacetone I, in *Xenopus* egg extracts. *Biochem. Biophys. Res. Commun.* 198: 536-545

Sorger, P.K. and Pelham, H.R.B. 1987. Cloning and expression of a gene encoding Hsc73, the major hsp70-like protein in unstressed rat cells. *EMBO J.* 6:993-998.

Srethapakdi, M., Liu, F., Tavorath, R. and Rosen, N. (2000) Inhibition of Hsp90 function by ansamycins causes retinoblastoma gene product-dependent G1 arrest. *Cancer Res.* 60: 3940-3946

Srinivasan, M., Edman, C.F. and Schulman, H. (1994) Alternative splicing introduces a nuclear localization signal that targets multifunctional CaM kinase to the nucleus. *J. Cell Biol.* 126: 839-852

Stade, K., Ford, C.S., Guthrie, C., Weis, K. (1997) Exportin 1 (Crm1p) is an essential nuclear export factor. *Cell* 90: 1041-1050

Stearns, T. (1995) Green fluorescent protein. The green revolution. *Curr Biol.* 5: 262-264

Stepanova, L., Leng, X. and Parker, S.B. (1996) Mammalian p50cdc37 is a protein kinase-targeting subunit of Hsp90 that binds and stabilizes ckd4. *Genes Dev.* 10: 1491-1502

Stochaj, U. and Silver, P.A. (1992) A conserved phosphoprotein that specifically binds nuclear localization sequences is involved in nuclear import. *J. Cell Biol.* 117: 473-482

Stochaj, U., Rassadi, R. and Chiu, J. (2000) Stress-mediated inhibition of the classical nuclear import pathway and nuclear accumulation of the small GTPase Gsp1p. *FASEB J*. 10.1096/fj.99-99-0751fje

Stock, J. (1999) Gyrating protein kinases. *Curr. Biol*. 9:R364.

Stokoe, D., Engel, K., Campbell, D.G., Cohen, P. and Gaestel, M. (1992) Identification of MAPKAP kinase 2 as a major enzyme responsible for the phosphorylation of the small mammalian heat shock proteins. *FEBBS lett.* 313: 307-313

Ström, A.C. and Weiss, K. (2001) Importin-β-like nuclear transport receptors. *Genome Biol.* 2: reviews3008.1-3008.9. http://genomebiology.com/2001/2/6/reviews/3008

Susuki, K. and Watanabe, M. (1992) Augmented expression of Hsp72 protein in normal human fibroblasts irradiated with ultraviolet light. *Biochem. Biophy. Res. Comm.* 186: 1257

Sweet, R.M. (1986) Evolutionary similarity among peptide seqments is a basis for prediction of protein folding. *Biopolymers* 25: 1565-1577

Tagawa, T.; Juroki, T.; Vogt, P.K. and Chida, K. (1995) The cell cycle-dependent nuclear import of v-jun is regulated by a phosphorylation of a serine adjacent to the nuclear localization signal. *J Cell Biol.* 130: 255-263

Talcott, B. and Moore, M.S. (1999) Getting across the nuclear pore complex. *Trends Cell Biol.* 9: 312:318

Tanner, D. (2001) Honours thesis, Rhodes University, South Africa

Te Poele, R.H., Okorokov, A.L. and Joel, S.P. (1999) RNA synthesis block by 5, 6-dichloro-1-beta-D-ribofuroanosylbenzimidazole (DRB) triggers p53-dependent apoptosis in human colon carcinoma cells. *Oncogene* 18: 5765-5772

Teitz, T., Eli, D., Penner, M., Bakhanashvili, M., Naiman, T., Timme, T.L., Wood, C.M., Moses, R.E. and Canaani, D. (1990) Expression of the cDNA for the beta subunit of human casein kinase II confers partial UV resistance on xeroderma pigmentosum cells. *Mutat. Res.* 236: 85-97*

Thomson, J.D., Higgins, D.G. and Gibson, T.J. (1994) CLUSTALW: Improving the sensitivity of progressive multiple sequence alignment through sequence weighting, position-specific gap penalties and weight matrix choice. *Nucleic Acids Res*. 22: 4673-4680

Tissieres, A., Mitchel, H.K. and Tracy, U.M. (1974) Protein synthesis in salivary glands of *Drosophila melanogaster*: relation to chromosome puffs. *J. Mol. Biol,* 84: 389-98

Towbin, H., Staehlin, T., and Gordon, J. (1979) Electrophoretic transfer of proteins from polyacrilamide gels to nitrocellulose sheets: procedure and some applications. *Proc. Natl. ac ad. Sci. U.S.A.* 76:4350-4354.

Toyoshima, F., Moriguchi, T., Wada, A., Fukuda, M. and Nishida, E. (1998) Nuclear export of cyclin B1 and its possible role in the DNA damage-induced G2 checkpoint. *EMBO J.* 17: 2728-2735

Ungewickell, E. (1985) The 70 kDa mammalian heat shock proteins are structurally and functionally related to the uncoating protein that releases clathrin triskelia from coated vesicles. *EMBO J.* 4:3385-3391.

Van den Heuvel, S. and Harlow, E. (1993) Distinct role for cyclin-dependent kinases in cell cycle control. *Science* 262: 2050-2054

Van der Spuy, J., Kana, B.D., Dirr, H.W., and Blatch, G.L. (2000) Heat shock cognate protein 70 chaperone-binding site in the co-chaperone murine stress-inducible protein 1 maps to within three consecutive tetratricopeptide repeat motifs. *Biochem J.* 345:645-651.

Vancurova, I., Paine, T.M., Lou, W. and Paine, P.L. (1995) Nucleoplasmin associates with and is phosphorylated by casein kinase II. *J. Cell Sci.* 108: 779-787

Vesely, J., Havlicek, L., Strnad, M., Blow, J.J., Donella-Deana, A., Pinna, L., Letham, D.S., Kato, J.Y., Détivaud, L., Leclerc, S. and meijer, L. (1994) Inhibition of cyclin-dependent kinases by purine derivatives. *Eur. J. Biochem.* 224: 771-786

Vidair, C.A., Huang, R.N. and Doxsey, S.J. (1996) Heat shock causes protein aggregation and reduced protein solubility at the centrosome and other cytoplasmic locations. *Int. J. Hyperthermia* 12: 681-695

Vogelstein, B. and Gillespie, D. (1979) Preparative and analytical purification of DNA from agarose. *Proc. Natl. Acad. Sci. U.S.A.* 76: 615-619

Vriend, G. (1990) WHATIF: A molecular modelling and drug design program. *J. Mol. Graph.* 8: 52-56

Wang, S. and Hazelrigg, T. (1994) Implications for bed mRNA localization from special distribution of exu protein in *Drosophila* oogenesis. *Nature*, 369:400-403

Weickert, M.J., Doherty, D.H., Best, E.A. and Olins, P.O. (1996) Optimization of heterologous protein production in *Escherichia coli*. *Curr Opin Biotech*. 7:494-499

Weiss, K. (1998) Importins and exportins: how to get in and out of the nucleus. *Trends Biochem Sci.* 23: 185-189

Welch, W.J. (1987) The mammalian heat shock (stress) response: a cellular defense mechanism. *Adv. Exp. Med. Biol*. 225:287-304.

Welch, W.J. (1991) The role of heat shock proteins as molecular chaperones. *Curr. Opin. Cell Biol.* 3: 1033-1038

Welch, W.J. and Diamond, M.I. (2001) Glucocorticoid modulation of androgen receptor nuclear aggregation and cellular toxicity is associated with distinct forms of soluble expanded polyglutamine protein. *Hum. Mol. Genet.* 10: 3063-3074

Welch, W.J. and Feramisco, J. R. (1984) Nuclear and nucleolar localization of the 72,000-dalton heat shock protein in heat-shocked mammalian cells. *J. Biol. Chem.* 259: 4501-4513

Welch, W.J. and Suhan, J.P. (1986) Cellular and biochemical events in mammalian cells during and after recovery from physiological stress. *J. Cell Biol.* 103(5):2035-52.

Wen, M., Meinkoth, J.L., Tsien, R.Y. and Taylor, S.S. (1995) Identification of a signal for rapid export of proteins from the nucleus. *Cell* 82: 463-473

Whitfield, M. L., Sherlock, G., Saldanha, A.J., Murray, J.I., Ball, C.A., Alexander, K.E., Matese, J.C., Perou, C.M., Hurt, M.M., Brown, P.O. and Botstein, D. (2002) Identification of genes periodically expressed in the human cell cycle and their expression in tumors. *Mol. Biol. Chem.* 13: 1977-2000

Wigley, D.B., Davies, G.J., Dodson, E.J., Maxwell, A. and Dodson, G. (1991) Crystal structure of an N-terminal fragment of the DNA gyrase B protein. *Nature* 351: 624-629

Wigley, W.C., Fabunmi, R.P., Lee, M.G., Marino, C.R., Muallem, S., DeMartino, G.N. and Thomas, P.J. (1999) Dynamic association of proteasomal machinery with the centrosome. *J. Cell Biol.* 145: 481-490

Williams, R.W.; Chang, A.; Juretic, D. and Loughran, S. (1987) Secondary structure predictions and medium range interactions. *Biochim. Biophys. Acta* 916: 200-204

Wolff, B., Sanglier, J.J. and Wang, Y. (1997) Leptomycin B is an inhibitor of nuclear export: inhibition of nucleo-cytoplasmic translocation of the human immunodeficiency virus type 1 (HIV-1) Rev protein and rev-dependent mRNA. *Chem. Biol.* 4: 139-147

Yagita, K., Tamanini, F., Yasuda, M., Hoeijmakers, J.H.J., van der Horst, G.T.J. and Okamura, H. (2002) Nucleocytoplasmic shuttling and mCRY-dependent inhibition of ubiquitylation of the mPER2 clock protein. *EMBO J.* 21: 1301-1314

Yamaga, M., Fujii, M., Kamata, H., Hirata, H. and Yagisawa, H. (1999) Phospholipase C-delta1 contains a functional nuclear export signal sequence. *J. Biol. Chem.* 274: 28537-28541

Yang, J., and Defranco, D.B. (1994) Differential roles of heat shock protein 70 in the *in vitro* nuclear import of glutocorticoid receptor and simian virus 40 large tumor antigen. *Mol. Cell Biol.* 14: 5088

Yano, M., Naito, Z., Tanaka, S. and Asano, G. (1996) Expression and roles of heat shock proteins in human breast cancer. *Jpn. J. Cancer res.* 87: 908

Yem, A.W., Tomasselli, A.G., Heinrikson, R.L., Zurcher-Neely, H., Ruff, V.A., Johnson, R.A., and Deibel, M.R., Jr. (1992) The Hsp56 component of steroid receptor complexes binds to immobilized FK506 and shows homolgy to FKBP12 and FKBP13. *J. Biol. Chem.* 267: 2868-2871

Yokoe, H. and Meyer, T. (1996) Spacial dynamics of GFP-tagged proteins investigated by local fluorescence enhancement. Nature Biotechnology 14: 1252-1256

Yoneda, Y. (1996a) Nuclear export and its significance in retroviral infection. *Trends Microbiol.* 4: 1-2

Yoneda, Y. (1996b) Nuclear pore-targeting complex and its role in nuclear protein transport. *Arch. Histol. Cytol.*59: 97-107

Yoneda, Y. (1997) How proteins are transported from cytoplasm to the nucleus. *Biochem. J.* 121: 811-817

Yoneda, Y., Arioka, T., Imamoto-Sonobe, N., Sugawa, H., Shimonishi, Y. and Uchida, T. (1987) Synthetic peptides containing a region of SV40 large T-antigen involved in nuclear localization direct the transport of proteins into the nucleus. *Exp. Cell Res.* 170: 439-452

Yoneda, Y., Semba, T., Kaneda, Y., Nobel, R.L., Matsuoka, Y., Kurihara, T., Okada, Y. and Imamoto, N. (1992) A long synthetic peptide containing a nuclear localization signal and its flanking sequences of SV40 T-antigen directs the transport of IgM into the nucleus efficiently. *Exp. Cell Res.* 201: 313-320

Yonehara, M., Minami, Y., Kawata, Y., Nagai, J. and Yahara, I. (1996) Heat-induced chaperone activity of Hsp90. *J. Biol. Chem.* 271: 2641-2645

Yoshida, K. and Blobel, G. (2001) The karyopherin Kap142p/Msn5p mediates nuclear import and nuclear export of different cargo proteins. *J. Cell Biol.* 152: 729-739

Yoshida, M., Nishikawa, M., Nishi, K., Abe, K., Horinouchi, S. and Beppu, T. (1990) Effects of leptomycin B on the cell cycle of fibroblasts and fission yeast cells. *Exp. Cell Res.* 187: 150-156

Young, J.C. and Hartl, F.U. (2002) Chaperones and transcriptional regulation by nuclear receptors. *Nature Struc. Biol.* 9: 640-642

Zakeri, Z.F., Wolgemuth, D.J. and Hunt, C.R. (1990) Identification and sequence analysis of a new member of the mouse HSP70 gene family and characterization of its unique cellular and developmental pattern of expression in the male germ line. *Mol. Cell Biol.* 8:2925-2932.

Zanata, S.M., Lopes, M.H., Mercadante, A.F., Hajj, G.N.M., Chiarini, L.B., Nomizo, R., Freitas, A.R.O., Cabral, A.L.B., Lee, K.S., Juliano, M.A., De Oliveira, E., Jachieri, S.G., Burlingame, A., Huang, L., Linden, R., Brentani, R.R. and Martins, V.R. (2002) Stress-inducible protein 1 is a cell surface ligand for cellular prion that triggers neuroprotection. *EMBO J.* 21:3307-3316.

Zeise, E., Kühl, N., Kunz, J. and Rensing, L. (1998) Nuclear translocation of stress protein Hsc70 during S-phase in rat C6-glioma cells. *Cell stress chap.* 3: 94

Zhang, G., Gurtu, V. and Kain, S.R. (1996) An enhanced green fluorescent protein allows sensitive detection of gene transfer in mammalian cells. *Biochem. Biophys. Res. Comm.* 227: 707-711

Zhao, C., Hashiguchi, A., Kondoh, K., Du, W., Hata, J. and Yamada, T. (2002) Exogenous expression of heat shock protein 90 kDa retards the cell cycle and impairs the heat shock response. *Exp. Cell Res.* 275: 200-214

Zhao, Y.G., Gilmore, L., Coffey, M.C., Weber, B. and Lee, P.W.K. (2001) Hsp90 phosphorylation is linked to its chaperoning function. *J. Biol. Chem.* 276: 32822-32827

Zhu, D., Dix, D.J. and Eddy, E.M. (1997) Hsp70 is required for cdc2 kinase activity at 37 degrees C and after heat shock. *Development* 124: 3007-3014